Roles of the Receptor Tyrosine Kinases EGFR and ErbB2, and their Downstream Signalling Pathways in Diabetes-induced Vascular Dysfunction

Sioned Mai Griffiths

Ph.D. 2007

Cardiff University

ProQuest LLC
789 East Eisenhower Parkway
P.O. Box 1346
Ann Arbor, MI 48106-1346

ACKNOWLEDGEMENTS

I would like to express my uttermost gratitude to my supervisors Prof Kenneth Broadley and Dr Iain Hutcheson, for accepting me as a student at such a late stage in my PhD, and turning the experience around for me into a happier and more productive one. I'd also like to thank the members of both the pharmacology group and the Tenovus Centre for Cancer Research for their support and assistance during the last year of my PhD.

I would also like to thank Prof Ibrahim Benter and Dr Mariam Yousif for completing the perfusion studies.

I am also truly grateful to my friends formally of the group CGT, whom supported and encouraged me during some very difficult times. Also, I'd like to thank other friends, new and old, for being there for me during the course of my PhD.

Lastly, I'd like to thank my family for their unwavering support during the last few years.

SUMMARY

Mechanisms involved in diabetes-induced vascular dysfunction are not clearly understood. Endothelial dysfunction, including an inability to produce the correct balance of vasoconstrictors and vasodilators, specifically nitric oxide (NO) is a major manifestation of vascular dysfunction. This study aimed to characterize the roles of the receptor tyrosine kinases (RTKs), epidermal growth factor receptor (EGFR) and ErbB2, and their downstream signalling pathways in diabetes-induced vascular dysfunction. Studies in the mesenteric vascular bed of streptozotocin (STZ)-induced diabetic rats showed that exaggerated vasoconstrictor responses to noradrenaline and endothelin-1, and attenuated vasodilator responses to carbachol in STZ-diabetic rats were normalized by treatment with either genistein (general RTK inhibitor) or with AG1478 (selective EGFR inhibitor). Higher levels of phosphorylated (p)EGFR and pErbB2 were seen in mesenteric tissues from diabetic rats, which were prevented by treatment with AG1478, AG825 (ErbB2 inhibitor) and with genistein, further suggesting a role for EGFR and ErbB2. Response to the endothelium-independent vasodilator sodium nitroprusside remained normal in tissue from STZ-diabetic animals, suggesting a dysfunction at the level of the endothelium. Studies in human endothelial-like ECV-304 cells grown in high glucose also showed alterations in EGFR and ErbB2 signalling. Glucose-induced upregulation of pEGFR and pErbB2 levels was accompanied by increased phosphorylation of the downstream molecule PKC and of eNOS at threonine 495, which inactivates the molecule and reduces NO production. Studies using isolated rat aortic tissue revealed that EGF has a vasodilator effect in endothelium-intact tissue but a vasoconstrictive effect in endothelium-denuded tissue. These studies along with cell culture studies also suggest that glucose changes EGFR signalling properties from mediating a pro-relaxant effect in normal glucose to producing a pro-contractile effect in high glucose conditions. These results suggest an important role for EGFR, ErbB2 and PKC signalling in mediating diabetes-induced vascular dysfunction, and as such may represent novel therapeutic targets.

CONTENS

ABBREVIATIONS

Ach	Acetyl choline
ADAM	A disintegrin and metalloproteinase
ADMA	Asymmetric dimethylarginine
AGE	Advanced glycation end-product
AMP	Adenosine monophosphate
AMPK	AMP-activated protein kinase
AngII	Angiotensin II
APS	Ammonium persulphate
AR	Amphiregulin
ATP	Adenosine tri-phosphate
BH_4	Tetrahydrobiopterin
BSA	Bovine serum albumin
BTC	Betacellulin
$[Ca^{2+}i]$	Intracellular calcium concentration
CaM	Calmodulin
cDNA	Complimentary DNA
cGMP	Cyclic guanosine monophosphate
CI	Confidence intervals
COX	Cyclooxygenase
DAG	Diacyl glycerol
DDT	DL-Dithiothreitol
DMSO	Dimethyl sulfoxide
DNA	Diribonucleic acid

dNTP	Deoxyribonucleotide triphosphate
DOCA	Deoxycorticosterone acetate
EDHF	Endothelium-dependent hyperpolarising factor
EDRF	Endothelium-derived relaxing factor
EDTA	Ethylenediamine tetraacetate
EGF	Epidermal growth factor
EGFR	EGF receptor
eNOS	Endothelial NOS
EPR	Epiregulin
ERK1/2	Extracellular signal-regulated kinase 1/2
ErbB	Avian erythroblastosis oncogene B
ET-1	Endothelin-1
FAD	Flavin adenine dinucleotide
FBS	Foetal Bovine Serum
FMN	Flavin mononucleotide
G3P	Glycerol-3 phosphate
GMP	Guanosine monophosphate
GPCR	G protein-coupled receptor
H_2O_2	Hydrogen peroxide
HB-EGF	Heparin-binding EGF
HRP	Horseradish peroxidase
HSP90	Heat shock protein 90
HUVECs	Human umbilical vein endothelial cells
ICAM	Intercellular cell adhesion molecule

iNOS	Inducible NOS
IP	Immunoprecipitation
IP_3	Inositol 1,3,5 – triphopshate
JNK	c-jun N-terminal protein kinase
K^+	Potassium
M199	Medium 199
MAPK	Mitogen activated protein kinase
Mch	Acetyl methylcholine
MMLV-RT	Moloney murine leukaemia virus reverse transcriptase
MMP	Matrix metalloproteinase
mRNA	Messenger RNA
NA	Noradrenaline-bitartrate
NADPH	Nicotinamide adenine dinucleotide phosphate
nNOS	Neuronal NOS
NO	Nitric oxide
NOS	NO synthase
NRG	Neuregulin
$O_2^{\cdot -}$	Superoxide
$ONOO^{\cdot -}$	Peroxynitrite
p	Phosphorylated
PAI-1	Plasminogen activator inhibitor-1
PBS	Phosphate buffered saline
PCR	Polymerase chain reaction
PDE	Cyclic AMP-specific phosphodiesterase

PE	Phenylephrine hydrochloride
PI3K	Phosphoinositide 3-kinase
PIP_2	Phosphatidyl inositol 4,5-bisphosphate
PKC	Protein kinase C
PLC-γ	Phospholipase-C-γ
PS	Phosphatidyl serine
PTK	Protein tyrosine kinase
PTP	Protein tyrosine phosphatase
RNA	Ribonucleic acid
ROS	Reactive oxygen species
RPM	Revolutions per minute
RTKs	Receptor tyrosine kinase
RT-PCR	Reverse Transcriptase-polymerase Chain Reaction
SEM	Standard error of mean
SDS	Sodium dodecyl sulphate
Ser	Serine
sGC	Soluble guanylate cyclase
SH2	Src-homology 2
SNP	Sodium nitroprusside
STZ	Streptozotocin
TAE	Tris-Acetate-EDTA
TBS	Tris buffered saline
TEMED	N,N,N,N′-tetramethylethylenediamine
TGF-α	Transforming growth factor-α

Thr	Threonine
TPA	12-O-tetra-decanoyl-phorbol-13-acetate
Tris	Tris(hydroxymethyl)aminomethane
Tyr	Tyrosine
UV	Ultraviolet
VCAM-1	Vascular cell adhesion molecule-1
VEGF	Vascular endothelial growth factor
VSM	Vascular smooth muscle
VSMC	VSM cell
vWF	Von Willebrand's factor

LIST OF FIGURES AND TABLES

1.0 Introduction

1.1. Diabetes Mellitus

Diabetes mellitus, most commonly referred to as diabetes, is a highly prevalent and complex metabolic disorder characterized by impaired insulin signalling and hyperglycaemia (Zierath and Kawano 2003). It is predicted to be one of the western world's biggest public health concerns of the 21st century (Engelgau, *et al* 2004, Zimmet, *et al* 2001).

There are two major types of diabetes, type I and type II; there is also a minor type known as gestational diabetes or type III (World Health Organization 1999). Type I diabetes, also known as insulin-dependent diabetes mellitus or as adolescence onset diabetes mellitus, is the least common of the two major types. It is characterized by an absolute lack of insulin due to the autoimmune destruction of β cells in the pancreatic islets of Langerhans (Donath, *et al* 2003, Tognini, *et al* 2003). A combination of genetic susceptibility (Jahromi and Eisenbarth 2006, Radha, *et al* 2003) and environmental factors such as viral infection (Tognini, *et al* 2003, Yoon and Jun 2006), exposure to toxins, perinatal infections (Dahlquist, *et al* 1995), vaccine administration, and early infant diet may be responsible for triggering the autoimmune process leading to the destruction of β cells (Zimmet, *et al* 2001). Type II diabetes, also known as non-insulin-dependent diabetes mellitus or as mature onset diabetes mellitus, accounts for more than 90 % of the diagnosed cases of diabetes world wide (Zimmet, *et al* 2001). Though its pathology is not very well understood, it is thought that over time the sufferer progressively

develops insulin resistance, and sometimes defective insulin secretion (Tognini, *et al* 2003, Zimmet, *et al* 2001) resulting from the adverse effects of chronic hyperglycaemia and hyperlipidaemia on β cell function (Poitout and Robertson 2002). The major causes are environmental and behavioural, including increasing obesity and the sedentary and stressful modern lifestyle (Ludvigsson 2006, Poitout and Robertson 2002). There is also believed to be some genetic component (Radha, *et al* 2003) as well as demographic characteristics such as ethnicity (Abate and Chandalia 2001), age (Kesavadev, *et al* 2003, Zimmet, *et al* 2001), and sex, in increasing the risk of developing type II diabetes. Gestational diabetes is uncommon, with only around 4 % of women developing this type of diabetes during their pregnancy, however in most cases the condition subsides soon after child-birth (Ben-Haroush, *et al* 2004).

1.1.1 Incidence and Prevalence of Diabetes

It is estimated that, world wide, over 180 million individuals suffer from diabetes (World Health Organization 2006). Over 1.9 million of these cases are in the United Kingdom, with a further 595,000 individuals believed to be suffering from the condition, but to remain undiagnosed (British Heart Foundation 2007). These figures are escalating at an alarming rate, if this trend continues it has been estimated that the number of people diagnosed with diabetes will more than double by the year 2030 (Wild, *et al* 2004, World Health Organization 2006). This metabolic disease and its associated complications puts a heavy economic burden on the health care services (Bagust, *et al* 2002). It has been estimated that around

£5.2 billion a year, 9 % of the National Health Service's annual expenditure, goes on treating diabetes and its complications (Currie, *et al* 1997).

1.1.2 The Development and Pathophysiology of Diabetes

Carbohydrates are used as the body's main source of fuel. Complex carbohydrates that are consumed are most commonly broken down into monosaccharides, mostly glucose molecules. Glucose molecules are then absorbed from the intestine into the blood stream. Once in the blood stream glucose is transported to all cells of the body where it is metabolized, providing energy to drive essential cellular processes. Cells need a constant supply of carbohydrates but excessive glucose can have deleterious consequences on the biological system. Thus, a steady blood glucose concentration must be maintained in order for the body to function normally. Throughout the day, typically, blood glucose concentration will fluctuate, for example after meals, between meals and during the overnight fast. The body maintains a constant blood glucose concentration during these times through a process known as glucose homeostasis (Fig. 1.1).

Glucose homeostasis is maintained by hormones produced in the pancreatic islets of Langerhans. Excess glucose in the blood stimulates the release of the hormone insulin, which is secreted and released by the β cells. Insulin stimulates the storage of excess glucose in the liver and muscles, as long chains known as glycogen, in a process known as glycogenesis. Insulin also increases glucose uptake from the

plasma into the peripheral tissues. In response to low blood glucose, the hormone glucagon is secreted from the pancreatic α cells to stimulate the breakdown of stored glycogen into glucose in a process known as glycogenolysis. Furthermore, in response to threatening or stressful situations, adrenaline is secreted by the adrenal medulla which acts on β-adrenoreceptors in the liver to rapidly increase glycogenolysis (Storey 2004).

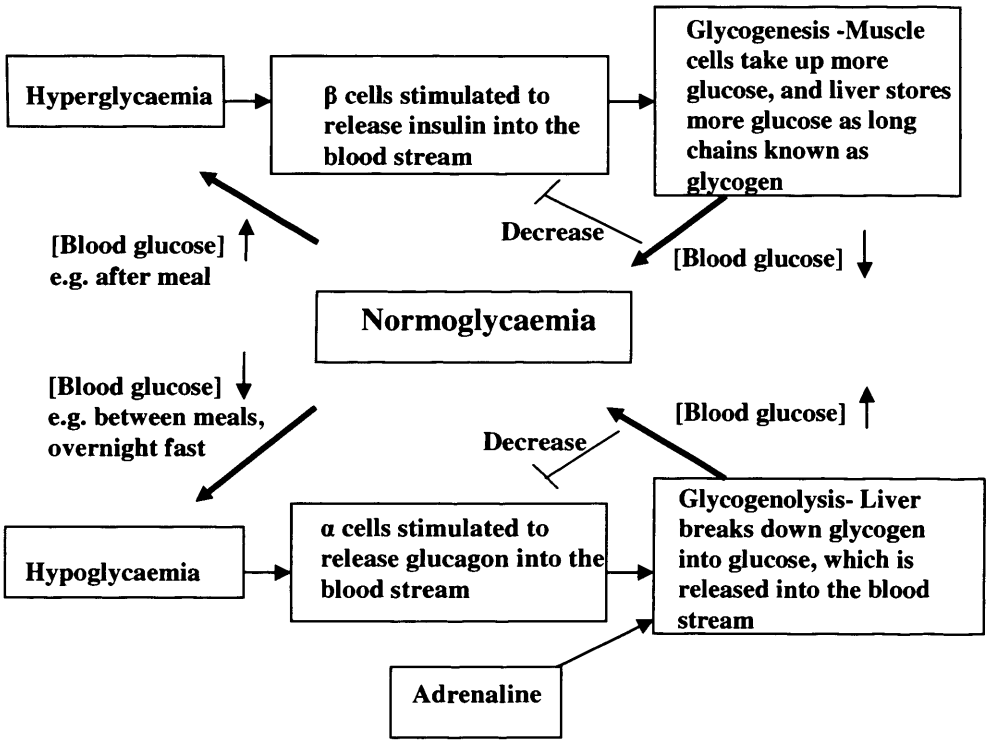

Figure 1.1 Glucose homeostasis

The interplay between these regulatory mechanisms keeps the whole blood glucose concentration of normoglycaemics within the range of 3.5 – 8 mM (Clark

and Kumar 2005). However occasionally there is a breakdown in these mechanisms, usually due to impaired insulin signalling, which can lead to chronic abnormally high blood glucose concentration. If left untreated, chronic hyperglycaemia can develop into full blown diabetes which is characterized by impaired insulin signalling and high blood glucose (Zierath and Kawano 2003). Diabetes is recognized when fasting plasma glucose concentration is over 7 mM, coupled with symptoms such as polydipsia, polyuria and unexplained weight loss (World Health Organization 1999).

1.1.3 Diabetes-induced Complications and Pathologies

Uncontrolled chronic diabetes is associated with the development of numerous pathologies and complications which can lead to a shortened expected life span and to a generally lower quality of life. Many of the major organs, the neuronal system and the vascular system can be affected by uncontrolled diabetes.

Diabetes-induced pathologies of the vasculature are often divided into microvascular and macrovascular complications (Hammes 2003, Tognini, *et al* 2003), both lead to impaired blood flow to organs and tissues. Diabetes-induced microvascular complications are frequently debilitating and include pathologies such as retinopathy due to damage of small arterioles and capillaries (Hammes 2003). Diabetes is one of the leading causes of blindness amongst adults in England and Wales (Bunce and Wormald 2006). Diabetes also increases the risk of non-traumatic lower-limb amputation due to impaired wound healing leading to

the development of gangrene in the feet, in a condition known as "diabetic foot infection"(Lipsky, *et al* 2006).

Diabetes-induced macrovascular complications are generally life threatening conditions such as coronary heart disease, atherosclerosis, and nephropathy. Diabetes sufferers are 2 - 4 times more likely than the general population to die from coronary artery disease or stroke (Du, *et al* 2001, Sacco 2002) and more than 75 % of deaths in diabetics are attributed to causes related to atherosclerosis (Hurst and Lee 2003). Diabetes can also lead to hypertension, which if left untreated can further increase the risk of developing heart disease (Vijan and Hayward 2003). Additionally these macrovascular events occur at a much earlier age in people suffering from diabetes, and progressive diseases such as carotid atherosclerosis occur at an accelerated rate (Wagenknecht, *et al* 2003). Much of the damaging effects of diabetes on the vascular system progresses from its effect on the vascular endothelium (Taylor 2001).

1.2 The Endothelium

Vascular smooth muscle cells (VSMCs) and macrovascular endothelial cells are the two major components of arteries. VSMCs are found in the middle thickest layer of the blood vessel known as the tunicia media, and the endothelial cells are found in the inner most layer of the vessel known as the endothelium, or tunicia intima. The tunica adventitia is the outer layer composed mostly of connective tissue.

The vascular smooth muscle (VSM) is important for regulating blood flow and blood pressure by contracting and relaxing in response to circulating hormones, shear stress, or local mediators secreted by sympathetic nerve terminals or by the endothelium (Rang, *et al* 1999). The VSM contracts via the actin-myosin cytoskeletal system which acts in response to increasing intracellular calcium concentration ($[Ca^{2+}]i$). Vasoconstrictors and vasodilators can either cause a change in $[Ca^{2+}]i$ or in the contractile machinery's sensitivity to $[Ca^{2+}]i$ (Hofmann, *et al* 2000).

The endothelium is a multifunctional inner layer found in all blood vessels and plays a major role in the control of vascular function, thus it is a key player in determining the state of health or disease of a blood vessel. Not only is the endothelium an efficient selective filter between plasma and the blood vessel, it also has many other actions, important for maintaining the blood vessel in an anti-atherogenic state (Galley and Webster 2004). The endothelium produces vasodilators such as prostacyclin, endothelium-dependent hyperpolarising factor (EDHF) and nitric oxide (NO), which act upon the VSM. It also produces vasoconstrictors including endothelin-1 (ET-1), thromboxane A_2 and prostaglandin H_2 (Avogaro, *et al* 2006, Gordon 2004, Schalkwijk and Stehouwer 2005). The endothelium is also important for controlling the processes of blood coagulation and haemostasis, by synthesizing anti-thrombotic factors such as tissue type plasminogen activator. However, the endothelium can also produce pro-coagulant

factors such as Von Willebrand's factor (vWF) and the anti-fibrinolytic factor plasminogen activator inhibitor-1 (PAI-1). It is also believed to play a role in inflammatory and immune responses through expressing selectins, intercellular cell adhesion molecules (ICAMs) and vascular cell adhesion molecule-1 (VCAM-1), which regulate adhesion of blood cells, including leucocytes, and permeability to the vascular tissue (Galley and Webster 2004, Guerci, *et al* 2001). It also regulates the composition of the sub-endothelial matrix by decreasing concentrations of components of the extracellular matrix such as collagen type I and II (Myers and Tanner 1998).

One of the most potent substances produced by the endothelium is NO. NO performs a myriad of functions which maintain the vessel in an anti-atherogenic, healthy state (Naruse, *et al* 1994).

1.2.1 Nitric Oxide (NO)

In 1980 Furchgott and Zawadzki demonstrated that an intact endothelium was necessary for the vasodilatory effects of acetylcholine. From this observation the group developed the concept of an endothelium-derived relaxing factor (EDRF), a mediator secreted by the endothelium, which was in part responsible for vasodilator-induced relaxation of VSM (Furchgott and Zawadzki 1980). Seven years later two groups found EDRF and NO to have undistinguishable biological and chemical characteristics, and thus concluded that EDRF was in fact NO

(Ignarro, *et al* 1988a, Ignarro, *et al* 1987a, Ignarro, *et al* 1987b, Ignarro, *et al* 1988b, Palmer, *et al* 1987).

1.2.1.1 The Role of NO in Blood Vessels

NO is a free radical gas secreted by the endothelium, it can also be released as a metabolic product of NO donor drugs such as sodium nitroprusside (SNP) (Marks, *et al* 1991), spermine NONOate (Keefer, *et al* 1996) and glyceryl trinitrate (Marks, *et al* 1992). These drugs can be used for the treatment of conditions such as ischemic heart disease and arterial hypertension (Ignarro, *et al* 2002). NO has many important roles to play in the cardiovascular system including the regulation of vascular tone through its relaxant effect on vascular tissue (Palmer, *et al* 1988, Palmer, *et al* 1987). It also plays a role in inflammatory and immune responses, and in blood coagulation by, among other processes, regulating leucocyte and monocyte adhesion and platelet aggregation (Bath, *et al* 1991, Guzik, *et al* 2003, Radomski, *et al* 1990). NO also plays a role in the inhibition of VSMC proliferation (Nunokawa and Tanaka 1992). Its importance in the cardiovascular system is reflected by the fact that a lack of NO can lead to cardiovascular damage, such as the damage seen in atherosclerosis (Naruse, *et al* 1994). It is now known that NO also plays an important role in the nervous system where it acts as a neurotransmitter (Belvisi, *et al* 1992, Bredt and Snyder 1992).

1.2.1.2 Nitric Oxide Synthase (NOS) Isozymes

NO is formed as a product of the reaction between L-arginine and molecular oxygen, catalysed by a family of dimeric enzymes known as the NO synthase (NOS) isozymes. A by-product of the reaction is citrulline (Andrew and Mayer 1999, Bredt and Snyder 1990, Mayer and Hemmens 1997, Palmer, *et al* 1988).

The NOS family of isozymes includes three distinct isoforms: neuronal (n)NOS/ NOS-I, endothelial (e)NOS/ NOS-III and inducible (i)NOS/ NOS-II. The first isozyme, nNOS, is found mainly in neurons including the central and peripheral nervous system, it can also be found in cardiac and skeletal muscles (Mungrue and Bredt 2004). eNOS is found mainly in the endothelium but can also be found in cardiac myocytes (Feron, *et al* 1998), gastrointestinal tract (Berg, *et al* 2004), brain hippocampus (Hashiguchi, *et al* 2004), ovaries (Zackrisson, *et al* 1996), and in platelets (Randriamboavonjy and Fleming 2005). Under physiological conditions both eNOS and nNOS are produced constitutively, however their production can be enhanced by certain stimuli. On the other hand, the expression of iNOS which is mostly found in immune cells such as macrophages and in most vascular cells is very low. High level expression of iNOS can be induced in response to inflammatory agents such as cytokines (Andrew and Mayer 1999).

NOS isozymes are dimers made up of two identical monomers. A NOS monomer possesses an N-terminal oxygenase domain and a C-terminal reductase domain, which makes NOS functionally bimodal (Andrew and Mayer 1999, Griffith and

Stuehr 1995). NOS has many bound prosthetic groups, the oxygenase domain binds protoporphyrin IX (haem), tetrahydrobiopterin (BH_4) and the NOS substrate L-arginine (Andrew and Mayer 1999, Griffith and Stuehr 1995). The reductase domain binds flavin mononucleotide (FMN), flavin adenine dinucleotide (FAD) and nicotinamide adenine dinucleotide phosphate (NADPH) (Nakane, *et al* 1993). In between the reductase and the oxygenase domains lies a calmodulin (CaM) binding domain (Abu-Soud and Stuehr 1993). These prosthetic groups and binding sites are necessary for the dimerization and activation of NOS and for the NOS catalysed production of NO (Fig. 1.2). The role of each prosthetic group and binding site is discussed in detail in a review by Andrew and Myer (1999). The enzyme catalysed reaction is complex and is believed to involve the transfer of electrons from NADPH through the flavins FAD and FMN to the haem iron. The haem iron then binds with oxygen and catalyses the oxidation of L-arginine to L-citrulline and NO. This mechanism is discussed in detail by Griffith and Stuehr (Griffith and Stuehr 1995).

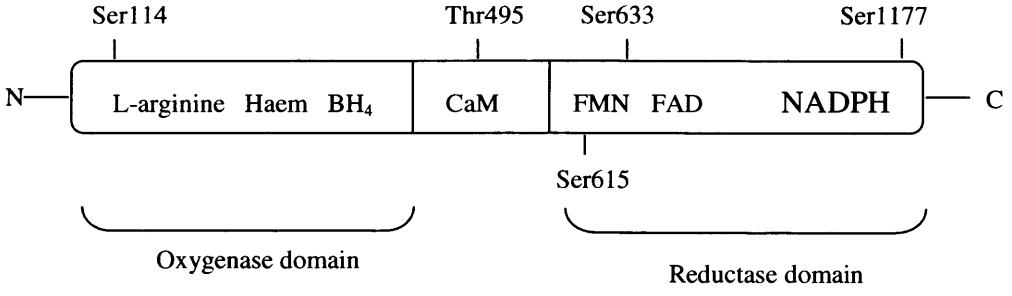

Figure 1.2 Domain structure, prosthetic groups and phosphorylation sites of an eNOS monomer. Haem = protoporphyrin IX, BH_4 = tetrahydrobiopterin, CaM = calmodulin, FMN = flavin mononucleotide, FAD = flavin adenine dinucleotide, NADPH = nicotinamide adenine dinucleotide phosphate.

1.2.1.3 eNOS Activation

As mentioned earlier, eNOS is constitutively but sub-maximally active under the basal conditions of resting endothelial cells. However, the catalytic activity of eNOS as well as nNOS can be enhanced or attenuated by certain mediators. The main mechanism for enhancement of eNOS activity involves an increase in $[Ca^{2+}]i$. This is in contrast to iNOS, where CaM is constitutively bound to the enzyme and its activity is thought to be independent of $[Ca^{2+}]i$ (Andrew and Mayer 1999, Boo and Jo 2003).

The two basic pathways for eNOS activation are receptor-stimulated, and flow-dependent. Receptor-stimulated eNOS activation is initiated by stimuli such as acetylcholine, bradykinin or substance P, which can activate downstream pathways that lead to an increase in the release of Ca^{2+} from intracellular stores, and an increase in extracellular Ca^{2+} influx. The increase in $[Ca^{2+}]i$ leads to Ca^{2+} binding to CaM, the Ca^{2+}/CaM then binds to eNOS, resulting in eNOS activation (Andrew and Mayer 1999, Griffith and Stuehr 1995, Rang, *et al* 1999).

Studies have revealed that mechanical, shear stress-induced eNOS activation occurs in two phases. The first phase is dependent on Ca^{2+}/CaM and lasts only seconds in response to the initial shear stress. The second phase is independent of $[Ca^{2+}]i$ and lasts as long as the shear stress is maintained. This second phase which is insensitive to Ca^{2+}/CaM is thought to involve activation of the signalling

molecules phosphoinositide 3-kinase (PI3K) and Akt. This mode of eNOS activation is important for the tonic production of NO to decrease systemic blood pressure (Boo and Jo 2003, Gallis, *et al* 1999).

The interaction between eNOS and proteins other than CaM is also important in controlling eNOS activity. For example heat shock protein 90 (HSP90) can act as a scaffold for eNOS, facilitating its affiliation with regulatory enzymes such as CaM and Akt, thus HSP90 enhances eNOS activity (Mount, *et al* 2006).

Post-translational modifications can also contribute to the regulation of eNOS catalytic activity through enhancing or reducing its activity, and mediating its stability in response to both hormones and shear stress. For example the posttranslational addition of lipid moieties palmitate and myristate at the N-terminus facilitate eNOS targeting to the caveolae. The association of eNOS with caveolin renders the enzyme inactive thus myrisotylation and palmitoylation negatively regulates eNOS activity (Goligorsky, *et al* 2002, Liu, *et al* 1996).

Another very important mediator of eNOS activity is the phosphorylation of certain residues of the enzyme. The activity of eNOS, in response to humoral factors such as bradykinin or insulin or shear stress can be enhanced or weakened at a given $[Ca^{2+}]i$ by the phosphorylation of specific eNOS residues. This can increase or decrease activity of eNOS without a corresponding alteration in $[Ca^{2+}]i$ or shear stress. There are five serine (Ser)/threonine (Thr) phosphorylation sites

know to affect eNOS activity upon phosphorylation. In the human eNOS sequence, these sites are Ser114 located in the oxygenase domain, Thr495 found in the CaM binding domain, and Ser633, Ser615 and Ser1177 located in the reductase domain (Mount, *et al* 2006). It is known that the phosphorylation of eNOS at Ser1177 and Ser633 increases eNOS activity (Bauer, *et al* 2003, Dimmeler, *et al* 1999, Mount, *et al* 2006), whilst eNOS phosphorylation at Thr495 inhibits eNOS activity (Fleming, *et al* 2001, Mount, *et al* 2006). However, it is not yet known what effect phosphorylation at Ser615 and Ser114 has on the enzyme's activity.

It is believed that phosphorylation of eNOS at site Ser1177 results in a conformational change of eNOS rendering the molecule more active (Lane and Gross 2002, Mount, *et al* 2006). Many factors have been implicated in the phosphorylation of eNOS at Ser1177 including cyclic adenosine monophosphate (AMP)-dependent protein kinase, AMP-activated protein kinase (AMPK), , Akt, Ca^{2+}/CaM dependent protein kinase II, protein kinase G and the phosphatase protein 2A. Also, protein kinase C (PKC) is known to inhibit eNOS activity by dephosphorylating Ser1177 (Boo and Jo 2003, Mount, *et al* 2006).

The residue Thr495 is found in the CaM binding domain of eNOS, this may explain the inhibitory effect that phosphorylation at this site has on eNOS activity, as it may interfere with the binding of Ca^{2+}/CaM to the enzyme (Fleming, *et al* 2001, Matsubara, *et al* 2003). PKC is known to phosphorylate eNOS at Thr495

both in vitro and in vivo (cultured endothelial cells), but it is not yet known which PKC isoform is responsible (Matsubara, *et al* 2003, Michell, *et al* 2001). It has been shown in rat hearts that AMPK also phosphorylates eNOS at Thr495 (Chen, *et al* 1999). In cultured endothelial cells, reduction in basal eNOS phosphorylation at Thr495 can contribute to the activation of eNOS. eNOS dephosphorylation at Thr495 is thought to happen in synchrony with the phosphorylation of eNOS at Ser1177 to activate the molecule in response to vasodilators such as bradykinin, vascular endothelial growth factor (VEGF), ionomycin and hydrogen peroxide (H_2O_2) (Mount, *et al* 2006, Thomas, *et al* 2002).

1.2.1.4 NO-mediated VSMC Relaxation

The enzyme eNOS is activated in the endothelium and catalyses the production of NO, which has a high affinity for haem. NO produced in the endothelium migrates to the VSM and activates soluble guanylate cyclase (sGC) through binding to its haem group. The activated sGC then goes on to initiate the intracellular production of the 2nd messenger cyclic guanosine monophosphate (cGMP). An increase in cGMP levels can modulate protein kinase G, cyclic nucleotide-gated cation channels, cyclic AMP-specific phosphodiesterases (PDE), cyclic GMP-dependent kinases and other smooth muscle proteins. The main action of cGMP is through these intermediary molecules to lower $[Ca^{2+}]i$, which subsequently affects the contractile machinery (actin-myosin cytoskeletal system) in a way that reduces VSMC contraction. Alternatively, cGMP through intermediary molecules can change the sensitivity of the contractile machinery to Ca^{2+} (Hofmann, *et al* 2000,

Murad 1986, Rang, *et al* 1999). The enzyme PDE5 inactivaes cGMP by hydrolysing it to the inactive form, GMP (Lincoln 2004) (Fig. 1.3).

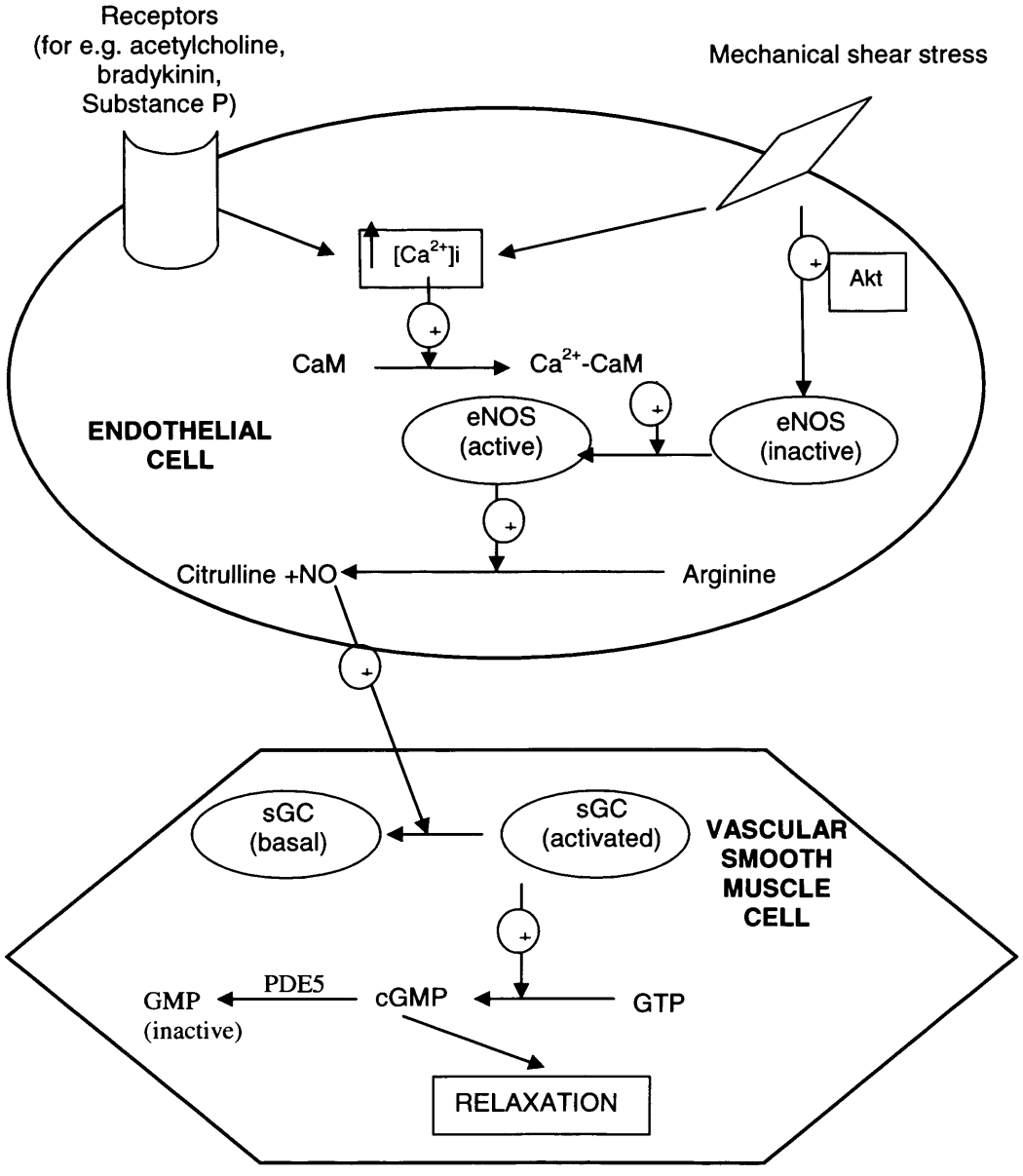

Figure 1.3 Regulation of soluble guanylyl cyclase (sGC) by nitric oxide (NO) which is produced in the endothelium. Adapted from (Rang, *et al* 1999). CaM = Calmodulin, PDE5 = Phosphodiesterase enzyme type 5, GMP = guanosine monophosphate, cGMP = cyclic GMP, GTP = guanosine tri phosphate.

1.3 Endothelial Dysfunction

Abnormalities in endothelial, or VSM function, or a breakdown in the relationship between the two can result in vascular dysfunction. A breach in the endothelial barrier leaves the blood vessel susceptible to the development of vascular disease. Initiation and progression of many of the commonest arterial diseases is partly due to endothelial dysfunction (Cuevas and Germain 2004).

Endothelial injury or dysfunction can lead to various kinds of vascular pathologies including atherosclerosis in which there is deposition of cholesterol at the sub-endothelial layer of arteries, this can form plaques. Macrophages can pass through the endothelium and scavenge these cholesterol deposits and accumulate in atherosclerotic lesions, which narrow the artery, this is known as stenosis. Also, blood clots can form at the site of the lesion, which is known as thrombosis (Gerrity 1981). This can lead to serious consequences such as myocardial infarction (heart attack) when a coronary artery becomes blocked. Also aneurysms can occur when the blood vessel becomes weakened at the site of the atheroma, leaving it susceptible to rupture, which is very serious if the blood vessel is a major artery such as the aorta or a brain artery, which can lead to a stroke (Clark and Kumar 2005). Also, importantly, damage caused to the endothelium impairs the endothelium's function as a regulator of vascular tone as it can no longer produce and secrete the appropriate balance of vasoactive factors such as NO and ET-1 to maintain vascular health (Galley and Webster 2004).

There are many factors that can contribute to endothelial dysfunction, including cigarette smoke (Heitzer, *et al* 1996), insulin resistance, obesity (Caballero 2003), hypercholesterolaemia (Steinberg, *et al* 1997), low levels of high-density lipoprotein cholesterol (Hurst and Lee 2003), hypertension (Panza 1997), and hyperglycaemia (Schalkwijk and Stehouwer 2005). Other than cigarette smoke, all of the risk factors mentioned above are associated with diabetes, thus it is not surprising that there is an increased risk of vascular dysfunction associated with diabetes.

1.3.1 Diabetes-induced Endothelial Dysfunction

Metabolic abnormalities such as hyperglycaemia and insulin resistance, associated with diabetes can induce a whole host of changes to the normal function of the vasculature. Such alterations include enhanced response to vasoconstrictors and attenuated response to vasodilators (Makino, *et al* 2000, Mayhan, *et al* 1999). The development of endothelial dysfunction is considered the major manifestation of diabetes that contributes to alterations in vascular function (Avogaro, *et al* 2006, De Caterina 2000). In fact it has been shown that in the presence of risk factors such as diabetes, endothelial dysfunction precedes the onset of vascular disease such as atherosclerosis, suggesting its role in the initiation of such pathologies (Reddy, *et al* 1994). Two groups have revealed that out of the risk factors for developing cardiovascular disease associated with diabetes, chronic hyperglycaemia is the biggest contributor to vascular damage in both type I and

type II diabetes (Diabetes Control and Complications Trial Research Group 1993, UK Prospective Diabetes Study (UKPDS) Group 1998). Studies have revealed that hyperglycaemic conditions elicit destructive actions upon the endothelium changing it deleteriously from functioning as an anti-atherogenic to functioning as a pro-atherogenic tissue.

High glucose concentrations have been shown to increase apoptosis, decrease proliferation and injure endothelial cells (Baumgartner-Parzer, *et al* 1995, Choy, *et al* 2001, Curcio and Ceriello 1992, Han, *et al* 2005, Ido, *et al* 2002), which can contribute to the development of endothelial dysfunction. Hyperglycaemia-induced dysfunctional endothelium can no longer act as a barrier to protect the vessel from atherosclerosis and thrombogenesis. Studies have revealed that even short-term hyperglycaemia increases vascular permeability (Zuurbier, *et al* 2005). Also diabetes-induced dysfunctional endothelium may produce increased amounts of adhesion molecules and C-reactive protein leading to increased inflammation. There may also be increased thrombogenesis due to increased production of procoagulant proteins such as vWF and PAI-1 (Du, *et al* 2000, King, *et al* 2003, Schalkwijk and Stehouwer 2005, Vaidyula, *et al* 2006). Furthermore, diabetes affects basement membrane composition as it increases the production of collagen type IV and fibronectin which thickens the basement membrane (Cagliero, *et al* 1988, Cagliero, *et al* 1991). However, a major consequence of diabetes-induced endothelial-dysfunction is reduced endothelium-dependent vasodilation

(Hogikyan, *et al* 1998, Makimattila, *et al* 1999, McVeigh, *et al* 1992, Watts, *et al* 1996, Williams, *et al* 1996).

1.3.2 The Effect of Diabetes on Endothelial Vasodilators and Vasoconstrictors

Hyperglycaemia or diabetes-induced dysfunctional endothelium results in aberrant vascular reactivity to vasodilators and vasoconstrictors, one of the main reasons is the reduced bioavailability of endothelium derived vasodilators, such as NO, required for maintaining normal vascular tone (Gordon 2004, Li and Forstermann 2000). There have been reports suggesting that the synthesis of NO is actually increased by diabetes and that it is only the bioavailability of NO that is reduced by high glucose (Cosentino, *et al* 1997). However, many studies have shown that high glucose can in fact reduce eNOS expression and activity, and NO synthesis (Ding, *et al* 2000, Du, *et al* 2001). Studies have shown diabetes-induced reductions in conversion of L-arginine to NO in type II diabetic patients (Avogaro, *et al* 2003b, Gomes, *et al* 2005, Williams, *et al* 1996). Also, studies have shown an increase in the level of the endogenous NOS competitor/ NO inhibitor, asymmetric dimethylarginine (ADMA), has been shown in type II diabetic patients after consuming a high fat meal. This rise in ADMA found in diabetic patients correlated inversely with vasodilation, suggesting its contribution to vascular dysfunction (Fard, *et al* 2000). It is known that insulin itself can stimulate the production of NO by signalling through PI3K and Akt. Thus it is not surprising that defective insulin signalling seen in diabetes results in defective insulin stimulated vasodilation (Scherrer, *et al* 1994, Zeng, *et al* 2000). Some

vasoconstrictors, including α adrenergic agonists such as noradrenaline, in synergy with their vasoconstrictor effect, can also release NO Thus, a decrease in NO bioavailability results in an imbalance between vasoconstrictor and vasodilator effect resulting in elevated noradrenaline-induced vasoconstriction and hypertension (Amerini, *et al* 1995). Furthermore, NO's other vasoprotective activities are diminished such as its anticoagulant activity and its role in immune responses, again contributing to the development of atherosclerosis (Russo, *et al* 2002).

Another endothelium-dependent vasodilator, namely prostacyclin is also found to be reduced in the diabetic person, which leads to impaired vasodilation. Also prostacyclin inhibits platelet adhesion and aggregation, thus reduced protacyclin increases these processes, which leads to the development of atherosclerosis (Gordon 2004, Jennings 1994). However, it has been shown that the inhibition of cyclooxygenase (COX), an essential enzyme for the generation of prostacyclin does not have an effect on agonist induced changes in vasodilation in type II diabetic patients. This suggests that the contribution of prostaglandins to diabetes induced abnormal endothelial function is only minor compared to the role of NO (Taylor 2001, Williams, *et al* 1996).

Diabetes not only decreases the production of important endothelial vasodilators but can also further tip the balance towards the development of atherosclerosis by increasing the production of vasoconstrictors, such as ET-1 and angiotensin II

(AngII). Renin secreted from the juxtaglomerular apparatus cleaves the precursor molecule angiotensinogen, giving rise to angiotensin I. Subsequently, angiotensin I is converted by angiotensin-converting enzyme into the potent vasoconstrictor AngII (Rang, *et al* 1999). It is believed that diabetes, through increased hyperglycaemia-induced production of reactive oxygen species (ROS), upregulates production of AngII. Increased AngII production increases NADPH oxidase which further catalyses ROS and superoxide production. Increased ROS production further induces vascular damage and NO scavenging, which is the reaction of NO with ROS, such as superoxide ($O_2^{\cdot-}$), to produce peroxynitrite ($ONOO^{\cdot-}$) in VSMC and cardiac cells. This not only leads to increased vascular tone but also to increased apoptosis and necrosis (Frustaci, *et al* 2000, Nakashima, *et al* 2006, Nickenig and Harrison 2002) and increased VSMC proliferation (Lee, *et al* 2003, Seshiah, *et al* 2002).

Prepro-ET-I is cleaved to big ET which is further processed by endothelin converting enzyme to produce the potent endothelium derived vasoconstrictor ET-1 (Rang, *et al* 1999). Elevated levels of ET-1 have also been observed in the plasma of patients with type II diabetes, again leading to increased vascular tone (Takahashi, *et al* 1990a).

1.3.3 Possible Mechanisms Responsible for Diabetes-induced Endothelial-dysfunction

1.3.3.1 Increased ROS Production

It is believed that a major contributor to diabetes-induced endothelial dysfunction is an increased production of ROS, triggered by hyperglycaemia. A large proportion of hyperglycaemia-induced ROS including $O_2^{\cdot-}$, H_2O_2 and $ONOO^{\cdot-}$ are produced and released by the mitochondria (Brownlee 2001, Nishikawa, *et al* 2000). However, studies have shown that NADPH oxidase is the most potent ROS provider in vascular cells (Lee, *et al* 2003), and increased NADPH oxidase activation has been shown in monocytes from patients with type II diabetes mellitus (Avogaro, *et al* 2003a).

Redox imbalance occurs when ROS production outweighs cellular antioxidative mechanisms, which leads to a state of oxidative stress. Under certain conditions of oxidative stress such as that caused by diabetes, BH_4, the essential co-factor for eNOS function, is destroyed. In the absence of BH_4, eNOS becomes uncoupled, resulting in the production of superoxide anions instead of NO. Superoxide can as mentioned earlier scavenge NO by reacting with it to form $OONO^{\cdot-}$ which causes further vascular damage partly by nitrating important vascular proteins such as actin, leading to the initiation of atherogenesis (Ballinger, *et al* 2000, Beckman and Koppenol 1996, Shinozaki, *et al* 1999, Vasquez-Vivar, *et al* 1998, White, *et al* 1994).

ROS can also activate oxidative stress triggered pathways, which initiate expression of genes whose products act destructively upon the vascular cells, initiating vascular pathologies and dysfunction (Griendling and FitzGerald 2003, Lee, *et al* 2003). It is thought that hyperglycaemia-induced ROS can also initiate endothelial-dysfunction by increasing flux through certain biochemical pathways, including advanced glycation end-product (AGE) production and the polyol pathway (sorbitol pathway). Initiation of these pathways can directly elicit destructive effects on endothelial function as well as further increase the production of ROS.

1.3.3.1.1 Advanced Glycation Endproduct Pathway

Nonenzymatic glycation, in which reducing sugars covalently attach to proteins, lipids and nucleic acids that accumulate in the vessel wall, can result in the production of AGEs. The first stage of the reaction leads to the production of a Schiff base, which rearranges itself into an Amadori product. This initial stage of the reaction is reversible, but Amadori products are fairly stable. However, if the concentration of glucose is persistently high, a series of subsequent reactions and rearrangements will occur which produces the irreversible AGE (Schalkwijk and Stehouwer 2005). Normally, AGE formation occurs during the aging process however studies have shown that hyperglycaemia associated with diabetes enhances the production of AGEs (Bierhaus, *et al* 1998). Increased AGE production can initiate an array of deleterious effects upon the vasculature such as initiating the production of foam cells, resulting in the development of

atherosclerosis (Brownlee, *et al* 1985). AGEs can also reduce the vessel wall's elasticity by cross-linking collagen and deleteriously changing its biochemistry, which may lead to vascular dysfunction (Reddy 2004). AGE generated ROS activate nuclear factor-kappa B which promotes the expression of genes such as those responsible for the production of inflammatory cytokines, adhesion molecules and procoagulant tissue factor, leading to vascular injury and dysfunction (Basta, *et al* 2004, Srivastava 2002). AGEs also induce the expression of VEGF which increases vasoconstriction through inducing the expression of ET-1 (Quehenberger, *et al* 2000). Importantly, AGEs can also quench NO activity, leading to impaired vasodilatory responses (Bucala, *et al* 1991, Hogan, *et al* 1992)..

1.3.3.1.2 The Polyol Pathway

The polyalcohol (polyol) pathway is a metabolic pathway in which a small portion of consumed glucose is reduced to the polyol sorbitol. This redox reaction is catalysed by the enzyme aldose reductase, which also catalyses the oxidation of NADPH to $NADP^+$ and reduces NAD^+ to NADH. Sorbitol is subsequently converted to fructose by sorbitol dehydrogenase.

Aldose reductase is the rate limiting enzyme in the polyol pathway. Normally aldose reductase has very low affinity for glucose so usually this reaction takes place very slowly. However, under hyperglycaemic conditions of diabetes more sugar is available and flux through the polyol reaction is increased (Brownlee

2001). Increased aldose reductase leads to vascular abnormalities. Accumulation of sorbitol leads to osmotic stress, AGE synthesis and oxidative stress which impair endothelial function (Schalkwijk and Stehouwer 2005, Williamson, *et al* 1993). It has been shown that inhibiting aldose reductase restores reduced endothelium-dependent vasodilation back to normal in diabetic rat aorta (Tesfamariam, *et al* 1993). Presently, an aldose reductase inhibiting, orally available drug named ranirestat is in development for the treatment of diabetic complications. Such complications include cataracts, due to the insoluble deposits of sorbitol in the lens, and also retinopathy, neuropathy and nephropathy (Giannoukakis 2006).

1.3.3.2 Activation of Receptor Tyrosine Kinase Signal Transduction Pathways

Protein tyrosine kinases (PTKs) are enzymes that catalyse the transfer of a phosphate group from adenosine tri-phosphate (ATP) to a tyrosine residue of the target protein. There are two main classes of PTKs: receptor tyrosine kinases (RTKs) and non-receptor tyrosine kinases. Examples of RTKs include the insulin receptor, platelet-derived growth factor receptor and the epidermal growth factor receptor (EGFR/ErbB1) (Alberts 2002). Activation of these RTKs initiates an array of downstream signal transduction cascades. It is known that diabetes and hyperglycaemia can induce abnormal signalling of various RTK-associated pathways including mitogen activated protein kinase (MAPK) pathways, the Akt pathway and the PKC pathway.

1.3.3.2.1 MAPK Pathways

MAPK signalling cascades are a group of signal transduction pathways which include the extracellular signal-regulated kinase 1/2 (ERK1/2), p38MAPK, c-jun N-terminal protein kinase, and bigMAPK 1 pathways (Cowan and Storey 2003).

Upon RTK activation, Ras, a small monomeric guanosine triphosphatase, relays the signal down to the ERK1/2 pathway, and through a series of serine threonine phosphorylations down to the nucleus, to regulate cell cycle, cell growth and differentiation (Jorissen, *et al* 2003, Kolch 2000). Diabetes and hyperglycaemia are known to increase MAPK signalling in various cell types and tissues. For example, studies have shown increased MAPK signalling in mesangial cells treated with high glucose (Haneda, *et al* 1995). Also there is increased MAPK signalling in glomeruli from streptozotocin (STZ)-induced diabetic rats (Awazu, *et al* 1999), which may contribute to the development of diabetic nephropathy. Also hyperglycaemia induced in patients using hyperglycaemic clamps, has been shown to increase MAPK signalling in veins (Schiekofer, *et al* 2003). In coronary arteries from the diabetic pig, hyperglycaemia-induced AGEs increased ERK1/2 activation, which induced the expression of inflammatory genes, leading to accelerated development of atherosclerosis (Zhang, *et al* 2003). These studies suggest that increased MAPK signalling may have a role to play in diabetes-induced pathologies and hyperglycaemia-induced atherosclerosis. Furthermore, ERK1/2 signalling is known to be associated with eNOS activity; however there are conflicting reports as to whether the inhibition of ERK1/2 enhances (Bernier,

et al 2000), attenuates (Mineo, *et al* 2003) or has no effect on eNOS activity (Schmidt, *et al* 2002). It is believed that the effect of ERK1/2 on eNOS activity depends very much upon the cell or tissue type used in the study and the agonist used to stimulate eNOS activity (Cale and Bird 2006). Thus, aberrant ERK1/2 signalling could lead to aberrant eNOS signalling and to endothelial-dysfunction.

The p38MAPK pathway can also be initiated through the activation of RTKs (Fitzgerald, *et al* 2005). However it is normally activated by various stress and inflammation signals including, oxidative stress (Sen, *et al* 2007), ultraviolet (UV) radiation (Keller, *et al* 1999), hyperosmolarity (Denkert, *et al* 1998), lipopolysaccaride (Nick, *et al* 1996), proinflammatory cytokines e.g. tumour necrosis factor-α and interleukin-1 (Modur, *et al* 1996, Raingeaud, *et al* 1995) and heat shock (Dorion, *et al* 2002). It has been shown that glucose can in part mediate endothelial dysfunction through activating stress activated pathways such as p38MAPK (Evans, *et al* 2002). Human aortic endothelial cells treated with high glucose undergo increased apoptosis in a mechanism involving increased p38MAPK phosphorylation (Nakagami, *et al* 2001). Also, using inhibitors of p38MAPK hyperglycaemia-induced increased p38MAPK signalling has been shown to contribute to the development of endothelial dysfunction by triggering an inflammatory response in STZ-induced diabetic rats (Riad, *et al* 2007), and by having an anti-proliferative effect on endothelial cells (McGinn, *et al* 2003). Also, in rat aortic VSMCs, high glucose has been shown to increase p38MAPK activity in a time-dependent manner, which is thought to affect cell survival, and

contribute to the development of vascular dysfunction (Igarashi, *et al* 1999). Furthermore, the p38MAPK pathway is also thought to have an involvement in NOS activity, specifically inducible NOS (iNOS). It has been shown in rat aortic VSMCs that hyperglycaemia and hyperinsulinaemia increase p38MAPK activity and block the induction of iNOS protein expression (Begum and Ragolia 2000). Thus, the p38MAPK pathway could also potentially be implicated in diabetes-induced vascular dysfunction.

1.3.3.2.2 The PI3K/Akt Pathway

Upon RTK activation in response to an external survival signal, signalling through the Akt (protein kinase B) pathway is initiated. Akt signalling promotes cell survival by inhibiting activators of cell death or by inhibiting the transcription of genes that encode them (Brunet, *et al* 1999, Cardone, *et al* 1998, Yao and Cooper 1995). Studies have shown the Akt pathway is also important in the control of insulin-mediated glucose transport and glycogen synthesis (Barthel, *et al* 1999, Cross, *et al* 1995, Hajduch, *et al* 1998). A previous study showed that by inhibiting PI3K which is the upstream mediator of Akt, increased responses to vasoconstrictors and attenuated responses to vasodilators induced by diabetes are normalized (Yousif, *et al* 2006). Furthermore, hyperglycaemia-induced impaired PI3K-Akt signalling has been shown to lead to a decrease in endothelial cell proliferation and cell survival (Varma, *et al* 2005). Also, insulin activation of Akt in endothelial cells can activate eNOS (Kim, *et al* 2001), thus it is plausible that

aberrant Akt activity leads to aberrant eNOS activity, and therefore vascular dysfunction.

1.3.3.2.3 The PKC Pathway

phospholipase-C-γ (PLC-γ) is activated by RTKs such as EGFR (Chattopadhyay, *et al* 1999, Kamat and Carpenter 1997), which then hydrolyses phosphatidyl inositol 4,5-bisphosphate (PIP_2) localized in the inner plasma membrane bilayer. The 2nd messengers, soluble inositol 1,3,5 – triphopshate (IP_3) and membrane bound diacyl glycerol (DAG) are generated. IP_3 mediates the release of Ca^{2+} from Ca^{2+} stores such as the endoplasmic reticulum. This increased Ca^{2+} can lead to the activation of serine/ threonine PKC. The other 2nd messenger, DAG, also acts as a cofactor in the activation of PKC. The rise in Ca^{2+} levels changes the conformation of PKC so that it translocates to the cytoplasmic side of the plasma membrane (Jorissen, *et al* 2003) (Fig 1.4).

Currently there are 12 known PKC isoforms which can be classified into 3 main groups. At the plasma membrane conventional or classical PKCs (α, βI, βII, γ) are activated by Ca^{2+}, DAG and the membrane phospholipid phosphatidyl serine (PS). Novel PKCs (δ, θ, η, ε, μ) are also activated by PS and DAG but do not require Ca^{2+}. The third class of PKCs, atypical PKCs (λ, ζ, ι), only require PS and phosphatidylinositides for activation (Newton 2001).

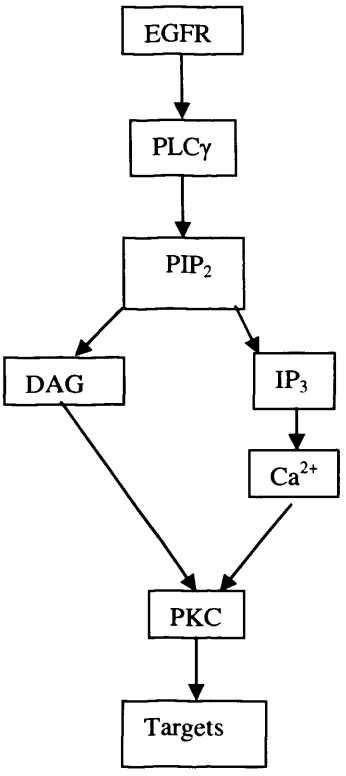

Figure 1.4 PKC pathway. EGFR = epidermal growth factor receptor, PLCγ = phospholipase-C-γ, PIP_2 = phosphatidylinositol 4,5-bisphosphate, DAG = diacyl glycerol, IP_3 = inositol 1,3,5 – triphopshate, PKC = protein kinase C.

Activation of PKC can initiate transcription of many gene regulatory proteins important in many cell processes. Cell processes that can be modulated by PKC signalling include permeability (Lynch, *et al* 1990), contraction (Webb 2003), migration (Wang, *et al* 2002), hypertrophy (Takeishi, *et al* 2000), proliferation (Leszczynski, *et al* 1996), and apoptosis (Niwa, *et al* 2002). PKC is also known to be involved in many vascular functions including the regulation of vascular cell growth and differentiation, vascular permeability, vasodilator mediator release and endothelial activation (Sheetz and King 2002). PKC is also involved in smooth

muscle contraction as receptors for contraction of smooth muscle e.g. phenylephrine through α adrenergic receptors or AngII through the angiotensin receptor, are believed to activate PLC and subsequently PKCs (Dixon, *et al* 1994, Husain, *et al* 2004). PKC can then phosphorylate downstream proteins that cause smooth muscle contraction for example L-type Ca^{2+} channels or proteins involved in the regulation of actin-myosin cross-bridge cycling. Also IP_3 can cause contraction by release of Ca^{2+} from the sarcoplasmic reticulum (Webb 2003). Furthermore, phorbol esters such as 12-O-tetra-decanoyl-phorbol-13-acetate which are synthetic compounds known to activate PKC through mimicking the actions of DAG, can cause smooth muscle contraction (Webb 2003).

Hyperglycaemia associated with diabetes increases glycolytic pathway flux, and the production of intermediates such as glycerol-3 phosphate (G3P). Increased G3P levels leads to an increases in the *de novo* synthesis of DAG, which subsequently increases PKC activation, mainly the β isoform (Hink, *et al* 2003, Koya and King 1998, Sheetz and King 2002, Xia, *et al* 1994). Increased PKC activation can lead to a host of deleterious changes in the vasculature that may lead to the development of diabetic vascular pathologies. Such changes include increased permeability of blood vessels, increased expression of adhesion molecules (ICAM, VCAM and E-selectin), increased leucocyte adhesion, increased platelet activation, increased basement thickening through production of collagen IV and increased activation of ROS generating enzymes such as NADPH

which has adverse effects on the vasculature (Avogaro, *et al* 2006, Fumo, *et al* 1994, Hink, *et al* 2003, Nonaka, *et al* 2000, Park, *et al* 2000, Sudic, *et al* 2006).

Importantly, increased PKC leads to NO dysregulation, as PKC can increase levels of uncoupled eNOS, that produce $O_2^{\cdot-}$ which reacts with and inactivates NO. Furthermore PKC can inhibit the activity of NO's downstream target sGC (Hink, *et al* 2003). As mentioned earlier PKC also phosphorylates eNOS at Thr495 which inhibits its enzymatic activity, thus reduces NO synthesis (Fleming, *et al* 2001, Mount, *et al* 2006). Also PKC's role in mediating smooth muscle contraction may result in enhancing the action of some vasoconstrictors such as AngII. PKC further tips the balance towards vasoconstriction by increasing production and release of ET-1 (Chen, *et al* 2000, Koya and King 1998, Sheetz and King 2002).

1.4 The ErbB Family of RTKs

As previously mentioned the signal transduction pathways mentioned above can be activated by a family of RTKs known as the type 1 ErbB family. EGFR is a 170 kDa, enzymatic cell surface receptor and was the first member of the ErbB family of RTKs to be discovered (Carpenter, *et al* 1978). The ErbB family includes three other members, ErbB2 (Neu/HER2), ErbB3 (HER3) and ErbB4 (HER4). The receptors share a similar structure made up of three domains: a ligand-binding glycosylated ectodomain, a predominantly hydrophobic amino acid transmembrane domain and an internal cytoplasmic domain which holds the

enzymatic tyrosine kinase activity (Garrett, *et al* 2003, Prenzel, *et al* 2001, Tommasi, *et al* 2004) (Fig. 1.5b). The ErbB family of receptors lie at the start of a complex network of signal transduction cascades. Signalling from ErbB receptors plays a part in the regulation of many cellular processes including mitogenesis, apoptosis, growth, angiogenesis, migration, proliferation and differentiation (Dreux, *et al* 2006).

1.4.1 The Biology of the ErbB Family of Receptor Tyrosine Kinases

The transduction of stimulus from the outside of the cell via the transmembrane ErbB receptors, through downstream transduction cascades and to the nucleus involves many steps. Firstly the ErbB receptor's intrinsic tyrosine kinase activity is stimulated in a mechanism involving ligand binding and receptor dimerization. Once activated, the receptor pair can *trans*-phosphorylate tyrosine residues within each other's cytoplasmic domain. Phosphorylated receptors can subsequently recruit target proteins, which then go on to initiate complex signalling cascades. The signal perpetuates downstream until it reaches and activates its targets, usually transcription factors that can promote the transcription of genes and produce the appropriate cellular output. To add to the complexity, ErbBs can also be activated in a ligand independent mechanism. The steps mentioned above are further discussed in the sections that follow.

1.4.2 Ligand Binding, Receptor Dimerization and Tyrosine Kinase Activation

Tyrosine kinase activity of an ErbB receptor can be initiated upon binding of a growth factor ligand to the receptor's ectodomain. Ligands include epidermal growth factor (EGF), heparin-binding epidermal growth factor (HB-EGF), transforming growth factor-α (TGF-α), amphiregulin (AR), neuregulin (NRG), betacellulin (BTC), epiregulin (EPR) and epigen (Yarden 2001). All of these ligands posses an EGF-like motif which contains six cysteine residues that interact to form three loops. Each ligand favours binding to a particular receptor or receptors (Table 1.1). The cysteine loops found in the EGF-like motif are essential to confer specificity for binding of ligand to the ectodomain of particular receptors (Casalini, *et al* 2004, Harris, *et al* 2003). Ligands originally exist in proform as transmembrane proteins which are cleaved from the cell membrane through regulated proteolysis by a disintegrin and metalloproteinases (ADAMs). The resulting 49-85 amino acid, soluble growth factor ligand can signal in an autocrine, paracrine or endocrine manner. However it is believed that certain ligands, including TGFα, amphiregulin and HB-EGF, can also signal in a juxtracrine manner i.e. from the signalling cell to the neighbouring target cell when still tethered to the membrane (Singh and Harris 2005).

Table 1.1 Binding specificities of ErbB family ligands to ErbB family members

Ligand	**Receptor**
EGF, AR, TGFα, epigen	EGFR
BTC, HB-EGF, EPR	EGFR, ErbB4
NRG-1, NRG-2	ErbB3, ErbB4
NRG-3, NRG-4	ErbB4

Each receptor has a protruding dimerization arm, this is essential for interacting with an adjacent receptor (Ogiso, *et al* 2002). The conformational arrangement of ErbB receptors is such that without external stimulation the receptor is in a "closed conformation", the dimerization arm is buried and unable to interact with other receptors. In this autoinhibited state receptors are unlikely to form stable dimers and are unable to phosphorylate tyrosine residues. Ligand binding induces substantial rearrangements of the receptor's allosteric conformation resulting in the receptor adopting an "open conformation" which releases the receptor from its autoinhibited state and frees the dimerization arm to interact with its dimerzation partner (Ferguson, *et al* 2003, Roskoski 2004). It was initially thought that ligand binding was necessary to facilitate receptor dimerization, however recent reports suggest that ErbB receptors can exist as dimers independently of ligands, however the binding of ligands facilitates dimer stability, receptor interaction and the activation of tyrosine kinase activity (Schlessinger 2000, Yu, *et al* 2002).

Dimerization occurs between two receptors, either two of a kind e.g. EGFR and EGFR, known as homodimerization, or two different members of the ErbB family e.g. ErbB2 and EGFR, known as heterodimerization. Theoretically all four EGFR family members can pair up with any other ErbB receptor in ten combinations to form four distinct homodimers and six distinct heterodimers (Tzahar, *et al* 1996). Following ligand binding and receptor dimerization the receptor tyrosine kinase activity is enhanced and it can catalyse ATP dependent self-phosphorylation as the

γ phosphate of ATP is transferred to the C-terminal domain of five tyrosine residues on the receptor (Fig. 1.5a). The tyrosine kinase domain on one of the receptors in the dimer can cross-phosphorylate its partner to complete the activation, this is known as *trans*-phosphorylation (Roskoski 2004, Sako, *et al* 2000).

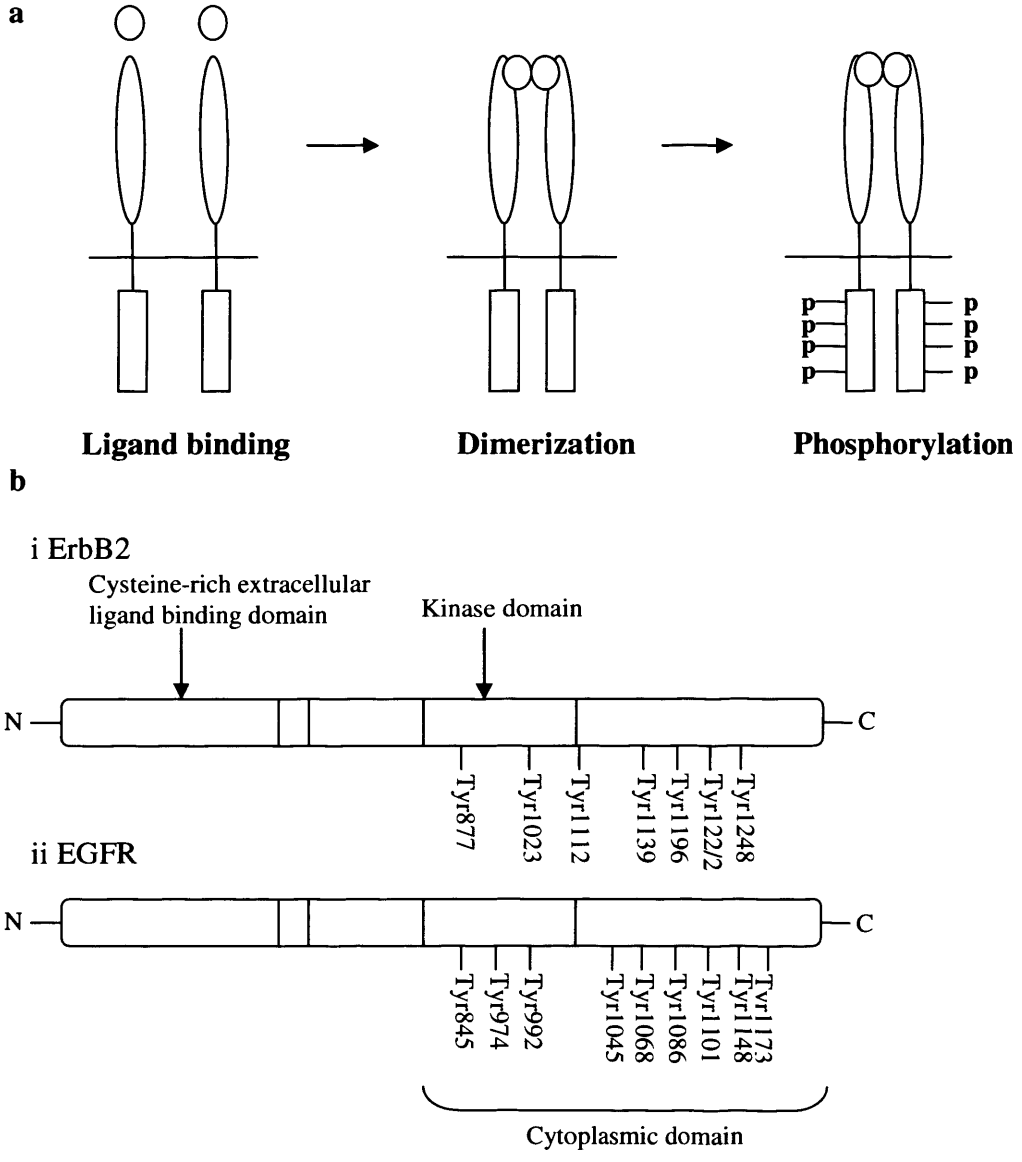

Figure 1.5 a) activation of ErbB receptor dimer b) domain structure and tyrosine residue phosphorylation sites of i) ErbB2 and ii) EGFR

Autophosphorylation of tyrosine residues increases receptor activity, however, phosphorylation of threonine residues deactivates the molecule. For example EGFR can be activated by phosphorylation of tyrosine residues 992, 1068, 1086, 1148 and 1173 (Fig 1.5b), however it can be deactivated by phosphorylation at Thr669 or Thr654 catalysed by PKC (Rijken, *et al* 1998, Roskoski 2004). Once phosphorylated the residues act as docking sites for proteins that transduce the signal downstream and initiate signalling cascades.

1.4.3 The Advantage of Heterodimerization for Diversity

As mentioned earlier each ligand has a certain affinitiy for each ErbB receptor, thus heterodimerization adds to the diversity of recognized ligands. The affinity of the ligand for the receptor conditions the strength and duration of the signal. To date, there is no known ligand that specifically binds and activates the 185 kDa receptor ErbB2. X-ray crystallographic studies have revealed that ErbB2 is in an autoactivated state, with a constitutively free dimerization arm poised to interact with other ErbB receptors, similar to ligand bound members of the ErbB family. Thus, ErbB2 is constitutively primed to dimerise without the need for growth factors. Studies have also revealed that the conformation of its ligand pockets makes it inaccessible to ligands (Garrett, *et al* 2003). Hence, ErbB2 homodimers cannot bind ligands, however, ErbB2 heterodimers formed with other family members can bind ligands and is indeed necessary for ErbB2 activation. (Citri, *et al* 2003, Garrett, *et al* 2003). Upon heterodimerization the other ErbB receptor

transphosphorylates the ErbB2. Then by an intermolecular mechanism ErbB2 undergoes autophosphorylation on five tyrosine residues 882, 1028, 1143, 1226/7 and 1253, leading to allosteric activation of its tyrosine kinase domian (Zhang, *et al* 1998) (Fig. 1.5b).

Heterodimerization further plays a part in diversity, since different receptor dimers have a unique set of phosphorylated C-terminal proteins that can be recognised by, and that can activate a unique set of second messengers. As such, distinct ErbB receptor dimers initiate distinct signaling pathways, leading to specific cellular responses (Graus-Porta, *et al* 1997). Also, the strength of the signal varies depending on the individual receptors in each pair. ErbB2 decreases ligand dissociation from the dimer, and dimer downregulation, thus signaling from an EGFR-ErbB2 heterodimer is more potent than signaling from an EGFR homodimer (Graus-Porta, *et al* 1997, Worthylake, *et al* 1999). ErbB2 is the preferential heterodimerization partner for all receptors regardless of which ligand is bound (Graus-Porta, *et al* 1997). Receptor dimers that contain ErbB2 are predominant, meaning a more potent signal resulting in increased activation of the cytoplasmic effectors and thus, increased number of signaling pathways activated (Tzahar, *et al* 1996).

1.4.4 EGFR Transactivation

Additional to direct modulation by soluble ligands, EGFR activity can be modulated by G protein-coupled receptors (GPCRs) through cross talk. EGFR can

mediate GPCR mitogenic signalling through a mechanism known as transactivation. Stimulation of GPCR with agonists such as AngII, ET-1, lysophosphatic acid and thrombin, causes a release of signalling molecules such as PKC, or a release of ROS which can activate metalloproteinases such as ADAMs. In turn ADAMs cleave membrane bound EGFR ligands such as pro HB-EGF which bind and activate EGFR, and initiate downstream signalling pathways (Daub, *et al* 1996, Eguchi, *et al* 2003, Hackel, *et al* 1999).

1.4.5 Alternative Mechanisms of EGFR Activation

The kinase activity of ErbB receptors can also be activated independently of ligand binding. For example the EGFR receptor can be activated by being phosphorylated by other kinases such as src (Tice, *et al* 1999) or janus tyrosine kinase 2 (Yamauchi, *et al* 1997).

Exogenous, non-physiologic agents such as gamma and UV irradiation are also known to mediate EGFR activation and have been shown *in vitro* (Warmuth, *et al* 1994) and *in vivo* (Fisher, *et al* 1998) to activate EGFR. One study indicated that UV irradiation activates EGFR in cultured human skin keratinocytes in a manner similar to activation induced by EGF or interleukin-1β ligand binding (Wan, *et al* 2001). Other activators of EGFR include heavy metal ions, substances that affect the osmotic state of the cell, oxidant and alkylating agents, H_2O_2 and iodoacetic acid. It is thought that the common mode of action of these agents is through

preventing EGFR dephosphorylation (Hackel, *et al* 1999, Knebel, *et al* 1996). Also Ca^{2+} influx can induce tyrosine phosphorylation and activation of EGFR (Rosen and Greenberg 1996).

1.4.6 Molecular Targets of Activated EGFR, and Intracellular Signalling

The phosphorylated ErbB receptor kinase domain can act as docking sites recognized by adaptor molecules such as growth factor receptor-bound protein 2 and Dok-R (Jorissen, *et al* 2003). These molecules interact with the receptor through their src-homology 2 (SH2) or phosphotyrosine-binding domains that bind to phosphotyrosine on the active receptor. Adaptor molecules with one or more src-homology 3 and SH2 domains can transduce the signal by phosphorylating other adaptor or effector molecules (Sudol 1998). This leads to the stimulation of a number of different signalling pathways such as the MAPK, PKC and Akt pathways, which leads to the activation of many transcription regulators (Jorissen, *et al* 2003). Molecules other than adaptor proteins, some with enzymatic activity (signal transducer proteins) can associate directly with EGFR e.g. PLC- γ, phosphatases such as protein tyrosine phosphatase-1B and SHP1, and tyrosine kinases such as Src and Abl can affect downstream molecules with no need for adapter proteins (Bogdan and Klambt 2001, Hackel, *et al* 1999, Jorissen, *et al* 2003). Other molecules such as the zinc-binding protein, ZPR-1, can associate with inactive, unphosphorylated EGFR but are released and activated upon EGFR activation (Galcheva-Gargova, *et al* 1996).

1.4.7 EGFR Signalling and its Role in Diabetes-induced Vascular Dysfunction

Studies have shown that signalling from EGFR is influenced by high glucose and diabetes, in organs and tissues of both genetically diabetic and chemically induced diabetic animals. Studies have revealed a decreased EGFR expression in the liver of both alloxan and STZ-induced diabetic rats (Lev-Ran, *et al* 1986). Another study showed depressed EGFR messenger ribonucleic acid (mRNA) expression in the liver of genetically diabetic, and STZ-induced diabetic mice (Kasayama, *et al* 1989). Tyrosine phosphorylation of EGFR was shown to be downregulated by high glucose in rat 1 fibroblasts (Obata, *et al* 1998). In contrast another study showed that the levels of EGFR and EGF mRNAs were higher in the kidney of STZ-induced diabetic rats (Sayed-Ahmed, *et al* 1996). A group working on kidney cells also showed increased local levels of EGF, and suggested that this might contribute to diabetic renal hypertrophy. However they did not observe a change in EGFR numbers (Yang, *et al* 1997). A marked increase in EGFR expression was shown in the gastric mucosa of STZ-induced diabetic rats. It is thought that EGFR activation, through TGF-α, initiated by diabetes is involved in inducing spontaneous gastric mucosal injury (Khan, *et al* 1999). Studies also suggest that there is dysregulation of endocytosis and recycling of the EGFR/ligand complex in diabetic tissues such as hepatocytes. This leads to a decrease in down regulation of EGFR and enhanced endocytosis leading to increased EGFR recycling and signalling (Dahmane, *et al* 1996).

EGFR and its downstream molecules are known to influence VSMC contraction (Berk, *et al* 1985, Florian and Watts 1999). EGFR and ErbB2 can alter Ca^{2+} homeostasis, which may lead to increased VSMC contraction (Dittmar, *et al* 2002, Feldner and Brandt 2002, Peppelenbosch, *et al* 1991). Also, vasoconstrictors such as AngII and ET-1 are known to transactivate EGFR, which initiates ERK1/2 signalling pathway and VSMC contraction (Kagiyama, *et al* 2002, Kawanabe and Nauli 2005). Also, as mentioned earlier some of EGFR's downstream signalling proteins are known to affect the synthesis of the potent endothelium-derived vasodilator NO, through modulating eNOS activity. Furthermore, a study showed that inhibiting RTKs, including EGFR and ErbB2, normalized diabetes-induced abnormal vascular reactivity in rat carotid artery (Yousif, *et al* 2005). The underlying mechanism that bridges hyperglycaemia and endothelial dysfunction remains unclear. It is plausible that EGFR and its signalling cascades may be key components in the mechanism leading to endothelial dysfunction induced by hyperglycaemia, possibly by modulating NO homeostasis.

1.5 Objectives of the Thesis

Studies have shown that diabetes leads to vascular complications such as an altered response to vasoconstrictors and vasodilators (Abebe, *et al* 1990, Kamata, *et al* 1989, Makino, *et al* 2000, Mayhan, *et al* 1999, Oyama, *et al* 1986). NO is a powerful endothelium derived vasodilator, and its bioavailability and activity is known to be reduced in diabetes. This lack of NO production from diabetic

endothelium is believed to contribute to diabetes induced vascular dysfunction (Avogaro, *et al* 2003b, Fard, *et al* 2000, Williams, *et al* 1996). The precise molecular mechanisms leading to diabetes induced impairment in vascular reactivity are not yet fully understood. However, there is evidence to implicate the involvement of RTKs, specifically EGFR and ErbB2 in the development of diabetes induced vascular pathologies. Studies have shown EGFR to be abnormally expressed or activated in tissues from diabetic animals (Kasayama, *et al* 1989, Kashimata, *et al* 1987, Khan, *et al* 1999, Lev-Ran, *et al* 1986, Okamoto, *et al* 1988, Sayed-Ahmed, *et al* 1996). Also, a study using the RTK inhibitor genistein and the EGFR and ErbB2 inhibitors AG1478 and AG825, have implicated RTKs including EGFR and ErbB2 in the development of vascular dysfunction in rat carotid artery (Yousif, *et al* 2005).

The aim of the present thesis was to investigate the roles of the RTKs, EGFR and ErbB2, in diabetes induced vascular dysfunction. Specifically to investigate the hypothesis that EGFR and ErbB2 activities, through downstream signalling, alter NO synthesis or activity in the diabetic endothelium, and that this alteration contributes to diabetes induced vascular dysfunction. Studies used to investigate this hypothesis include:

1. Perfusion studies to examine the response to vasodilators and vasoconstrictors, of vascular tissue from diabetic rats and from diabetic rats treated with EGFR and RTK inhibitors.

2. Establishing a suitable cell model system for studying the effects of hyperglycaemia on EGFR and ErbB2 signalling.

3. Western blotting and immunoprecipitation to examine the effect of diabetes and hyperglycaemia on EGFR and ErbB2 activity in diabetic rat tissue, and cells grown in high glucose.

4. Western blotting to investigate the effect of hyperglycaemia on downstream molecules Akt, p38MAPK, ERK1/2 and PKC in cells grown in high glucose.

5. Western blotting and pharmacological techniques to investigate the effect of hyperglycaemia on NO, and to examine the role of EGFR activity in the regulation of NO production.

2.0 Materials and Methods

2.1 Materials

2.1.1 General Equipment

Eppendorf centrifuge 5417R was purchased from Eppendorf, Germany. Hearaeus multifuge 3 S-R with a BIOshield rotor was obtained from Kendro, UK. Sartorius CP124S and CP620I weighing scales were purchased from Sartorius AG, Germany. Fisherbrand hydrus 300 pH meter and FB300 powerpack was purchased from Fisher scientific, UK. Techne dri-block® heating block was purchased from Techne, UK. Millipore Elix water purification system and milli-Q synthesis system was from Millipore Corporation, MA. Nine hundred and fifty Watt microwave was from Currys, UK.

2.1.2 Disposables and Plastic Ware

Kwill filling tubes and BD plastipak syringes were obtained from Western Laboratory Service Ltd. Ministart® 0.2 μm filters were from Sartorius, Germany. Sterile disposable stripettes (5 ml, 10 ml and 25 ml), 50 ml falcon tubes, T-25, T-75 and T-150 flasks, 24 well plates and 96 well plates were purchased from Corning Inc, USA. Eppendorf tubes were purchased from Elkay, Ireland. Universals and cell scrapers were purchased from Fisher scientific, UK. Sterile needles (BD microlance™) were purchased from Becton Dickinson Ltd, UK. Gilson pipetman pipettes were purchased from Anachem Ltd, UK. Powerpette plus pipette controller and sealpette multi-channel pipettor were purchased from Jencons Ltd, UK. Disposable pipette tips and polymerase chain reaction (PCR) tubes were purchased from Elkay, Ireland.

2.1.3 General Chemicals and Drugs

Methanol, ethanol, electrode storage solution, buffer solution pH 10, buffer solution pH 7, buffer solution pH 4, hydrochloric acid (5 M), molecular biology grade chloroform and laboratory reagent grade propan-2-ol (isopropanol) were all purchased from Fisher scientific, UK. NaCl was obtained from USB Corporation, USA. Dimethyl sulfoxide (DMSO) was from Sigma Aldrich, UK. Tris (tris(hydroxymethyl)aminomethane) was purchased from Amersham Biosciences. Liquid nitrogen and 95 % O_2: 5 % CO_2 were supplied by BOC.

2.1.4 Vascular Pharmacology

Streptozotocin (STZ), (±) noradrenaline-bitartrate (NA), endothelin-1 (ET-1), carbachol, sodium nitroprusside (SNP), (-) phenylephrine hydrochloride (PE) and acetyl methylcholine (Mch) were purchased from Sigma-Aldrich Co Ltd., UK. Citric acid, $MgSO_4$, KCl, $CaCl_2.6H_20$, KH_2PO_4 and $NaHCO_3$ were all from Fisher, UK. Diadzein was purchased from Tocris-Cookson Ltd, UK. Female Wistar rats (200-500g) were bred in house and male Sprague Dawley rats (250-300g) were purchased from Harlan UK Ltd, UK.

2.1.5 Cell Culture

ECV-304 (human urinary bladder carcinoma) cells were purchased from European Collection of Cell Cultures, UK. Medium 199 (M199), and trypan blue solution (0.4 % w/v), L-glucose and epidermal growth factor (EGF) were purchased from

Sigma-Aldrich Co Ltd., UK. FBS (Foetal Bovine Serum), trypsin/ethylenediamine tetraacetate (EDTA), L-glutamine 200 mM (100 x), sterile phosphate buffered saline (PBS), penicillin-streptomycin and cell culture freezing medium-DMSO were purchased from Invitrogen Life Technologies Corporation, UK. AG1478 and AG825 were purchased from Tocris, UK. Bisindoylmaleimidine (Ro-31-8220) was purchased from Sigma-Aldrich, UK. GO6983 and TPA (12-O-tetra-decanoyl-phorbol-13-acetate) were purchased from Calbiochem, UK. D-glucose was purchased from Fisher, UK.

2.1.6 Cell Lysis and Western Blotting

Ethylene glycol tetracetic acid, Triton-X 100, sodium orthovanadate, sodium fluoride, phenyl-methyl-sulfonyl-fluoride, sodium molybdate, leupeptin, aprotinin and bovine serum albumin (BSA) were purchased from Sigma-Aldrich Co Ltd, UK. Acrylamide/bis-acrylamide 30 % v/v solution, glycerol and bromophenol blue, Tween® 20 (Polyethylenesorbitan monolaurate), ponceau S stain, and sodium azide were purchased from Sigma-Aldrich Co Ltd, UK. Ammonium persulphate (APS) and TEMED (N,N,N,N′-tetramethylethylenediamine) were purchased from Usb Co, USA. Bio-Rad protein assay kit, upper buffer pH 6.8 and lower buffer pH 8.8 were purchased from BioRad laboratories Ltd, UK. Sodium dodecyl sulphate (SDS) was purchased from Fisher scientific Ltd, UK. DDT (DL-Dithiothreitol) was purchased from Promega Corporation, USA. Protan®Nitrocellulose transfer membrane (0.2 μM) was purchased from Schleicher and Schuell bioscience GmbH

Whatman group, Germany. Filter paper grade 3 was purchased from Whatman, UK. Western blocking reagent was purchased from Roche Diagnostics Ltd, Germany. Marvel® dried skimmed milk was purchased from Premier international foods, UK. Full range and low range rainbow™ molecular weight markers were purchased from Amesham biosciences Ltd, UK. Chemiluminescent supersignal® west dura and femto substrates were purchased from Pierce, USA. X-0-fix-fixer and X-0-dev-develpoer were purchased from X-0-graph Imaging System, UK. The primary antibodies used, their source, the molecular weight of the protein they detect, the company they were purchased from and their catalogue number can be seen in table 2.1. The secondary antibodies used were anti-rabbit IgG, horse radish peroxidase linked whole antibody (from donkey) and anti mouse Ig, horseradish peroxidase linked whole antibody (from sheep) and were purchased from Amersham biosciences Ltd, UK. Protein A-agarose immunoprecipitation reagent (beads) SC-2001 was purchased from Santa Cruz Biotechnology, USA.

Table 2.1 A list of primary antibodies with their source, the molecular weight of the protein they detect, the company they were purchased from and their catalogue number. Epidermal growth factor receptor (EGFR), extracellular signal-regulated kinase 1/2 (ERK1/2), p38 mitogen activated protein kinase (p38MAPK), protein kinase C (PKC) and endothelial nitric oxide syhthase (eNOS).

Antibody	Source	Molecular weight (kDa)	Company and catalogue number
EGFR	Rabbit	175	Cell Signalling Technology, UK (2232)
Phospho EGFR(Tyr1068)	Rabbit	175	Cell Signalling Technology, UK (2234)
ErbB2	Rabbit	185	Santa Cruz Biotechnology, USA (Sc-284)
Phospho ErbB2 (Tyr1248)	Rabbit	185	Upstate Biotechnology, UK (06-229)
Akt	Rabbit	60	Cell Signalling Technology, UK (9272)
Phospho Akt (Ser473)	Mouse	60	Cell Signalling Technology, UK (4051)
ERK1/2	Rabbit	42,44	Cell Signalling Technology, UK (9102)
Phospho ERK1/2 (Thr202, Tyr204)	Rabbit	42,44	Cell Signalling Technology, UK (4377)
p38MAPK	Rabbit	43	Cell Signalling Technology, UK (9212)
Phospho p38MAPK(Thr189/ Tyr182)	Rabbit	43	Cell Signalling Technology, UK (9211)
Phospho PKC (Pan) (betaII Ser660)	Rabbit	78,80,82,85	Cell Signalling Technology, UK (9371)
eNOS	Rabbit	140	Cell Signalling Technology, UK (9572)
Phospho eNOS (Thr495)	Rabbit	140	Cell Signalling Technology, UK (9574)
Phospho eNOS (Ser1177)	Rabbit	140	Cell Signalling Technology, UK (9571)
β-actin	Mouse	42	Sigma-Aldrich, UK (A1978)

2.1.7 Reverse Transcriptase-polymerase Chain Reaction (RT-PCR)

Tri-reagent, 1M magnesium chloride, 2 % gelatine and ethidium bromide were purchased from Sigma-Aldrich Co Ltd., UK. Molecular grade pure water was purchased from Invitrogen Life Technologies Corporation, UK. Moloney murine leukaemia virus reverse transcriptase (MMLV-RT) and DTT were purchased from Invitrogen. Agarose, *BioTaq*™ diribonucleic acid (DNA) polymerase, hyperladder I and hyperladder IV were purchased from Bioline, UK. RNase inhibitor was purchased from Promega, UK. Deoxyribonucleotide triphosphates (dNTPs) and random hexamers were purchased from Amersham, UK. PCR primers were purchased from MWG biotechnology (Table 2.2). Primers were designed using the OLIGO primer design software from Med probe AS, Norway. The specificity of primers was tested using the basic local alignment search tool program from the European Molecular Biology Laboratory – Genebank database software.

Table 2.2 Forward and reverse sequences of PCR primers

	Forward sequence	Reverse sequence
ErbB2	5` CCTCTGACGTCCATCATCTC 3`	5`ATCTTCTGCTGCCGTCGCTT 3`
EGFR	5' CAACATCTCCGAAAGCCA 3'	5' CGGAACTTTGGGCGACTAT 3'
TGFα	5' CCACACTCAGTTCTGCTTCC 3'	5' TCTTTATTGATCTGCCACAGTC 3'
Epiregulin	5' TCCATCTTCTACAGGCAGTCC 3'	5' AGAATCACGGTCAAAGCCAC 3'
Amphiregulin	5' TCCTCGGGAGCCGACTATGAC 3'	5' GGACTTTTCCCCACACCG 3'
HB-EGF	5' CGGACCCTCCCACTGTATC 3'	5' TGACAGCACCACAGCCAC 3'
Betacellulin	5' ACTGCATCAAAGGGAGATGC 3'	5' CCTGAGACACATTCTGTCCA 3'
EGF	5' GAGTCTGACTCAGTCCAGAA 3'	5' TCTACTTGGAGCAACAGTGG 3'
Connexin 43	5' TTCATGCTGGTGGTGTCCTTGGTG 3'	5' GCTCACTTGCTTGCTTGTTGTAATTGC 3'
β-actin	5' GGAGCAATGATGTTGATCTT 3'	5' CCTTCCTGGGCATGGAGTCCT 3'

2.2 Methods

2.2.1 Isolated Mesenteric Bed Studies

Methods in section 2.2.1 were carried out by Dr Mariam Yousif and Prof Ibrahim Benter of the Department of Pharmacology and Toxicology, Faculty of Medicine, Kuwait University (Benter, *et al* 2005a).

The following experiments conform to the guidelines for the care and the use of laboratory animals published by the US National Institute of Health (publication Number 85-23, revised 1985).

2.2.1.1 Induction of Diabetes and Treatment with Genistein, Diadzein and AG1478

Diabetes was induced in rats using STZ (Fig. 2.1e). The basal glucose levels of female Wistar rats (200-250g) were determined using an automated blood glucose analyser (Glucometer Elite XL). Then diabetes was induced by a single intraperitoneal injection of STZ (55 mg/kg body weight) dissolved in citrate buffer (pH 4.5). Age-matched control rats were injected with citrate buffer vehicle only. Blood glucose was determined again 48 hours after STZ injection. Rats with a blood glucose concentration above 300 mg/dl were declared diabetic.

Eight groups of rats were used in this study. These groups are shown in table 2.3. Rats were treated with 1.5 mg/kg body weight (intraperitoneal on alternate days, n = 8) of genistein (receptor tyrosine kinase inhibitor) (Fig. 2.1a),

AG1478 (EGFR inhibitor) (Fig 2.1c), diadzein (inactive analogue of genistein) or vehicle only (Fig. 2.1b), with groups 5, 6, 7 and 8 treated on the same day as the induction of diabetes and every other day for 4 weeks. The concentrations of AG1478 and genistein used to treat the rats were based on preliminary experiments in which the effects of these drugs were tested at different concentrations (Personal communication with Dr Mariam Yousif). Genistein, diadzein and AG1478 were not present ex-vivo in the perfusion studies.

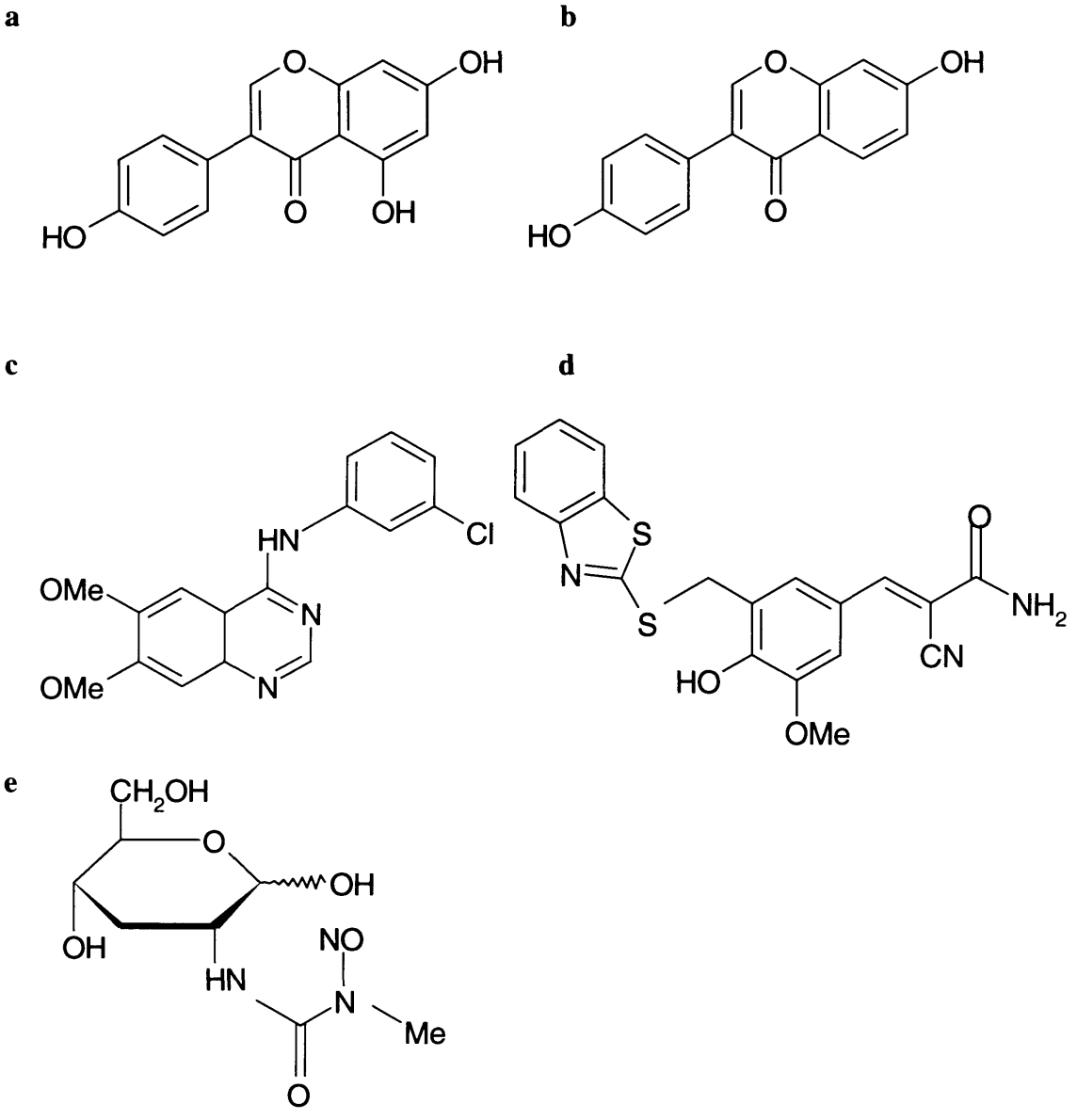

Figure 2.1 Chemical structures of a) genistein, b) diadzein, c) AG1478, d) AG825 and e) STZ

Table 2.3 The eight groups of rats used in the perfusion studies

Group	Rat
1	**Control (non-diabetic)-vehicle treated**
2	**Control-genistein treated**
3	**Control-AG1478 treated**
4	**Control-diadzein treated**
5	**Diabetic-vehicle treated**
6	**Diabetic-genistein treated**
7	**Diabetic-AG1478 treated**
8	**Diabetic-diadzein treated**

2.2.1.2 Isolation of the Mesenteric Vascular Bed

The mesenteric bed was carefully removed and placed in a dish of oxygenated Krebs solution (118 mM NaCl, 4.6 mM KCl, 2.5 mM $CaCl_2$, 1.2 mM $MgSO_4$, 25 mM $NaHCO_3$, 1.2 mM KH_2PO_4 and 11.2 mM glucose) and then it was cannulated via the mesenteric artery using a polyethylene cannula. The cannulated mesenteric bed was placed in a warm water jacketed chamber at 37°C and perfused with Kreb's solution at a constant flow rate of 6 ml/min using a multichannel masterflex® peristaltic pump (Cole-Palmer Instrument Co LTD, UK) The Krebs solution was oxygenated with 95 % O_2 and 5 % CO_2.

2.2.1.3 Measurement of Perfusion Pressure

Perfusion pressure was recorded using a pressure transducer connected to a Lectromed chart recorder. Preparations were always allowed to equilibrate for at least 30 minutes. Tissue responsiveness was tested at the beginning of each experiment using a bolus injection of NA (10^{-7} mol).

2.2.1.4 Vasoconstriction Studies

After the period of equilibration, successive doses of NA (10^{-8}, 10^{-7} and 10^{-6} mol) or ET-1 (10^{-11}, 10^{-10} and 10^{-9} mol) were added to the perfusate at regular intervals and the vasoconstrictor response of the perfused mesenteric bed was recorded in mmHg.

2.2.1.5 Vasodilation Studies

After the period of equilibration, the perfused mesenteric bed was preconstricted by a constant infusion of NA (10^{-5} M). After establishing a steady level of preconstriction, successive doses of carbachol (10^{-9} and 10^{-8} mol) or SNP (10^{-10}, 10^{-9} and 10^{-8} mol) were added to the perfusate at regular intervals. The vasodilator response was recorded and was expressed as % of the preconstriction induced by NA (10^{-5} M).

It should be noted that each vasoconstrictor and vasodilator was tested using the same vascular bed. The order of testing was NA, carbachol, SNP then ET-1. The order used was based on the time needed to establish dose response curves for each vasoconstrictor and vasodilator. The response to ET-1 develops slowly and may be difficult to wash out, thus, it was always tested last (personal communication with Dr Mariam Yousif).

2.2.1.6 Statistics and Data Analysis for Isolated Mesenteric Bed Studies

Results were analyzed using Graph Pad Prism 4 software. Where indicated in the text the number of experiments (*n*) is the number of rats used and the standard error of mean (± SEM) is represented with vertical bars on graphs.

Values were compared using analysis of variance (ANOVA) followed by *post hoc* Bonferroni tests. A value of $p < 0.05$ was considered to be significant.

2.2.2 Aortic Rings

2.2.2.1 Preparation of Isolated Tissue

Animals were maintained in accordance with the Animals (Scientific Procedures) Act 1986. Male Sprague Dawley rats (250-300g) were sacrificed by a blow to the back of the head followed by fracturing of the neck. The rib cage, heart and lungs were removed exposing the thoracic aorta. After removing the connective tissue, the whole aorta was removed and dispensed into a dish of Krebs solution (118.4 mM NaCl, 4.7 mM KCl, 25.0 mM $NaHCO_3$, 1.2 mM $MgSO_4 \cdot 2H_2O$, 1.2 mM $KH_2PO_4 \cdot 2H_2O$, 11.7 mM glucose and 2.5 mM $CaCl_2 \cdot 2H_2O$ dissolved in double distilled water). The aorta was cut into 3 mm rings and suspended between two stainless steel hooks. Then the preparations were placed in 20 ml tissue baths containing Krebs solution oxygenated with 95 % O_2 and 5 % CO_2 and maintained at 37°C. As a control, previous studies had shown that aortic rings behave similarly when treated the same (Personal communication with Prof Kenneth Broadley).

2.2.2.2 Measurement of Contractile Tension

The upper hook was connected to a Dynamometer UF1 isometric transducer (± 55 g sensitivity range) (Pioden Controls, UK). The signal was amplified using a bridge amplifier (PowerLab, ADInstruments, UK) and was converted from analogue to digital data and passed to a computer with Powerlab 200 hardware and Chart v.5.5 (sampling frequency 4 Hz) software both from PowerLab, ADInstruments, UK. An initial tension of approximately 0.5 g was applied to all tissues. The preparations were washed and then allowed to equilibrate for a minimum of 60 minutes before the addition of any drugs.

2.2.2.3 Denuding Endothelium

Where stated in the text, a proportion of aortic rings were denuded of endothelium. For this, before mounting the aorta in the tissue bath, the aorta was gently rotated on a needle. Removal of endothelium was confirmed by loss of endothelium-dependent responses to Mch in preconstricted tissue. For any given experiment preparations were either all with- or all without-endothelium.

2.2.2.4 Effects of EGF on Resting Unconstricted Aorta

Preparations were taken from the animal and placed in organ baths. After the period of equilibration tissue either with- or without- endothelium was exposed to a singe concentration of EGF (100 ng/ml) or vehicle alone for 10 minutes and the tension was recorded.

2.2.2.5 Cumulative Concentration-response Curve to Mch

In order to determine a submaximal concentration suitable for relaxing the aorta, a cumulative concentration-response curve to Mch was constructed. Firstly the aortic rings were preconstricted using 5 x 10^{-9} M U46619 (thromboxane A2 mimetic). When the tension had reached a plateau a cumulative concentration-response curve was constructed using Mch starting at a concentration of 10^{-9} M and increasing at half log intervals up to a maximum of $10^{-3.5}$ M. From the concentration response curve the EC50 (concentration (M) required to induce 50% of the response to Mch) was calculated.

2.2.2.6 Effect of EGF on Mch-induced Relaxation

The effects of a single concentration or cumulative concentrations of EGF were examined on rat aorta preconstricted and submaximally relaxed with Mch. Two preparations were taken from the animal and placed in organ baths. Both aortic rings were preconstricted with 5 x 10^{-9} M U46619 and then relaxed with Mch. To the first tissue bath a single concentration (100 ng/ml) of EGF or cumulative concentrations (1, 10 and 100 ng/ml) of EGF were added. To the other tissue bath vehicle alone (10 mM acetic acid + 0.1% BSA) was added.

2.2.2.7 Effect of EGF on U46619 Cumulative Concentration-response Curve

The effect of a single concentration of EGF (100 ng/ml) was examined on the EC50 and maximum response of a U46619 cumulative concentration-response curve. Two preparations were taken from the animal and placed in organ baths.

Both were exposed to cumulative concentrations of U46619 starting with a concentration of 10^{-13} M and increasing at log intervals up to a maximum of 10^{-10} M. The baths were then washed out 3 times with Krebs solution. After the tension had stabilized back to a base line, 100 ng/ml of EGF was added to the first organ bath. To the second organ bath vehicle alone (10 mM acetic acid + 0.1 % BSA) was added. After 10 minutes of exposure the cumulative concentration-response curve to U46619 was repeated.

2.2.2.8 Effect of EGF on PE Cumulative Concentration-response Curve

The effect of a single concentration of EGF (100 ng/ml) was examined on the concentration-response curve to an alternative vasoconstrictor, PE, on aorta with- or without endothelium. Three preparations were taken from each animal and placed in organ baths. All three were exposed to cumulative concentrations of PE starting with a concentration of 10^{-10} M and increasing at log intervals up to a maximum of 10^{-5} M. The baths were then washed out 3 times with Krebs solution. When the tension had stabilized back to a base line, 100 ng/ml of EGF was added to the first organ bath. To the second organ bath vehicle alone (10 mM acetic acid + 0.1 % BSA or PBS + 0.1 % BSA as stated in the text) was added. To the last bath Krebs solution was added as a naïve control. After 10 minutes of exposure the cumulative concentration-response curve to PE was repeated.

2.2.2.9 Effect of EGF on PE Preconstricted Aorta

The effect of a single concentration of EGF was examined on the EC50 and maximum response of a PE constricted aorta with endothelium. Two preparations were taken from the animal and placed in organ baths. Both were constricted with 10^{-7} M PE. After the contraction had reached a plateau, 100 ng/ml of EGF was added to the first organ bath. To the second organ bath vehicle alone (PBS + 0.1 % BSA) was added for 10 minutes.

2.2.2.10 Statistics and Data Analysis for Aortic Ring Studies

The data was analyzed using Graph Pad Prism 4 software. Where indicated in the text the number of experiments (*n*) is the number of rats used and the standard error of mean (± SEM) is represented with vertical bars on graphs.

EC50 with 95 % confidence intervals and maximum response values (± SEM) were derived from individual non-linear curve fitted concentration-response curves for PE. An example of non-linear curve fitting for an individual data set (from +EGF) is shown in figure 2.2. Values were calculated for the first PE-induced contractions in the absence of EGF (or vehicle) and for the second PE-induced contractions in the presence of EGF (or vehicle). EC50 and maximum response were also calculated for naïve control 1 and naïve control 2, which are the first and second PE-induced contractions without EGF or vehicle.

Also calculated was the % of maximum or EC50 of the second concentration response curve (in the presence of EGF or vehicle) to the maximum or EC50 of the first concentration response curve (in their absence).

For comparing two measurements from the same sample (before and after treatment), and two samples from the same animal (EGF treated and vehicle treated), mean values were compared using a 2 tailed, paired Student's t-test and a 2 tailed, unpaired Student's t-test respectively. A value of $p < 0.05$ was considered to be significant.

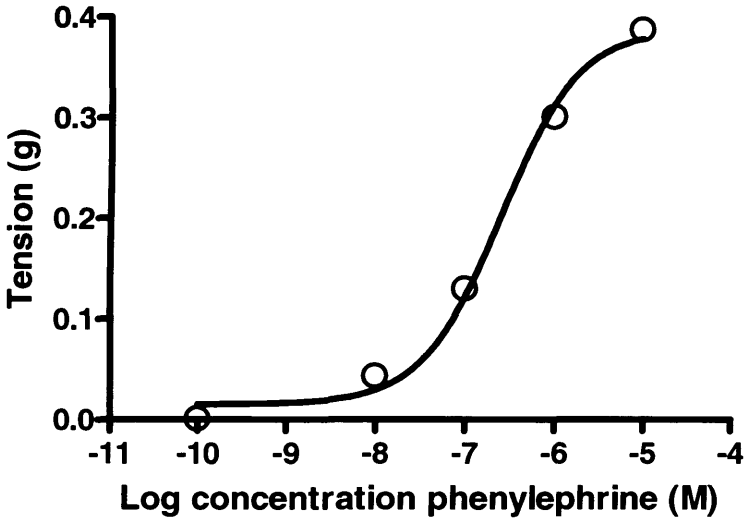

Figure 2.2 Example of non-linear curve fitting for an individual data set (set 2 from +EGF). The R2 value for the plot is 0.9936 and the equation is $y = \text{min} + (\text{max-min}) / (1x10^{(\text{logEC50-x})})$ (Y = Response, X= Logarithm of concentration). From the plot the -logEC50 and the maximum were calculated as -6.539 and 0.4207 respectively. –logEC50 and maximum values for each individual data set were meaned.

2.2.3 Cell Culture

2.2.3.1 Cell Culture Conditions

Cell culture was performed in a Heraeus safe type II laminar hood (Jencons PLS, UK) that had been decontaminated firstly with Precept® and then with a

70 % ethanol wash. All consumables used for cell culture were sterile and were decontaminated using 70 % ethanol and opened inside the hood. Cells were incubated and maintained in a Heraeus Hera Cell incubator (Jencons PLS, UK) with atmosphere of 5 % CO_2 and a temperature of 37°C, 95 % humidified with water humidifying trays containing copper II sulphate. Medium and PBS were always warmed to 37°C before adding to the cells.

2.2.3.2 Cell Line and Culture Medium

ECV-304 cells were grown in M199 medium supplemented with 10 % FBS, and 1 % penicillin streptomycin. For certain studies serum-free media was required, for this, the above media was used without the addition of FBS. To avoid the possibility of phenotypic drift, each batch of cells was used for a maximum of 10 passages.

2.2.3.3 Subculturing (Passaging) and Maintenance of Cells

Stock cultures were fed with fresh medium every 2-3 days and subcultured every 3 days or upon reaching 70-80 % confluency. To subculture, spent medium was aspirated, and cells washed 3 times with PBS. Then 1 x Trypsin/ EDTA was added to the cells (1 ml for every 25 cm^2 vessel surface area) and incubated until cells were detached from the flask. Adding 10 ml of fresh medium to the flask stopped trypsinisation, due to the presence of trypsin inhibitors in serum. The cell-containing medium was then transferred to a centrifuge tube and centrifuged at 150 gravity (g) for 5 minutes. The supernatant was aspirated and the cells were resuspended in the appropriate

volume of fresh medium. Cells were counted using an inverted Nikon Eclipse TS100 microscope (Jencons PLS, UK), on a Neubauer haemocytometer (Marinefield, Germany) and aliquoted into flasks at the required seeding density.

2.2.3.4 Cryopreservation of Cells

Cells were grown in culture flasks to around 60 % confluency, and trypsinised as described above, counted and pelleted by centrifugation at 150 g for 5 minutes. The pellet was reconstituted in normal medium and pelleted again at 150 g for 5 minutes. The resulting pellet was reconstituted in freezing media with an average of 10^6 cells/ml of freezing medium. One ml was placed in each cryovial, and these were kept at -80°C overnight, and the following day stored in liquid nitrogen at -196°C.

2.2.3.5 Thawing Frozen Cells

Cells were taken out of liquid nitrogen storage and quickly thawed at 37°C in a water bath. The cells were transferred to a centrifuge tube containing 10 ml of normal medium and centrifuged at 150 g for 5 minutes. The supernatant was then decanted, and the pellet gently resuspended in 7.5 ml of fresh medium and then placed in a 25 cm flask to grow as normal. After 24 hours spent media was aspirated and fresh media was added.

2.2.3.6 Cell Count and Viability

The trypan blue exclusion test was used to assay the viability of cells. Cells were washed with PBS, and then trypsinised and resuspended in a known volume of medium. One hundred µl of trypsinised cells was mixed with 100 µl of trypan blue (0.4 % solution) and left to stand for 2-3 minutes. A coverslip was placed on the haemocytometer and 10 µl of the suspension was taken and transferred to the counting chambers of a two counting grid Neubaeur haemocytometer with a depth of 0.1 mm and an area of 1/400 mm^2. The cells in the 5 x 5 counting grid were counted using a light microscope at a magnification of x100, this was repeated four times. For calculating the number of cells/ml the mean count was taken excluding the non-viable cells stained with trypan blue and used in the calculation formula:

$$\text{Cells/ml} = \text{mean count} \times 10^4 \times \text{dilution factor}$$

2.2.3.7 Cell Growth Curve for ECV-304 Cells

Cells were plated at a seeding density of either 12,500, 25,000 or 50,000 in a 24 well cell culture plate using 1 ml of medium per well. After 12 hours spent medium was aspirated from 3 wells for each seeding density and the wells were washed 3 times with PBS. Trypsin (100 µl) was added to each well and the plate was incubated for 5 minutes. The trypsinisation was stopped by adding 100 µl of normal medium to each well. The detached cells were transferred into an eppendorf tube, and the cells counted. This was repeated

every 12 hours for 5 days, and every 24 hours thereafter up to 9 days. Every 3rd day, spent medium was aspirated and replaced with fresh medium.

2.2.3.8 Cell Growth Curve for ECV-304 Cells Grown in Normal and High Glucose Conditions

Cells were plated at a seeding density of 25,000 cells/well in a 24 well cell culture plate using 1 ml of medium per well, and incubated for 24 hours. Cell medium was then changed to either fresh medium with a concentration of 5.5 mM glucose or to medium containing 25.5 mM glucose. After 8 hours, spent medium was aspirated from 6 of the wells (3 with normal medium and 3 with medium containing 25.5 mM glucose), and the wells were washed 3 times with PBS. The cells were detached for counting as described above, in section 2.2.3.7. This was repeated every 10-12 hours for the first 4 days and just once on the 5th day. On the 3rd day after treatment with glucose, spent medium was aspirated and replaced with fresh medium and treatments. For ECV-304 growth curves, SEM is represented with vertical bars on graphs.

2.2.3.9 Exposing Cells to EGF

ECV-304 cells were seeded in a T-75 T-flask at a seeding density of 1 million cells per flask with 20 ml of medium. Cells were incubated for 24 hours, after which 1, 10 or 100 ng/ml of EGF was added for 1, 10 or 60 minutes (as stated in the text). After which the cells were lysed as described in section 2.2.4.

2.2.3.10 Exposing Cells to Glucose and Treatment with ErbB Inhibitors: AG1478 and AG825

ECV-304 cells were seeded in a T-75 T-flask at a seeding density of 1 million cells per flask with 20 ml of medium. Cells were incubated for 24 hours, after which the medium was aspirated and cells washed 3 times with PBS. Then serum-free medium was added to the cells, and incubated for a further 24 hours. Stock solution of 1.4 M of D-glucose was prepared and filtered. The appropriate volume of the stock solution was added to serum free medium to give the final concentration of glucose, as stated in the text. For control cells conventional serum-free medium that contained 5.5 mM glucose was added straight to the cells. For osmotic control D-glucose was replaced with L-glucose (Fig. 2.3)

Where stated, and at concentrations stated in the results section, AG1478 or AG825 (Fig. 2.1d) (in DMSO) was added simultaneously with glucose. The overall DMSO concentration in medium was kept at 1 %. Cells were incubated with treatment for various time periods as stated in the results section and then lysed for western blotting as described in section 2.2.4 or ribonucleic acid (RNA) was extracted as described in section 2.2.5.

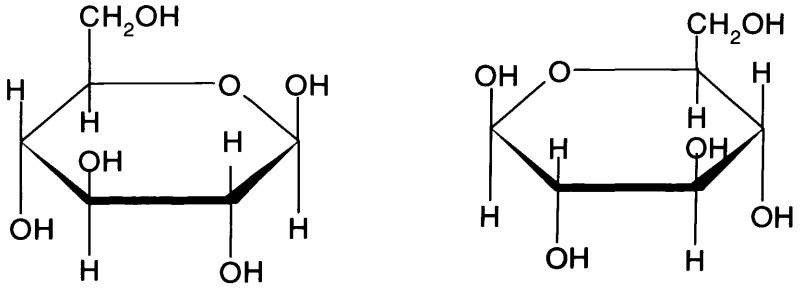

D-glucose L-glucose

Figure 2.3 Chemical structure of a) D-glucose and b) L-glucose

2.2.3.11 Treatment of Cells with PKC Activator TPA, and PKC Inhibitors RO-31-8220 and GO6983

ECV-304 cells were seeded in T-75 T-flasks at a seeding density of 1 million cells per flask and incubated for 24 hours in 20 ml of serum-containing media. Then media was aspirated and replaced with fresh media alone for untreated control, or containing the following treatments: 100 nM TPA for 3, 24 and 48 hours; 0.05, 0.1, 0.25 and 0.5 μM RO-31-8220 for 24 hours; and 0.1, 0.5, 1, 5 and 10 μM GO6983 for 24 hours. After which cells were lysed as described in section 2.2.4 for western blotting.

2.2.4 Cell Lysis and Western Blotting

Western blotting is a semi-quantitative technique used for the analysis of protein, and was first introduced by Towbin and co-workers in 1979 (Towbin, *et al* 1979). It involves many steps, first of which is the harvesting of protein from cells or tissue and the loading of protein samples onto an SDS-gel. Negatively charged SDS binds to protein molecules, causing each protein moecule to become negatively charged. Molecules of similar size bind the same amount of SDS, thus have a similar negative charge. Thus, an electrical current can be used to separate proteins according to mass and not to charge, since all proteins will migrate towards the anode with larger proteins retarded by the gel matrix more so than smaller proteins. The separated proteins are then transferred from the gel onto a nitrocellulose membrane. After transfer, the blot is blocked using milk, this reduces background interference from antibody

binding to non-specific sites on the nitrocellulose blot. Following this the blot is incubated in diluted primary antibody which binds specifically to the protein of interest. Then after washing off excess primary antibody, the blot is incubated in diluted secondary antibody, which in this case is conjugated with the enzyme horseradish peroxidase (HRP). The secondary antibody binds to the primary antibody, and since each primary antibody has several epitopes that can be identified and bound by the labeled secondary antibody the signal is amplified. After washing off excess secondary antibody, substrate is added to the blot. The substrate is catalysed by HRP on the secondary antibody, to produce light (Fig. 2.4), which can be detected by means of a photographic film.

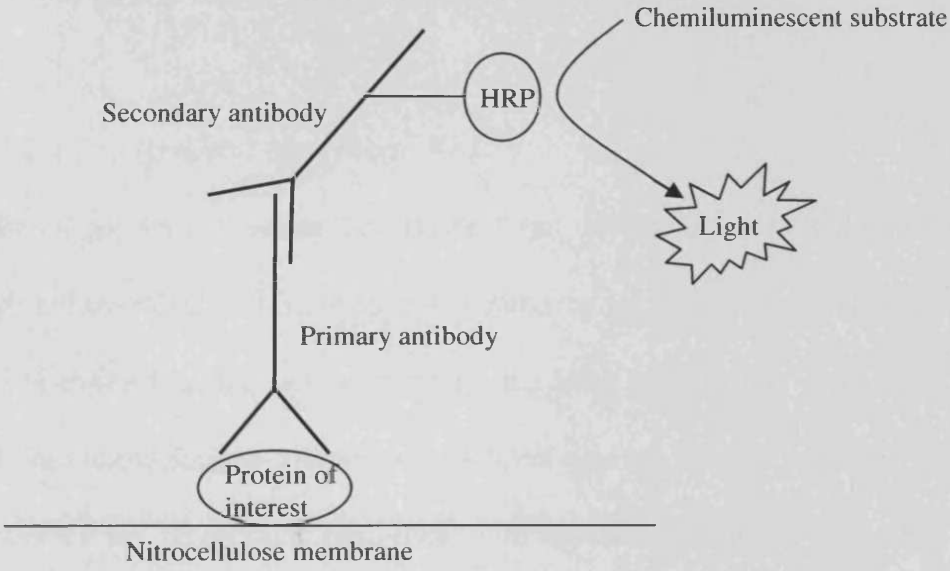

Figure 2.4 Nitrocellulose membrane with protein of interest bound to the primary antibody/secondary antibody complex. Substrate is added which is catalysed by HRP to produce light.

2.2.4.1 Preparation of ECV-304 Cell Lysates

Cell medium was aspirated and cells washed 3 times with PBS. For every 1 cm^3 of culture vessel area approximately 10 µl of lysis buffer (50 mM tris base, 5 mM EGTA, 150 mM NaCl, Triton 1 %) was added to the cells. To protect the cellular protein from proteolysis by peptidases, protease inhibitors (2 mM Na_3VO_4, 50 mM NaF, 1 mM PMSF, 20 µM phenylarsine, 10 mM sodium molybdate, 10 µg/ml leupeptin and 8 µg/ml aprotinin) were added to the lysis buffer immediately prior to lysis. Cells were scraped with a cell scraper, and left on ice for 15 minutes. Cells were further scraped, transferred to eppendorf tubes and left on ice for a further 15 minutes. Samples were then centrifuged for 15 minutes at 13,000 g at 4°C. The supernatant was then collected, aliquoted and frozen at -20°C and the pellet was discarded.

2.2.4.2 Lysis of Rat Mesenteric Bed

Rat mesenteric vascular bed tissue from the perfusion experiments had been stored at –80°C until the tissue was required for further experiments. The tissue was thawed on ice. After complete thawing, lysis buffer was added, and the tissue homogenised 3 times with a homogenizer (Fisher scientific Inc, UK) at speed 2 for 20 seconds each time. The tissue was then left on ice for a further 30 minutes. The lysates were centrifuged at 13,000 g for 20 minutes at 4°C. The resulting supernatant was collected, aliquoted and frozen at –20°C until required and the pellet was discarded.

2.2.4.3 Protein Determination

The Bio-Rad protein assay was used for the Bradford method of total protein determination in prepared cell or tissue lysates. A BSA standard curve was set up in triplicate in a plastic 96 well plate, at concentrations of 0, 0.05, 0.1, 0.15, 0.2, 0.29 and 0.5 nM to a final volume of 10 µl. Protein samples were also set up in triplicates containing 1/10 dilution of sample in ultra pure water to a final volume of 10 µl. Then 200 µl of a 1:5 dilution of 0.2 µM filtered Bio-rad protein assay reagent was added to each well. This was left to stand for 5 minutes and absorbencies of standards and protein samples were read at 595 nM using a sunrise absorbance reader (Tecan, Austria). A graph of the concentration versus absorbance (595 nm) was drawn for standards, see example in figure 2.5 below. The concentration was then worked out as shown in the example below:

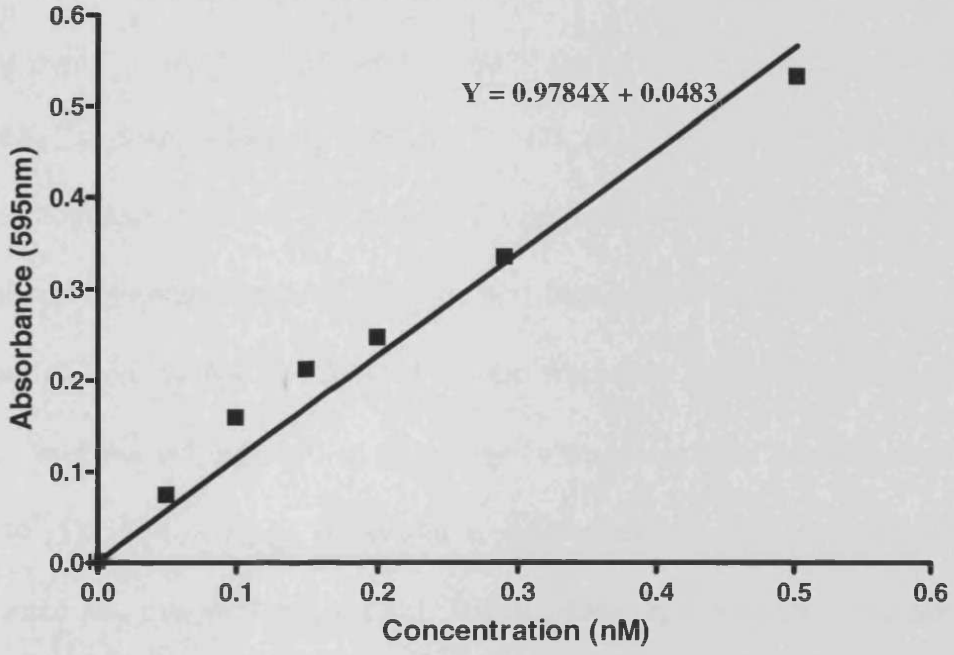

Figure 2.5 Example standard curve showing absorbance (595 nM) of proteins at standard concentrations with the linear curve equation.

The linear equation y = mx + c (y = absorbance, m = slope of the line, x = concentration and c = y intercept) was used to calculate the protein concentration of lysate samples. From a best-fit line through the standard curve the values for 'm' and 'c' were derived. Using the protein sample's absorbance value as 'y', the equation (x = (y-c)/m) was rearranged to find 'x'. Then 'x' was multiplied by the dilution factor (in this case 10) which gave the protein sample's concentration in nM.

2.2.4.4 SDS Polyacrylamide Gel Electrophoresis

Electrophoresis was completed using Mini-PROTEAN® 3 electrophoresis cell with accessories (BioRad Laboratories, UK). Polyacrylamide gel was prepared and placed in a gel tank filled with running buffer (25 mM tris base, 192 mM glycine and 0.01 % SDS at pH 8.3 dissolved in double distilled water). Recipes for acrylamide gels are shown in table 2.4 and table 2.5. The percentage of resolving gel used depends on the size of the protein to be detected as shown in table 2.4. Sample loading buffer (2 % SDS, 10 % glycerol, 60 mM tris pH 6.8, bromophenol blue and 20 mM DTT dissolved in double distilled water) was added to protein samples (1:1, v/v) and then heated at 100°C for 10 minutes. Samples containing 20-50 μg of protein were then loaded, into the pre-formed wells of the gel. Also 10 μl full range molecular weight rainbow marker (10-250 kDa) or low range molecular weight rainbow marker (2.5- 45 kDa) was loaded into one well of each gel. The gel was run at a constant voltage of 150 V and 35 mA per gel for 90 minutes or until the blue bromophenol dye in the sample-loading buffer had run off the bottom of the gel.

Table 2.4 Recipes for 8, 10 and 12 % resolving gels with the protein range of separation

% Resolving gel	8	10	12
Protein range for separation (kDa)	70-200	20-100	10-70
Acrylamide (30 %) (ml)	2.7	3.3	4.0
Distilled water (ml)	4.6	4.0	3.3
1.5M Tris pH 8.8 (ml)	2.5	2.5	2.5
10% SDS (ml)	0.1	0.1	0.1
10% APS (ml)	0.1	0.1	0.1
TEMED (ml)	0.02	0.02	0.02

Table 2.5 Recipe for 5% stacking gel

5% Stacking gel	(ml)
Acrylamide	1.67
Distilled water	5.83
1.5M Tris pH 6.8	2.5
10% SDS	0.1
10% APS	0.05
TEMED	0.01

2.2.4.5 Electrophoretic Transfer

The separated proteins were transferred onto protan nitrocellulose transfer membrane with 0.2 μm pores using mini trans-blot® cell apparatus (BioRad Laboratories, UK). Transfer buffer was made up of 0.25 M tris base, 1.92 M glycine and 20 % methanol dissolved in double distilled water. A sandwich consisting of sponge, 3 sheets of filter paper, SDS gel, nitrocellulose, another 3 sheets of filter paper, and sponge (all first soaked in transfer buffer) was assembled. Air bubbles caught between the gel and nitrocellulose were carefully removed, and the entire group was placed inside a support grid (Fig. 2.6). This was placed in the transfer apparatus full of transfer buffer making sure that the transfer from gel to nitrocellulose was going from cathode to

anode, due to the negative charge on the proteins. Transfer was performed at 250 mA and 100 V for 90 minutes.

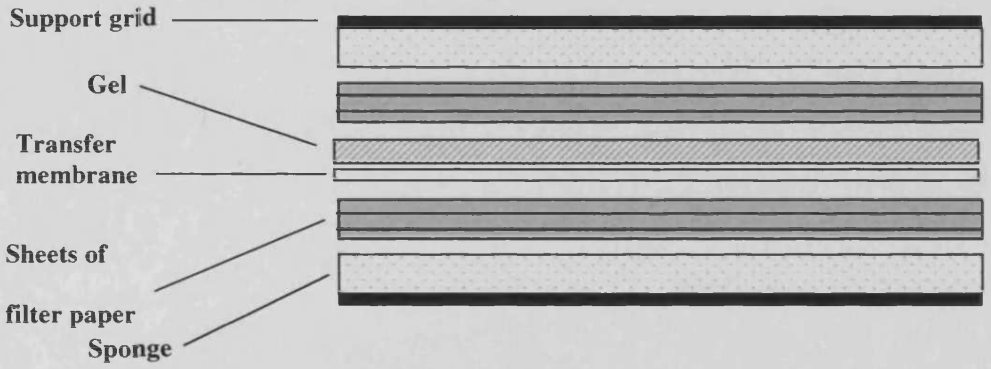

Figure 2.6 Diagrammatic representation of the electrophoretic transfer sandwich

2.2.4.6 Ponceau S Staining and Membrane Blocking

Following blotting the nitrocellulose was placed in ponceau S stain for visualizing of transferred proteins, showing efficiency of transfer. The red ponceau S stain was then washed off with tris buffered saline (10 mM tris base and 150 mM NaCl dissolved in double distilled water) containing 0.05 % tween20 (TBS/tween). The blot was blocked by incubating it in 5 % (w/v) Marvel® dried skimmed milk in TBS/tween for 1 hour at room temperature with gentle agitation.

2.2.4.7 Western Blot Membrane Probing with Antibodies

Following blocking, the nitrocellulose blot was washed for 10 minutes with TBS/tween, and then the appropriate primary antibody was added, diluted 1:1000 in TBS/tween and 5 % Western blocking reagent. The concentrations of

antibody used were based on preliminary experiments were each antibody was fully optimized. The blots were incubated in the primary antibody overnight at 4°C on a Stuart roller mixer SRT2 (Bibby Sterilin Ltd, UK). Following primary antibody treatment, the nitrocellulose membrane was washed 3 times with TBS/tween for 10 minutes each time on an orbital shaker at room temperature. Then the membrane was treated with HRP-conjugated secondary antibody diluted 1:10,000 in TBS/tween and 5% Western blocking reagent. This was incubated at room temperature on a roller mixer for 1 hour.

2.2.4.8 Chemiluminescence Detection

After antibody treatments the membrane was washed again 3 times with TBS/tween for 10 minutes each time at room temperature on an orbital shaker at high speed. Excess TBS/tween was carefully taken off the membrane before it was placed between sheets of thin clear plastic. Under safe light, equal volumes of chemiluminescence reagents 1 (peroxide buffer) and 2 (luminol/enhancer solution) supersignal west dura extended duration substrate (supersignal west femto substrate was used to detect endothelial nitric oxide synthase (eNOS) at Thr495) was then applied to the blot and left for 5 minutes. Excess chemiluminescence substrate was removed, and the blot was placed in an autoradiograph cassette. An autoradiograph film was placed in the cassette with the membrane, and the film was developed.

2.2.4.9 Measurement of β-actin as an internal control

Under most conditions the level of β-actin should not vary between samples, thus can be used as an internal control (Liao, *et al* 2000). To ensure that an equal amount of protein was loaded into each lane, after western blotting for a specific protein, the blot was washed 3 times with TBS/tween. The blot was then probed with antibodies and subjected to chemiluminescence detection as above, except the primary antibody was at a concentration of 1:10000 incubated for 30 minutes.

2.2.4.10 .Co-immunoprecipitation

Co-immunoprecipitation is a method used for the analysis of protein:protein interactions. The protein of interest and any proteins that are complexed with it are precipitated from the rest of the cell lysate. Antibody specific for the protein of interest is added to the sample and an antibody:protein complex forms. Then an immobilized antibody binding protein, in this case protein A-agarose beads, is added to the sample. The protein A recognizes and binds to the Fc region of the antibody in the antibody:protein complex and due to the bound agarose beads the complex can then be easily isolated out of solution by centrifugation. Unbound proteins are washed away and the antibody:protein complex is eluted from the immobilized protein A. The protein of interest and any protein in complex with it can then be analysed using western blotting.

Co-immunoprecipitation was performed as follows: Anti-EGFR antibody was added to 1 mg of cell lysate samples at a dilution of 1:50, and incubated on a

tube rotator (NeoLab, Germany) overnight at 4°C. Then 20 µl of protein A-agarose beads was added to the samples and incubated on a tube rotator at 4°C for a further 3 hours. Then the bead pellets were washed 5 times with excess lysis buffer (400 µl), making sure to keep the samples on ice for the duration of the washes. Between each wash the samples were centrifuged at the maximum speed for 5 seconds. Finally the pellets were resuspended in 20 µl of 2 x SDS-sample buffer and vortexed for 3 seconds. Then the samples were centrifuged again, after which the samples were heated to 100°C for 5 minutes. Finally 10 µl of sample per well was added to two SDS-gels and western blotting was performed. One blot was probed for EGFR and the other for ErbB2.

2.2.5 RT-PCR

PCR is a technique used to enzymtically amplify DNA, invented by Kary Mullis in 1983 (Mullis 1990). In this instance total RNA was isolated and converted into the more stable c (complimentary) DNA by the process of RT-PCR. Then cDNA was amplified using PCR, and was detected on a stained agarose gel.

2.2.5.1 Isolation of Total RNA

Spent medium was aspirated from a 25 cm^2 flask of confluent ECV-304 cells, and washed 3 times with excess PBS. After removing all PBS, 2 ml of TRI reagent was added. Then a cell scraper was used to harvest the cells. The cell-containing suspension was aliquoted into 1 ml portions in eppendorf tubes. Then 0.2 ml of chloroform was added and vortexed for approximately 20

seconds. These were centrifuged for 15 minutes at 19,000 g and 4°C. This resulted in 3 layers; the clear fraction at the top containing RNA, the middle DNA containing layer and the bottom protein fraction. The top RNA fraction was removed very carefully and transferred into a new sterile eppendorf tube, and then 0.5 ml of isopropanol was added. This was then left to stand at room temperature for 10 minutes. Then it was centrifuged again at 19,000 g and 4°C for 10 minutes, a pellet of RNA resulted. Then very carefully not to disturb the pellet the supernatant was removed, and the pellet washed with 75 % ethanol, by vortexing, and then centrifuging at 19,000 g and 4°C for 5 minutes. The ethanol was pipetted off, and the pellet of RNA was left to air dry. Then the pellet of RNA was resuspended in 50 µl of deionised water.

2.2.5.2 Assessing Purity and Yield of Total RNA

A denaturing gel was used to asses the purity of RNA. A 1 % denaturing agarose gel was prepared. 10 µl of RNA loading solution was added to 1 µl of total RNA, mixed and heated for 15 minutes at 70°C. This was then cooled on ice for 1 minute and loaded onto the denaturing gel. The gel was left to run at 50 V, until the dye had migrated 3-4 cm from the wells. Two bright bands at approximately 4.5 and 1.9 kb (28S and 18S ribosomal RNA) indicated pure RNA

Total RNA's absorbencies at 260 nm and 280 nm were measured using an Ultrospec 3100 pro UV/visible spectrophotometer (Amersham Biosciences, UK). The ratio of the absorbencies at 260 and 280 nm indicated RNA's purity.

RNA with a ratio of 1.7-2.0 was declared pure. Since an absorbance of 1 unit at 260nm corresponds to 40 μg RNA/ml based on an extinction coefficient calculated for RNA in water, then to determine RNA concentration in μg/ml the absorbance at 260 nm was multiplied by 40 and then by the dilution factor.

2.2.5.3 RT: Preparation of cDNA

RT-PCR and PCR were undertaken in a Labconco purifier PCR enclosure (GRI, UK). RNA (1 μg) made up in RNase/DNase free water in a total volume of 7.5 μl was added to 11 μl of RT master mix comprising of 5 μl dNTPs (2.5 mM), 2 μl (10 x) PCR buffer (100 mM tris HCl (pH 8.3), 500 mM KCl, 15 mM $MgCl_2$ and 0.01 % gelatine dissolved in RNase/DNase free water), 2 μl DTT (0.1 M) and 2 μl of random hexamers. Samples were vortexed then denatured at 95°C for 5 minute in a MJ research PTC-100 programmable thermal controller PCR machine (GRI, UK). Then they were incubated on ice for 2 minutes. 1 μl of MMLV-RT and 0.5 μl of RNase inhibitor was added. A negative control was always used which was a reaction excluding RNA, presence of a band or bands in an RT-PCR gel picture would indicate contamination with RNA from an external source. The samples were gently flick mixed and pulse spun in a micro-centrifuge. The tubes were returned to the PCR machine and reverse transcribed following the protocol: 22°C for 10 minutes (annealing), 42°C for 40 minutes (RT extension) and finally 95°C for 5 minutes (denaturing).

2.2.5.4 PCR

cDNA coding for known genes was amplified exponentially using PCR. First, 0.5 µl of cDNA produced in the RT step was added to the master mix comprising of: 18.24 µl of ddH20, 2.5 µl PCR buffer (10x), 2 µl dNTPs (2.5 mM), 0.625 µl each of 100 pmol/µl forward and reverse primers, 0.156 µl each of 100 pmol/µl β-actin forward and reverse primers and 0.2 µl of Taq polymerase giving a final volume of 25 µl per sample. Then, PCR reactions were set up in PCR tubes on ice and the Taq was always added at the latest possible time. A negative control was always used which was a reaction excluding cDNA, presence of a band or bands in a PCR gel picture would indicate contamination with DNA from an external source. In preliminary experiments the annealing conditions were fully optimized for each primer pair. Tubes were placed in the PCR machine and amplified using the following thermocycling program:

First cycle:
95°C for 2 min
55°C for 1 min
72°C for 5 min
PCR cycles (x no. cycles):
95°C for 1 min
55°C for 30sec
72°C for 1 min
Final cycle:
94°C for 1 min
60°C for 5 min

The number of PCR cycles varied between primers as shown in table 2.6.

Table 2.6 Primers and the number of PCR cycles performed

Primer	Number of PCR cycles
EGFR	27
ErbB2	27
TGF α	30
Betacellulin	35
Epiregulin	27
Amphiregulin	30
HB-EGF	35
EGF	35
Connexin 43	30

The product was resolved on a 2 % agarose gel containing ethidium bromide in 1x Tris-Acetate-EDTA (TAE) buffer at 70 V for 30 minutes. Samples were loaded using 1x loading buffer (50 % glycerol in 1 x TAE with 1 % bromophenol blue). Then gels were viewed and analysed using an alpha innotech corporation alpha digidoc RT gel documentation system and the alphaEase FC software (v4.1.0) (GRI, UK).

3.0 Results

3.1 Modulation of Epidermal Growth Factor Receptor and ErbB2, and the Effect of Receptor Tyrosine Kinase Inhibition on Vascular Tone in the Mesenteric Bed of Streptozotocin-induced Diabetic Rats

Introduction

It has previously been shown that diabetic vascular tissues show an enhanced response to vasoconstrictors and an attenuated response to vasodilators (Abebe, *et al* 1990, Kamata, *et al* 1989, Makino, *et al* 2000, Mayhan, *et al* 1999, Oyama, *et al* 1986). Studies suggest that this aberrant vascular response could be due to diabetes-induced abnormalities of several important mechanisms involved in vascular reactivity. Possibilities include a diabetes-induced rise in calcium levels or sensitivity (Abebe, *et al* 1990, Beenen, *et al* 1995), diabetes-induced changes in vascular response to endothelium derived hyperpolarising factor (EDHF) (Makino, *et al* 2000) and a diabetes-induced reduction in the levels of vascular cyclic GMP (cGMP), due to aberrant nitric oxide (NO) production (Kamata, *et al* 1989, Li and Forstermann 2000). However, the exact underlying mechanisms involved remain unclear.

It is known that epidermal growth factor (EGFR) activity is increased in some diabetic tissues from streptozotocin (STZ)-induced diabetic rats, such as the gastric mucosa (Khan, *et al* 1999). Also, under high glucose conditions, the transactivation of EGFR is increased in the proximal tubules of human kidneys (Saad, *et al* 2005). Additionally, the involvement of EGFR and ErbB2 signalling pathways have been implicated in the development of diabetes-

induced vascular dysfunction in rat carotid artery (Yousif, *et al* 2005). The aim of this section was to investigate the involvement of EGFR in diabetes-induced abnormal vascular reactivity in rat mesenteric bed, by use of receptor tyrosine kinase (RTK) inhibitors, and to look at the levels of phosphorylated (p)EGFR and pErbB2 in the mesenteric bed of diabetic rats.

Results

Effects of Genistein and AG1478 on Vascular Tone of Perfused Mesenteric Bed from STZ-induced Diabetic Rats

Firstly the effect of EGFR inhibition on aberrant vascular reactivity seen in diabetic vascular tissues was examined using perfusion experiments. Perfusion experiments were carried out by Dr Mariam Yousif and Prof Ibrahim Benter of the Department of Pharmacology and Toxicology, Faculty of Medicine, Kuwait University (Benter, *et al* 2005a).

Before commencing with the experiments, the blood glucose concentration of each rat was tested. STZ is a potent diabetogenic agent that destroys the insulin-producing β cells and was thus used to generate a type I diabetes experimental animal model. The STZ-treated diabetic rats had significantly higher blood glucose concentrations at 4 weeks (610 ± 24 mg/dl) as compared to the non-diabetic control rats (86 ± 5 mg/dl). Treatment of diabetic rats with the highly potent and specific EGFR inhibitor AG1478 (550 ± 28 mg/dl) or the general tyrosine kinase inhibitor genistein (538 ± 26mg/dl) did not have a

significant effect on blood glucose concentration as compared to the diadzein control (532 ± 23 mg/dl), which is an inactive analogue of genistein.

Upon confirmation of the successful induction of diabetes in the STZ treated rats, perfusion studies within the isolated mesenteric vascular bed were carried out using the vasoconstrictors noradrenaline (NA) (adrenergic agonist) and endothelin-1 (ET-1). The vasoconstrictor responses to 10^{-8}, 10^{-7} and 10^{-6} mol NA were significantly exaggerated in the perfused mesenteric vascular bed from STZ-diabetic rats (85 ± 9, 160 ± 7 and 177 ± 7 mmHg) as compared to non-diabetic control rats (39 ± 7, 106 ± 11 and 124 ± 6 mmHg) (Figs. 3.1a and 3.1b). The augmented responses to 10^{-7} and 10^{-6} mol NA were significantly (n = 8, $p < 0.05$) prevented by 4 week treatment of diabetic rats with the tyrosine kinase inhibitors genistein (97 ± 18 and 119 ± 23 mmHg) (Fig. 3.1a) and AG1478 (91 ±_13 and 114 ± 11 mmHg) (Fig. 3.1b). The vasoconstrictive responses to 10^{-10} and 10^{-9} mol ET-1 were also significantly (n = 8, $p < 0.05$) exaggerated in the perfused mesenteric beds from STZ-diabetic rats (138 ± 14 and 198 ± 7 mmHg) as compared to control (75 ± 14 and 99 ± 8 mmHg) (Figs. 3.2a and 3.2b). The exaggerated response to 10^{-10} mol ET-1 was again significantly normalized by 4 week treatment of diabetic rats with either genistein (66 ± 18 mmHg) (Fig. 3.2a) or AG1478 (80 ± 25 mmHg) (Fig. 3.2b). The effect of AG1478 and genistein were overcome at the highest concentration of ET-1 (10^{-9} mol) (Figs. 3.2a and 3.2b).

Perfusion studies were next carried out using the vasodilators, carbachol (muscarinic agonist) and sodium nitroprusside (SNP, NO donor) to examine the effect of endothelium-dependent and independent vasodilators, respectively. There was a significant (n = 8, $p < 0.05$) reduction in the vasodilator response to 10^{-9} and 10^{-8} mol carbachol in the perfused mesenteric vascular bed from STZ-diabetic rats (44 ± 7 and 59 ± 6 %) compared to non-diabetic control rats (78 ± 5 and 100 ± 6 %) (Figs. 3.3a and 3.3b). This reduced response to 10^{-9} and 10^{-8} mol carbachol was significantly (n = 8, $p < 0.05$) prevented in STZ-diabetic rats treated with either genistein (89 ± 17 and 86 ± 6%) (Fig. 3.3a) or AG1478 (78 ± 9 and 92 ± 14%) (Fig. 3.3b).

The vasodilator responses to 10^{-10}, 10^{-9} and 10^{-8} mol SNP in the perfused mesenteric vascular bed of the STZ-diabetic rats (37 ± 8, 66 ± 6 and 80 ± 7 %) were similar to those observed in the perfused mesenteric beds of the control rats (28 ± 3, 69 ± 7 and 94 ± 6 %). The treatment of STZ-diabetic rats with genistein (56 ± 9, 75 ± 8 and 86 ± 6 %) or AG1478 (38 ± 10, 62 ± 8 and 73 ± 8 %) did not have a significant effect on SNP-induced changes in perfusion pressure in STZ-diabetic rats (Fig. 3.4).

Control studies were carried out, which showed that 4 week treatment of non-diabetic rats with either genistein or AG1478 did not have a significant effect on vasoconstrictor response to NA (10^{-8}, 10^{-7} and 10^{-6} mol) and ET-1 (10^{-11}, 10^{-10} and 10^{-9} mol) nor on vasodilator response to carbachol (10^{-9} and 10^{-8} mol) and SNP (10^{-10}, 10^{-9} and 10^{-8} mol) (Figs. 3.1c, 3.2c, 3.3c and 3.4c). Control

studies were also carried out using diadzein. A 4 week diadzein treatment of control rats and STZ-diabetic rats did not have a significant effect on NA (10^{-8}, 10^{-7} and 10^{-6} mol) or ET-1 (10^{-11}, 10^{-10} and 10^{-9} mol) induced vasoconstrictor response nor on carbachol (10^{-9} and 10^{-8} mol) or SNP (10^{-10}, 10^{-9} and 10^{-8} mol) vasodilator response as compared to control (Figs. 3.1d, 3.2d, 3.3d and 3.4d).

The Effect of RTK Inhibition on EGFR Phosphorylation at Tyrosine 1068 in STZ-induced Diabetic Rats

Next western blot studies were conducted to examine whether the level of pEGFR was increased at tyrosine (Tyr)1068 in the mesenteric bed of STZ-induced diabetic rats, and whether the level of pEGFR could be reduced using the inhibitors AG1478 and genistein. This would show whether the recovery of vasoconstrictor and vasodilator response following genistein and AG1478 treatment was a result of these agents inhibiting EGFR activity.

In all cases throughout this text, western blots for pEGFR and pErbB2 showed single bands at 175 kDa and 185 kDa respectively as estimated using molecular weight markers, these were the expected molecular weights for each protein. To ensure that an equal amount of protein was loaded into each lane levels of β-actin were always detected by means of western blot. In all cases throughout the text, levels of β-actin remained constant, indicating equivalent loading of protein.

Higher level of pEGFR in mesenteric bed tissue from STZ-diabetic rats was seen as compared to control rats. This increase in pEGFR seen in the diabetic rats was prevented by treatment with AG1478 and with genistein (Fig. 3.5a).

The Effect of RTK Inhibition on ErbB2 Phosphorylation at Tyrosine 1248 in STZ-Induced Diabetic Rats

Since ErbB2 is the preferred heterodimerization partner for EGFR (Graus-Porta, *et al* 1997), whether ErbB2 phosphorylation at Tyr1248 was also elevated in mesenteric bed from STZ-induced diabetic rats, and whether phosphorylation of ErbB2 could be reduced using genistein, or using the ErbB2 inhibitor AG825 which is selective for ErbB2 over EGFR was examined.

Western blotting showed a higher level of pErbB2 in the mesenteric bed tissue from STZ-diabetic rats as compared to control rats. This increase in pErbB2 seen in mesenteric bed tissue from diabetic rats was reduced back to near control levels by treatment with genistein and with AG825 (Fig. 3.5b).

Figure 3.1

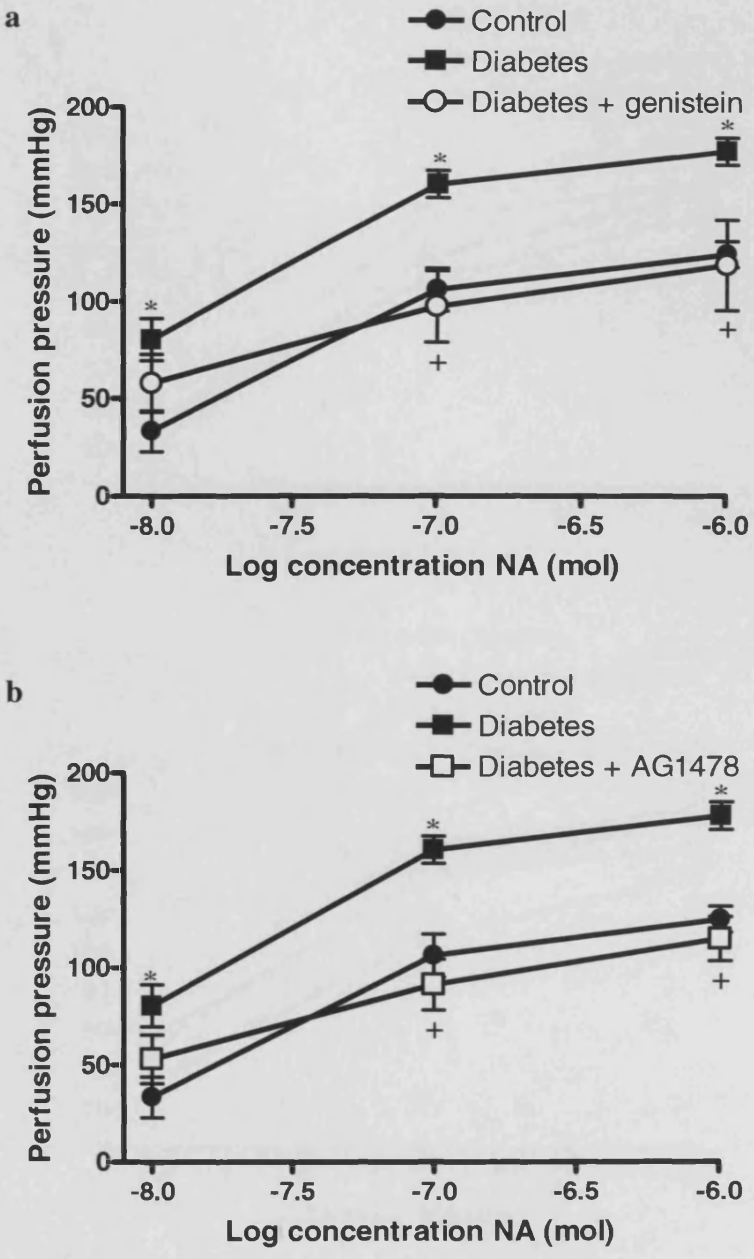
a
Control
Diabetes
Diabetes + genistein
Perfusion pressure (mmHg)
200
150
100
50
0
-8.0
-7.5
-7.0
-6.5
-6.0
Log concentration NA (mol)
b
Control
Diabetes
Diabetes + AG1478
Perfusion pressure (mmHg)
200
150
100
50
0
-8.0
-7.5
-7.0
-6.5
-6.0
Log concentration NA (mol)

Figure 3.1 continued

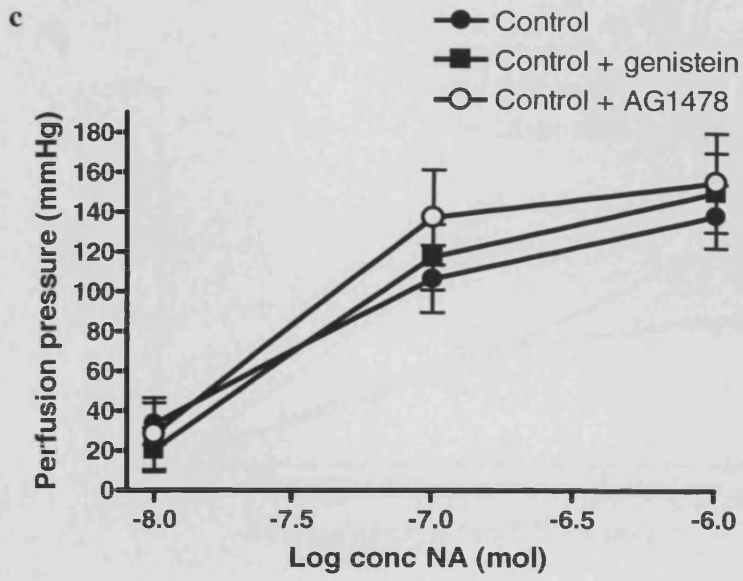

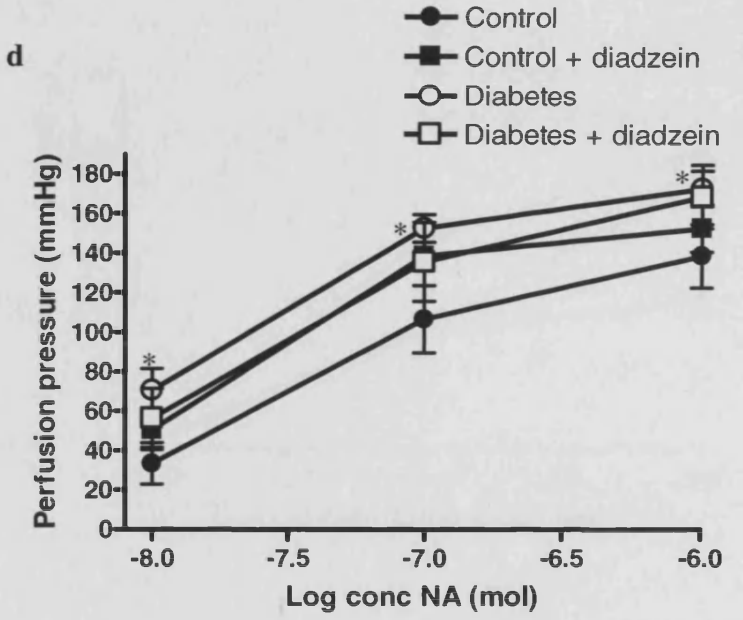

Effect of NA on the mesenteric vascular bed of control, diabetic and RTK antagonists chronically treated control and diabetic rats. NA-induced vasoconstriction was measured as perfusion pressure (mmHg) in the mesenteric vascular bed perfused with Krebs' solution (mean ± SEM). a) Responses in control, diabetic, and chronic genistein-treated diabetic rats b) control, diabetic and chronic AG1478-treated diabetic rats c) control, chronic genistein-treated control and chronic AG1478-treated control rats and d) control, diabetic, chronic diadzein-treated control and chronic diadzein-treated diabetic rats. Genistein, AG1478 and diadzein treatments were for four weeks with 1.5 mg/kg body weight intraperitoneal injections on alternate days. Diabetic rats were STZ-induced with a single intraperitoneal injection of 55 mg/kg body weight. Values were compared using ANOVA followed by *post hoc* Bonferroni tests, * significantly different from control, + significantly different from diabetic, $P < 0.05$, $n = 8$.

Figure 3.2

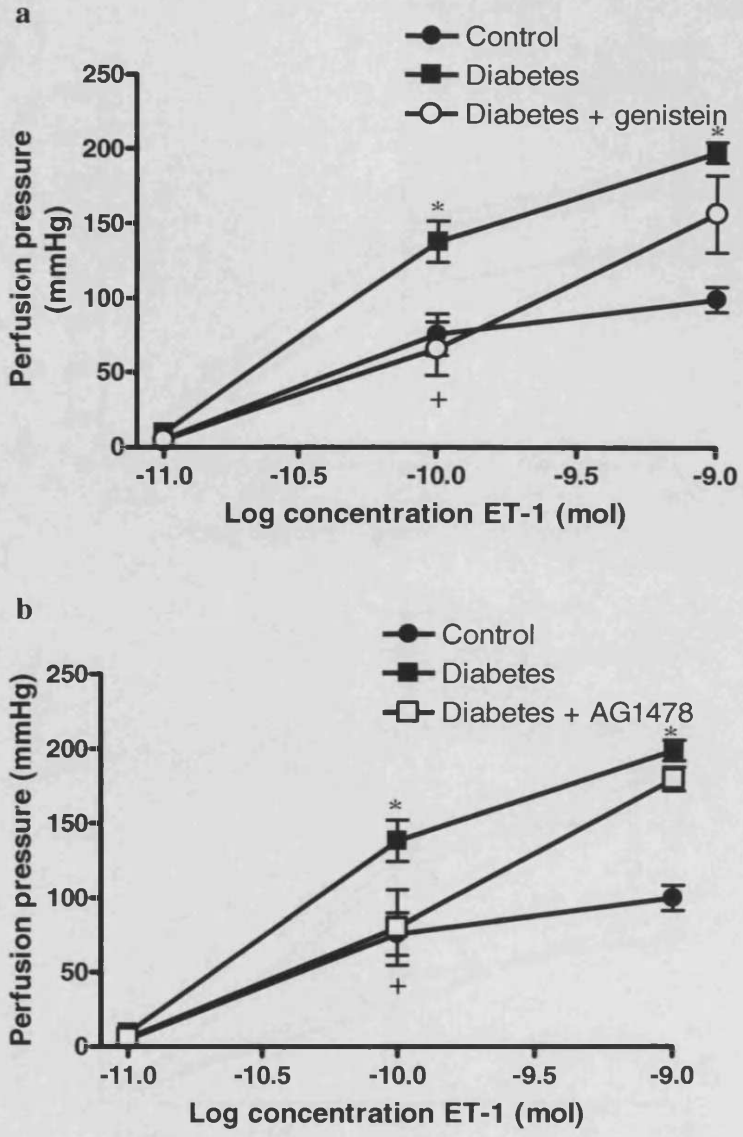
a
Control
Diabetes
Diabetes + genistein
Perfusion pressure (mmHg)
250
200
150
100
50
0
-11.0
-10.5
-10.0
-9.5
-9.0
Log concentration ET-1 (mol)
b
Control
Diabetes
Diabetes + AG1478
Perfusion pressure (mmHg)
250
200
150
100
50
0
-11.0
-10.5
-10.0
-9.5
-9.0
Log concentration ET-1 (mol)

Figure 3.2 continued

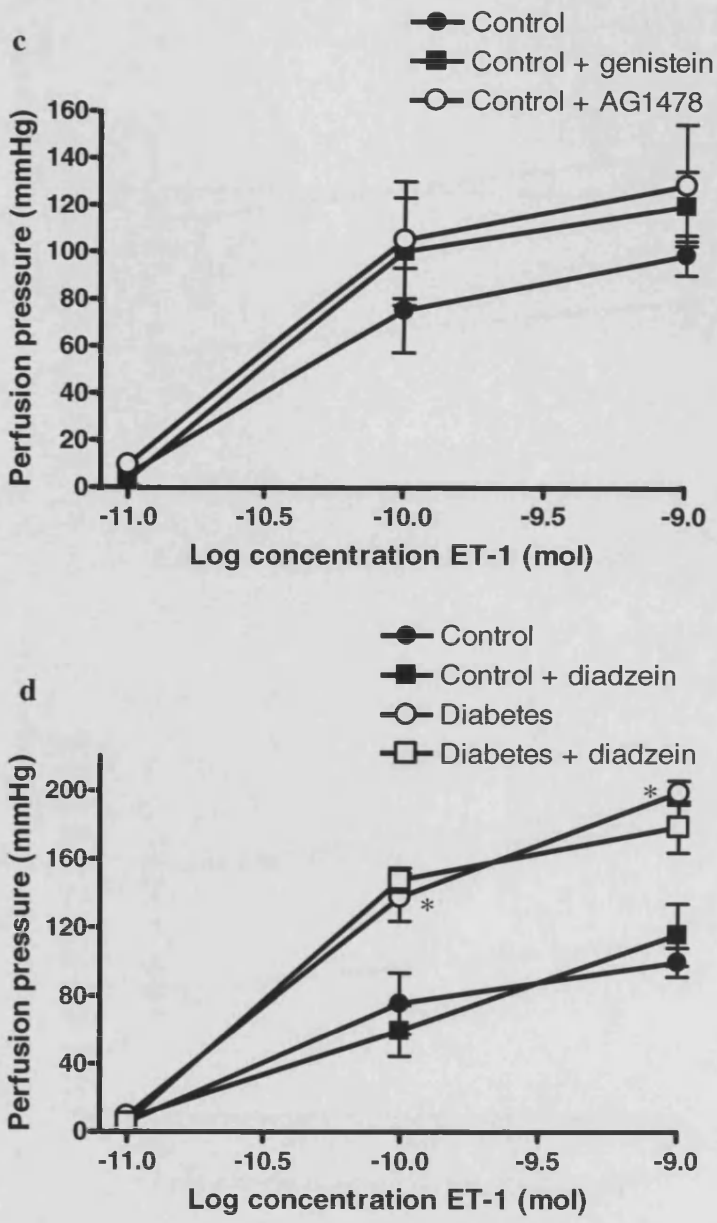

Effect of ET-1 on the mesenteric vascular bed of control, diabetic and RTK antagonists chronically treated control and diabetic rats. ET-1-induced vasoconstriction was measured as perfusion pressure (mmHg) in the mesenteric vascular bed perfused with Krebs' solution (mean ± SEM). a) Responses in control, diabetic, and chronic genistein-treated diabetic rats b) control, diabetic and chronic AG1478-treated diabetic rats c) control, chronic genistein-treated control and chronic AG1478-treated control rats and d) control, diabetic, chronic diadzein-treated control and chronic diadzein-treated diabetic rats. Genistein, AG1478 and diadzein treatments were for four weeks with 1.5 mg/kg body weight intraperitoneal injections on alternate days. Diabetic rats were STZ-induced with a single intraperitoneal injection of 55 mg/kg body weight. Values were compared using ANOVA followed by *post hoc* Bonferroni tests, * significantly different from control, + significantly different from diabetic, $P < 0.05$, $n = 8$.

Figure 3.3

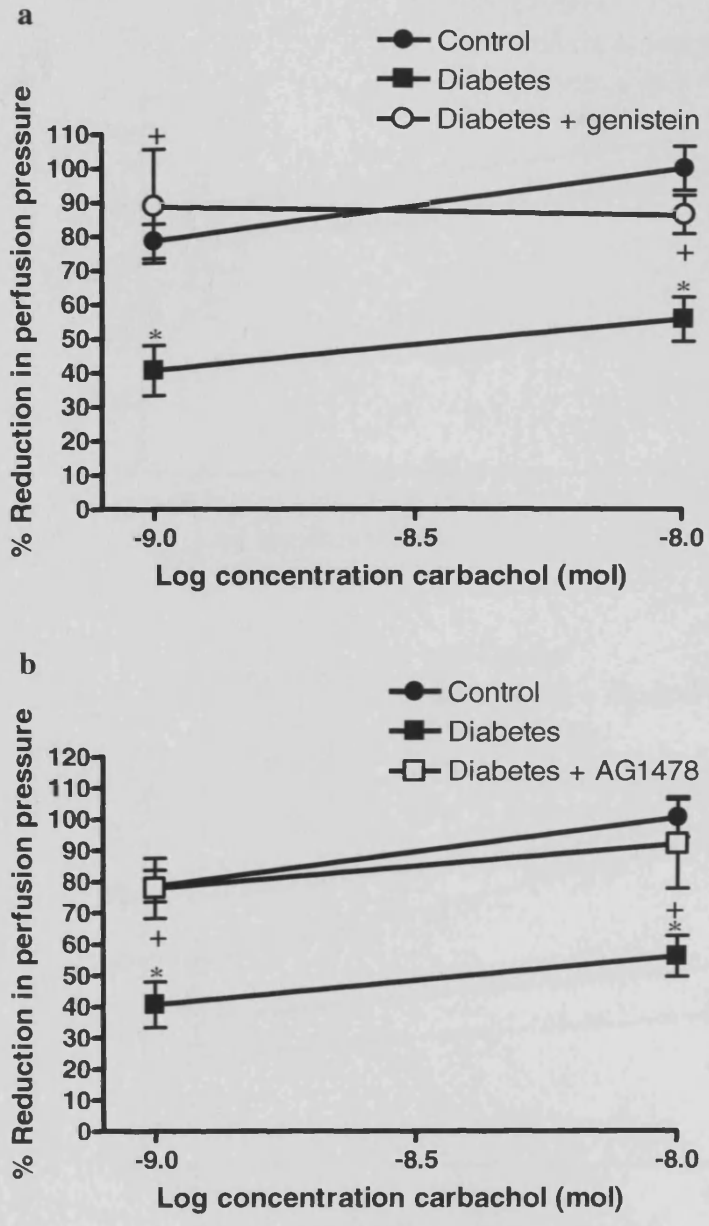

Figure 3.3 continued

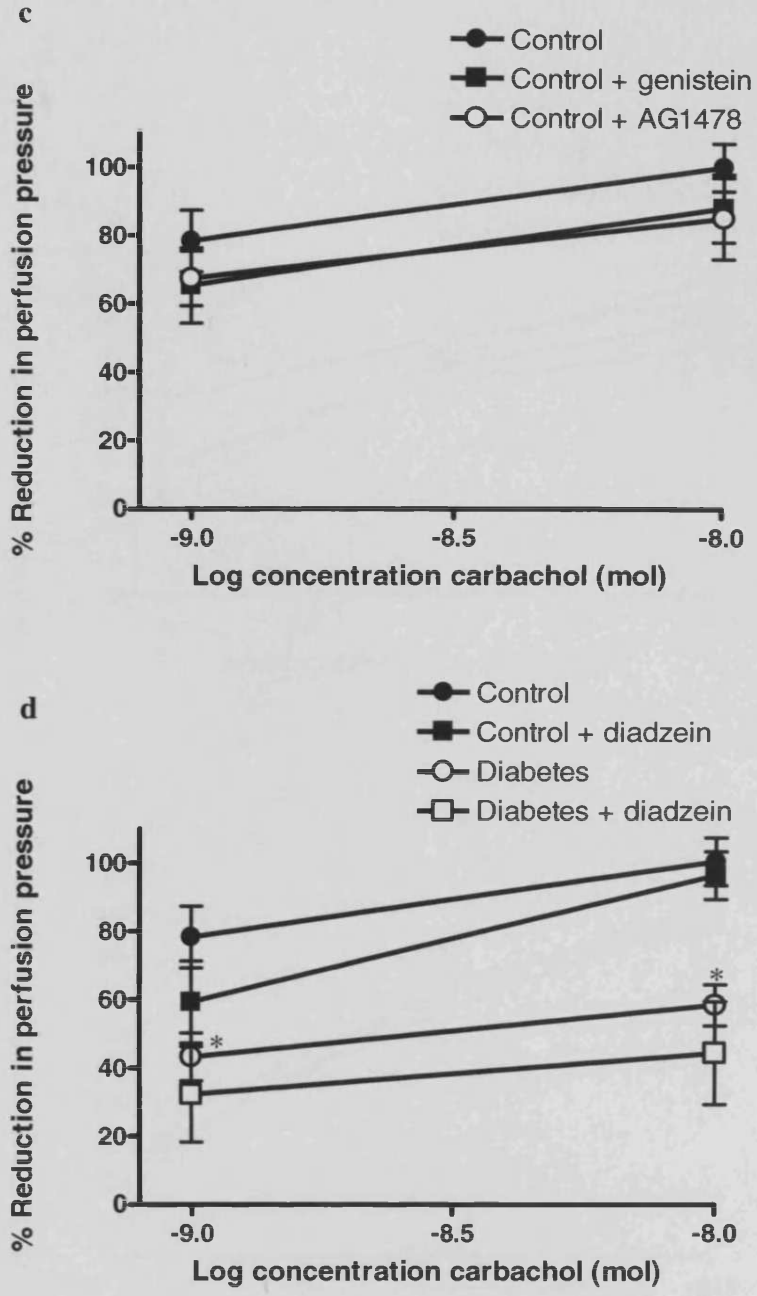

Effect of carbachol on the mesenteric vascular bed of control, diabetic and RTK antagonists chronically treated control and diabetic rats. Carbachol-induced vasodilation was measured as % reduction in perfusion pressure of 10^{-5} M NA induced contraction in the mesenteric vascular bed perfused with Krebs' solution (mean ± SEM). a) Responses in control, diabetic, and chronic genistein-treated diabetic rats b) control, diabetic and chronic AG1478-treated diabetic rats c) control, chronic genistein-treated control and chronic AG1478-treated control rats and d) control, diabetic, chronic diadzein-treated control and chronic diadzein-treated diabetic rats. Genistein, AG1478 and diadzein treatments were for four weeks with 1.5 mg/kg body weight intraperitoneal injections on alternate days. Diabetic rats were STZ-induced with a single intraperitoneal injection of 55 mg/kg body weight. Values were compared using ANOVA followed by *post hoc* Bonferroni tests, * significantly different from control, + significantly different from diabetic, $P < 0.05$, $n = 8$.

Figure 3.4

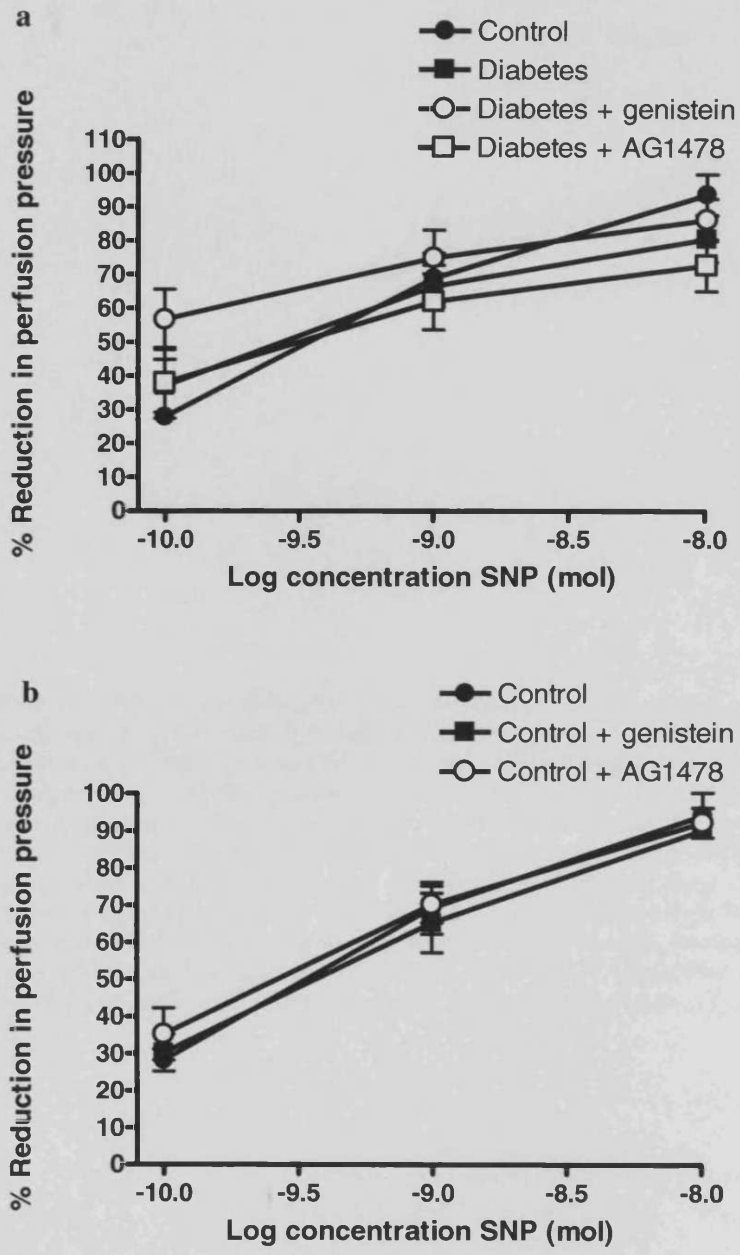
a
Control
Diabetes
Diabetes + genistein
Diabetes + AG1478
% Reduction in perfusion pressure
110
100
90
80
70
60
50
40
30
20
10
0
-10.0
-9.5
-9.0
-8.5
-8.0
Log concentration SNP (mol)
b
Control
Control + genistein
Control + AG1478
% Reduction in perfusion pressure
100
90
80
70
60
50
40
30
20
10
0
-10.0
-9.5
-9.0
-8.5
-8.0
Log concentration SNP (mol)

Figure 3.4 continued

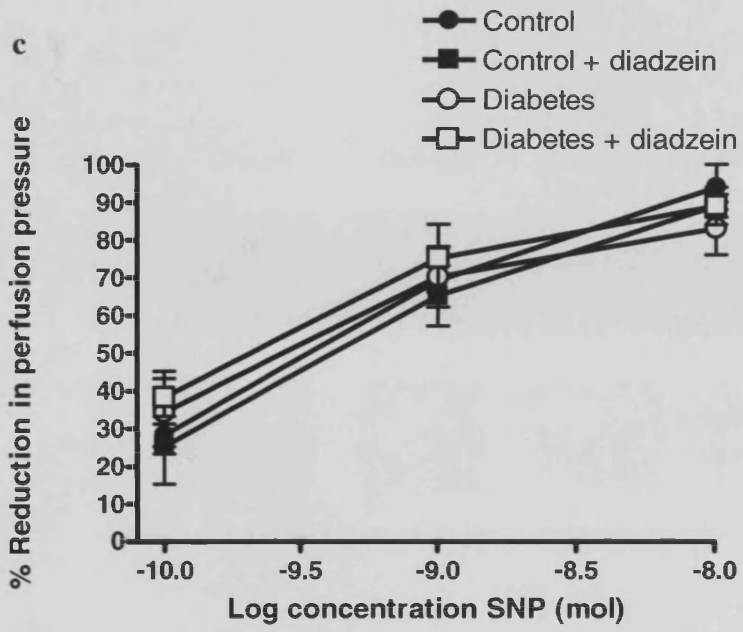

Effect of SNP on the mesenteric vascular bed of control, diabetic and RTK antagonists chronically treated control and diabetic rats. SNP-induced vasodilation was measured as % reduction in perfusion pressure of 10^{-5} M NA induced contraction in the mesenteric vascular bed perfused with Krebs' solution (mean ± SEM). a) Responses in control, diabetic, chronic genistein-treated diabetic and chronic AG1478-treated diabetic rats b) control, chronic genistein-treated control and chronic AG1478-treated control rats c) control, diabetic, chronic diadzein-treated control and chronic diadzein-treated diabetic rats. Genistein, AG1478 and diadzein treatments were for four weeks with 1.5 mg/kg body weight intraperitoneal injections on alternate days. Diabetic rats were STZ-induced with a single intraperitoneal injection of 55 mg/kg body weight. Values were compared using ANOVA followed by *post hoc* Bonferroni tests, * significantly different from control, + significantly different from diabetic, $P < 0.05$, $n = 8$.

Figure 3.5

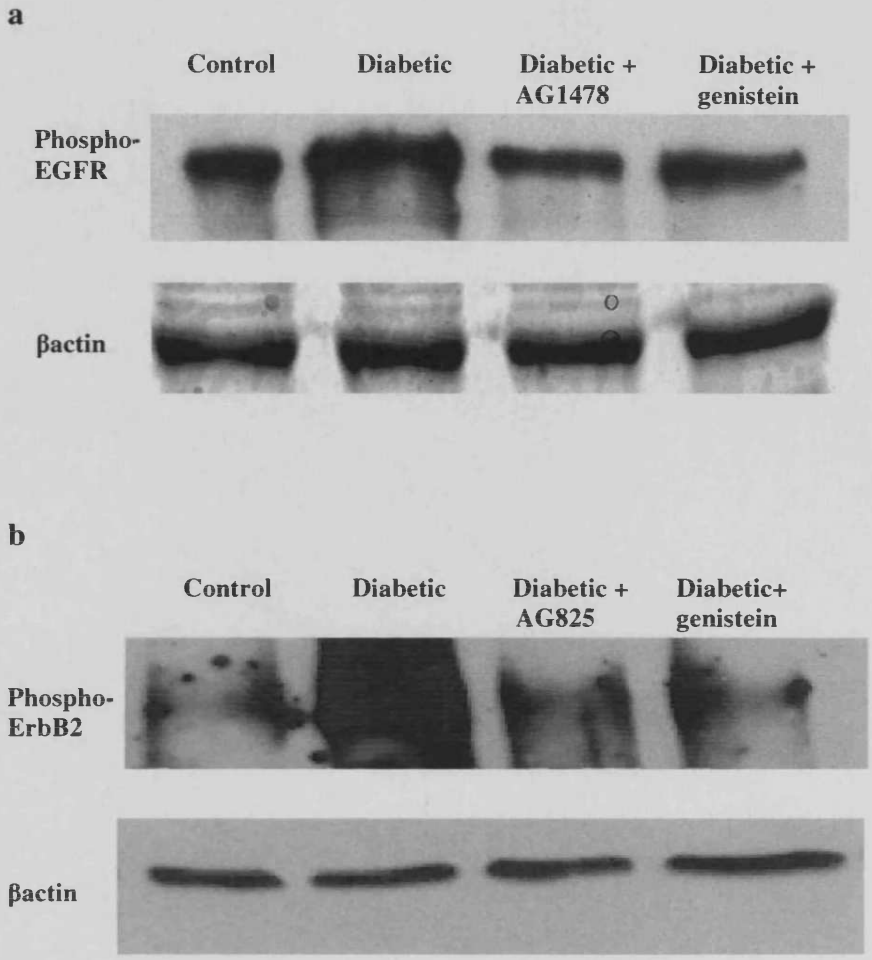

Effects of chronic genistein and AG1478 treatments on EGFR phosphorylation, and the effects of chronic genistein and AG825 treatments on ErbB2 phosphorylation in the mesenteric bed of diabetic rats. a) Western blot analysis of EGFR phosphorylation in the mesenteric vascular bed tissue of control, diabetic, chronic AG1478-treated diabetic and chronic genistein-treated diabetic rats and b) western blot analysis of ErbB2 phosphorylation in the mesenteric bed tissue of control, diabetic, chronic AG825-treated diabetic and chronic genistein-treated diabetic rats. Genistein, AG1478 and AG825 treatments were for four weeks with 1.5 mg/kg body weight intraperitoneal injections on alternate days. Diabetic rats were STZ-induced with a single intraperitoneal injection of 55 mg/kg body weight. β-actin was used as a control to verify an equal protein loading in each lane, $n = 3$ for both a) and b).

3.2 Characterization of Human ECV-304 Cells and the Effect of High Glucose on EGFR and ErbB2 in These Cells

Introduction

Section 3.1 demonstrated reduced action of the endothelium-dependent vasodilator carbachol in tissues from STZ-induced diabetic rats, suggesting reduced NO-mediated vasodilation. Additionally, vascular response to SNP, a NO donor, was unaltered in STZ-induced diabetic rats suggesting that vascular smooth muscle responses to NO were unaffected. These results suggest that the attenuated vasodilator effect observed in the STZ-induced diabetic rat tissue is due to an abnormality at the level of the endothelium. The more common human endothelial cell model human umbilical vein endothelial cells (HUVECs) were not available for the present studies. As a result, further investigations of the role of EGFR in diabetes induced vascular dysfunction were carried out using the human endothelial-like cell line ECV-304. ECV-304 cells were until recently believed to be spontaneously transformed endothelial cells derived from human infant's umbilical cord (Takahashi, *et al* 1990b). However, more recently there have been some discrepancies regarding the cell line's true identity and questions raised regarding its validity as a human endothelial cell model (Brown, *et al* 2000, Masters, *et al* 2001). Nevertheless, studies have shown that ECV-304 cells display many features and markers characteristic of endothelial cells (Takahashi, *et al* 1990b), thus ECV-304 is still widely used as an endothelial cell model (Paulino, *et al* 2007, Shi, *et al*

2007). In this section, the aim was to further investigate the effects of high glucose on EGFR and ErbB2 using the human ECV-304 cells.

Results

Characterization of ECV-304 Cells

Before proceeding with the investigations, a basic characterization of the cell line was undertaken to confirm the usefulness of ECV-304 as an endothelial cell model. Polymerase chain reaction (PCR) or western blotting techniques were used to confirm the presence of endothelial nitric oxide synthase (eNOS) (140kDa) and connexin 43 (289 bp), which are both proteins found in the endothelium. Also the presence of EGFR (636 bp/ 175kDa) and ErbB2 (98 bp/ 185kDa) were confirmed in these cells (Figs. 3.6a and 3.6b). For each protein western blotting revealed a single band at the expected molecular weight, as estimated by means of molecular weight markers. Also for each gene PCR showed a single band at the expected size, as estimated using hyperladder IV.

ECV-304 Growth Curve

Cell sets at 3 seeding densities (12,500, 25,000 and 50,000 cells/well) showed similar growth profiles and growth rates, with exponential growth from 24 up to approximately 120 hours. By approximately 168 hours after seeding, growth rates of all three cell sets slowed proportional to seeding density. By 218 hours after seeding the number of cells was equivalent for all three cell sets (Fig. 3.7).

Effect of High Glucose on ECV-304 Cell Growth

Cells grown in 5.5mM glucose showed exponential growth (log phase) until approximately 62 hours after seeding. Following which a plateau was reached indicating cell confluency. Cells grown in 25.5mM glucose demonstrated a lag phase between 0 and approximately 24 hours after seeding, where there was no growth. Then these cells grew exponentially for approximately 48 hours after which a short plateau was reached. Then at the 72 hour point cell numbers began to decline. At the final count, approximately 120 hours after seeding the number of cells was less than the number originally seeded (Fig. 3.8).

Effect of High Glucose on EGFR and ErbB2 Expression and Phosphorylation: Concentration-response Relationships

ECV-304 cells exposed to 10.5 - 25.5 mM of glucose in serum free medium for 72 hours demonstrated increased levels of pEGFR and pErbB2 as compared to control cells grown in 5.5mM glucose. A glucose concentration of 25.5 mM was subsequently chosen for further studies, and is further referred to as high glucose in this text (Figs. 3.9a and 3.9b).

Time Course

Treatment of ECV-304 cells with 25.5 mM (high) glucose for 1 hour and 6 hours had no observable effect on levels of pEGFR or pErbB2. Twenty four hours of high glucose treatment increased levels of both pEGFR and pErbB2, as compared to their respective controls. EGFR and ErbB2 phosphorylation

was further increased following 72 hours of treatment with high glucose (Figs. 3.10a and 3.10b).

Seventy two hours of high glucose exposure had no effect on levels of EGFR protein and mRNA expression shown by western blot and PCR respectively (Figs. 3.11a and 3.11b). Similarly 72 hours of high glucose exposure failed to affect the levels of ErbB2 protein and mRNA expression (Figs. 3.12a and 3.12b).

Osmotic Control

To account for the osmotic effect of glucose, ECV-304 cells were exposed to its metabolically inactive stereoisomer L-glucose. The treatment of ECV-340 cells for 72 hours with L-glucose did not have any observable effect on the levels of pEGFR and pErbB2 as shown by western blot (Figs. 3.13a and 3.13b).

Effect of EGFR and ErbB2 Blockade with AG1478 and AG825

AG1478 and AG825 were both solubilized using dimethyl sulfoxide (DMSO). However, above a particular concentration DMSO becomes cytotoxic, therefore, before using this solvent the threshold concentration for DMSO cytotoxicity in ECV-304 cells was established. ECV-304 cells survived when exposed to ≤ 2 % DMSO before a major drop in cell numbers was observed. At 4 % DMSO was cytotoxic, reducing cell numbers by more than 50 % (Fig.

3.14). Therefore, 1 % (v/v, final concentration) of DMSO was used in experiments involving the use of AG1478 or AG825.

Treatment of ECV-304 cells grown in high glucose with increasing concentrations of AG1478 for 72 hours resulted in a concentration-related inhibition of EGFR phosphorylation at Tyr1068 (Fig. 3.15a). In all further cell culture studies that involved the use of this inhibitor maximal effect was desired thus, from the inhibitor concentration-response relationship 0.5 μM of AG1478 was always used. At this concentration 72 hours of AG1478 treatment was more selective for reducing phosphorylation of EGFR compared to ErbB2 in ECV-304 cells grown in high glucose, although a reduction in the levels of pErbB2 was observed with this agent (Fig. 3.16).

Treatment of cells grown in high glucose with increasing concentrations of AG825 similarly decreased levels of ErbB2 phosphorylation at Tyr1248 in a concentration dependent manner (Fig. 3.15b). Again maximal effect was desired thus, from the inhibitor concentration-response relationship 20 μM of AG825 was used in future cell culture studies that involved the use of this inhibitor. At this concentration AG825 was more selective for reducing phosphorylation of ErbB2 compared to EGFR following a 72 hour treatment of ECV-304 cells (Fig. 3.16).

Also the effect of AG1478 and AG825 on EGFR and ErbB2 phosphorylation in control ECV-304 cells grown in 5.5 mM glucose was investigated. In these

cells, AG1478 treatment for 72 hours decreased levels of pEGFR and pErbB2 as compared to control. A 72 hour treatment with AG825 had little effect on EGFR phosphorylation in these cells but markedly lowered ErbB2 phosphorylation (Figs. 3.17a and 3.17b).

Effect of High Glucose on EGFR and ErbB2 Heterodimerization

A co-immunoprecipitation assay was developed to detect protein-protein interactions between EGFR and ErbB2. The effect of high glucose, AG1478 and AG825 on EGFR/ErbB2 heterodimerization was investigated in these cells.

Immunoprecipitation revealed a direct interaction between EGFR and ErbB2 in ECV-304 cells that was increased by 72 hours of high glucose. The increase in molecular interaction induced by high glucose was decreased by treatment of the cells for 72 hours with AG1478 and decreased to less than control levels by treatment with AG825. Levels of immunoprecipitated EGFR remained equal, indicating equal total EGFR protein level (Fig. 3.18).

In this section in each case where β-actin was used to verify an equal loading of protein or mRNA levels of β-actin which were found at the expected size (204 bp/ 42 kDa) remained constant.

Figure 3.6

a

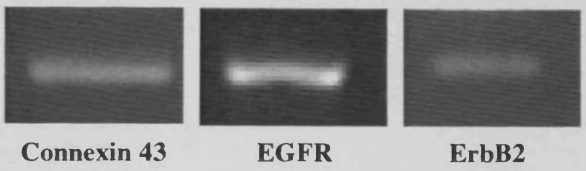

b

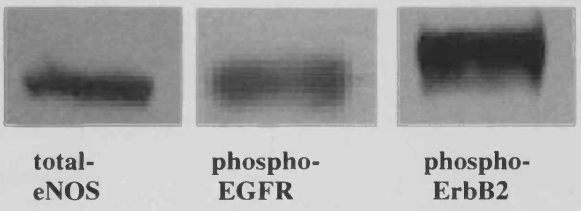

Characterization of ECV-304 cells. a) PCR showing connexin 43, EGFR and ErbB2 mRNA expression and b) western blot analysis of EGFR and ErbB2 phosphorylation and total eNOS protein expression in control ECV-304 cells grown in normal M199 medium for 72 hours, n = 3 for both a) and b).

Figure 3.7

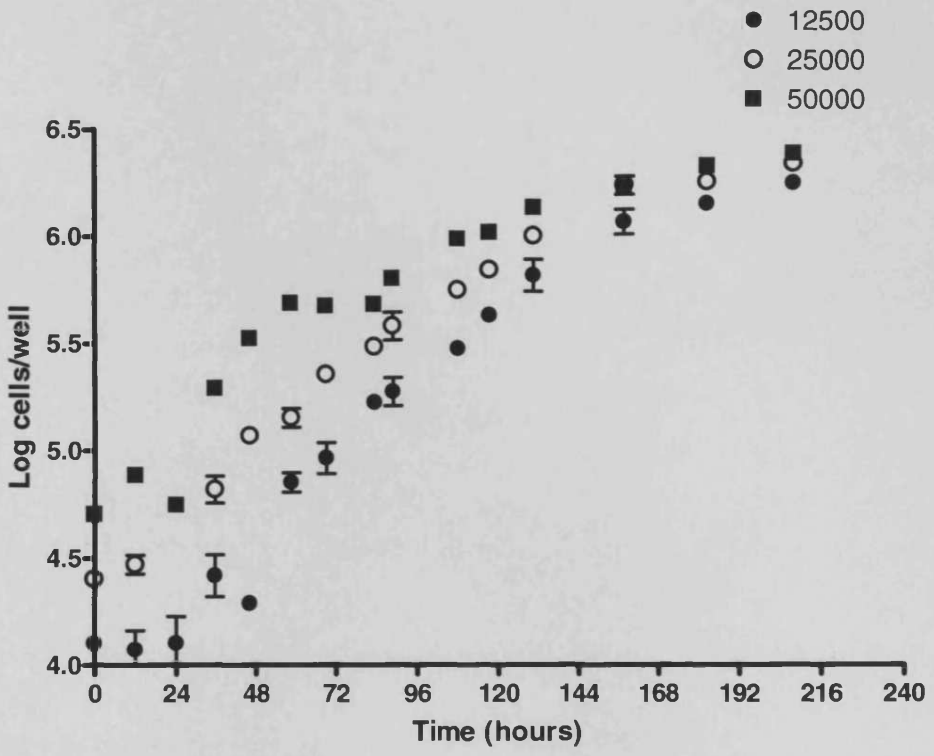

Effect of seeding density on ECV-304 cell growth. Growth curves for ECV-304 cells over 9 days in normal M199 medium (± SEM). Cells were seeded in 24 well plates at seeding densities of 12500, 25000 and 50000 and were counted every 12 hours for the first 5 days and every 24 hours thereafter, $n = 3$.

Figure 3.8

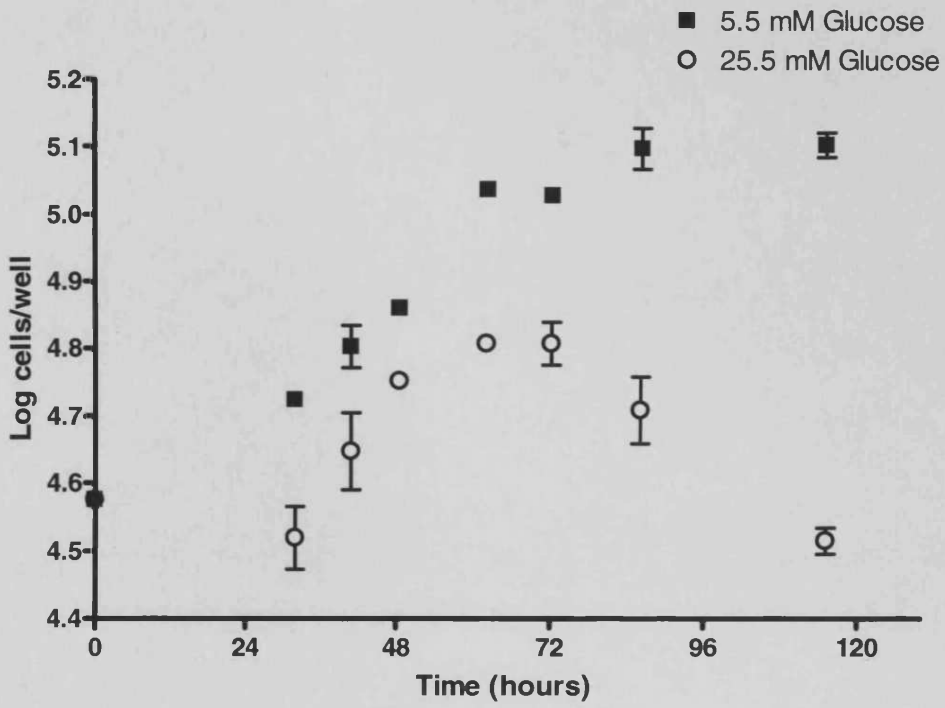

Effect of high glucose on ECV-304 cell growth. Cells were seeded in 24 well plates at a seeding density of 25000 cells per well and were incubated for 24 hours in normal M199 medium. Then the cell medium was changed to M199 with 5.5 mM or 25.5 mM glucose. Cells were counted every 10 - 12 hours on days 2 - 4 and only once on day 5 (± SEM, n = 3).

Figure 3.9

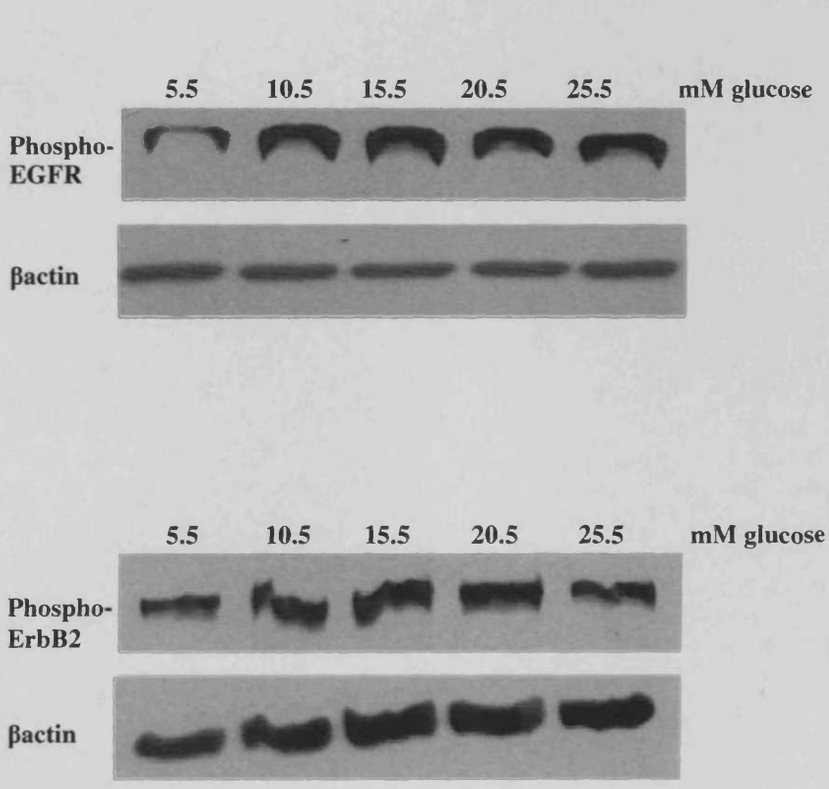

Effects of increasing glucose concentrations on EGFR and ErbB2 phosphorylation in ECV-304 cells. Cells were grown in normal M199 medium for 24 hours and in serum-free medium for a further 24 hours. Then the cells were exposed to various concentrations of glucose for 72 hours, then protein was extracetd for western blotting. a) Western blot analysis of pEGFR and b) western blot analysis of pErbB2. β-actin was used as a control to verify and equal protein loading in each lane, n = 3 for both a) and b).

Figure 3.10

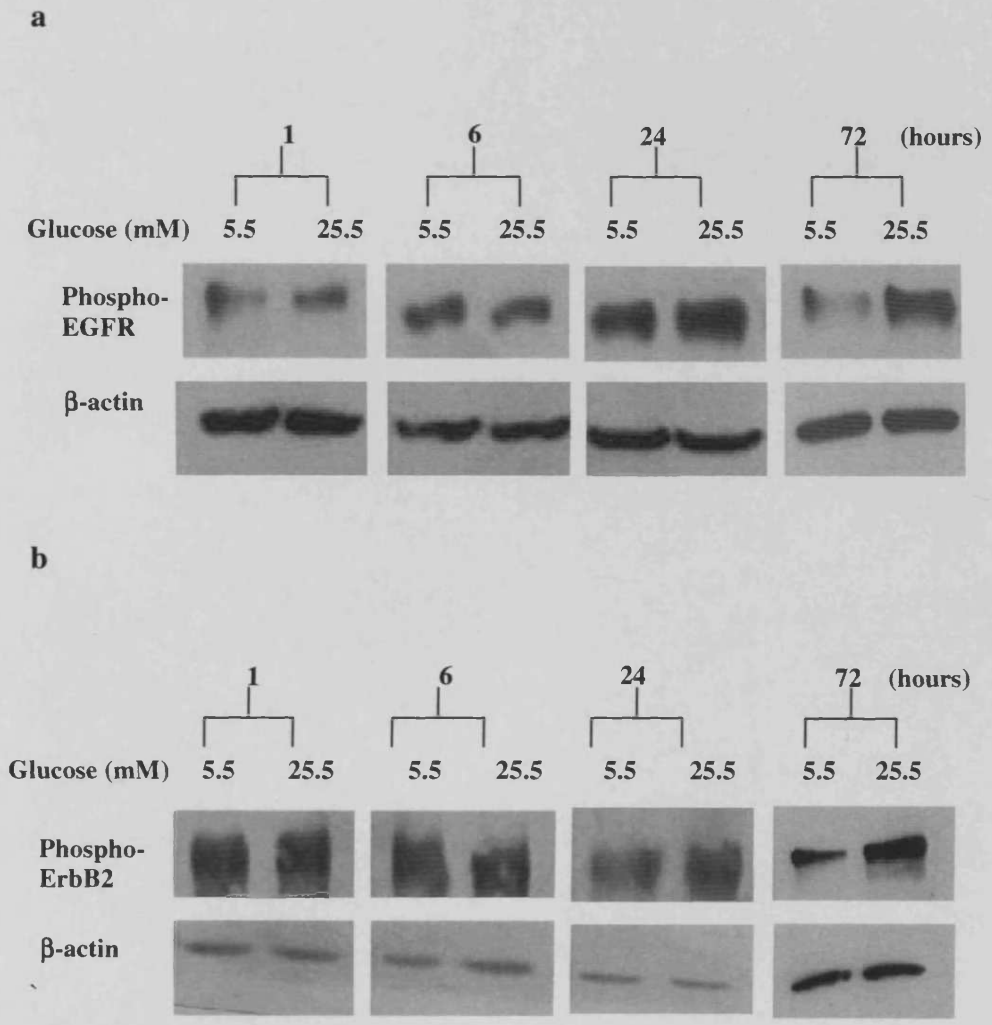

Effect of high glucose on EGFR and ErbB2 phosphorylation at increasing time points in ECV-304 cells. Cells were grown in normal M199 medium for 24 hours and in serum-free medium for a further 24 hours. Then the cells were exposed to 5.5 and 25.5 mM glucose and protein was extracted for western blotting at various time points. a) Western blot analysis of pEGFR and b) western blot analysis of pErbB2. β-actin was used as a control to verify and equal protein loading in each lane, $n = 3$ for both a) and b).

Figure 3.11

a

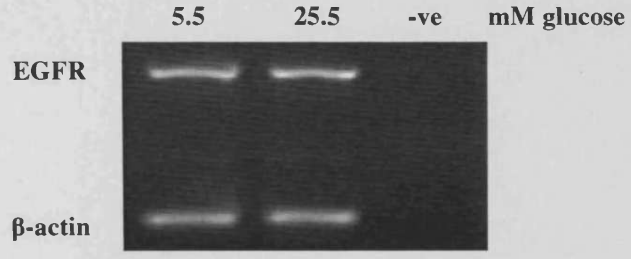

b

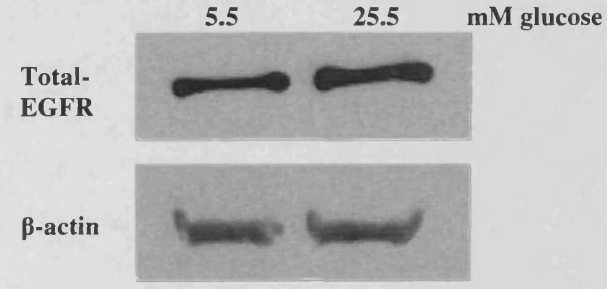

Effects of high glucose on EGFR mRNA and protein expression in ECV-304 cells. Cells were grown in normal M199 medium for 24 hours and in serum-free medium for a further 24 hours. Then the cells were exposed to 5.5 and 25.5 mM glucose for 72 hours and RNA was extracted for PCR analysis or protein was extracted for western blotting. a) PCR analysis of EGFR mRNA expression and b) western blot analysis of total EGFR protein expression. β-actin was used as a control to verify and equal mRNA or protein loading in each lane, n = 3 for both a) and b).

Figure 3.12

a

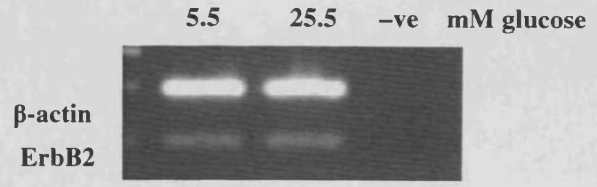

b

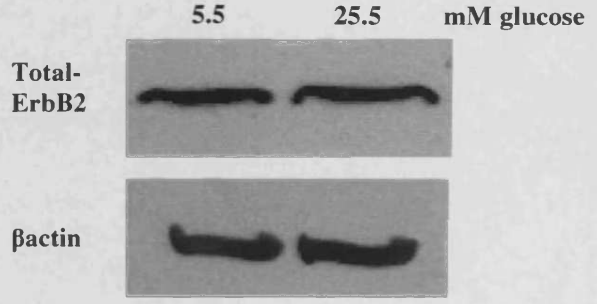

Effects of high glucose on ErbB2 mRNA and protein expression in ECV-304 cells. Cells were grown in normal M199 medium for 24 hours and in serum-free medium for a further 24 hours. Then the cells were exposed to 5.5 and 25.5 mM glucose for 72 hours and RNA was extracted for PCR analysis or protein was extracted for western blotting. a) PCR analysis of ErbB2 mRNA expression and b) western blot analysis of total ErbB2 protein expression. β-actin was used as a control to verify and equal mRNA or protein loading in each lane, n = 3 for both a) and b).

Figure 3.13

a

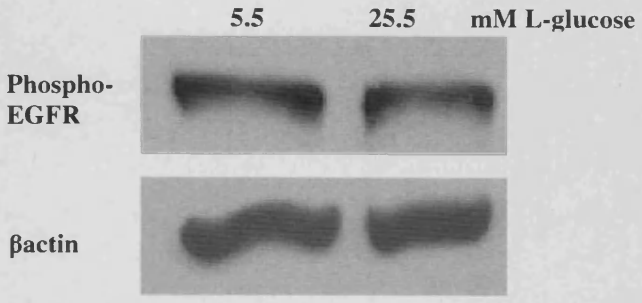

b

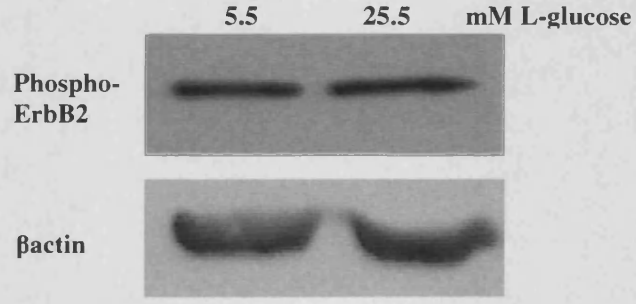

Effects of high L-glucose on EGFR and ErbB2 Phosphorylation in ECV-304 cells. Cells were grown in normal M199 medium for 24 hours and in serum-free medium for a further 24 hours. Then the cells were exposed to 5.5 and 25.5 mM L-glucose for 72 hours and protein was extracted for western blotting. a) Western blot analysis of pEGFR and b) western blot analysis of pErbB2. β-actin was used as a control to verify and equal protein loading in each lane, $n = 3$ for both a) and b).

Figure 3.14

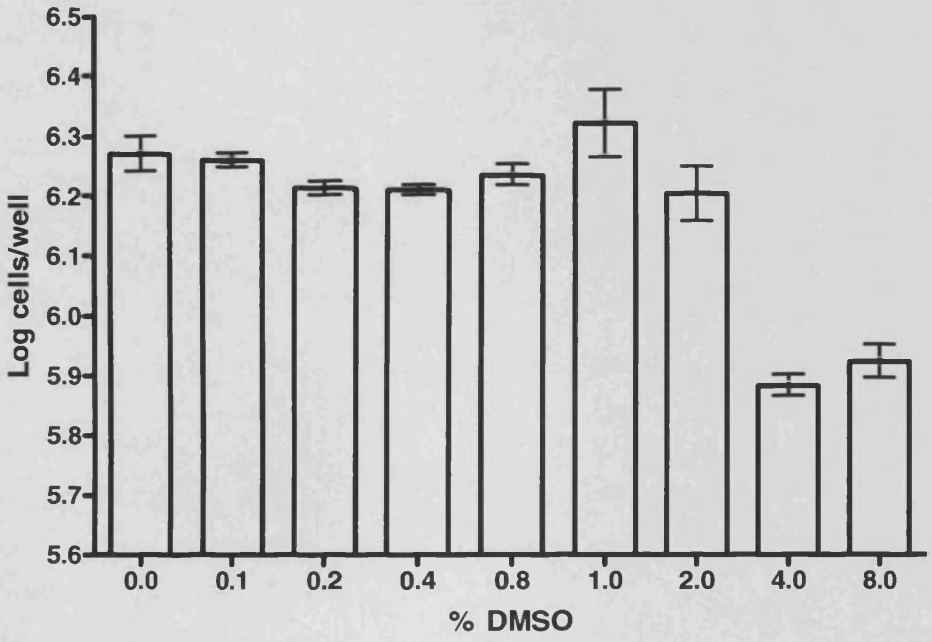

Effect of DMSO exposure on ECV-304 cell survival. Cells were grown for 72 hours in serum free medium in the absence or in the presence of DMSO at various concentrations, and then the cells were counted. Cell numbers are expressed as log cells per well (± S.E.M, n = 3).

Figure 3.15

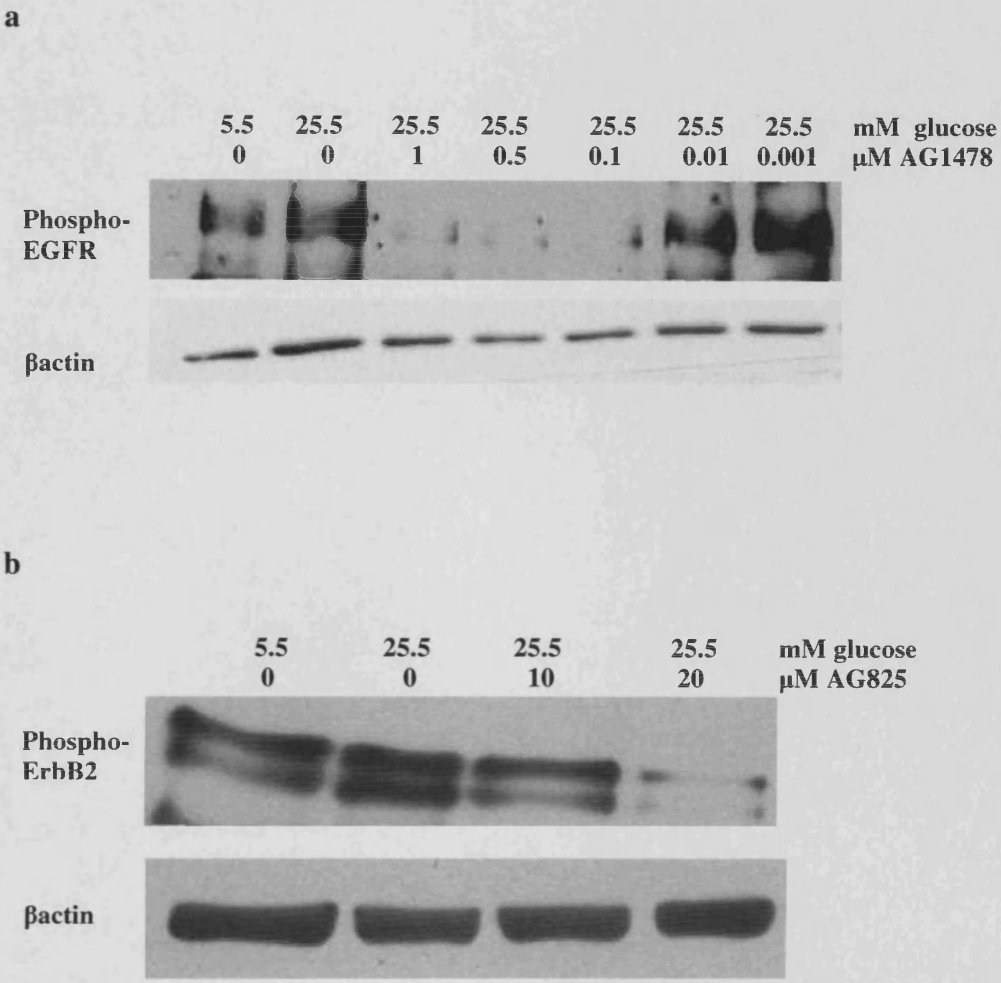

AG1478 and AG825 concentration-responses for inhibiting the phosphorylation of EGFR and ErbB2 respectively in ECV-304 cells. Cells were grown in normal M199 medium for 24 hours and in serum-free medium for a further 24 hours. Then the cells were exposed to high glucose + RTK inhibitors for 72 hours and protein was extracted for western blotting. a) Western blot of EGFR phosphorylation in untreated cells, in cells treated with 25.5mM glucose and in cells treated with 25.5mM glucose + various concentrations of AG1478 and b) western blot of ErbB2 phosphorylation in untreated cells, in cells treated with 25.5mM glucose and in cells treated with 25.5mM glucose + various concentrations of AG825. β-actin was used as a control to verify and equal protein loading in each lane, $n = 3$ for both a) and b).

Figure 3.16

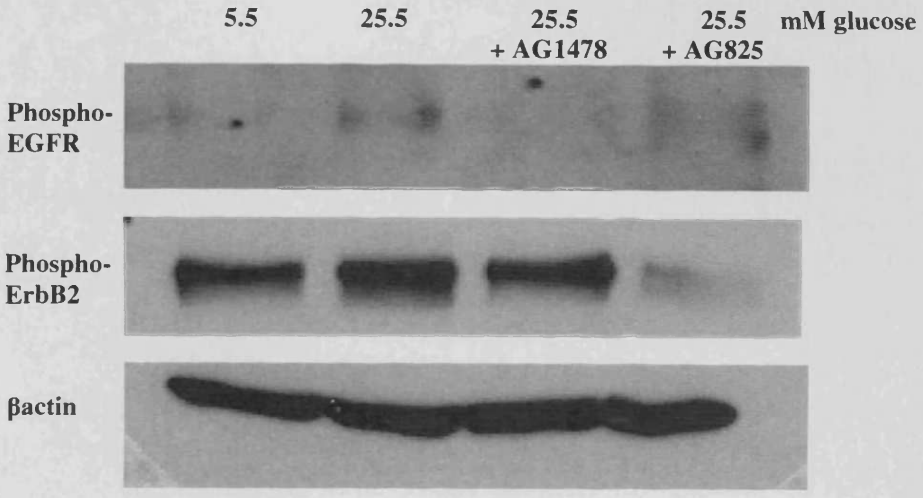

Effects of AG1478 and AG825 on EGFR and ErbB2 phosphorylation in ECV-304 Cells exposed to high glucose. Cells were grown in normal M199 medium for 24 hours and in serum-free medium for a further 24 hours. Then the cells were exposed to high glucose and RTK inhibitors for 72 hours and protein was extracted for western blotting. Western blot analysis of EGFR and ErbB2 phosphorylation in untreated cells, in cells treated with 25.5 mM glucose, in cells treated with 25.5 mM glucose + AG1478 (0.5 μM) and in cells treated with 25.5 mM glucose + AG825 (20 μM). β-actin was used as a control to verify and equal protein loading in each lane, $n = 3$.

Figure 3.17

a

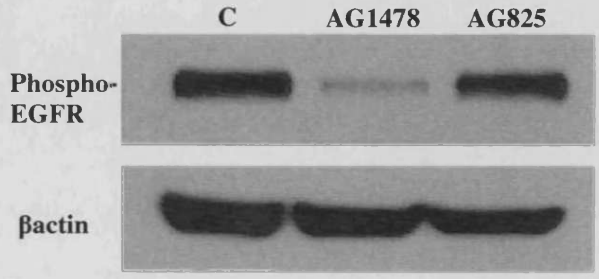

b

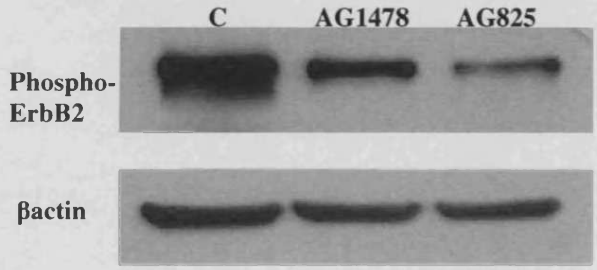

Effects of AG1478 and AG825 on EGFR and ErbB2 phosphorylation in ECV-304 cells grown in normal glucose levels. Cells were grown in normal M199 medium for 24 hours and in serum-free medium for a further 24 hours. Then the cells were exposed to RTK inhibitors for 72 hours and protein was extracted for western blotting. Western blot analysis of a) EGFR in control cells, in control cells treated with AG1478 (0.5 μM) and in control cells treated with AG825 (20 μM) and b) ErbB2 phosphorylation in control cells, in control cells treated with AG1478 (0.5 μM) and in control cells treated with AG825 (20 μM). β-actin was used as a control to verify and equal protein loading in each lane, $n = 3$ for both a) and b).

Figure 3.18

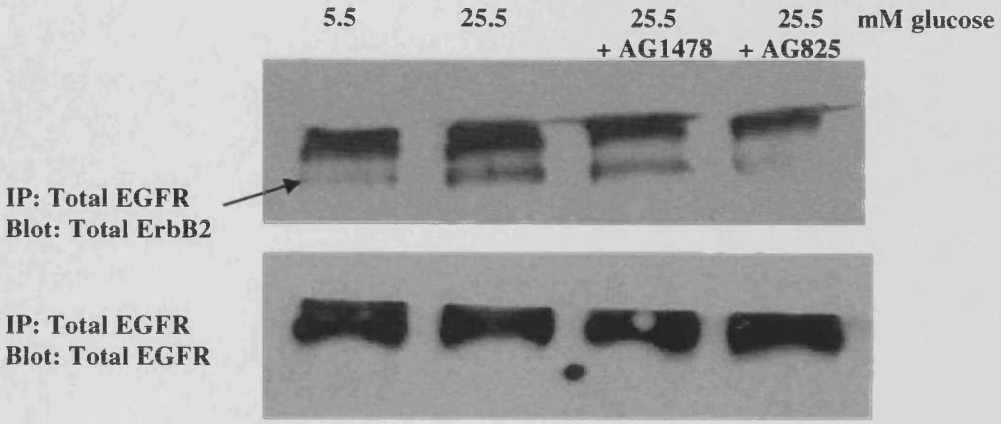

Effects of AG1478 and AG825 on EGFR and ErbB2 heterodimerization in ECV-304 cells exposed to high glucose for 72 hours. Cells were grown in normal M199 medium for 24 hours and in serum-free medium for a further 24 hours. Then the cells were exposed to high glucose and to RTK inhibitors for 72 hours and then protein was extracted for immunoprecipitation. By means of immunoprecipitation total EGFR antibody was used to pull down EGFR protein and any proteins that had complexed with it from the total lysate. This was then analysed via western blotting to examine the levels of ErbB2. Western blot shows control, 25.5 mM glucose, 25.5 mM glucose + AG1478 (0.5 μM) and 25.5 mM glucose + AG825 (20 μM) treated cells (upper panel). To verify an equal protein loading in each lane total levels of EGFR was also detected by western blotting (lower panel), $n = 3$.

3.3 The Effect of High Glucose on EGFR Ligand Production

Introduction

Results from previous sections suggest that pEGFR and pErbB2 levels are increased by high glucose. However, the mechanisms involved remain elusive. Studies have suggested that glucose acts upon some upstream component of EGFR such as increasing EGFR transactivation (Konishi and Berk 2003) or increasing EGFR ligand production (Asakawa, *et al* 1996). Hyperglycaemia-induced aberrant ligand production could indirectly alter EGFR phosphorylation. The aim of this section was to investigate the effect of high glucose on the mRNA expression of some common EGFR ligands.

Results

Exposure of ECV-304 cells to high glucose for 72 hours had no effect on the EGFR ligands: amphiregulin (AR) (350 bp), betacellulin (BTC) (395 bp), epiregulin (EPR) (304 bp), epidermal growth factor (EGF) (478 bp), heparin binding – EGF (HB-EGF) (300 bp) or transforming growth factor α (TGFα) (379 bp) mRNA expression. PCR showed a single band at the expected size, as estimated by means of hyperladder IV. In each case levels of β-actin did not change between samples (Fig. 3.19).

Figure 3.19

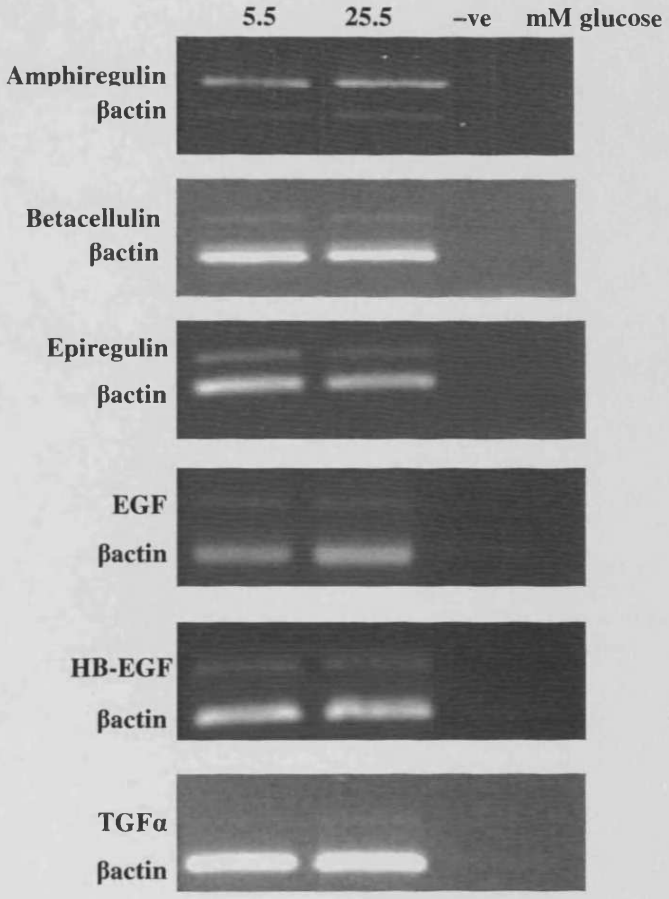

Effect of high glucose exposure on mRNA expression of EGFR ligands in ECV-304 cells. Cells were grown in normal M199 medium for 24 hours and in serum-free medium for a further 24 hours. Then the cells were exposed to 5.5 and 25.5 mM glucose for 72 hours and RNA was extracted for PCR. PCR analysis of amphiregulin, betacellulin, epiregulin, EGF, HB-EGF and TGFα mRNA. β-actin was used as a control to verify equal mRNA loading in each lane, $n = 1$.

3.4 Downstream Pathways Associated with the Activation of EGFR in ECV-304 Cells

Introduction

The heterodimerization and activation of EGFR and ErbB2 initiate signalling of a number of diverse pathways including the protein kinase C (PKC) phospholipid hydrolysis pathway, the exracellular signal-regulated kinase 1/2 (ERK1/2) cell proliferation and differentiation pathway, the Akt anti-apoptotic pathway and the p38 mitogen activated protein kinase (p38MAPK) stress activated pathway. The aim of this section was to confirm that the activation of EGFR by the ligand EGF is associated with the activation of these downstream pathways.

Results

EGF Concentration-response in Cells Grown in 5.5 mM Glucose

The level of pEGFR was relatively low in unstimulated ECV-304 cells but increased in a concentration-dependent manner when stimulated for 10 minutes with 1, 10 and 100 ng/ml of EGF (Fig. 3.20a). A similar response to 1, 10 and 100 ng/ml of EGF was seen for pErbB2 levels (Fig. 3.20b).

For blots showing pPKC levels both bands seen on the blot represent levels of pPKC and the same applies for all other pPKC blots shown in this text. The expected molecular weights of the PKC isoforms detected using the pan antibody (α, β I, β II, δ, ε, η and θ) are 78, 80, 82 and 85 kDa. As expected,

both bands were found at around 78-85 kDa as estimated using molecular weight markers. Western blots for p38MAPK and Akt always showed single bands at 43 and 60 kDa respectively as estimated using molecular weight markers, which were the expected molecular weights for these proteins. Also, as expected, western blots for ERK1/2 always showed a double band at 42 and 44 kDa.

The levels of pPKC and pp38MAPK were also relatively low in unstimulated ECV-304 cells. 10 minutes of EGF at 1, 10 and 100 ng/ml activated both in a concentration-dependent manner with maximal activation observed at 10 ng/ml. Interestingly 100 ng/ml promoted activation of both proteins but not to the same extent as 10 ng/ml (Figs. 3.21a and 3.21b).

Relatively low levels of pAkt and pERK1/2 were present in unstimulated ECV-304 cells. These levels were again markedly increased upon stimulation with 1, 10 and 100 ng/ml of EGF for 10 minutes with maximal activation being achieved at a concentration of 1 ng/ml of EGF (Figs. 3.21c and 3.21d).

EGF Time Course Studies in Cells Grown in 5.5 mM Glucose

Due to time constraints only time courses for pEGFR, pErbB2, pPKC and pAkt were completed.

Increased phosphorylation of both EGFR and ErbB2 was observed as early as 1 minute following 10 ng/ml EGF treatment and was maximal at 10 minutes.

Maximal activation of both receptors was maintained up to 60 minutes following initial exposure of the cells to EGF (Figs. 3.22a and 3.22b).

Exposure of cells to 10 ng/ml of EGF increased pPKC after 1 minute and maximal activation was observed 10 minutes after initial exposure. Maximal activation was again maintained up to 60 minutes following initial exposure of cells to EGF (Fig. 3.23a).

Stimulation of cells with 10 ng/ml of EGF for as little as 1 minute maximally phosphorylated Akt, and maximal activation was observed up to 10 minutes following initial exposure of cells to 10 ng/ml EGF. After 60 minutes the level decreased from maximal but not back down to control levels (Fig. 3.23b).

In each case in this section the level of β-actin remained constant between each sample.

Figure 3.20

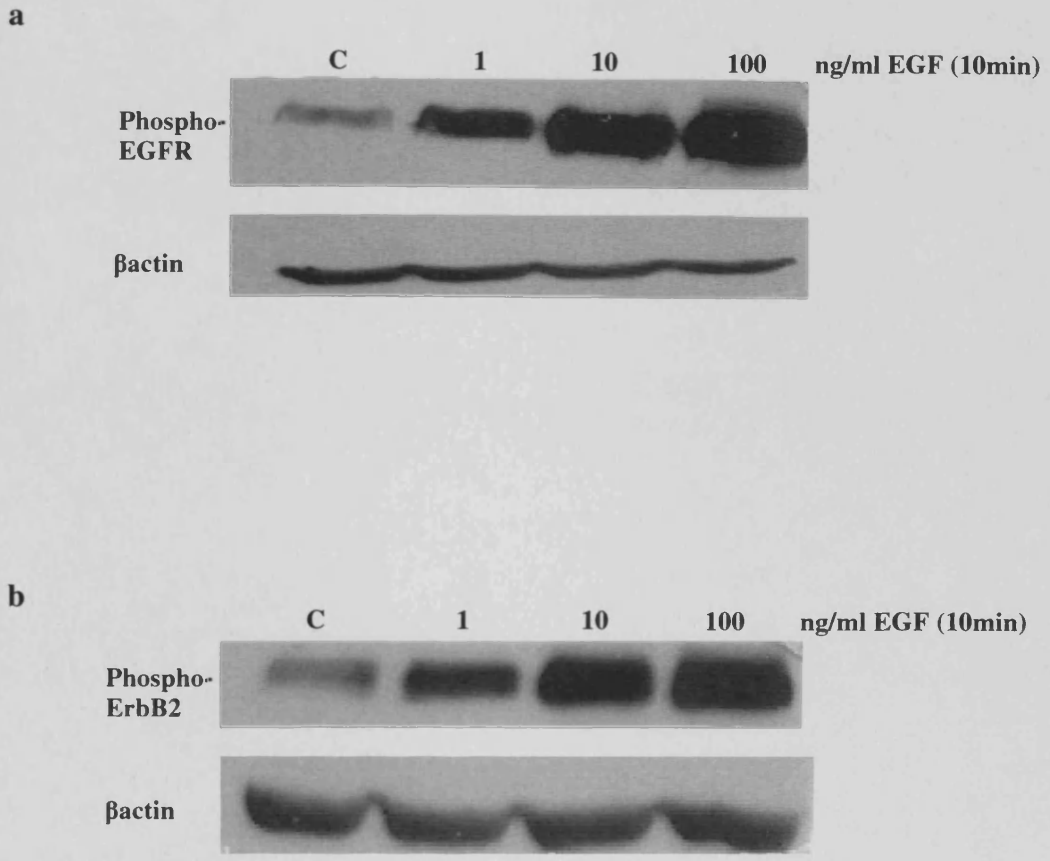

Effects of increasing EGF concentrations on EGFR and ErbB2 phosphorylation in ECV-304 cells. Cells were grown in normal M199 medium for 24 hours and then various concentrations of EGF was added, after 10 minutes the protein was extracted for western blotting. Western blot of a) EGFR phosphorylation and b) ErbB2 phosphorylation in ECV-304 cells in the absence or following treatment with EGF. β-actin was used as a control to verify and equal protein loading in each lane, $n = 3$ for both a) and b).

Figure 3.21

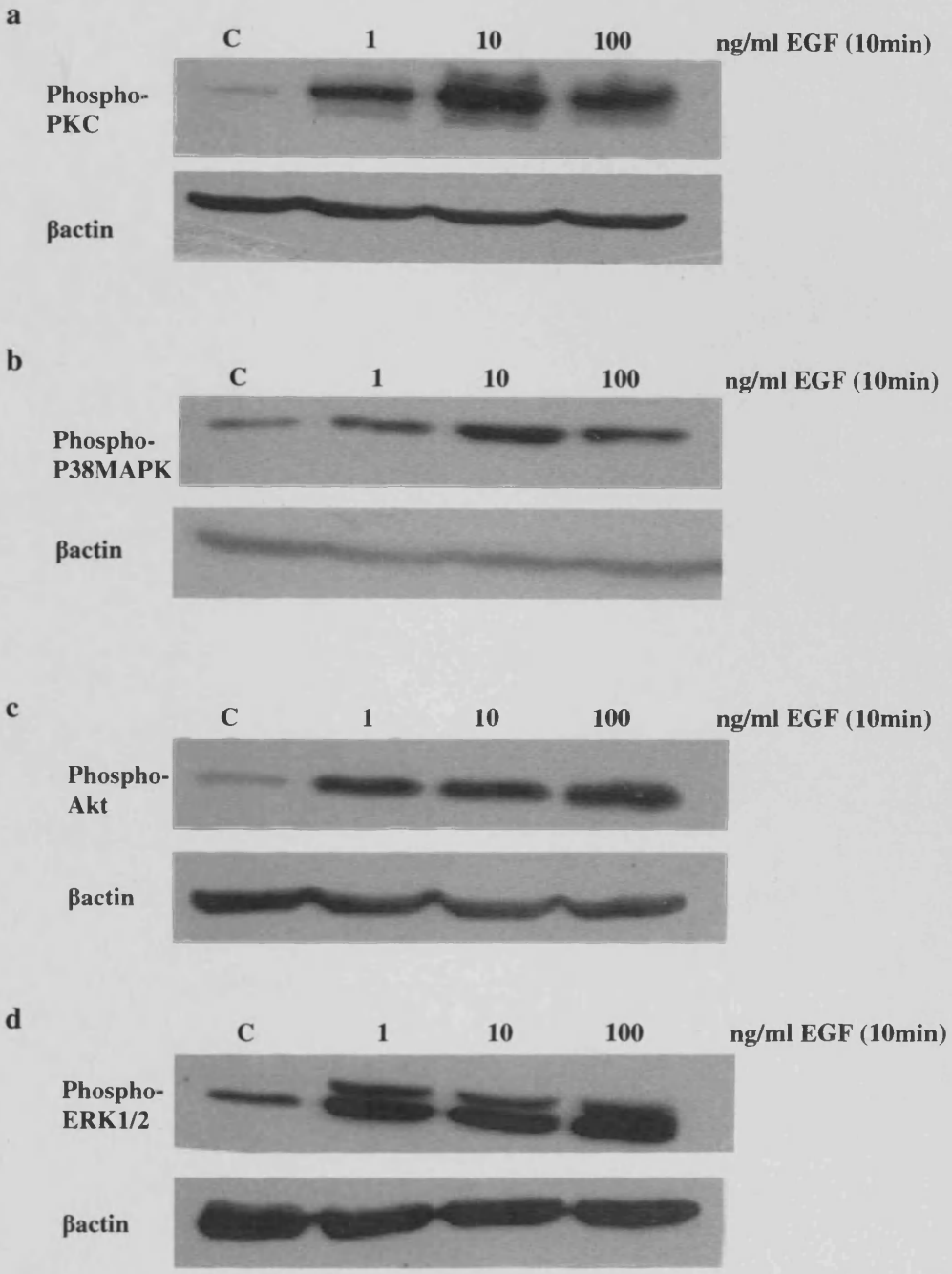

Effects of increasing EGF concentrations on PKC, p38MAPK, Akt and ERK1/2 phosphorylation in ECV-304 cells. Cells were grown in normal M199 medium for 24 hours and then various concentrations of EGF was added, after 10 minutes the protein was extracted for western blotting. Western blot of a) PKC phosphorylation, b) p38MAPK phosphorylation, c) Akt phosphorylation, and d) ERK1/2 phosphorylation in ECV-304 cells in the absence or following treatment with EGF. β-actin was used as a control to verify and equal protein loading in each lane, $n = 3$ for a), b), c) and d).

Figure 3.22

a

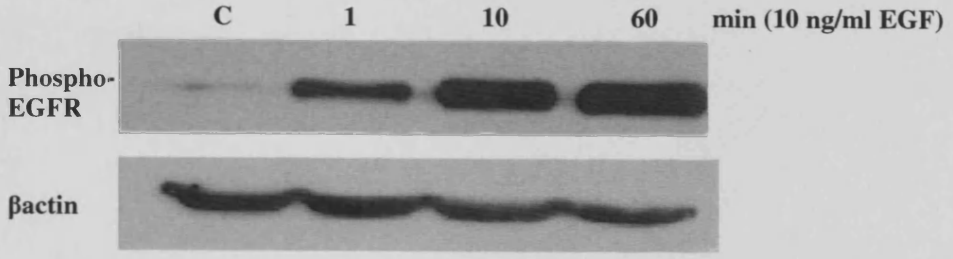

b

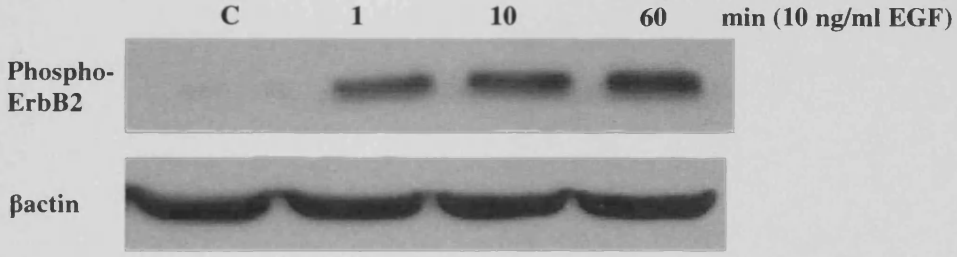

Effect of EGF on EGFR and ErbB2 phosphorylation in ECV-304 cells at various time points. Cells were grown in normal M199 medium for 24 hours and then 10 ng/ml EGF was added. At various time points the protein was extracted for western blotting. Western blot of a) EGFR phosphorylation and b) ErbB2 phosphorylation in ECV-304 cells in the absence or following treatment with EGF. β-actin was used as a control to verify and equal protein loading in each lane, $n = 3$ for both a) and b).

Figure 3.23

a

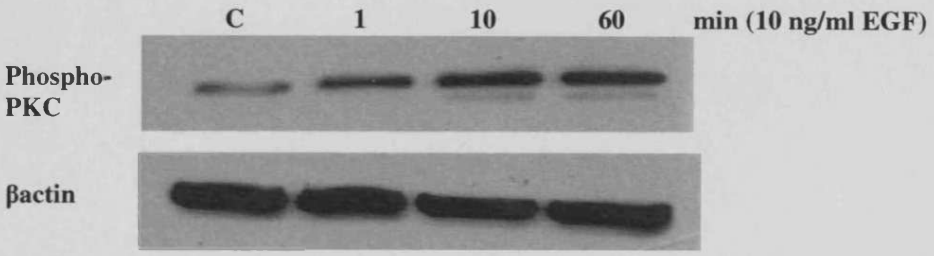

b

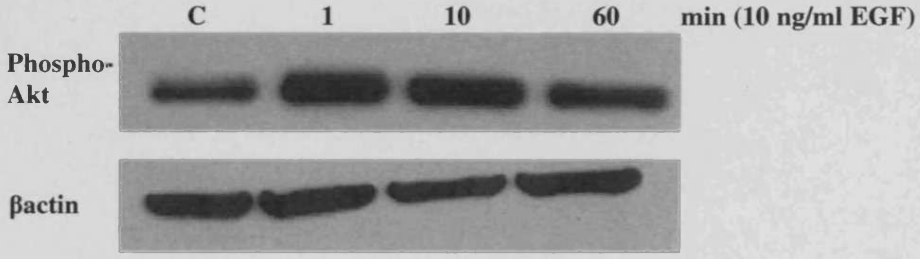

Effect of EGF on PKC and Akt phosphorylation in ECV-304 cells at various time points. Cells were grown in normal M199 medium for 24 hours and then 10 ng/ml EGF was added, at various time points. Then the protein was extracted for western blotting. Western blot of a) phosphorylated PKC and b) phosphorylated Akt expression in cells grown in the absence of or following treatment with EGF. β-actin was used as a control to verify and equal protein loading in each lane, $n = 3$ for both a) and b).

3.5 Effects of AG1478 and AG825 on PKC, p38MAPK, Akt and ERK1/2 Phosphorylated and Total Protein Levels in ECV-304 Cells Exposed to High Glucose for 72 Hours

Introduction

The present studies clearly implicate a role for EGFR in diabetes-induced vascular dysfunction. Furthermore, the cell culture studies suggest that high glucose conditions also leads to aberrant ErbB2 activation and to increased EGFR-ErbB2 heterodimerization. This study has already shown that PKC, p38MAPK, Akt and ERK1/2 are downstream effectors of EGFR and ErbB2 since EGF-induced activation of EGFR and ErbB2 increases the phosphorylation of all four pathways. Potentially any one of these pathways might be involved downstream of EGFR/ErbB2 in cascades that become aberrant under diabetic conditions. The aim of this section was to investigate the effect of high glucose on PKC, p38MAPK, Akt and ERK1/2 phosphorylated and total protein levels.

Results

Seventy two hours of high glucose exposure increased pPKC levels in ECV-304 cells. AG1478 decreased this glucose-induced increase in pPKC, specifically the lower band. AG825 treatment for 72 hours normalized glucose-induced increase in PKC phosphorylation more effectively than AG1478 treatment (Fig. 3.24).

ECV-304 cells exposed to high glucose for 72 hours showed slightly increased levels of pp38MAPK. Treatment with AG1478 and with AG825 reduced the glucose-induced increase back to control levels (Fig. 3.25a). Neither exposure of cells to high glucose nor treatment with AG1478 or AG825 had any effect on the total expression of p38MAPK (Fig. 3.25b).

Exposure of ECV-304 cells to high glucose for 72 hours did not have an effect on the levels of pAkt and pERK1/2. AG1478 reduced the levels of pAkt and pERK1/2 to below control levels. However AG825 treatment did not have an effect on the levels of Akt and ERK1/2 phosphorylation (Figs. 3.26a and 3.27a). Total levels of Akt and ERK1/2 proteins were not affected by high glucose, AG1478 or AG825 treatments (Figs. 3.26b and 3.27b).

The effect of AG1478 and AG825 treatments on pPKC levels in cells grown in 5.5 mM glucose was also investigated. Treatment with AG1478 increased levels of pPKC as compared to control cells, whilst treatment of cells with AG825 lowered levels of pPKC (Fig. 3.28).

In each case in this section levels of β-actin remained constant between samples.

Figure 3.24

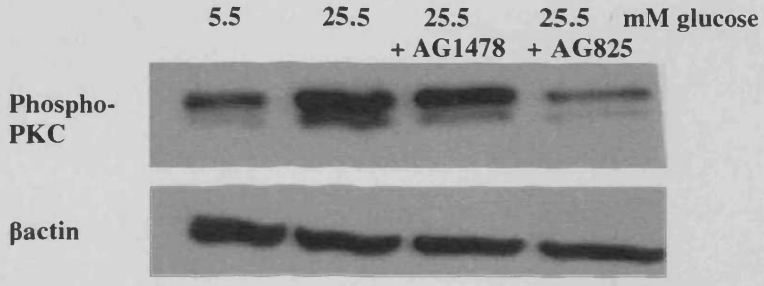

Effects of AG1478 and AG825 on PKC phosphorylation in ECV-304 cells exposed to high glucose. Cells were grown in normal M199 medium for 24 hours and in serum-free medium for a further 24 hours. Then the cells were exposed to high glucose and RTK inhibitors for 72 hours and protein was extracted for western blotting. Western blot analysis of PKC phosphorylation in untreated cells, in cells treated with 25.5 mM glucose, in cells treated with 25.5 mM glucose + AG1478 (0.5 μM) and in cells treated with 25.5 mM glucose + AG825 (20 μM). β-actin was used as a control to verify and equal protein loading in each lane, $n = 3$.

Figure 3.25

a

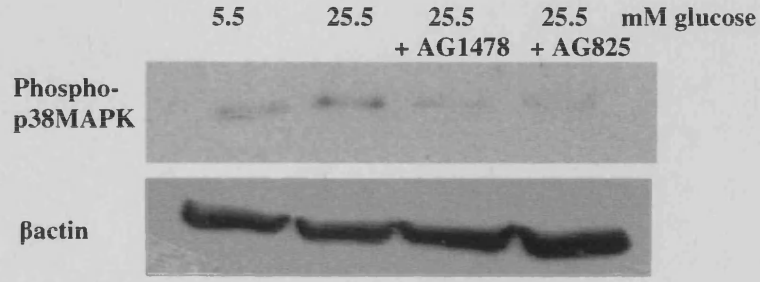

b

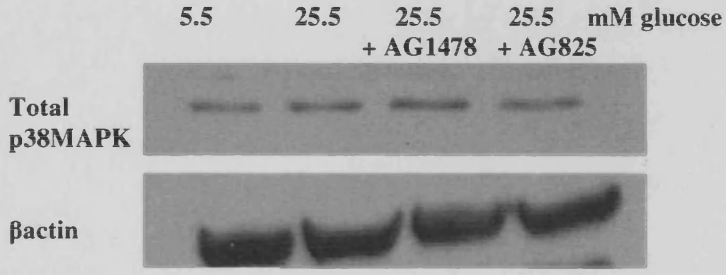

Effects of AG1478 and AG825 on p38MAPK phosphorylation and total protein expression in ECV-304 cells exposed to high glucose. Cells were grown in normal M199 medium for 24 hours and in serum-free medium for a further 24 hours. Then the cells were exposed to high glucose and RTK inhibitors for 72 hours and protein was extracted for western blotting. Western blot analysis of a) p38MAPK phosphorylation and b) p38MAPK total protein expression in untreated cells, in cells treated with 25.5 mM glucose, in cells treated with 25.5 mM glucose + AG1478 (0.5 μM) and in cells treated with 25.5 mM glucose + AG825 (20 μM). β-actin was used as a control to verify and equal protein loading in each lane, $n = 3$ for both a) and b).

Figure 3.26

a

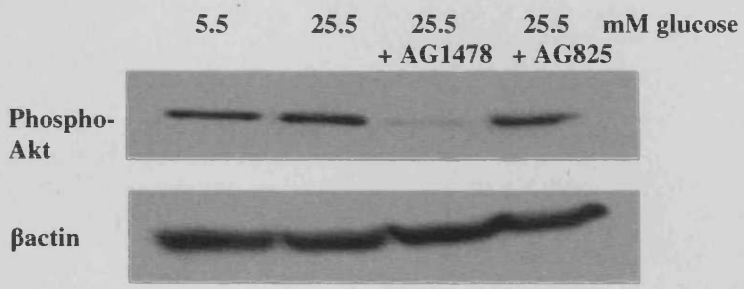

b

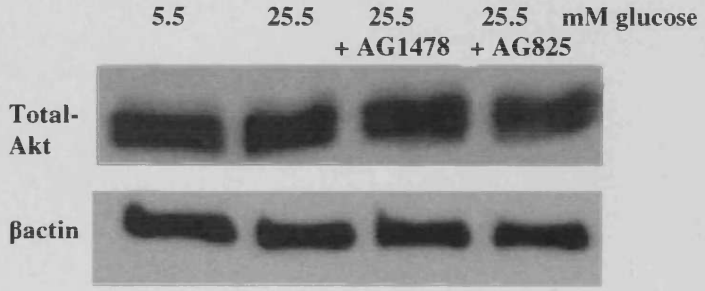

Effects of AG1478 and AG825 on Akt phosphorylation and total protein expression in ECV-304 cells exposed to high glucose. Cells were grown in normal M199 medium for 24 hours and in serum-free medium for a further 24 hours. Then the cells were exposed to high glucose and RTK inhibitors for 72 hours and protein was extracted for western blotting. Western blot analysis of a) Akt phosphorylation and b) Akt total protein expression in untreated cells, in cells treated with 25.5 mM glucose, in cells treated with 25.5 mM glucose + AG1478 (0.5 μM) and in cells treated with 25.5 mM glucose + AG825 (20 μM). β-actin was used as a control to verify and equal protein loading in each lane, $n = 3$ for both a) and b).

Figure 3.27

a

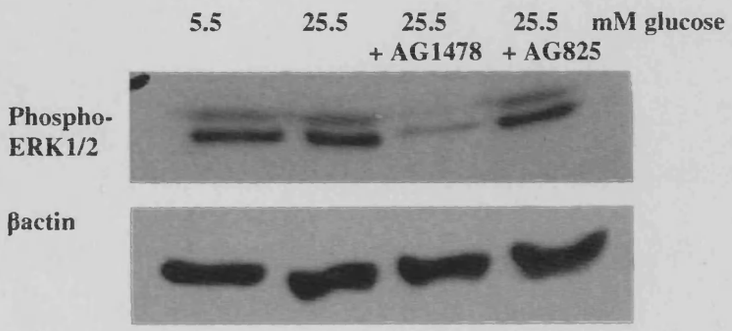

b

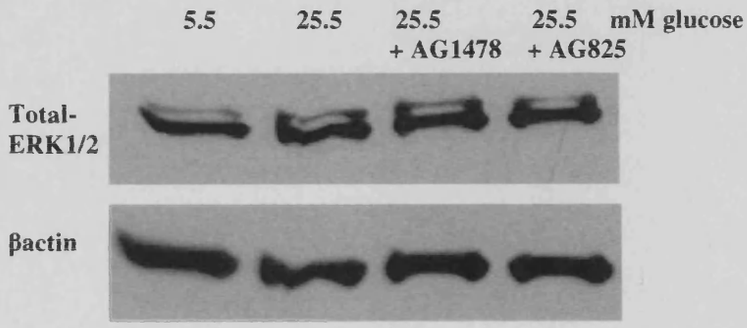

Effects of AG1478 and AG825 on ERK1/2 phosphorylation and total protein expression in ECV-304 cells exposed to high glucose. Cells were grown in normal M199 medium for 24 hours and in serum-free medium for a further 24 hours. Then the cells were exposed to high glucose and RTK inhibitors for 72 hours and protein was extracted for western blotting. Western blot analysis of a) ERK1/2 phosphorylation and b) ERK1/2 total protein expression in untreated cells, in cells treated with 25.5 mM glucose, in cells treated with 25.5 mM glucose + AG1478 (0.5 μM) and in cells treated with 25.5 mM glucose + AG825 (20 μM). β-actin was used as a control to verify and equal protein loading in each lane, $n = 3$ for both a) and b).

Figure 3.28

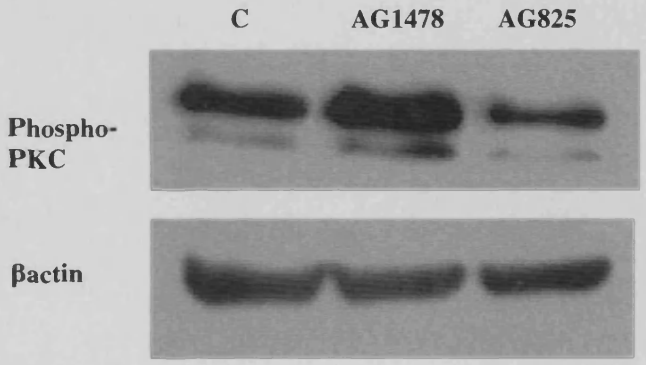

Effects of AG1478 and AG825 on PKC phosphorylation in ECV-304 cells grown in normal glucose levels. Cells were grown in normal M199 medium for 24 hours and in serum-free medium for a further 24 hours. Then the cells were exposed to RTK inhibitors for 72 hours and protein was extracted for western blotting. Western blot analysis of PKC phosphorylation in control cells, in control cells treated with AG1478 (0.5 μM) and in control cells treated AG825 (20 μM). β-actin was used as a control to verify and equal protein loading in each lane, n =3.

3.6 Identification of eNOS as a Downstream Target of EGFR/ErbB2 and PKC in ECV-304 Cells

Introduction

The previous section identified molecules downstream of EGFR and ErbB2 which may be involved in cascades leading to diabetes induced vascular dysfunction. Of the downstream molecules identified, high glucose induced-increase in PKC phosphorylation was most consistent and robust. PKC signalling is already known to be aberrant under hyperglycaemic conditions and in diabetic tissues, and it is known to have an important role to play in the initiation and progression of diabetes induced vascular dysfunction (Way, *et al* 2001), but the exact mechanism governing this remains unknown. However, it is known that PKC can negatively regulate eNOS activity by phosphorylating eNOS at Threonine (Thr)495 (Matsubara, *et al* 2003, Michell, *et al* 2001). One possibility is that PKC mediated eNOS inhibition is increased in diabetic conditions (Rask-Madsen and King 2005). Moreover results from section 3.1 suggest that the abnormal vascular reactivity observed in the STZ-induced diabetic rats is due to dysfunction at the level of the endothelium. This is apparent since vasodilator response to carbachol which is mediated via NO release from the endothelium, is reduced in the mesenteric tissue of STZ treated rats. This suggests that NO synthesis might be impaired in the diabetic tissue. Also the results in section 3.1 showed vasodilation to be unaltered in STZ-induced diabetic rats in response to the NO donor SNP; further suggesting impaired NO synthesis, rather than responses to NO in the mesenteric bed

tissue of STZ-induced diabetic rats. The enhanced vasoconstrictor responses observed in STZ-induced diabetic rats could also be due to decreased synthesis of NO to oppose vasoconstrictor effects.

Thus, the aim of this section was to identify whether eNOS is downstream of EGFR/ ErbB2 and PKC, and to investigate the effect of high glucose exposure and the inhibition of EGFR and ErbB2 on eNOS protein expression and phosphorylation. The presence of eNOS downstream of PKC and its dysregulation by glucose would implicate an EGFR/ErbB2-PKC-eNOS pathway leading to vascular dysfunction.

Results

In all cases western blots for peNOS Thr495 and peNOS Ser1177 showed single bands both at 140 kDa as estimated using molecular weight markers, this was the expected molecular weight for both proteins.

Effect of EGF on eNOS Phosphorylation

Stimulation of ECV-304 cells with 1, 10 and 100 ng/ml of EGF for 10 minutes had no effect on levels of peNOS at Thr495, (phosphorylation at this site decreases eNOS activity) and increased levels of peNOS at Serine (Ser)1177 (phosphorylation at this site increases eNOS activity) in a concentration-dependent manner as compared to control (Figs. 3.29a and 3.29b).

Effect of PKC Activity on eNOS Phosphorylation

Treatment with 12-O-tetra-decanoyl-phorbol-13-acetate (TPA)

TPA is a direct activator of classical and novel PKCs, however prolonged TPA-induced activation (6 – 12 hours) leads to downregulation of PKC activity (Rask-Madsen and King 2005). In order to observe the activator and inhibitor effects of TPA on PKC activity and also its effects on eNOS phosphorylation, ECV-304 cells were treated with TPA for up to 48 hours.

Treatment of ECV-304 cells with TPA for 3 hours slightly increased levels of pPKC and peNOS at Thr495. After 24 hours of treatment with TPA, levels of pPKC were markedly decreased and the levels of peNOS at Thr495 were also decreased. Forty eight hours of treatment with TPA also markedly decreased the level of pPKC and decreased levels of peNOS at Thr495 compared to control levels (Figs. 3.30a and 3.30b).

Treatment with PKC Inhibitors

RO-31-8220 and GO6983 are both selective PKC inhibitors. Here the effect of PKC inhibition on eNOS phosphorylation at Thr495, was investigated using these selective inhibitors of PKC.

Treatment of cells with 0.1, 0.25 and 0.5 μM of RO-31-8220 for 24 hours resulted in decreased levels of pPKC compared to control untreated cells and a similar decrease in peNOS at Thr495 was observed (Figs. 3.31a and 3.31b). Treatment of ECV-304 cells with 0.1, 0.5, 1, 5 and 10 μM of the PKC inhibitor

GO6983 for 24 hours did not affect levels of pPKC as compared to control (Fig. 3.32). Therefore, studies investigating the effect of this agent on eNOS phosphorylation were not pursued.

Effect of High Glucose and the Inhibition of EGFR and ErbB2 Activity on eNOS Protein Expression and Phosphorylation

The previous studies indicate that PKC can regulate inhibitory phosphorylation of eNOS on Thr495 in ECV-304 cells. This section investigated whether this mechanism could be activated via hyperglycaemia-induced EGFR/ErbB2 activation.

High glucose AG1478 and AG825 did not have any observable effect on the total levels of eNOS (Fig 3.33a). However, exposure of ECV-304 cells to high glucose for 72 hours increased levels of eNOS phosphorylation at Thr495. Treatments with both AG1478 and with AG825 decreased the glucose-induced increase in peNOS at Thr495, with AG825 reducing levels to a much greater extent than AG1478 (Fig. 3.33b). Exposure of cells to high glucose for 72 hours had no effect on the levels of eNOS phosphorylation at Ser1177. Treatment with AG1478 lowered peNOS levels at Ser1177 to lower than control. Treatment of cells with AG825 had no effect on peNOS levels at Ser1177 (Fig. 3.33c)

The effect of AG1478 and AG825 on eNOS phosphorylation at Thr495, in cells grown in 5.5 mM glucose was also investigated. ECV-304 cells treated with AG1478 had higher levels of peNOS at Thr495 than control cells. However treatment with AG825 decreased peNOS levels at Thr495 as compared to control cells (Fig 3.34).

For each case in this section the levels of β-actin remained constant, indicating equal protein loading for each sample.

Figure 3.29

a

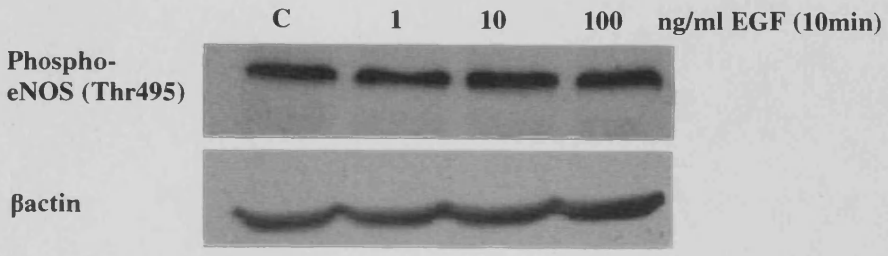

b

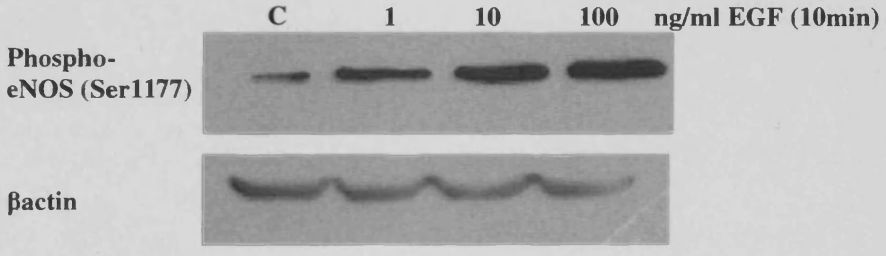

Effects of increasing EGF concentrations on eNOS phosphorylation at Thr495 and Ser1177 in ECV-304 cells. Cells were grown in normal M199 medium for 24 hours and then various concentrations of EGF was added, after 10 minutes the protein was extracted for western blotting. Western blot analysis of eNOS phosphorylation at a) Thr495 and b) at Ser1177 in cells grown in the absence of or following treatment EGF. β-actin was used as a control to verify and equal protein loading in each lane, $n = 3$ for both a) and b).

Figure 3.30

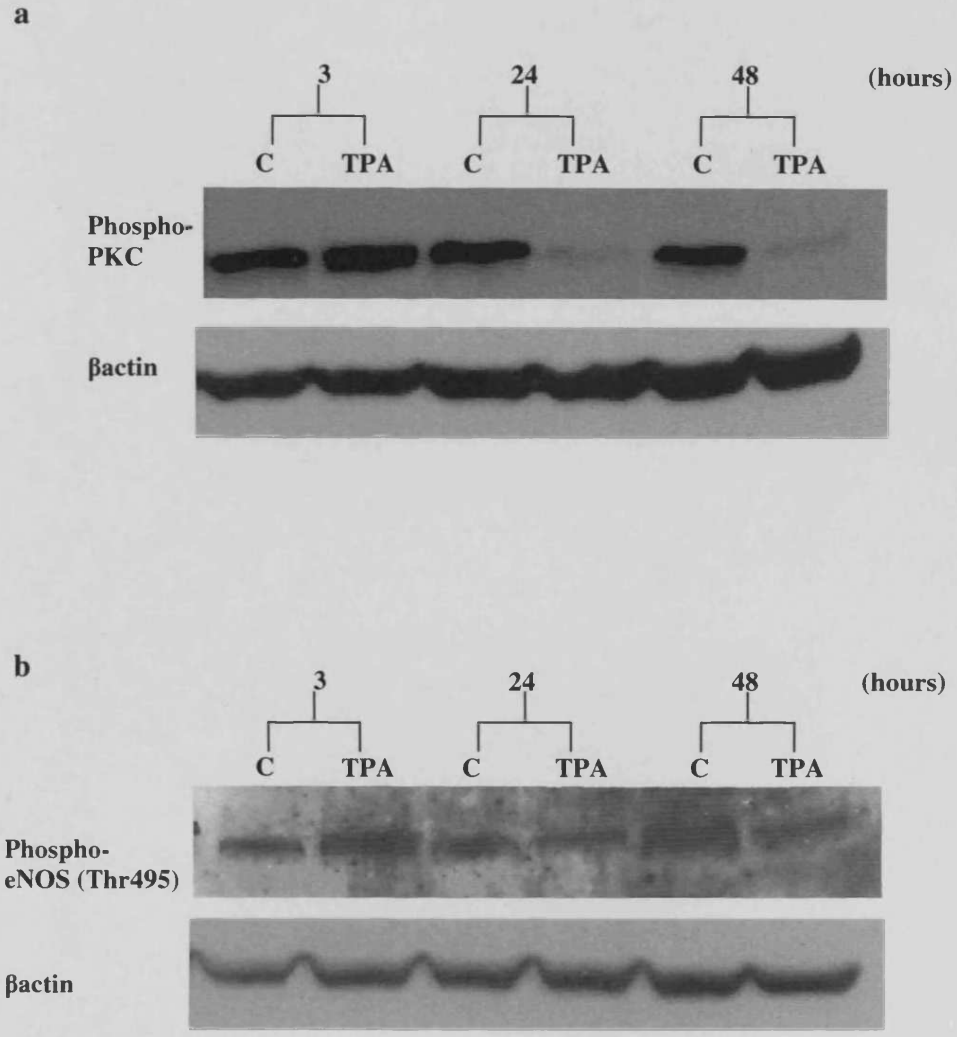

Effects of TPA on PKC phosphorylation and eNOS phosphorylation at Thr495. Cells were grown in normal M199 medium for 24 hours and then TPA was added. Then protein was extracted for western blotting at various time points. Western blot analysis of a) phosphorylated PKC and b) phosphorylated eNOS at Thr495 in cells grown in the absence of and following treatment with 100 nM TPA. β-actin was used as a control to verify and equal protein loading in each lane, $n = 3$ for both a) and b).

Figure 3.31

a

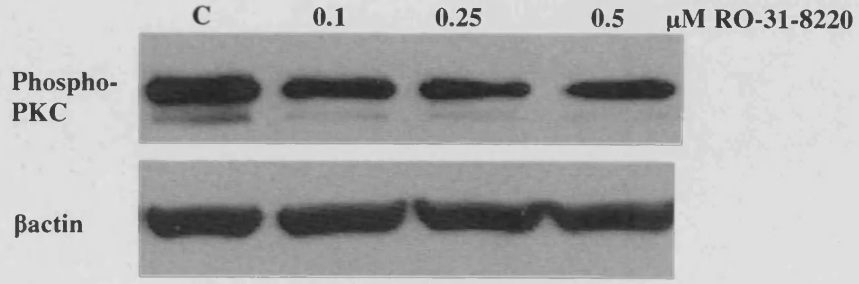

b

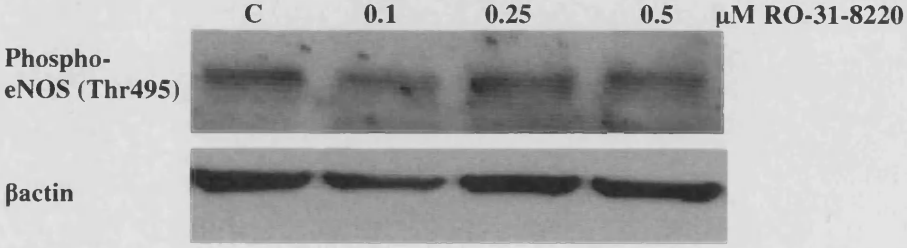

Effects of PKC inhibitor RO-31-8220 on PKC phosphorylation and eNOS phosphorylation at Thr495. Cells were grown in normal M199 medium for 24 hours and then various concentrations of RO-31-8220 was added, after 24 hours the protein was extracted for western blotting. Western blots of a) phosphorylated PKC and b) phosphorylated eNOS at Thr495 in cells grown in the absence of and following treatment with RO-31-8220. β-actin was used as a control to verify and equal protein loading in each lane, $n = 3$ for both a) and b).

Figure 3.32

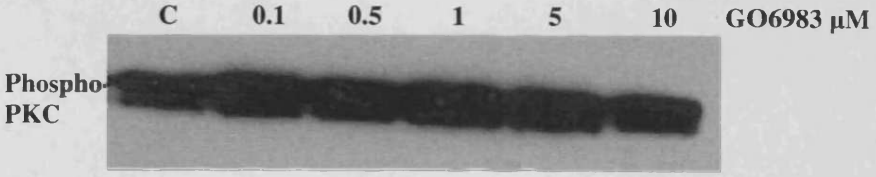

Effect of PKC inhibitor GO6983 on PKC phosphorylation. Cells were grown in normal M199 medium for 24 hours and then various concentrations of GO6983 was added, after 24 hours the protein was extracted for western blotting. Figure shows western blot of phosphorylated PKC in cells grown in the absence of or following treatment with GO6983, $n = 2$.

Figure 3.33

a

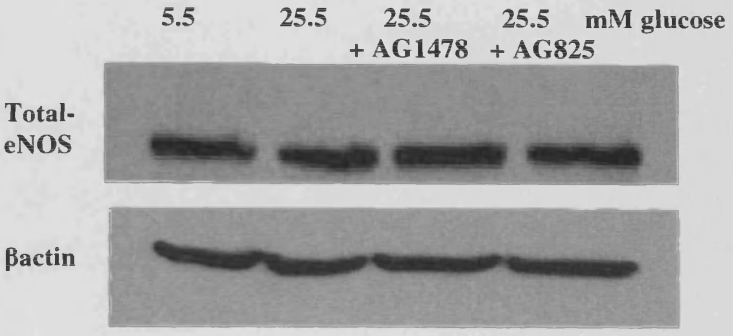

b

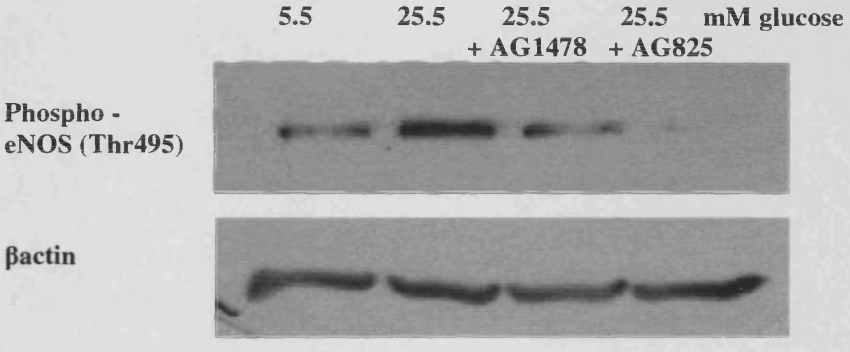

c

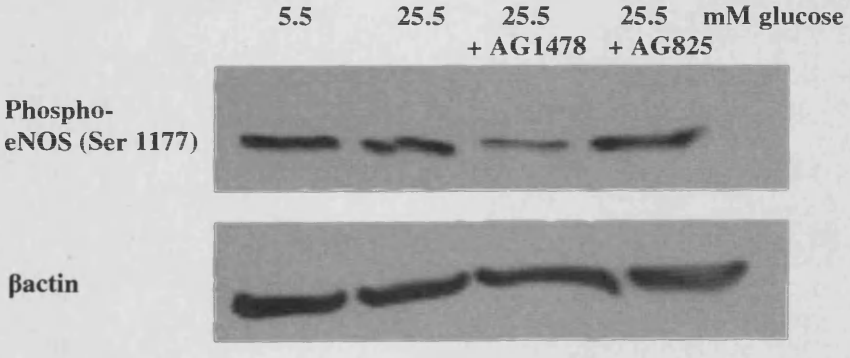

Effects of AG1478 and AG825 on eNOS phosphorylation at Thr495 and Ser1177 and total protein expression in ECV-304 cells. Cells were grown in normal M199 medium for 24 hours and in serum-free medium for a further 24 hours. Then the cells were exposed to high glucose and RTK inhibitors for 72 hours and protein was extracted for western blotting. Western blot analysis of a) eNOS total protein expression, b) eNOS phosphorylation at Thr495 and c) eNOS phosphorylation at Ser1177 in untreated cells, in cells treated with 25.5 mM glucose, in cells treated with 25.5 mM glucose + AG1478 (0.5 μM) and in cells treated with 25.5 mM glucose + AG825 (20 μM. β-actin was used as a control to verify and equal protein loading in each lane, $n = 3$ for a), b) and c).

Figure 3.34

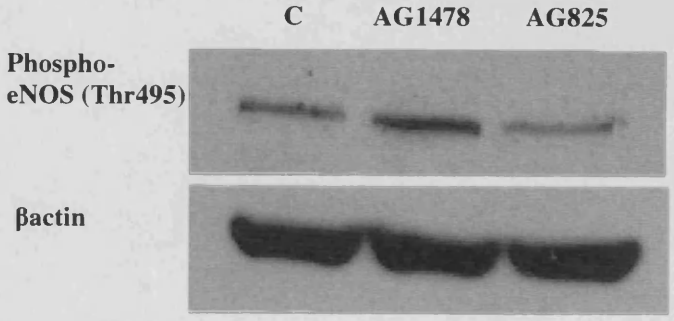

Effects of AG1478 and AG825 on eNOS phosphorylation at Thr495 in ECV-304 cells grown in normal glucose levels. Cells were grown in normal M199 medium for 24 hours and in serum-free medium for a further 24 hours. Then the cells were exposed to RTK inhibitors for 72 hours and protein was extracted for western blotting. Western blot analysis of eNOS phosphorylation at Thr495 in control cells, in control cells treated with AG1478 (0.5 μM) and in control cells treated with AG825 (20 μM). β-actin was used as a control to verify and equal protein loading in each lane, $n = 3$.

3.7 Effects of EGF on Isolated Rat Aortic Rings

Introduction

Perfusion experiments carried out in section 3.1 suggest that abnormal vascular reactivity observed in the mesenteric bed of STZ-induced diabetic rats was due to dysfunction of the endothelium, in a mechanism involving increased EGFR activity. Furthermore, the cell culture studies implicate eNOS as a downstream target of EGFR/ErbB2 in a cascade that includes PKC. Thus, diabetes-induced increased EGFR/ErbB2 activity may reduce NO synthesis through modulating eNOS activity. The aim of this section was to further investigate the ability of EGFR activity to regulate NO production. Using isolated ring preparations from Spague-Dawley rats as a bioassay for NO production, this section aimed to establish whether EGF could influence NO-mediated endothelium-dependent vasodilator responses.

Results

Where stated in the text, a proportion of the aortic rings used were denuded of endothelium. In each vessel, endothelium-dependent relaxation to acetyl methylcholine (Mch) was used to confirm the presence or absence of the endothelium.

Effect of EGF on Resting Aorta

Endothelium-intact aorta was used to investigate whether EGF could itself induce aortic contraction, possibly by interfering with basal NO synthesis. As a control, the effect of EGF on endothelium-denuded aorta was also tested.

Exposure of unconstricted rat aorta to 100 ng/ml of EGF or to vehicle alone (10 mM acetic acid + 0.1 % bovine serum albumin (BSA)) for 10 minutes had no effect on vascular tone in endothelium intact aorta (Figs. 3.35a and 3.35b). However exposure of endothelium-denuded aorta to 100 ng/ml of EGF for 10 minutes caused an immediate contraction (mean maximum tension 0.5 ± 0.1 g), with vehicle alone having no effect (Figs. 3.36a, 3.36b and 3.36c).

Effects of EGF on Mch-induced Relaxation

Mch relaxes vessels mainly by increasing NO production from the endothelium. Here the effect of EGF upon Mch-induced relaxation was investigated to see whether EGF could influence Mch-induced NO synthesis.

Firstly, a cumulative concentration-response curve for Mch was constructed in tissues preconstricted with the thromboxane A2 mimetic U46619 (5×10^{-9} M). Mch caused a concentration-dependent relaxation of rat aorta (Fig. 3.37) and from this curve the EC50 was estimated to be 10^{-6} M. This concentration of Mch was therefore selected for relaxing aortic rings in subsequent experiments.

In aorta preconstricted with U46619, EGF had a variable effect on Mch-induced relaxation of the aortic rings, in half the experiments (2/4) causing a further relaxation (Fig. 3.38a) and in the other half (2/4) having no effect on Mch-induced relaxation (Fig. 3.38b). EGF vehicle (10 mM acetic acid + 0.1 % BSA) alone had no effect on Mch-induced response (Fig 3.38c). Figure 3.39 shows mean % relaxation to U46619 induced contraction in response to Mch alone and with added 1, 10 and 100 ng/ml EGF. Although a trend for concentration-dependent EGF-induced relaxation can be seen, mean % relaxation to U44619 was not significantly different between Mch and the highest concentration of EGF (100 ng/ml).

To discount possible desensitisation by the cumulative concentrations of EGF used in the first experiment, only the highest concentration of EGF (100 ng/ml) was used. 100 ng/ml of EGF further relaxed Mch-induced relaxation, but only slightly (Fig. 3.39).

Effect of Treatment with EGF on U46619 Cumulative Concentration-response Curve

Since the effect of EGF on Mch-induced relaxation was variable, the effect of EGF on aortic responses to vasoconstrictors was investigated. The effect of EGF was initially tested on the thromboxane A2 mimetic U46619, which is a powerful vasoconstrictor.

Following a U46619 cumulative concentration-response curve and washout, either EGF or vehicle alone was added to the bath prior to a second cumulative concentration-response curve to U46619 in endothelium-intact aorta. The highest concentration of EGF (100 ng/ml) was used to ensure that a substantial effect could be observed. Neither the presence of EGF nor vehicle alone (10 mM acetic acid + 0.1 % BSA) had an effect on the ability of U46619 to constrict endothelium-intact rat aorta (Figs. 3.40a, 3.40b, 3.41a and 3.41b). Thus, an alternative vasoconstrictor- phenylephrine (PE) was also examined.

Effect of Treatment with EGF on PE Cumulative Concentration-response Curve

a) With 10 mM Acetic Acid + 0.1 % BSA Vehicle

Following a PE cumulative concentration-response curve and washout, 100 ng/ml of EGF or vehicle alone was added to the bath prior to a second cumulative concentration-response curve to PE in endothelium-intact aorta. As compared to the maximum contractions induced by PE in the absence of EGF (0.6 ± 0.2 g), the maximum contractions in the presence of EGF were reduced (0.2 ± 0.1 g). The PE-induced maximum contractions were reduced in the presence of vehicle (0.07 ± 0.03 g) as compared to maximum contractions in the absence of vehicle (0.4 ± 0.03 g). The EC50 value was increased in the presence of EGF (8.5 (1.3 – 16.2) x 10^{-7} M), as compared to EC50 in the absence of EGF (0.7 (0.3 – 1.0) x 10^{-7} M). However, in the presence of vehicle the EC50 was decreased (1.6 (0.7 – 2.3) x 10^{-7} M) as compared to EC50 in the

absence of vehicle (2.4 (0.6 – 3.1) x 10^{-7} M) (Figs. 3.42a, 3.42b, 3.43a and 3.43b and table 3.1).

Since the vehicle, 10 mM acetic acid + 0.1% BSA, alone reduced PE-induced maximum contractions, more so than the effect of EGF, further investigations were carried out using an alternative vehicle for EGF, namely, phosphate buffered saline (PBS) + 0.1 % BSA.

b) With PBS + 0.1 % BSA Vehicle

The maximum response of PE concentration-response curve was significantly less in aorta in the presence of 100 ng/ml EGF (0.3 ± 0.1 g) compared to aorta not exposed to EGF (0.8 ± 0.1 g) (n = 5, $p < 0.01$). The EC50 value for PE concentration-response curve was significantly higher in aorta exposed to EGF (6.1 (1.3 -7.9) x 10^{-7} M) as compared to aorta not exposed to EGF (1.0 (0.3 – 1.6) x 10^{-7} M) (n = 5, $p < 0.01$) (Figs. 3.44a and 3.45a; table 3.2).

Vehicle control (PBS + 0.1 % BSA) significantly reduced PE-induced maximum contraction in rat aortic rings (0.5 ± 0.1 g) as compared to aorta unexposed to vehicle (0.6 ± 0.1 g) (n = 5, $p < 0.05$) but significantly increased the EC50 value (1.5 (0.8 – 2.1) x 10^{-7} M) as compared to control aorta unexposed to vehicle (0.8 (0.5 – 1.1) x 10^{-7} M) (n = 5, $p < 0.001$) (Figs. 3.44b and 45b) and (Table 3.2). However the reduction in maximum by exposure of aorta to vehicle (to 84.3 ± 5.4 % of original), was significantly less than the reduction in maximum by exposure of aorta to EGF (to 41.8 ± 4.4 % of

original) (n = 5, $p < 0.01$). Also the increase in EC50 was significantly more in aorta exposed to EGF (to 560 ± 151.7 % of original) than in aorta exposed to vehicle (to 163 ± 13.1 % of original) (n = 5, $p < 0.05$) (Table 3.3).

To check that these changes were not the result of repeating the PE concentration-response curve, two successive curves were obtained in the same tissue and the effect of the first concentration-response curve (naïve control 1) was observed on the second concentration-response curve (naïve control 2). The maximum response (1.0 ± 0.2 g) and EC50 (1.5 (0.7 – 2.2) x 10^{-7} M) for the second concentration-response curve were not significantly different form those of the first concentration-response curve (1.1 ± 0.2 g) and (2.4 (0.4 – 3.9) x 10^{-7} M) (Figs. 3.44c and 3.45c) (Table 3.2).

As shown earlier (Fig. 3.36a), endothelium-denuded rat aorta markedly contracted in response to 100 ng/ml of EGF (mean maximum contraction 0.5 ± 0.1 g). This occurred when EGF was added before the second cumulative concentration-response curve. Addition of 10^{-10}, 10^{-8}, 10^{-7} M of PE did not increase the EGF-induced constriction any further. However 10^{-6} and 10^{-5} M PE increased the EGF-induced contraction even further until aortic constriction had reached its maximum (Fig 3.46a). Vehicle alone did not have this effect (Fig. 3.46b). The mean maximum response of the second concentration-response curve to PE in the presence of EGF (0.8 ± 0.1 g) was not significantly different from the mean maximum response of the first concentration-response

curve prior to exposure to EGF (0.8 ± 0.1 g). Thus, EGF did not significantly increase maximum aortic response (Fig 3.47).

Effects of EGF on PE- preconstricted Aorta

The effect of EGF on PE-preconstricted aorta was investigated to see whether EGF could modulate aortic-tone induced by PE. Exposure of rat aorta pre-constricted with 10^{-7} M PE to 100 ng/ml of EGF for 10 minutes caused relaxation (39 ± 14 %) to PE-induced contraction (Figs. 3.48a and 3.48b). Exposure to the vehicle control (PBS + 0.1 % BSA) for 10 minutes had no effect on aortic tone (Fig. 3.48c). Due to time constraints the effect of EGF on PE-preconstricted aorta in endothelium-denuded aorta was not investigated.

Figure 3.35

a

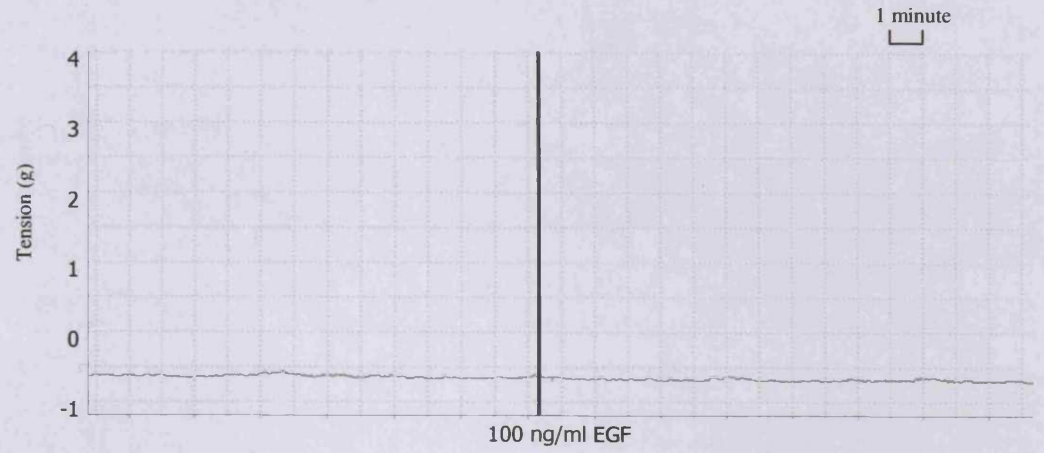

b

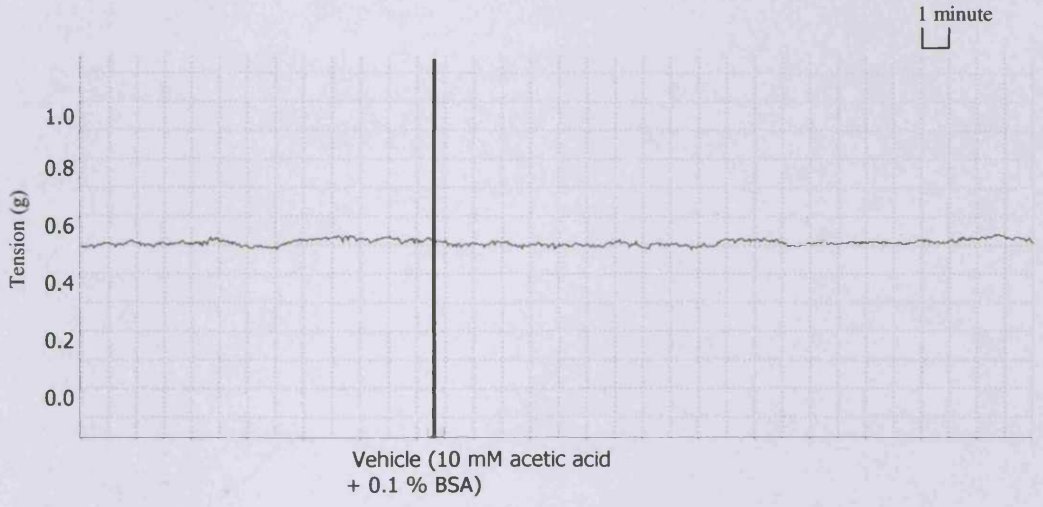

Example traces showing a) the effect of a single exposure of EGF and b) the effect of vehicle alone on resting endothelium-intact rat aortic rings, $n = 4$ for both a) and b).

Figure 3.36

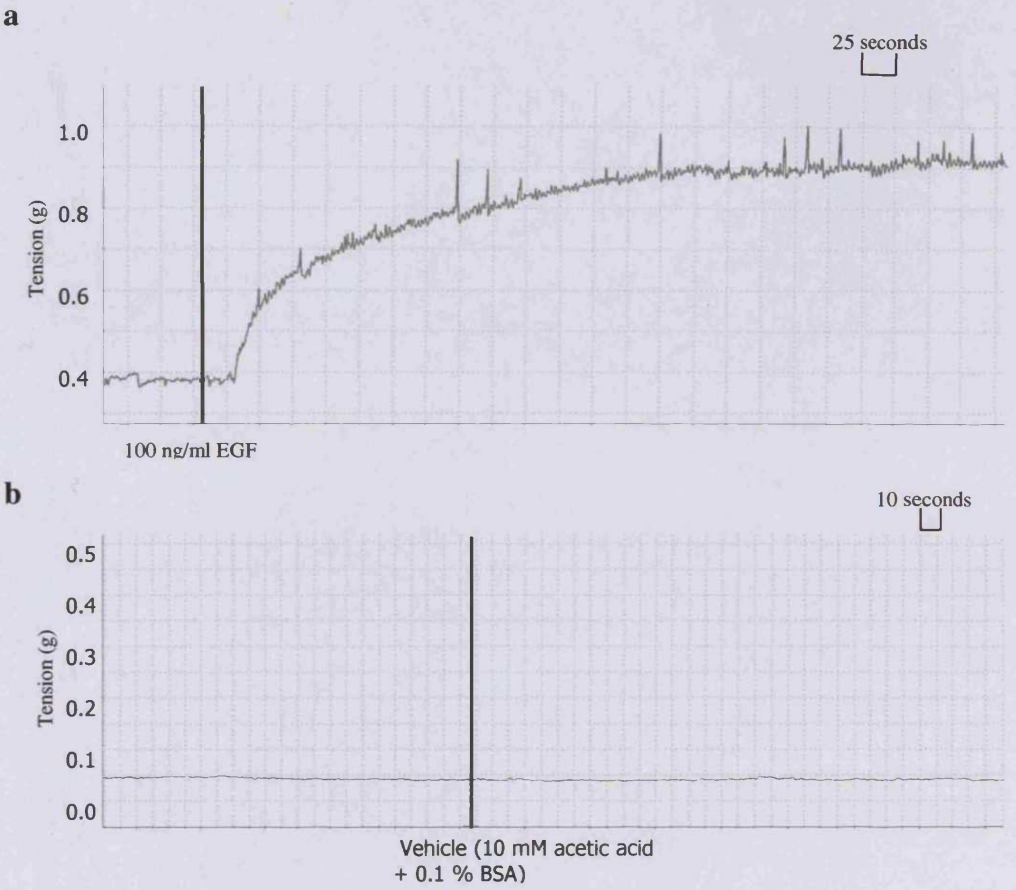

a) Example trace from an experiment showing the effect of a single exposure of EGF on resting endothelium-denuded rat aortic rings and b) vehicle alone as a control and c) mean maximum tension (g) of EGF-induced contraction, measured from the pre-EGF baseline (± SEM), $n = 4$.

Figure 3.37

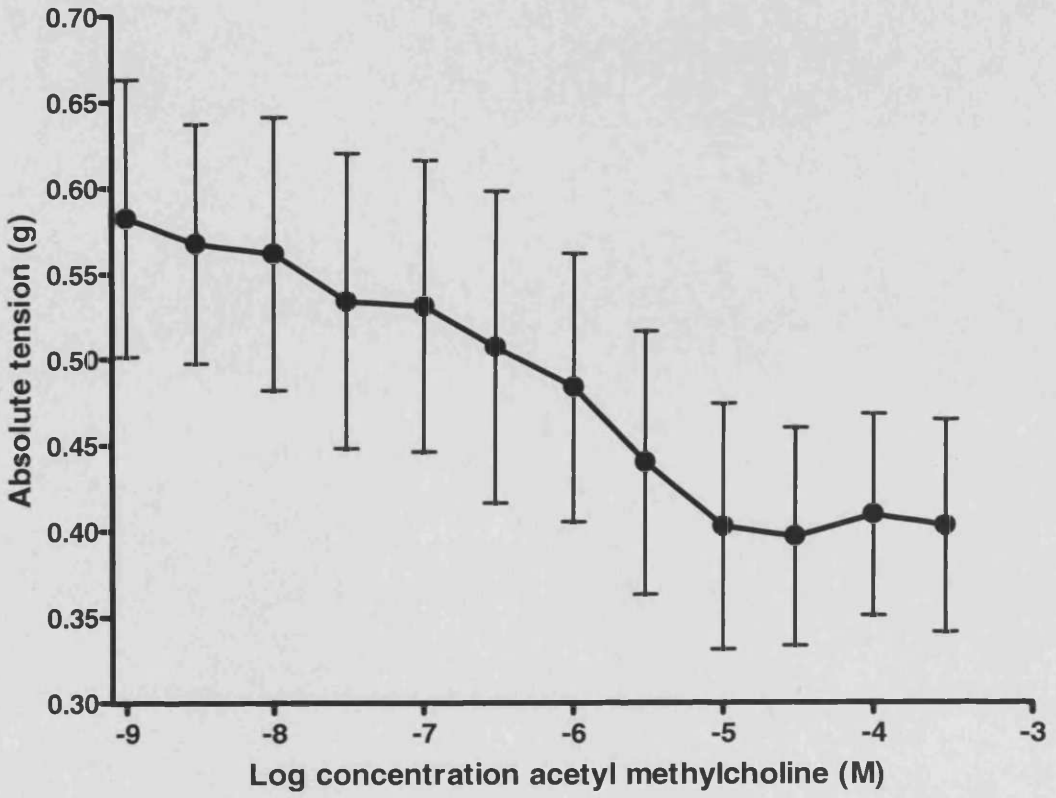

Mean cumulative concentration-response curve for the relaxation of endothelium-intact rat aortic rings in response to Mch in tissues preconstricted with U46619 (5 x 10^{-9} M). EC50 = 10^{-6} M (± SEM), n = 2.

Figure 3.38

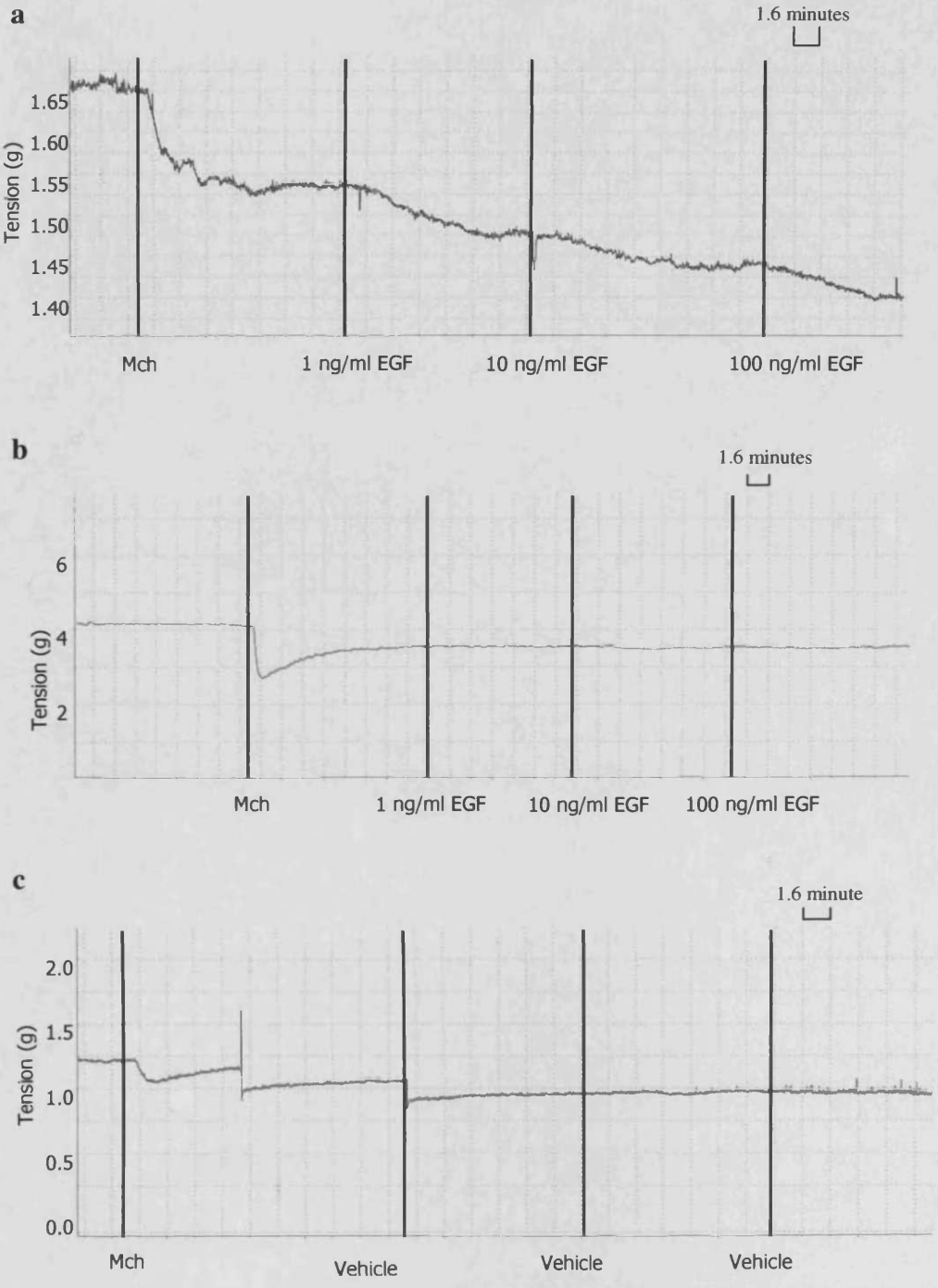
a
1.6 minutes
Tension (g)
1.65
1.60
1.55
1.50
1.45
1.40
Mch
1 ng/ml EGF
10 ng/ml EGF
100 ng/ml EGF
b
1.6 minutes
Tension (g)
6
4
2
Mch
1 ng/ml EGF
10 ng/ml EGF
100 ng/ml EGF
c
1.6 minute
Tension (g)
2.0
1.5
1.0
0.5
0.0
Mch
Vehicle
Vehicle
Vehicle

Figure 3.38 continued

d

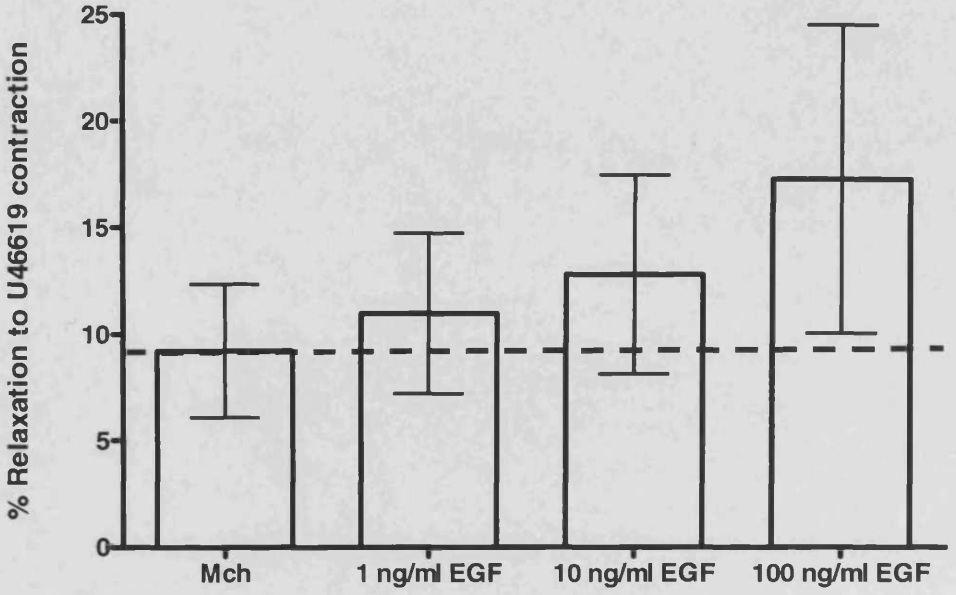

Example traces from an experiment showing the effect of cumulative concentrations of EGF on Mch induced relaxation in endothelium-intact rat aorta preconstricted with 5 x 10^{-9} M U46619. EGF had a variable effect, trace a) shows EGF having a concentration-dependent relaxant effect upon the aorta and trace b) shows EGF having no effect, also shown in c) is the effect of vehicle alone. Figure d) shows mean % relaxation to U46619 induced contraction in response to Mch and to EGF (± SEM), $n = 4$.

Figure 3.39

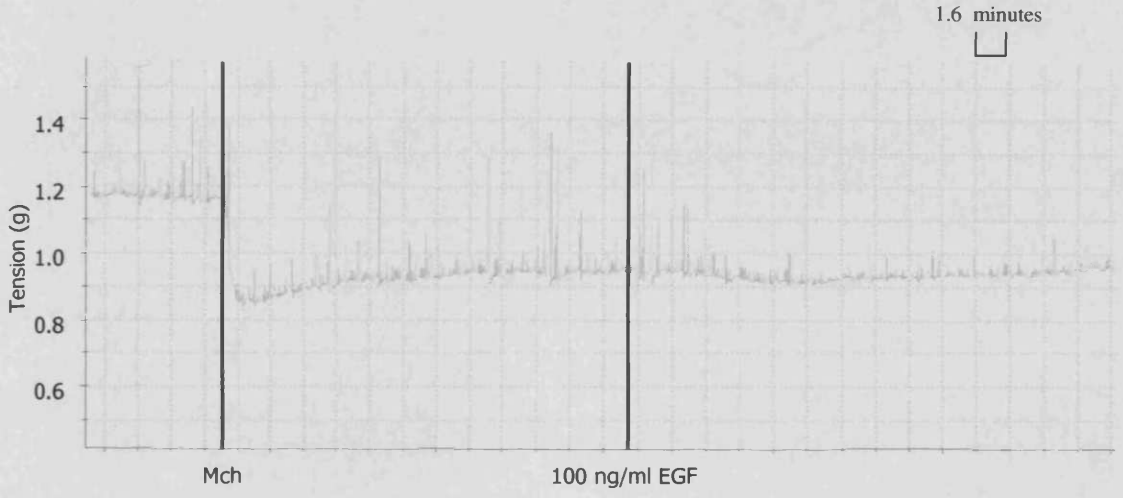

Example trace from an experiment showing the effect of a single exposure of EGF on Mch-induced relaxation of endothelium-intact rat aortic rings preconstricted with 5 x 10^{-9} M U46619, $n = 2$.

Figure 3.40

a

First cumulative concentration-responses to U46619 in endothelium-intact rat aortic ring

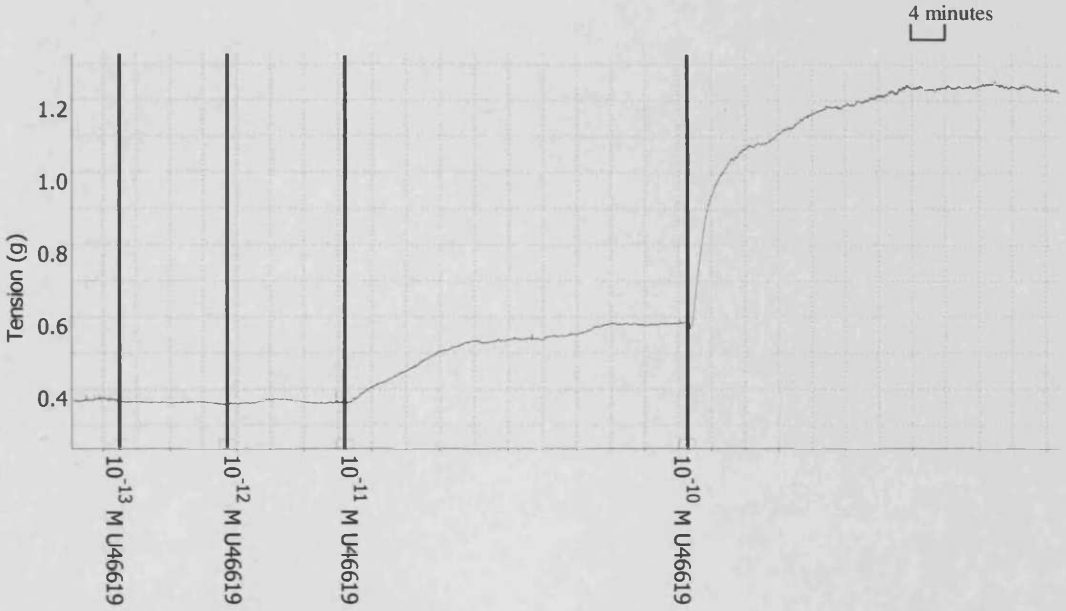

Second cumulative concentration-responses to U46619 in endothelium-intact rat aortic ring exposed to EGF (100ng/ml)

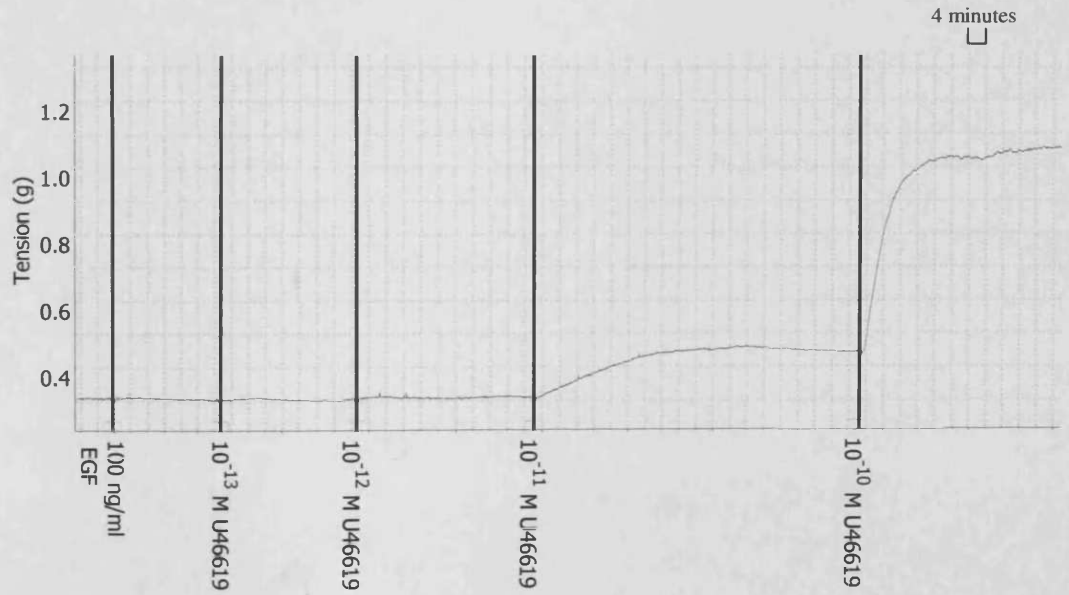

Figure 3.40 continued

b

First aortic cumulative concentration-response to U46619 in endothelium-intact rat aortic ring

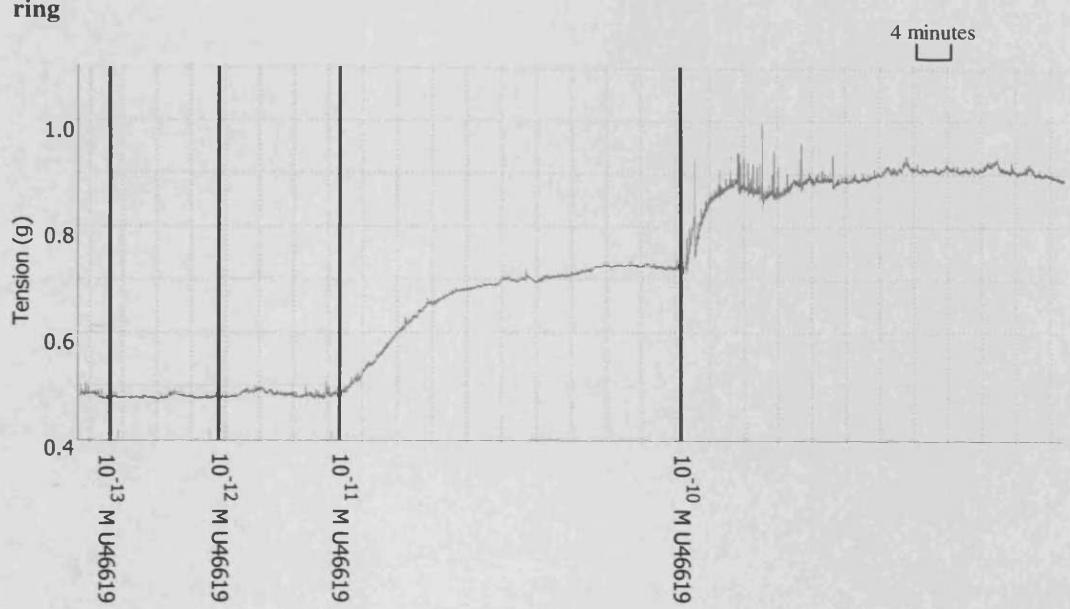

Second aortic cumulative response to U46619 in endothelium-intact rat aortic ring exposed to vehicle alone

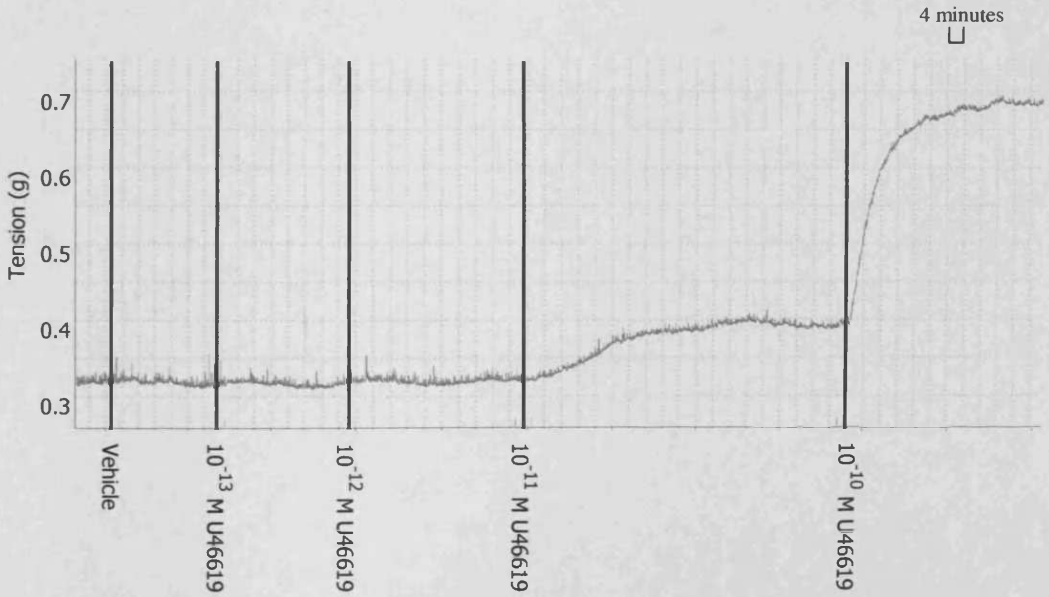

Example traces from experiments showing the effect of a) EGF and b) vehicle alone on aortic response to cumulative concentrations of U46619, in endothelium-intact rat aortic rings, $n = 2$.

Figure 3.41

a

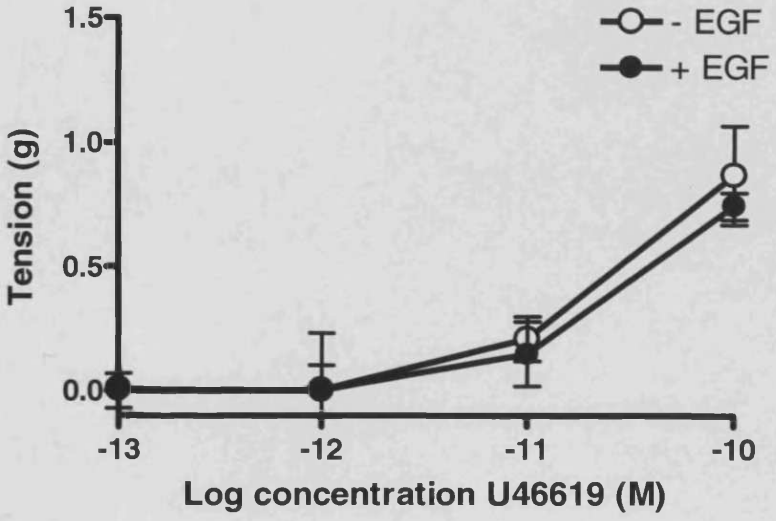

b

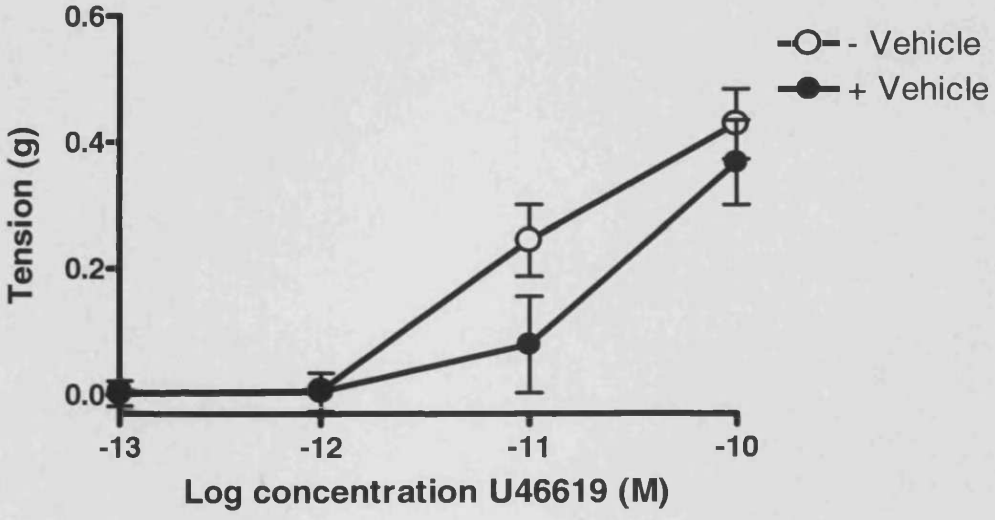

Graphs showing mean cumulative concentration-response curves for U46619 in endothelium-intact rat aortic rings a) + EGF and – EGF and b) + vehicle and – vehicle (± SEM). Results are of the absolute tension values relative to U46619 concentration, $n = 2$.

Figure 3.42

a

First cumulative concentration-response to PE in endothelium-intact rat aortic ring

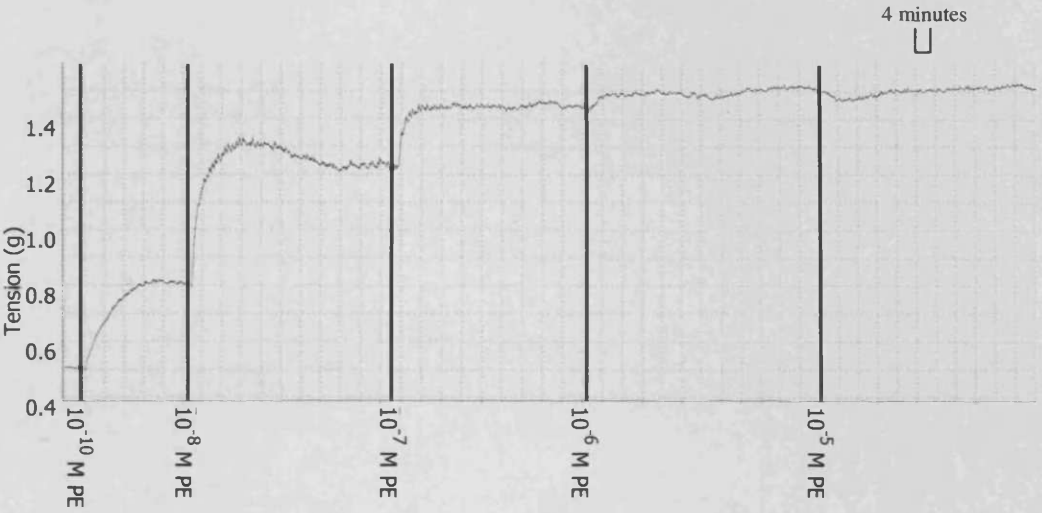

Second cumulative concentration-response to PE in endothelium-intact rat aortic ring exposed to EGF (100 ng/ml)

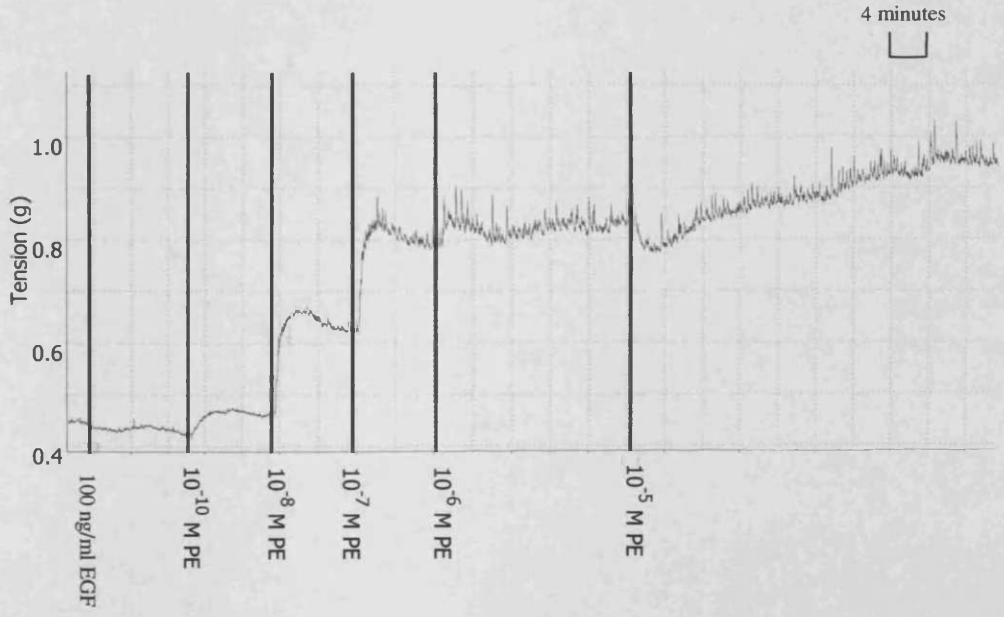

Figure 3.42 continued

b

First cumulative concentration-response to PE in rat endothelium-intact aortic ring

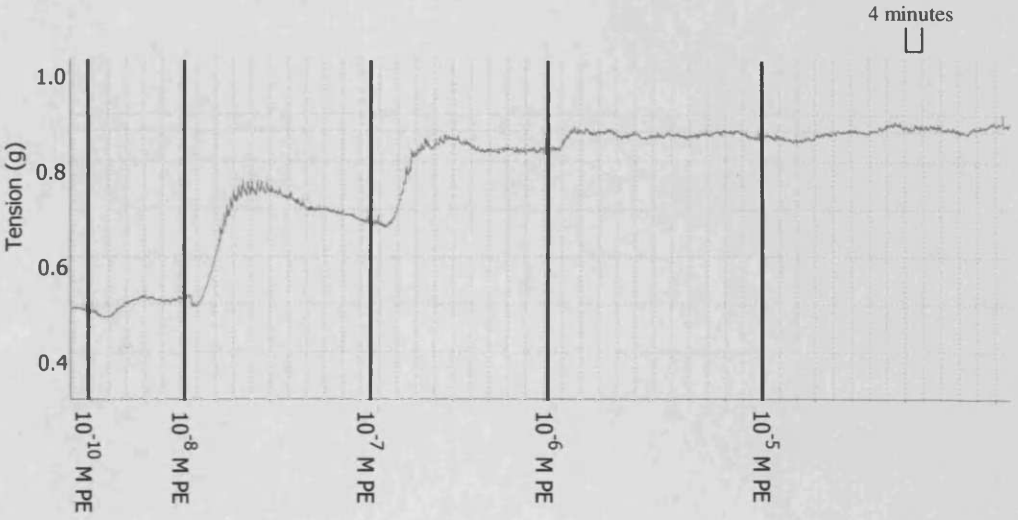

Second aortic cumulative concentration-response to PE in endothelium-intact rat aortic ring exposed to vehicle alone

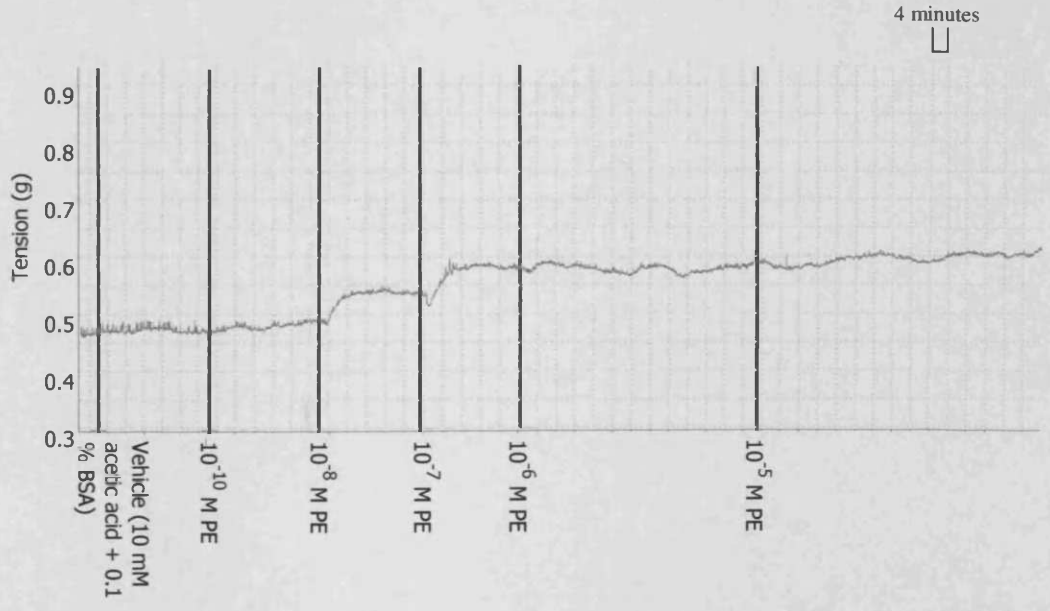

Example traces from experiments showing the effect of a) EGF and b) vehicle alone on aortic response to cumulative concentrations of PE in endothelium-intact rat aortic rings, $n = 4$.

Figure 3.43

a

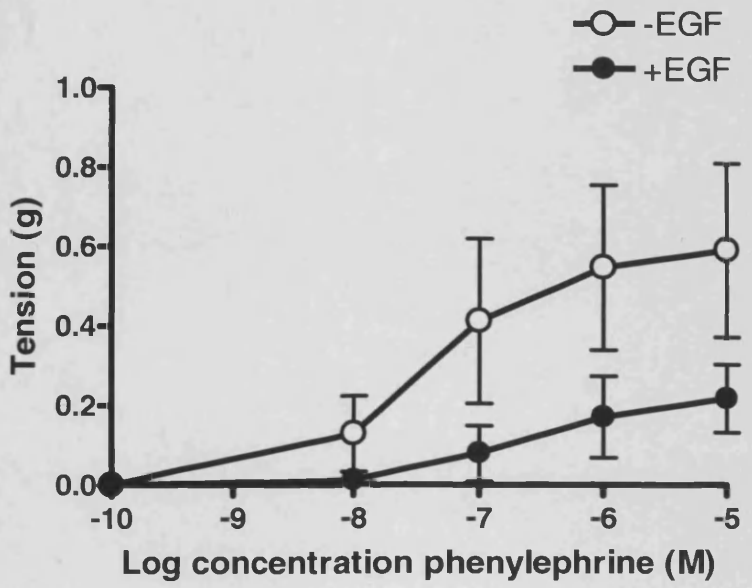

b

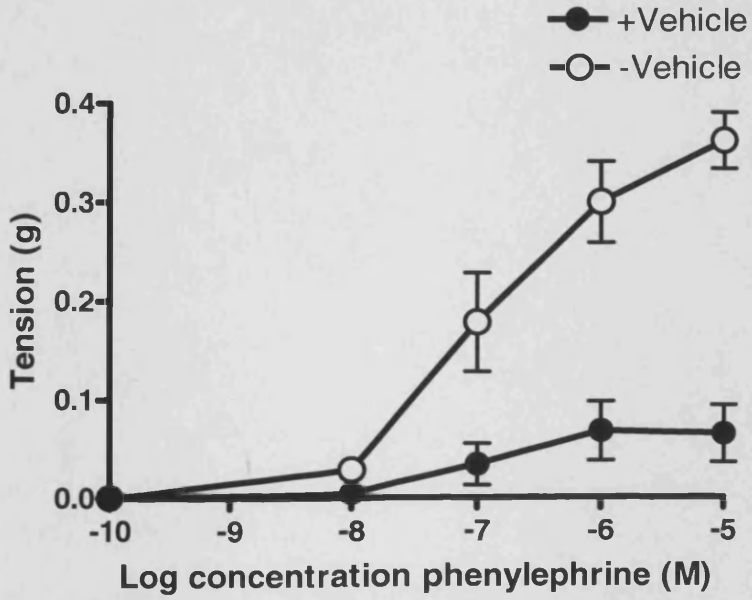

Graphs showing mean cumulative concentration-response curves for PE in endothelium-intact rat aortic rings a) + EGF or – EGF and b) + vehicle and – vehicle (± SEM). Results are of the absolute tension values relative to PE concentration, $n = 3$.

Table 3.1 EC50 and Maximum Values Derived from Individual Non-linear Curve Fitting for Phenylephrine Concentration-response Curves +/- EGF and +/- Vehicle (10 mM Acetic Acid + 0.1 % BSA)

The values are EC50 and maximum responses for the first PE-induced contractions in the absence of EGF (or vehicle) and for the second PE-induced contractions in the presence of EGF (or vehicle). 95% confidence intervals (CI) are shown for EC50 values and the ±SEM is shown for the maximum values.

Agonist response (g)	n	EC50 (M) (95% CI)	Maximum (g)
- EGF	3	0.7 (0.3 – 1.0) x 10^{-7}	0.6 ± 0.2
+ EGF	3	8.5 (1.3 – 16.2) x 10^{-7}	0.2 ± 0.1
- Vehicle	3	2.4 (0.6 – 3.1) x 10^{-7}	0.4 ± 0.03
+ Vehicle	3	1.6 (0.7 – 2.3) x 10^{-7}	0.07 ± 0.03

Figure 3.44

a

First cumulative concentration-response to PE in endothelium-intact rat aortic ring

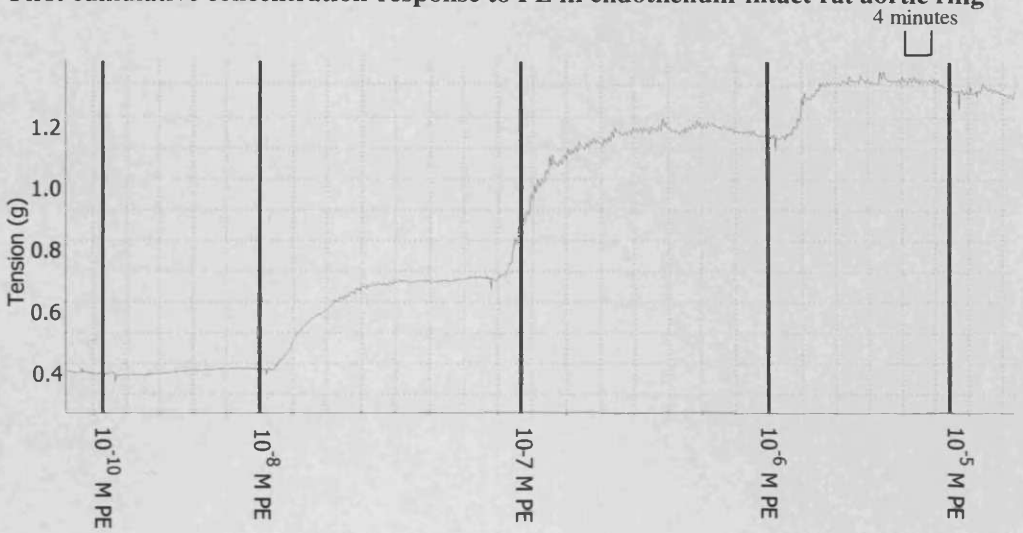

Second aortic cumulative concentration-response to PE in endothelium-intact rat aortic ring exposed to EGF (100 ng/ml)

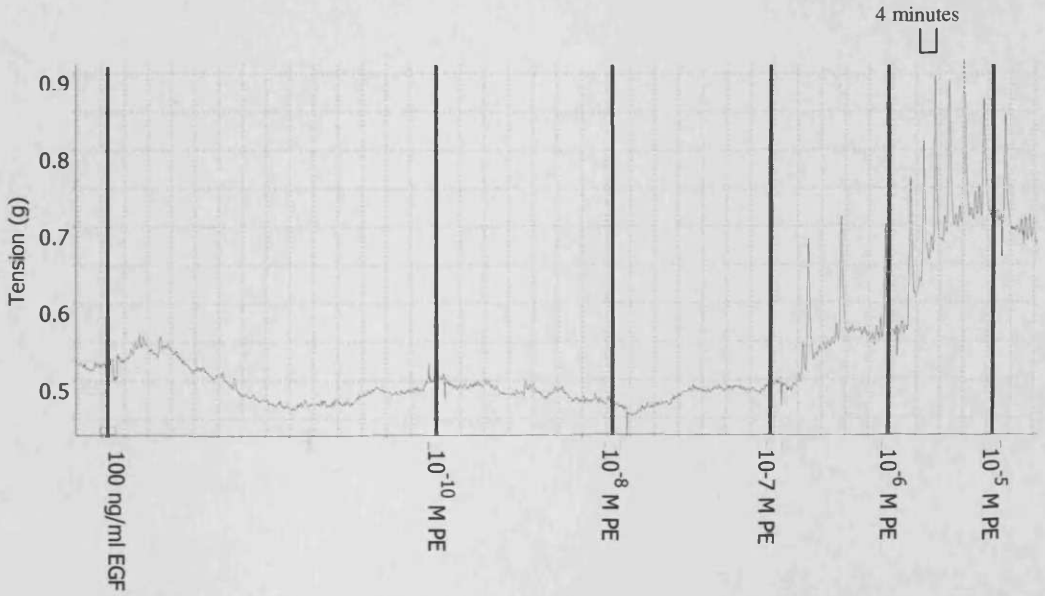

Figure 3.44 continued

b

First cumulative concentration-response to PE in endothelium-intact rat aortic ring

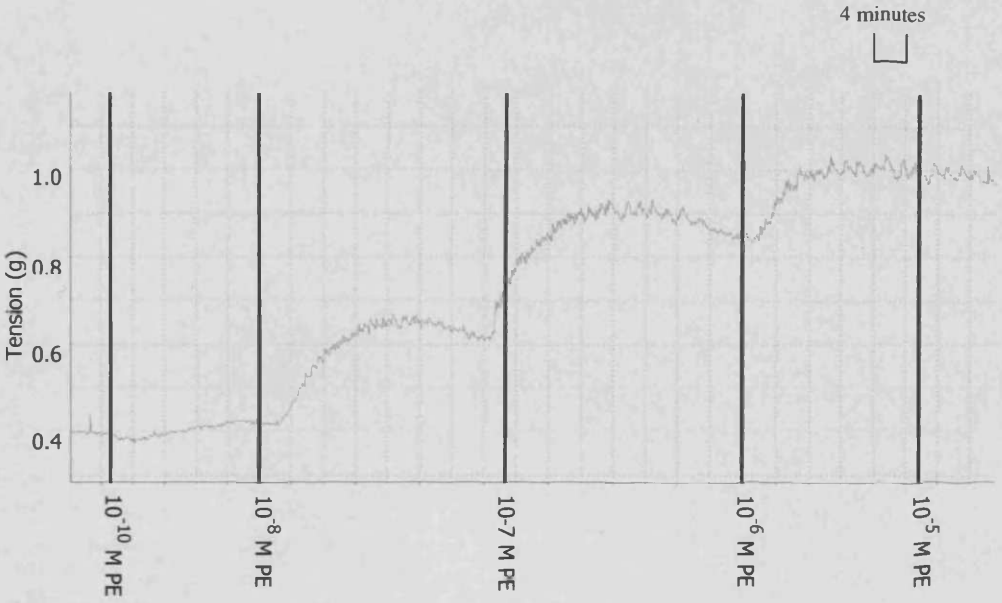

Second aortic cumulative concentration-response to PE in endothelium-intact rat aortic ring exposed to vehicle alone

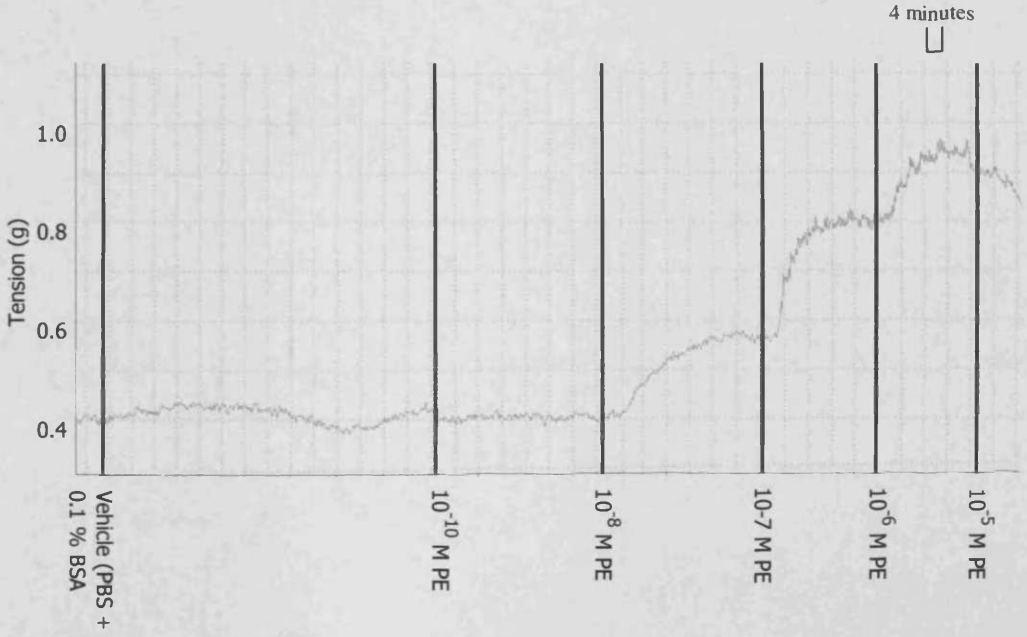

Figure 3.44 continued

c

First cumulative-concentration response to PE in endothelium-intact rat aortic ring (naïve control 1)

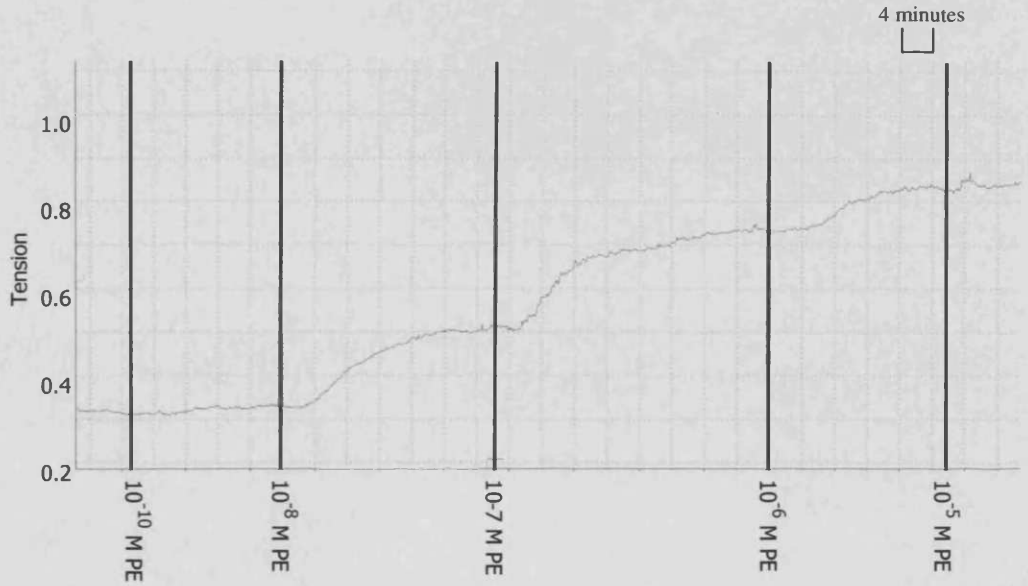

Second aortic cumulative concentration-response to PE in endothelium-intact rat aortic ring (naïve control 2)

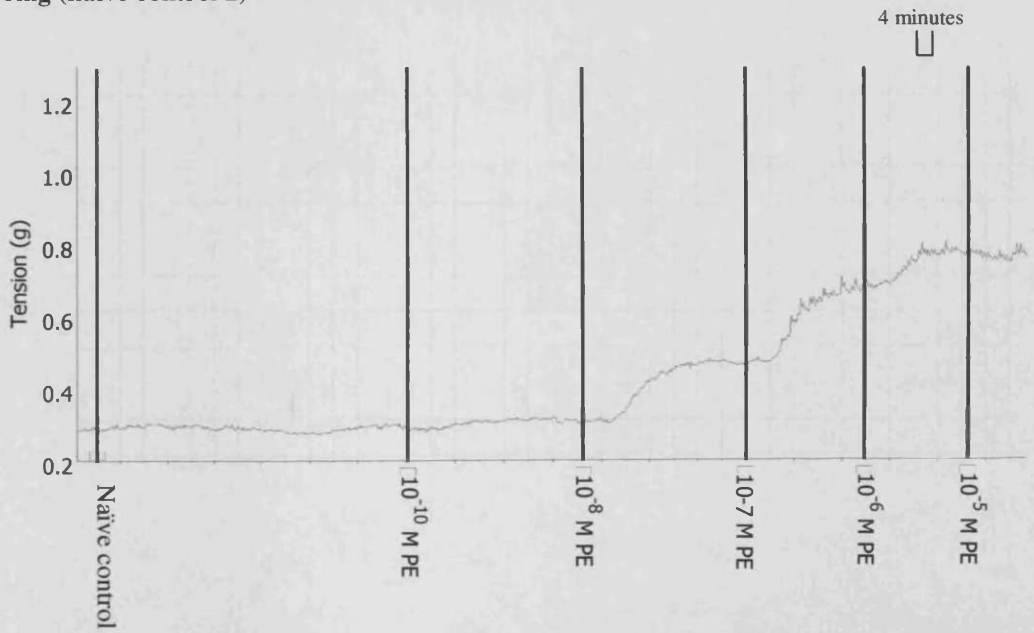

Example traces from experiments showing the effect of a) EGF, b) vehicle alone (n = 5 for both a) and b)) and c) naïve control (n = 4) on aortic response to cumulative concentrations of PE in endothelium-intact rat aortic rings.

Figure 3.45

a

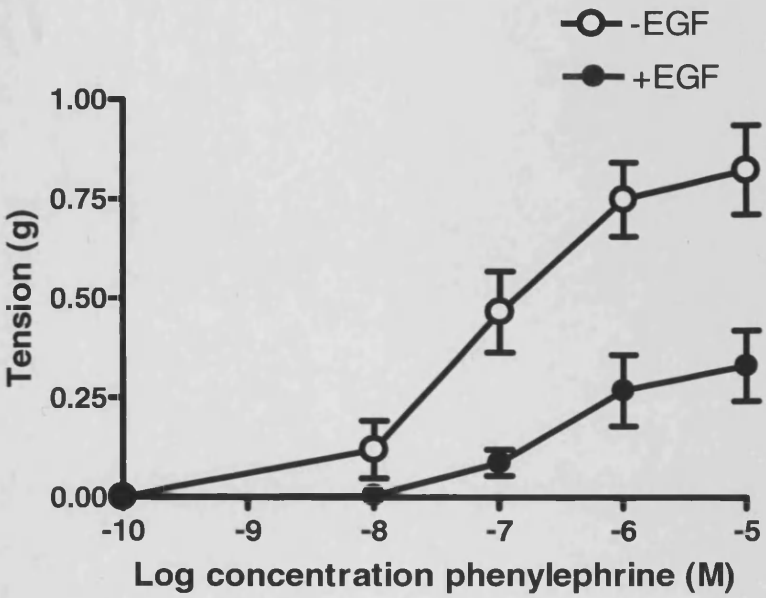

b

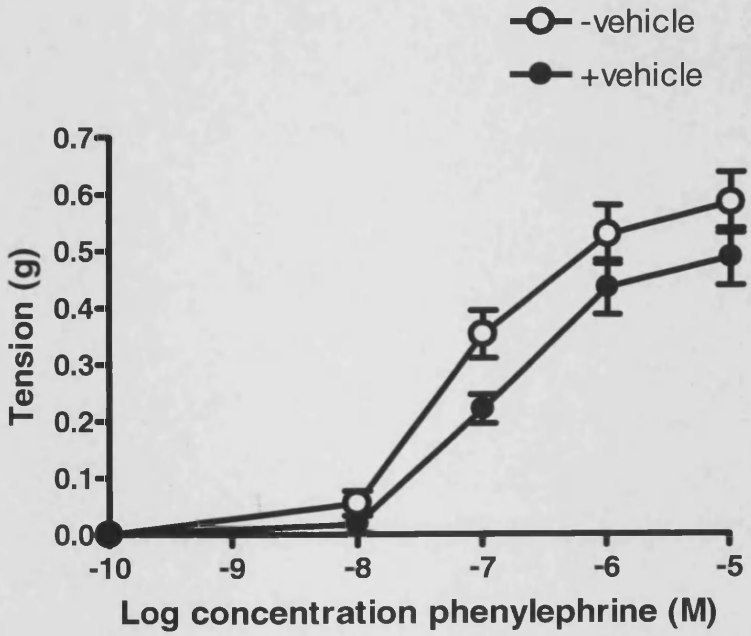

Figure 3.45 continued

c

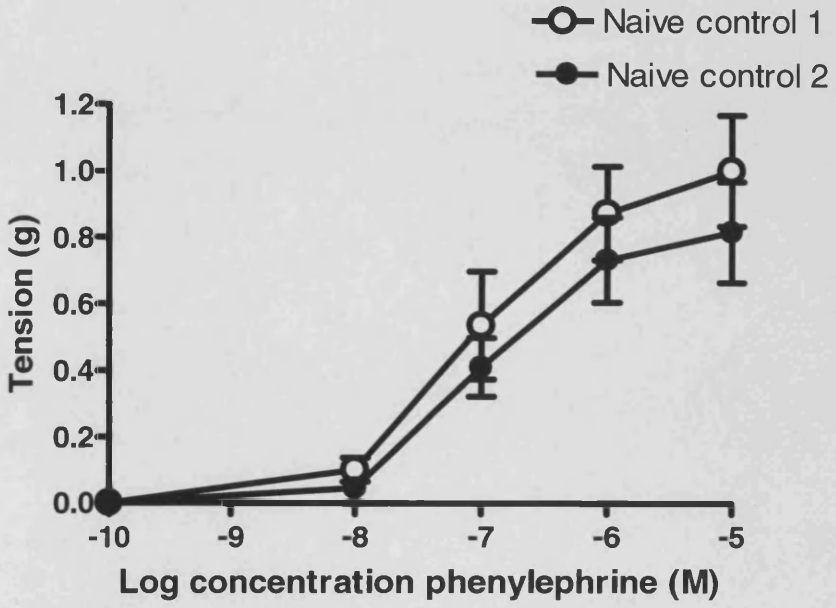

Graphs Showing mean cumulative concentration-response curves for PE in rat aortic rings a) + EGF and – EGF and b) + vehicle and – vehicle (PBS + 0.1 % BSA) (± SEM), n = 5 for both a) and b)). In figure c) naïve control 1 and naïve control 2 are first and second cumulative-concentration response contractions to PE without EGF and vehicle (± SEM), n = 4. Results are of the absolute tension values relative to PE concentration

Table 3.2 EC50 and Maximum Values Derived from Individual Non-linear Curve Fitting for Phenylephrine Concentration-response Curves +/- EGF and +/- Vehicle (PBS + 0.1 % BSA)

The values are EC50 and maximum responses for the first PE-induced contractions in the absence of EGF (or vehicle) and for the second PE-induced contractions in the presence of EGF (or vehicle). Naïve control 1 and naïve control 2 are first and second cumulative-concentration response contractions to PE without EGF or vehicle. 95% confidence intervals (CI) are shown for EC50 values and the ±SEM is shown for the maximum values. * $P < 0.05$, ** $P < 0.01$, *** $P < 0.001$ for second contraction with EGF or vehicle as compared to their respective controls (-EGF or –vehicle) as estimated using a 2 tailed paired Student's t-test.

Agonist response (g)	n	EC50 (M)(95% CI)	Maximum (g)
- EGF	5	$1.0\ (0.3 - 1.6) \times 10^{-7}$	0.8 ± 0.1
+ EGF	5	$6.1\ (1.3 - 7.9) \times 10^{-7}$**	0.3 ± 0.1**
- Vehicle	5	$0.8\ (0.5 - 1.1) \times 10^{-7}$	0.6 ± 0.1
+ Vehicle	5	$1.5\ (0.8 - 2.1) \times 10^{-7}$***	0.5 ± 0.1*
Naïve control 1	4	$2.4\ (0.4 - 3.9) \times 10^{-7}$	1.1 ± 0.2
Naïve control 2	4	$1.5\ (0.7 - 2.2) \times 10^{-7}$	1.0 ± 0.2

Table 3.3 Percentage (%) of Maximum Response and EC50 Values

% values are the % of maximum or EC50 of the second concentration response curve (in the presence of EGF or vehicle) to the maximum or EC50 of the first concentration response curve (in their absence). * $P < 0.05$, ** $P < 0.01$ compared with vehicle % as estimated using a 2 tailed, unpaired Student's t-test.

Ratio of	n	EGF (%)	Vehicle (%)
Maximum response	5	41.8 ± 4.4 **	84.3 ± 5.4
EC50	5	560.8 ± 151.7 *	163.8 ± 13.1

Figure 3.46

a

First cumulative-concentration response to PE in endothelium-denuded rat aortic ring

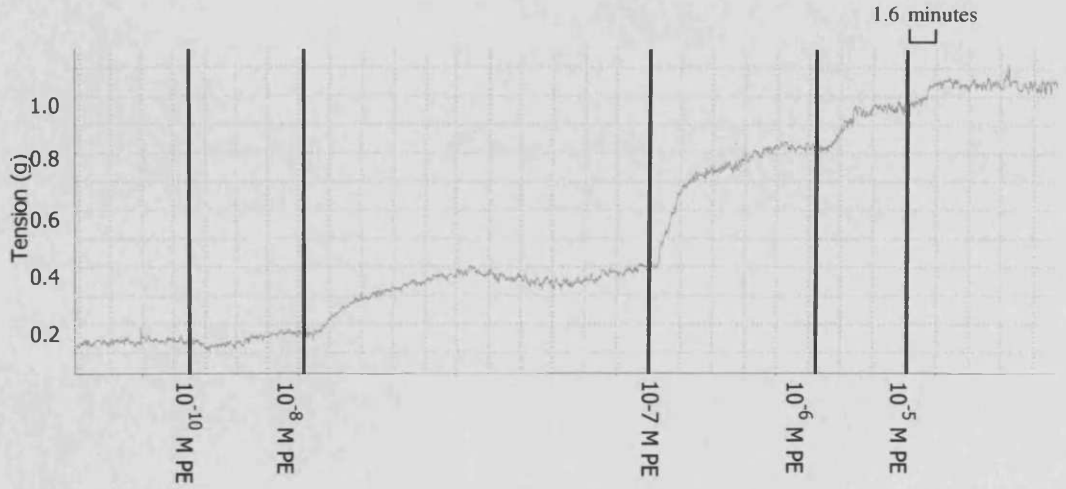

Second aortic cumulative concentration-response to PE in endothelium-denuded rat aortic ring exposed to EGF (100 ng/ml)

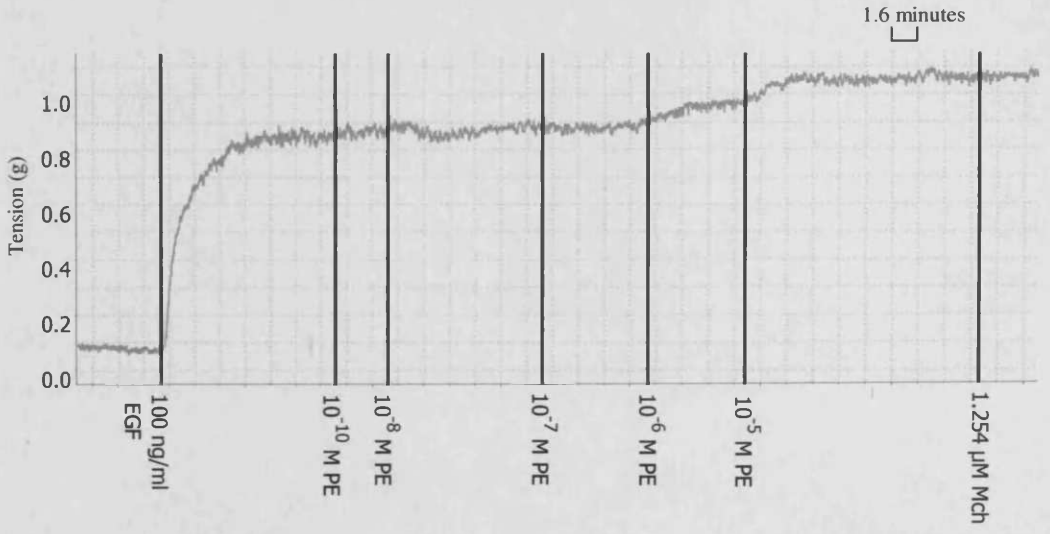

Figure 3.46 continued

b

First cumulative concentration-response to PE in endothelium-denuded rat aortic ring

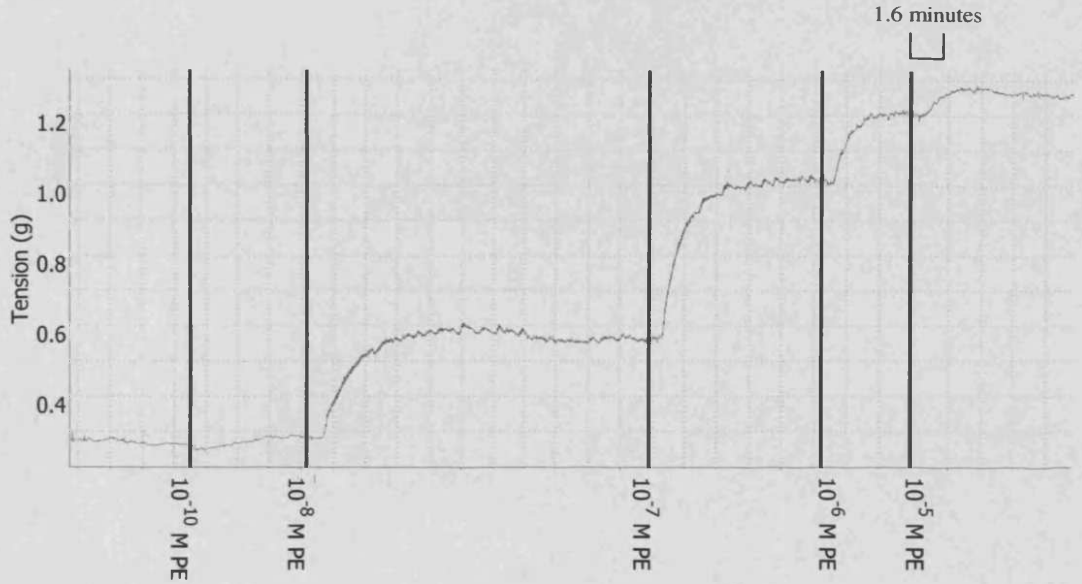

Second aortic cumulative concentration-response to PE in endothelium-denuded rat aortic ring exposed to vehicle alone

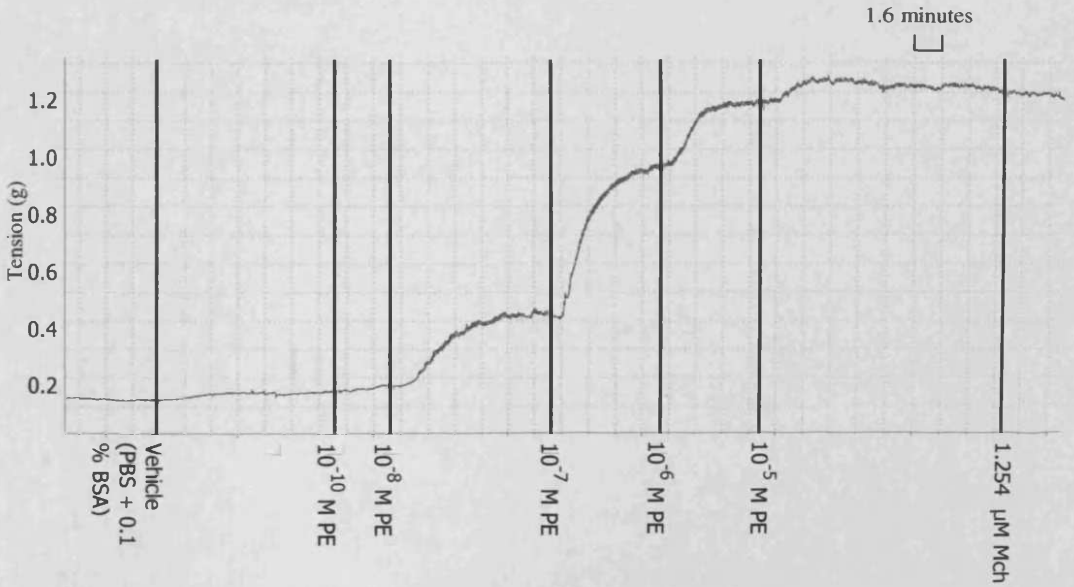

Example traces from experiments showing the effect of a) EGF and b) vehicle alone on aortic response to cumulative concentrations of PE in endothelium-denuded aortic rings, n = 5 for both a) and b).

Figure 3.47

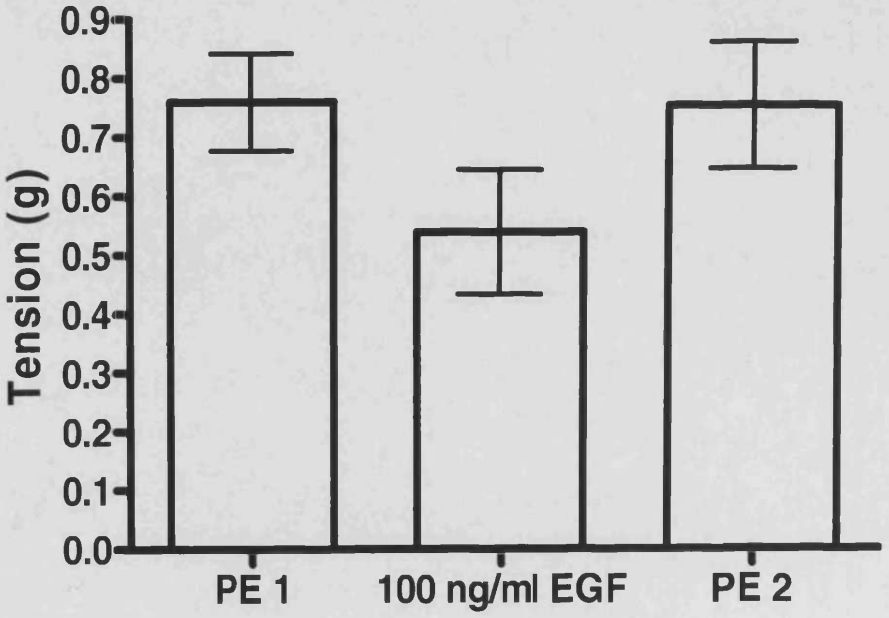

Mean maximum tension (g) of first PE concentration-response contraction, EGF-induced contraction and second cumulative concentration-response contraction, measured from the pre-EGF baseline.

Figure 3.48

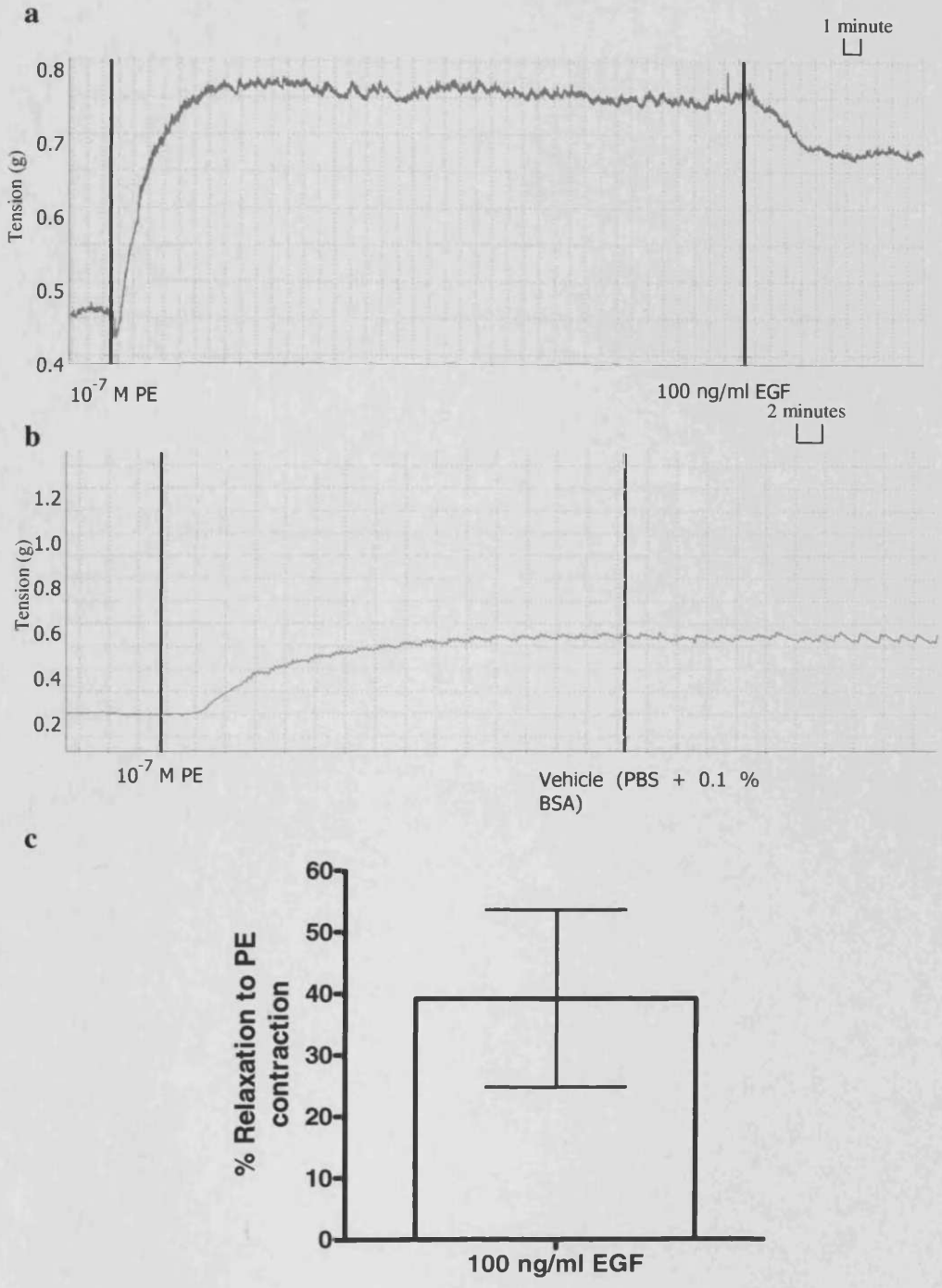

Example traces from experiments showing the effect of EGF on a PE-induced contraction a) shows EGF reversing PE induced contraction b) shows the effect of vehicle on PE induced contraction and c) shows mean % relaxation to PE-induced contraction in response to EGF (± SEM), $n = 4$.

4.0 Discussion

It is well known that uncontrolled diabetes can induce the development of microvascular and macrovascular pathologies, including retinopathy, nephropathy, atherosclerosis and myocardial infarction (Hammes 2003, Hurst and Lee 2003). These pathologies mostly develop as a result of diabetes-induced endothelial dysfunction (Avogaro, *et al* 2006, De Caterina 2000). One feature of endothelial dysfunction is an inability to produce the correct balance of vasoconstrictors and vasodilators, including the potent vasodilator nitric oxide (NO) (Gordon 2004, Li and Forstermann 2000). The present study provides new insights into the role of the receptor tyrosine kinases (RTKs), epidermal growth factor receptor (EGFR) and ErbB2 in the mechanism governing hyperglycaemia-induced aberrant endothelium-dependent NO production.

In the first part of this thesis, it was demonstrated that mesenteric bed tissue of streptozotocin (STZ)-induced diabetic rats showed an enhanced response to the vasoconstrictors noradrenaline (NA) and endothelin-1 (ET-1) and an attenuated response to the endothelium-dependent vasodilator carbachol. However, the response to the endothelium-independent vasodilator sodium nitroprusside (SNP) was similar in mesenteric vascular bed from STZ-induced diabetic rats to that seen in normal control rats (studies completed by Dr Mariam Yousif and Prof Ibrahim Benter (Benter, *et al* 2005a)). These findings support previous studies in mesenteric arteries (Fukao, *et al* 1997, Makino, *et al* 2000, Taylor, *et al* 1995) and aortae (Kamata, *et al* 1989, Oyama, *et al* 1986, Pieper and Gross 1988) from STZ-induced diabetic rats which reveal that the response to

endothelium-dependent vasodilators such as acetylcholine (Ach) are impaired. The present findings are also comparable with studies which show that responses to endothelium-independent vasodilators such as SNP, nitroglycerin, papaverine and atrial natriuretic peptide remain unaltered in the vasculature of diabetic rats (Kamata, *et al* 1989, Pieper and Gross 1988, Taylor, *et al* 1995). Moreover, again consistent with the present findings, previous studies have shown an enhanced response to vasoconstrictors in aortae and mesenteric arteries from diabetic rats (Abebe, *et al* 1990), and cheek pouch arterioles from diabetic hamsters (Mayhan, *et al* 1999).

Interestingly, the increased response to vasoconstrictors, ET-1 and NA, and the attenuated response to the vasodilator, carbachol, seen in the mesenteric vascular bed of STZ-induced diabetic rats could be prevented by pre-treating the rats with the RTK inhibitor genistein or with AG1478, a specific inhibitor of the RTK, EGFR. Diadzein, the inactive analogue of genistein, had no significant effect on vascular responses in STZ-induced diabetic rats. Also, no effect of AG1478, genistein or diadzein was seen in control rats. This suggests that RTK pathways, including EGFR pathways are involved in a mechanism that leads to diabetes-induced altered vascular reactivity.

Western blotting analysis of the mesenteric vascular bed tissue revealed an increase in EGFR phosphorylation in tissue from STZ-induced diabetic rats as compared to normal control rats. Furthermore, pre-treatment of STZ-induced diabetic rats with genistein or with AG1478 normalized the levels of

phosphorylated (p)EGFR in the mesenteric bed of these rats. This further strengthened the hypothesis that EGFR has a role to play in the mechanism of diabetes-induced vascular dysfunction. However, genistein also has effects on other molecules apart from EGFR, including other RTKs and also it has been shown to inhibit the activity of certain Ca^{2+} channels including the L-type Ca^{2+} channel in VSMC from rat portal vein (Liu and Sperelakis 1997). Thus, genistein's effects on molecules other than EGFR cannot be excluded in the present study. The present study is the first to demonstrate an elevation in the level of pEGFR in the mesenteric bed of diabetic animals as compared to non-diabetic controls. However, previous studies have shown EGFR and its main ligand, the epidermal growth factor (EGF) to be altered in other tissues from diabetic animals. An increase in EGFR activity has been reported in the gastric mucosa and kidneys of diabetic animals (Khan, *et al* 1999, Sayed-Ahmed, *et al* 1996) whereas, a decrease in EGFR activity has been demonstrated in the pancreas, liver, and placenta of diabetic animals (Korc, *et al* 1984, Okamoto, *et al* 1988, Sissom, *et al* 1987). Thus, it seems that upregulation or downregulation of EGFR in diabetic tissues depends on the type of tissue. Furthermore, it has been reported that RTKs, specifically EGFR and ErbB2 have a role to play in diabetes-induced vascular dysfunction in rat carotid artery, as inhibiting the activity of these receptors prevents diabetes-induced aberrant response to vasoconstrictors and vasodilators (Yousif, *et al* 2005). Similarly, inhibition of RTKs, specifically EGFR has been shown to prevent vascular dysfunction in the renal artery (Benter, *et al* 2005b).

Interestingly, western blotting further revealed that levels of pErbB2 were also increased in the mesenteric vascular bed of STZ-induced diabetic rats. Furthermore, in the same manner as pEGFR, increased ErbB2 phosphorylation was normalized by treatment with genistein and also with the specific ErbB2 inhibitor AG825. This is also the first study to show increased levels of pErbB2 in the mesenteric vascular bed tissue of diabetic animals. However, as mentioned earlier a previous study reported enhanced responses to vasoconstrictors and attenuated response to vasodilators observed in the carotid artery of diabetic rats could be normalized by inhibiting ErbB2 with AG825 (Yousif, *et al* 2005). Together with this study, the present results suggest that ErbB2, EGFR's favoured heterodimerization partner (Graus-Porta, *et al* 1997) also has a role to play in the mechanism which leads to diabetes-induced vascular dysfunction.

It has been suggested that diabetes-induced changes in cardiovascular reactivity can be attributed in part to diabetes-induced changes in calcium homeostasis, for example this has been demonstrated in whole tissue studies in heart (Beenen, *et al* 1995), aorta and mesenteric artery (Abebe, *et al* 1990) from diabetic rats. However, evidence is accumulating to suggest that dysfunctional abnormalities of the endothelium are major contributors to diabetes-induced aberrant vascular reactivity. This includes the aberrant production of endothelium-derived vasoactive agents, for example, hyperglycaemia has been shown to induce an increase in the generation of endothelium-derived vasoconstrictor prostanoids such as thromboxane A_2 in

rabbit aortae, which leads to reduced effect of vasodilators and increased vasoconstriction (Tesfamariam, *et al* 1990). Also, it has been suggested that an attenuated response to the vasodilator potassium (K^+), which is thought to be one of the endothelium-derived hyperpolarizing factors (EDHFs) (Edwards, *et al* 1998) has some part to play, as its function as a vasodilator is impaired in the mesenteric arterial bed of STZ-induced diabetic rats (Makino, *et al* 2000). However, relaxant responses to endothelium-dependent vasodilators such as Ach or carbachol are mainly due to the release of the powerful endothelium-derived vasodilator NO. Thus, a reduction in endothelium-dependent vasodilation may reflect decreased NO bioavailability. It is well known that the bioavailability of NO and also NO-mediated vascular dilation are reduced in diabetic animals and humans (Meininger, *et al* 2000, Pieper 1998). The present study identifies a dysfunction, specifically at the level of the endothelium, with an impaired response to endothelium-dependent vasodilators and a normal response to the endothelium-independent vasodilator and NO donor, SNP, being observed in the mesenteric vascular bed of STZ-induced diabetic rats. Thus, in the present model, a diabetes-induced reduction in NO production is a likely candidate for impairing vasodilation, and increasing the potency of vasoconstrictors due to a reduction in the opposing effect of NO. Previous studies have also found decreased production of cyclic guanosine monophosphate, which is downstream of NO, in response to Ach stimulation, in aortic strips from STZ-induced diabetic rats. However, these vessels responded normally to SNP, suggesting decreased production of endothelium-dependent vasodilators, most likely NO (Kamata, *et al* 1989).

The mechanisms that lead to aberrant synthesis and activity of endothelium derived vasodilators such as NO are not fully understood. Studies have suggested that diabetes-induced oxidative stress may have a major role to play. A previous study has shown that diabetic aortas become particularly sensitive to free radical damage, that impairs endothelium-dependent vasodilation in chronic diabetic rats (Pieper and Gross 1988). Also advanced glycation endproducts (AGEs), which are found at increased levels in diabetic vessels are known to quench NO both *in vitro* and *in vivo*, and thus contribute to reduce NO-induced vasodilation (Bucala, *et al* 1991). Also, studies have shown that high glucose can reduce NO synthesis through inhibiting eNOS expression and activity (Ding, *et al* 2000, Du, *et al* 2001). However, the exact mechanisms underlying these changes are not precisely known. The present studies suggest RTKs, in particular EGFR and ErbB2, as potential candidates involved in a mechanism which leads to diabetes-induced vascular dysfunction. Therefore, the subsequent aim of this study was to further elucidate the involvement of EGFR and ErbB2 in diabetes-induced vascular dysfunction, particularly how increased EGFR and ErbB2 activity might affect NO production. Identification of such a mechanism would lead to a better understanding of diabetes-induced vascular dysfunction and as such may lead to the development of novel therapies for the prevention or treatment of diabetes-induced vascular disease.

To further investigate the hypothesis a cell model was established using the human, endothelial-like cell line, ECV-304. Recently, there have been some doubts regarding the validity of ECV-304 as an endothelial cell model (Brown, *et al* 2000, Masters, *et al* 2001). However, studies have shown that ECV-304 cells display many features and markers characteristic of endothelial cells, such as their polygonal shape and the typical contact-inhibited cobble stone monolayer growth pattern, and also the presence of Weibel-Palade bodies (Takahashi, *et al* 1990b). Additionally, the present study revealed that ECV-304 cells express connexin 43 and endothelial NO synthase (eNOS), molecules which are characteristically found in endothelial cells. The cells were also shown to have detectable levels of pEGFR and pErbB2, thus, it was concluded that the cell line was suitable for further investigating the effect of diabetes on EGFR and ErbB2, and downstream mediators including NO.

Groups such as Varma *et al.* (2005) have mimicked the high glucose conditions associated with the diabetic state by growing cells of interest in cell medium containing high glucose. A fasting blood glucose concentration of around 7 mM or above indicates diabetes (World Health Organization 1999). However, blood glucose concentration fluctuates throughout the day and can reach concentrations well above 7 mM in diabetic individuals (World Health Organization 1999). Thus, to study the effect of high glucose on EGFR and its pathways, under the controlled conditions of cell culture, ECV-304 cells were incubated in control normoglycaemic (5.5 mM) conditions and in hyperglycaemic conditions, at concentrations of up to 25.5 mM glucose. These

studies were performed only following full optimization of conditions for this particular cell line. Incubation of cells with 25.5 mM glucose considerably reduced the rate of ECV-304 cell proliferation and cell survival as compared to cells grown in 5.5 mM glucose. After ≥ 72 hours of exposure to high glucose, proliferation of ECV-304 ceased and survival of cells decreased. This correlates with a study showing reduced proliferation and survival of HUVECs grown in 20 mM and 40 mM glucose, believed to be due to glucose-induced impairment of the anti-apoptotic PI3 kinase-Akt signalling pathway (Varma, *et al* 2005).

Studies using ECV-304 cells confirmed that high glucose treatment increased both EGFR and ErbB2 phosphorylation with no effect on total protein and mRNA expression being observed. This increase in phosphorylation of EGFR and ErbB2 was observed when glucose was increased to 10.5 mM. This suggests that a modest increase in glucose concentration for 72 hours is adequate to cause aberrant EGFR and ErbB2 signalling. Moreover, phosphorylation of both EGFR and ErbB2 were observed in ECV-304 cells after as little as 24 hours of high glucose treatment and was maximal after 72 hours of exposure. This may explain why such tight control of blood glucose concentration is necessary to prevent vascular damage, as a slight increase in glucose concentration over a relatively short period of time may cause biochemical changes which lead to vascular dysfunction. For example, a previous study demonstrated that acute (≤ 12 hours) high glucose (25.5 mM)

exposure can lead to pro-atherogenic changes in human aortic endothelial cells, by increasing the production of adhesion molecules and chemotactic factors (Piga, *et al* 2006). Also, a study of type I diabetic patients revealed that poor glycaemic control over relatively short periods of time (48 hours), can lead to adverse effects on the vasculature, by initiating vascular smooth muscle (VSM) or endothelial dysfunction (Sorensen, *et al* 2005). Furthermore, population studies have revealed that a modest increase above normal glucose levels is sufficient to increase the risk of developing cardiovascular disease. In this study an increased risk for cardiovascular disease development was seen when the blood glucose concentration of individuals was raised from 4.2 to 6.1 mM, which is still below the diabetic threshold (Coutinho, *et al* 1999).

The exact mechanism for hyperglycaemia-induced increased EGFR and ErbB2 activation is unknown. Conventionally, activation of EGFR is initiated upon binding of EGF, or other EGF-like ligands, to the receptor (Yarden 2001). ErbB2 on the other hand can only be activated through heterodimerizing with another ErbB receptor, as it has no cognate ligand (Garrett, *et al* 2003). Therefore, high glucose conditions could potentially be upregulating EGFR activation and ErbB2 dimerization through promoting transcription of EGFR ligands. However, in the present study this was found to be unlikely since preliminary polymerase chain reaction studies showed that mRNA levels of the EGFR ligands- amphiregulin, betacellulin, epiregulin, EGF, HB-EGF and TGFα, remained unchanged by 72 hours of high glucose exposure in ECV-304 cells.

There are alternative mechanisms for activating EGFR. For example glucose is known to increase the production of some external mediators of EGFR activity, including osmotic stress (Rosette and Karin 1996), AGEs (Cai, *et al* 2006) and oxidative stress (Rao 1996), which are all known to increase EGFR activity. However, osmotic stress-induced EGFR and ErbB2 activation can be excluded in the present study, since, in contrast to the effect seen after treating the cells with D-glucose, the osmotic control L-glucose did not induce EGFR or ErbB2 phosphorylation. Another mechanism for activation is EGFR transactivation, where stimulation of a G-protein coupled receptor by agonists such as angiotensin II (AngII) and ET-1 activate matrix metalloproteinases (MMPs) or ADAMs which cleave and release preformed, cell membrane bound ligands such as HB-EGF. The released ligands can subsequently transactivate EGFR (Eguchi, *et al* 2003). In fact, EGFR transactivation is known to take place in the endothelium (Fujiyama, *et al* 2001) and transactivation of EGFR receptor has previously been shown to be an important step in the development of diabetic nephropathy (Nose, *et al* 2003). Studies have shown that levels of AngII are increased in rat mesangial cells incubated with high glucose for 24 hours (Singh, *et al* 2003). Also, an increase in AngII induced transactivation of EGFR was shown in rat VSM cells (VSMCs) incubated with high glucose for 48 hours (Konishi and Berk 2003). This may explain in part how AngII receptor blockers or angiotensin converting enzyme inhibitors can prevent and reverse cardiovascular complications and neuropathy in diabetic patients (Coppey, *et al* 2006, Podar and Tuomilehto 2002). Further studies using

neutralising antibodies for EGFR ligands and MMP inhibitors could help determine the potential role for this mechanism in high glucose-induced aberrant EGFR activation in the present model. Protein tyrosine phosphatases (PTPs), enzymes that dephosphorylate EGFR, are also important external mediators of EGFR activity, thus, may be implicated in the present model. It has been suggested that oxidative stress such as the production of hydrogen peroxide induces the phosphorylation of EGFR partly through inactivating PTPs, leading to a reduced rate of EGFR dephosphorylation (Kamata, *et al* 2000).

It is also possible that the activities of EGFR and ErbB2 are not altered by glucose through intermediary molecules, but instead are directly altered by the glucose molecule itself. A previous study has shown that cells exposed to high glucose for 48 hours express an N-glycosylated form of EGFR, which compared to its non-glycosylated counterpart, is transactivated by AngII at an increased rate. This transactivated glycosylated EGFR then activates Akt and ERK1/2, and promotes VSMC proliferation (Konishi and Berk 2003). Further investigation would be necessary to investigate this as a potential mechanism.

To further investigate the effects of hyperglycaemia on EGFR, ErbB2 and downstream signal transduction pathways, the EGFR inhibitor, AG1478, and the ErbB2 inhibitor, AG825, were used. Both AG1478 and AG825 can be solubilized using dimethyl sulfoxide (DMSO). Studies showed that only 1 % final volume of DMSO could be used in experiments, before DMSO became

toxic to the cells. Inhibitor concentration-response experiments were conducted to elucidate the concentration of inhibitors to use in order to inhibit EGFR and ErbB2 phosphorylation in ECV-304 cells. From these 0.5 μM of AG1478 and 20 μM of AG825 were used in experiments. In ECV-304 cells the specificity of the inhibitors for their targets were tested by looking at the effect of AG1478 on ErbB2 phosphorylation and the effect of AG825 on EGFR phosphorylation under normal and high glucose conditions. AG1478 demonstrated greater selectivity towards EGFR but also caused a small inhibition of ErbB2 phosphorylation. In contrast, AG825 was more selective for inhibiting ErbB2 phosphorylation, but also caused a small decrease in EGFR phosphorylation. However, this is not surprising considering that EGFR and ErbB2 heterodimerize, thus inhibiting the activity of one of the pair would undoubtedly affect the activity of the other. This correlates with a previous study showing that the inhibition of EGFR with an EGFR specific inhibitor, also blocks ErbB2 phosphorylation in breast carcinoma cells (Moulder, *et al* 2001). Additionally, although these inhibitors are selective for their specific targets they do also have some inhibitory effects upon other members of the ErbB family if used at higher concentrations (Tocris bioscience 2007a, Tocris bioscience 2007b).

Indeed, this study showed for the first time that high glucose induces an increase in the level of co-immunoprecipitated EGFR and ErbB2. This suggests that high glucose treatment increases EGFR and ErbB2

heterodimerization. However, the involvement of the other dimerization partners, ErbB3 and ErbB4, cannot be excluded. Further studies would be necessary to deduce the importance of each family member in the mechanism leading to diabetes-induced vascular dysfunction. As expected, AG1478 reduced the levels of hyperglycaemia-induced co-immunoprecipitated EGFR and ErbB2, and AG825 completely prevented co-immunoprecipitation of the receptors.

To investigate the mechanisms by which EGFR and ErbB2 signalling might mediate vascular dysfunction, studies were performed to examine the effects of high glucose-induced activation of EGFR and ErbB2 on initiation of downstream signal transduction cascades and NO production. The possibility of hyperglycaemia-induced EGFR activity modulating the production or activity of endothelium-derived agonists other than NO, such as EDHF and prostacyclin cannot be excluded; however, these were not investigated in the present study.

EGFR regulates its cellular function through initiating multiple downstream signal transduction cascades, including mitogen activated protein kinase (MAPK), phosphoinositide 3-kinase (PI3K) and diacyl glycerol/ protein kinase C (DAG/PKC) pathways (Hackel, *et al* 1999, Holbro, *et al* 2003, Prenzel, *et al* 2001). In the present study, the external addition of EGF to ECV-304 cells, increased levels of EGFR and ErbB2 phosphorylation in a concentration- and time-dependent manner. Furthermore, EGF increased phosphorylation of PKC,

Akt, ERK1/2 and p38MAPK, suggesting that these pathways are modulated by EGFR activity in ECV-304 cells.

Increased levels of PKC and DAG, the upstream mediator of PKC, have been reported in the renal glomeruli, aorta, heart and retina of STZ-induced diabetic rats (Craven and DeRubertis 1989, Inoguchi, *et al* 1992, Shiba, *et al* 1993). Also, hyperglycaemia has been shown to induce the *de novo* synthesis of DAG in cultured retinal and aortic endothelial cells isolated from diabetic animals (Koya and King 1998). These findings are consistent with the present study which showed increased levels of pPKC in ECV-304 cells treated with high glucose for 72 hours. PKC is thought to play a crucial role in mediating diabetes or hyperglycaemia-induced vascular dysfunction, as PKC activation has adverse effects on both the endothelium and the VSM. Increased PKC activation is known to increase production of cytokines and enhance permeability, vascular cell proliferation and contractility (Koya and King 1998). Studies also suggest that increased PKC induces endothelial dysfunction via a number of mechanisms, most of which stem from the fact that hyperglycaemia-induced PKC activation generates superoxide ($O_2^{\cdot-}$) by activating $O_2^{\cdot-}$ producing enzymes such as nicotinamide adenine dinucleotide phosphate oxidase (Hink, *et al* 2003). For example, the paradox of reduced NO bioavailability but increased eNOS mRNA and protein expression reported by some in cultured human aortic endothelial cells and vessels from STZ-induced diabetic rats is partly due to increased PKC activity, as PKC can induce uncoupling of eNOS which then produces $O_2^{\cdot-}$ that reacts with NO, and

produces the destructive reactive oxygen species peroxynitrite (Cosentino, *et al* 1997, Hink, *et al* 2003). Furthermore, PKC-induced oxidative stress has been shown to upregulate cyclooxygenase-2 (COX-2) in human aortic endothelial cells. COX-2 further decreases NO bioavailability, decreases the production of vasodilatory prostanoids and increases the production of vasoconstrictor prostanoids (Cosentino, *et al* 2003). PKC-induced $O_2^{\cdot-}$ produced in the VSM may also inactivate or reduce the expression of the soluble guanylate cyclase, which is the downstream target of NO (Hink, *et al* 2003). PKC can also influence NO production through phosphorylating eNOS at threonine residue 495 (Fleming, *et al* 2001, Mount, *et al* 2006) found within the calmodulin binding domain. Phosphorylation at this site reduces binding of calmodulin to eNOS, resulting in reduced catalytic activity (Matsubara, *et al* 2003). PKC can also dephosphorylate eNOS at the activator site Ser1177, by increasing activity of the phosphatase PPA2, thus, reducing eNOS activity and NO production (Michell, *et al* 2001).

The PKC isoform mostly associated with hyperglycaemia-induced vascular pathologies and the reduction of eNOS activity in endothelial cells is PKC β (Beckman, *et al* 2002, Chu and Bohlen 2004, Way, *et al* 2001). However, the PKC δ isoform is also believed to have an involvement in the development of diabetes-induced vascular abnormalities (Koya and King 1998, Rask-Madsen and King 2005, Srivastava 2002). The PKC pan antibody used for western blotting in this study detects α, β I, β II, δ, ε, η and θ isoforms, and was thus

suitable for examining the role of PKC in diabetes-induced vascular dysfunction.

A previous study has reported a decrease in eNOS activity in response to increased glucose concentrations, through a PKC mechanism, in diabetic mouse kidney glomeruli (Chu and Bohlen 2004). Based on present studies showing that in ECV-304 cells, high glucose phosphorylates PKC, which is reduced by treatment with AG1478 and normalized by treatment with AG825, and the knowledge that PKC phosphorylates eNOS at Thr495, a hypothesis was formulated. This was that hyperglycaemia-induced increase in EGFR and ErbB2 activity leads to increased PKC activity which subsequently reduces the activity of eNOS via phosphorylation at Thr495, leading to aberrant NO synthesis. Initial evidence to support this hypothesis was provided via a western blotting assay which revealed that hyperglycaemia and thus, increased EGFR/ ErbB2 activity, was associated with increased eNOS phosphorylation at Thr495. However, high glucose treatment had no effect on eNOS phosphorylation at Ser1177, which is consistent with another study in human aortic endothelial cells, showing that high glucose treatment for 48 hours was without effect on eNOS phosphorylation at Ser1177 (Salt, *et al* 2003). Also, high glucose concentration did not have an effect on total eNOS protein expression.

To further test the involvement of PKC in the regulation of eNOS phosphorylation in ECV-304 cells, 12-O-tetra-decanoyl-phorbol-13-acetate

(TPA), a direct activator of classical and novel PKCs, was used. However, prolonged TPA exposure (6 – 12 hours) is known to downregulate PKC activity (Rask-Madsen and King 2005). The present study strongly suggests that PKC modulates activation of eNOS at Thr495, since both PKC and eNOS Thr495 activity were increased in response to TPA after 3 hours of exposure but inhibited after 24 hours and 48 hours of TPA treatment. Furthermore, the inhibition of PKC in control cells using the specific PKC inhibitor RO-31-8220 inhibited both PKC activation and eNOS activation at Thr495. Although these studies suggest that in the cell model used eNOS phosphorylation at Thr495 is modulated by PKC activity, further studies using cells grown in high glucose would be needed to see if the same effect were seen under hyperglycaemic conditions. In fact, other studies have suggested increased PKC activation as a mechanism for a hyperglycaemia-induced decrease in NO production, and demonstrated that high glucose-induced impaired endothelium-dependent vasodilation can be prevented or corrected through inhibiting PKC activity (Beckman, *et al* 2002, Tesfamariam, *et al* 1991).

The specific PKC inhibitor GO6983 had no effect on PKC in the ECV-304 cell model. This may be because GO6983 inhibits only the α, β, δ, and ζ isoforms of PKC, it is not known for certain which specific isoforms (α, β I, β II, δ, ε, η and θ) that the PKC (pan) antibody detects in the ECV-304 cell model. Thus, it could be that the inhibitor does not specifically target the PKC isoforms present in the cell model used.

An interesting observation made from the present studies is that the inhibition of ErbB2 activation using AG825 is more effective at downregulating the phosphorylation of PKC and eNOS at Thr495, than inhibiting EGFR with AG1478. This could mean that ErbB2 with a dimerization partner such as ErbB3 is more important in regulating NO activity in this system. However an alternative explanation is that AG825 is simply a more potent inhibitor than AG1478 at the concentrations used in this study.

As previously mentioned, activation of EGFR in ECV-304 cells activates MAPK and PI3K signalling pathways alongside PKC. ERK1/2, p38MAPK and Akt have all been implicated to have some role in modulating NOS activity (Begum and Ragolia 2000, Cale and Bird 2006, Kim, *et al* 2001). In the present study, high glucose treatment for 72 hours increased levels of phosphorylated but not total p38MAPK, with both AG1478 and AG825 treatment preventing this activation. Similarly, high glucose treatment slightly increased Akt phosphorylation, with AG1478 inhibiting Akt phosphorylation and AG825 having no effect. Thus, both p38MAPK and Akt may also have a role to play in diabetes-induced vascular dysfunction, but further studies would be required to confirm their importance in the development of diabetes-induced vascular dysfunction. However, in the present study, high glucose treatment for 72 hours had little effect upon the level of ERK1/2 phosphorylation, indicative of no role for this pathway in high glucose-induced dysfunction of ECV-304 cells.

To further investigate the ability of EGFR activity to regulate NO synthesis, isolated aortic ring preparations from non-diabetic Spague-Dawley rats were used, as a bioassay for NO production. To stimulate EGFR activity, human recombinant EGF, expressed in *Escherichia coli* was used. Studies have shown that although the degree of homology between human and rat EGF is not as high as between human and mouse EGF, the biological-effects are not species specific (Schaudies and Savage 1986). Thus, human EGF could be used in the present study to investigate EGF effects on rat vascular reactivity. The concentrations of EGF used in this study, 1, 10 and 100 ng/ml, were higher than that found in free plasma which is around 0.30 - 0.35 ng/ml (Brzezinski and Lewinski 1998, Oka and Orth 1983). However, it has been suggested that the levels of available EGF at sites of active platelet-vessel wall interaction is higher than that found in free plasma (Berk, *et al* 1985). Studies using ECV-304 cells suggested that diabetes-induced EGFR activity reduced endothelial NO synthesis by modulating eNOS activity. Therefore, it was expected that exposure of aortic rings to EGF would reduce endothelial NO production and thus potentiate the effect of vasoconstrictors and attenuate vasodilation.

EGF exposure alone had no effect on the resting tone of endothelium-intact aorta, but induced a significant and immediate contraction in endothelium-denuded aorta. This contraction would appear to be mediated directly on the VSM as endothelium was absent. Previous studies have also shown that EGF can have a vasoconstrictive effect directly upon the VSM, believed to be due to an EGF-induced increase in calcium efflux and calcium channel activation, as

demonstrated in cultured rat aortic VSMCs (Berk, *et al* 1985) and in isolated endothelium-denuded aorta from deoxycorticosterone acetate (DOCA)-salt hypertensive rats (Florian and Watts 1999). However, Muramatsu *et al.* (1985) suggested that EGF causes contraction through a COX pathway, since the COX inhibitor indomethacin abolished EGF-induced contractions. A more recent study suggests that EGF induces vasoconstriction in hypertensive rats through a PI3K-mediated MAPK pathway (Kim, *et al* 2006).

In contrast to the present study, previous studies have shown that EGF also induces vasoconstriction in endothelium-intact rat arterial strips (Berk, *et al* 1985, Muramatsu, *et al* 1985). However, one study showed that EGF induced contraction in both intact and endothelium-denuded aortic strips from DOCA-salt hypertensive rats, and that contraction was slightly attenuated in the endothelium-intact aortic strips, suggesting that the presence of the endothelium could partly counteract the contractile effect of EGF (Florian and Watts 1999).

Interestingly, the present study suggests that EGF may act at both the level of the endothelium and the VSM, producing diametrically opposing actions. Thus, in intact non-diabetic aorta, EGF acts on the endothelium to promote the release of a vasodilator that then opposes its direct constrictor action on VSM, ultimately resulting in little or no effect of EGF being observed in endothelium-intact aortic rings. This is opposite to what the present studies suggest is occurring in diabetic tissues.

Further evidence to support the theory that EGF induces a release of an endothelium-derived vasodilator was provided by results showing that EGF caused significant relaxation in phenylephrine (PE)-preconstricted aortic rings. Also, although the effect was variable, a trend could be seen showing EGF enhancing acetyl methylcholine induced relaxations in a concentration-dependent manner. Consistent with the present study, one group showed that EGF induced an endothelium-dependent relaxation in isolated rat aortic strips preconstricted with prostaglandin F2 α and with NA, and to a lesser extent preconstricted with K^+. NO is known to be more effective against an agonist induced contraction compared to K^+ induced contraction, which suggested the involvement of NO in counteracting the effect of the vasoconstrictors. Thus, this group proposed that EGF binds to EGFR on endothelial cells, increasing NO production and inducing cGMP, and a subsequent relaxation of VSM (Namiki and Akatsuka 1990). Also, EGF has been shown to increase eNOS protein and mRNA expression and NO synthesis, believed to be important for placental blood flow and the onset of labour, in endothelial cells from ovine fetoplacental artery (Zheng, *et al* 1999) and in rat placentae (Ribeiro, *et al* 2005). Thus, it could be speculated that in the present study the vasodilator released by the endothelium in response to EGF, which counteracts the direct contractile effect of EGF upon the VSM, is NO. However, further investigation into the role of EGF in modulating the production of NO in the present model would be required, which could be done using specific eNOS inhibitors such as nitro-L-arginine methyl ester.

The possibility that EGF is acting upon other endothelium-derived factors such as prostacyclin or EDHF in the present model cannot be excluded. This is especially true since previous studies have shown that EGF can activate cytosolic phospholipase A2c, an enzyme that catalyses the release of arachidonic acid from phospholipids, which is a precursor for eicosanoids such as the effective vasodilator prostacyclin (Bonventre, *et al* 1990).

Due to the unexpected effect of EGF on aortic tension, further studies were undertaken to confirm the role of EGF in modulating NO production. Experiments were conducted to investigate the effects of EGF treatment on the vasoconstrictor action of U46619 in endothelium-intact aortic rings. Surprisingly pre-treatment with EGF had no effect on U46619-induced contractions. However, previous studies have indicated that the modulation of U46619-induced contraction by levels of NO is variable. Some experiments have shown NO to influence contractile responses to U46619 (Lamping and Faraci 2003, Oyekan 2003, Sillau, *et al* 2002, Wilson, *et al* 1997) whilst other studies have shown NO to have no effect (Heijenbrok, *et al* 2000, Vedernikov, *et al* 2001). One study showed in eNOS deficient mice (eNOS-/-) or acute absences of eNOS activity following N(G)-nitro-L-arginine treatment only modestly increased mouse aortic contraction induced by U46619, and no effect at all when U46619 was used at a high concentration (Lamping and Faraci 2003). Thus, EGF-induced alterations in eNOS in the present study might not influence U46619-induced contractions, due to higher concentrations of

U46619 masking any effect of EGF. In support of this theory an interesting observation made from the present studies was that in vessels preconstricted with U46619 and relaxed with acetyl methylcholine a relaxation to EGF was only seen when U46619-induced tone was low e.g. < 2g but was lost when U46619-induced tone was high e.g. > 2g.

Due to this complication with U46619 an alternative vasoconstrictor was assessed, the α adrenergic agonist PE. Like other α adrenergic agonists, in most blood vessels the vasoconstrictor activity of PE is affected by NOS activity (Vanhoutte 2001), also PE can indirectly stimulate NO production (Dora, *et al* 2000). Therefore PE may be a better constrictor than U46619 to assess EGF's potential to influence NO release and thus affect PE-induced constriction. Firstly these experiments were conducted using EGF solubilized in 10 mM acetic acid with 0.1 % bovine serum albumin (BSA). However, alone this vehicle had a significant effect on PE-induced contractions, thus PBS with 0.1 % BSA was subsequently used as an EGF vehicle. Pre-treatment of aorta with EGF solubilized in this alternative vehicle attenuated PE-induced contractions, shifting the concentration-response curve to the right, which confirmed the previous findings showing EGF-induced relaxation. In agreement with the earlier study on endothelium-denuded aorta, EGF treatment of aorta denuded of endothelium caused contraction but had no effect on the aorta's maximum response to PE.

In the present study, aorta from healthy non-diabetic rats showed a reduced response to vasoconstrictors when exposed to EGF. However, in STZ-diabetic rats EGFR activity seemed to be involved in the mechanism increasing response to vasoconstrictors. This suggests that EGF has opposite effects on aortic tone in vessels from diabetic and non-diabetic animals. Therefore, a component of diabetes, such as hyperglycaemia, must not only increase the activity of EGFR, but also convert the effects of EGFR activation from initiating a prorelaxant output to a procontractile output. A hyperglycaemia-induced alteration in EGFR signalling pathways is further suggested by cell culture studies. These studies show increased eNOS phosphorylation at Ser1177 in cells grown in control (5.5 mM) glucose when treated with EGF for 10 minutes, with high glucose having no effect on phosphorylation at this site. This suggests an EGF-induced increase in NO synthesis under normal glucose levels. Also, in cells grown in normoglycaemia, inhibiting the activity of EGFR with AG1478 for 72 hours induces eNOS Thr495 phosphorylation. However, in cells grown in high glucose the opposite effect is seen, where inhibition of EGFR with AG1478 reduces eNOS Thr495 activity. Interestingly, AG1478 treatment also has the opposite effect on pPKC levels in control cells as to cells grown in high glucose. This suggests that under both normal and high glucose conditions EGFR signalling modulates eNOS phosphorylation through the activation of PKC. However, EGF-induced phosphorylation occurs at Ser1177 in normal cells, with no effect of EGF seen at Thr495, but changes to EGF-induced Thr495 phosphorylation in diabetic cells. Thus, under normoglycaemic

conditions, activation of EGFR has the opposite effect on NO production to that seen in hyperglycaemic conditions.

5.0 Conclusions

As of yet there is no cure for diabetes, the main aim of treating diabetic patients is to prevent or delay major cardiovascular events such as heart attacks and strokes associated with diabetes, and diabetes-induced microvascular complications. Thus, current treatments modify the risks factors contributing to these vascular events. For type I diabetic patients treatment is mostly insulin injections and for type II diabetic patients, treatment is mostly oral hypoglycaemics that reduce blood glucose concentration in combination with guidelines for leading a healthier lifestyle (Krentz and Bailey 2005, Ward, *et al* 2005). However up to one third of patients fail to respond to these oral hypoglycaemics (Bullock, *et al* 2002) and many patients find it difficult to live completely healthy "sugar-free" lifestyles. This puts them at increased risk of developing diabetic-complications. Moreover, even patients with well controlled diabetes almost always develop organ and vascular damage eventually. Thus, it is important to find potential therapeutic targets for the prevention of diabetes-induced vascular dysfunction, which is what was attempted in the present study.

This study revealed for the first time that levels of pEGFR are increased in the mesenteric bed of diabetic rats. Also, using EGFR and RTK inhibitors the involvement of EGFR and its downstream signal transduction cascade were implicated in the development of diabetic vascular dysfunction. Furthermore, for the first time a role for ErbB2 was implicated in the mechanism leading to vascular dysfunction by showing that ErbB2 is activated in the mesenteric bed of diabetic rats and in ECV-304 cells grown in high glucose, and that

hyperglycaemia increases the rate of EGFR and ErbB2 heterodimerization. The present study also suggests that high glucose induced activation of EGFR and ErbB2 initiates a signalling cascade which activates PKC and subsequently phosphorylates eNOS at Thr495. It is well known in the literature that increased phosphorylation of eNOS at Thr495 decreases the rate of NO biosynthesis (Matsubara, *et al* 2003). It is possible that this mechanism contributes to diabetes-induced exaggerated response to vasoconstrictors and attenuated response to vasodilators. Using isolated aortic ring preparations this study attempted to confirm that increased EGFR signalling reduced NO production. However, interestingly the results revealed that EGFR activation did not increase contraction in aortic tissue from healthy non-diabetic aortic rats. In fact, EGF had the opposite effect upon the aorta by reducing contractile activity to PE. Furthermore EGF induced an immediate contraction in endothelium-denuded aortae, suggesting that EGFR induces the release of a vasodilator such as NO from the endothelium, which counteracts the contractile effect of EGF upon the VSM. The opposite effects of EGFR activation upon vessels from non-diabetic and diabetic rats suggests that high glucose not only increases EGFR phosphorylation but also alters its downstream effects, converting a prorelaxant effect to a procontractile effect.

Thus this study has identified the involvement of EGFR and ErbB2 in the development of diabetes-induced vascular dysfunction and implicated a novel mechanism for which increased EGFR/ ErbB2 signalling may impair vascular response via the attenuation of NO synthesis. Figure 5.2 summarises the key

results from this study and how these fit into previous findings found in the literature. In conclusion, the RTKs EGFR and ErbB2 and also the PKC pathway may be potential new therapeutic targets for the prevention or treatment of diabetes-induced vascular dysfunction.

a

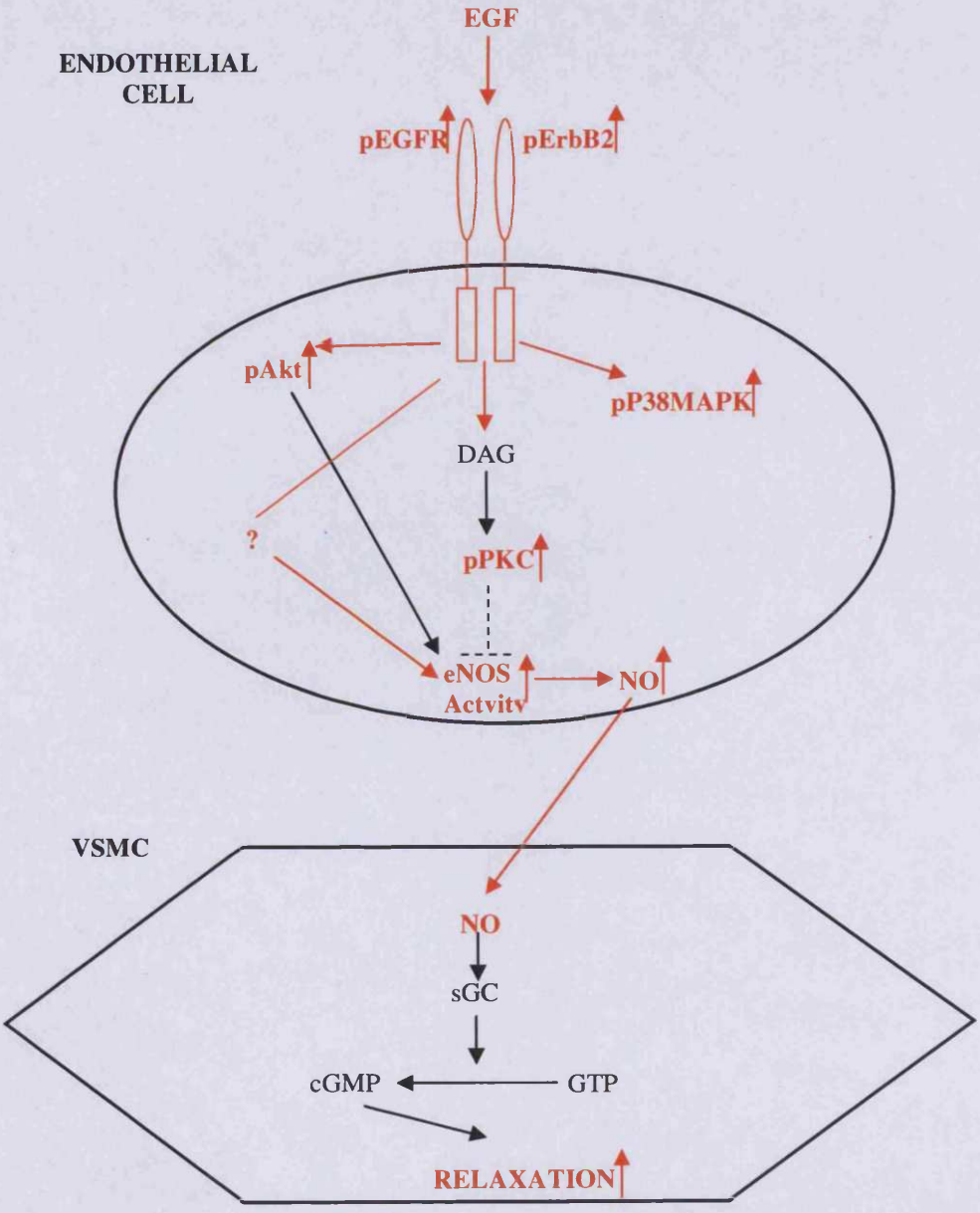

b

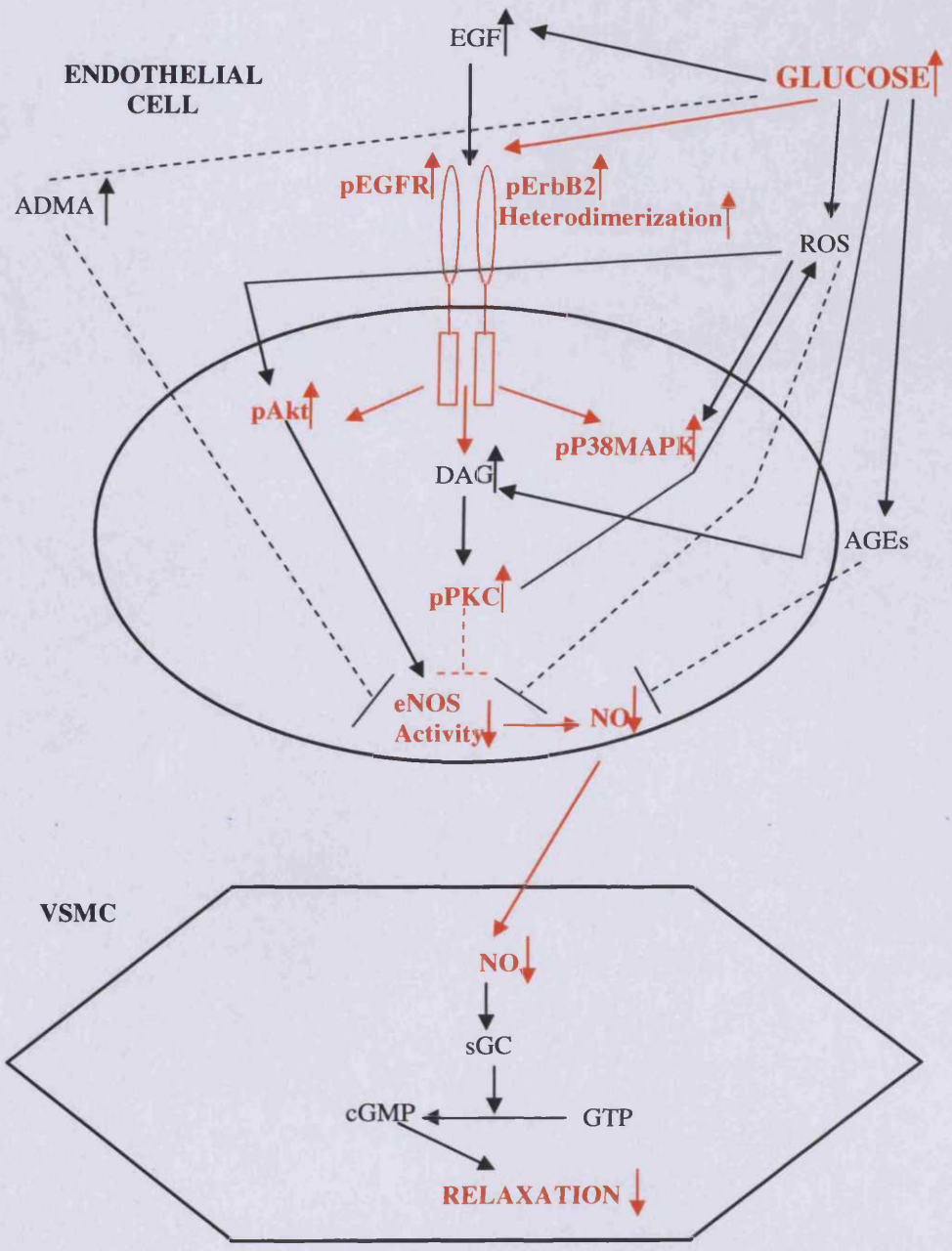

Figure 5.1 Summary of the results obtained in the thesis in normal and high glucose. a) Summary of the effect of EGF upon EGFR/ErbB2 and NO signalling in endothelial and VSM cells under normal glucose conditions. b) Summary of the effect of high glucose upon EGFR/ErbB2 and NO signalling in endothelial and VSM cells. In both a) and b) the parts of the figure shown in red represent findings from the present study. Dashed lines represent inhibition of the downstream molecule induced by the molecule upstream from it. ADMA = asymmetric dimethylarginine, AGEs = advanced glycation end products.

6.0 References

Abate, N. & Chandalia, M. (2001) Ethnicity and type 2 diabetes: focus on Asian Indians. ***J Diabetes Complications,*** **15, 320-327.**

Abebe, W., Harris, K.H. & MacLeod, K.M. (1990) Enhanced contractile responses of arteries from diabetic rats to alpha 1-adrenoceptor stimulation in the absence and presence of extracellular calcium. ***J Cardiovasc Pharmacol,*** **16, 239-248.**

Abu-Soud, H.M. & Stuehr, D.J. (1993) Nitric oxide synthases reveal a role for calmodulin in controlling electron transfer. ***Proc Natl Acad Sci U S A,*** **90, 10769 -10772.**

Alberts, B. (2002) ***Molecular biology of the cell.*** **Garland Science, New York.**

Amerini, S., Mantelli, L. & Ledda, F. (1995) Enhancement of the vasoconstrictor response to KCL by nitric oxide synthesis inhibition: a comparison with noradrenaline. ***Pharmacol Res,*** **31, 175-181.**

Andrew, P.J. & Mayer, B. (1999) Enzymatic function of nitric oxide synthases. ***Cardiovasc Res,*** **43, 521-531.**

Asakawa, H., Miyagawa, J., Higashiyama, S., Goishi, K., Hanafusa, T., Kuwajima, M., Taniguchi, N. & Matsuzawa, Y. (1996) High glucose and hyperosmolarity increase heparin-binding epidermal growth factor-like growth factor (HB-EGF) production in cultured human aortic endothelial cells. ***Cell Biochem Funct,*** **14, 181-186.**

Avogaro, A., Pagnin, E. & Calo, L. (2003a) Monocyte NADPH oxidase subunit p22(phox) and inducible hemeoxygenase-1 gene expressions are increased in type II diabetic patients: relationship with oxidative stress. ***J Clin Endocrinol Metab,*** **88, 1753-1759.**

Avogaro, A., Toffolo, G., Kiwanuka, E., de Kreutzenberg, S.V., Tessari, P. & Cobelli, C. (2003b) L-arginine-nitric oxide kinetics in normal and type 2 diabetic subjects: a stable-labelled 15N arginine approach. ***Diabetes,*** **52, 795-802.**

Avogaro, A., Fadini, G.P., Gallo, A., Pagnin, E. & de Kreutzenberg, S. (2006) Endothelial dysfunction in type 2 diabetes mellitus. ***Nutr Metab Cardiovasc Dis,*** **16 Suppl 1, S39-45.**

Awazu, M., Ishikura, K., Hida, M. & Hoshiya, M. (1999) Mechanisms of mitogen-activated protein kinase activation in experimental diabetes. ***J Am Soc Nephrol,*** **10, 738-745.**

Bagust, A., Hopkinson, P.K., Maslove, L. & Currie, C.J. (2002) The projected health care burden of Type 2 diabetes in the UK from 2000 to 2060. ***Diabet Med,*** **19 Suppl 4, 1-5.**

Ballinger, S.W., Patterson, C., Yan, C.N., Doan, R., Burow, D.L., Young, C.G., Yakes, F.M., Van Houten, B., Ballinger, C.A., Freeman, B.A. & Runge, M.S. (2000) Hydrogen peroxide- and peroxynitrite-induced mitochondrial DNA damage and dysfunction in vascular endothelial and smooth muscle cells. ***Circ Res,*** **86, 960-966.**

Barthel, A., Okino, S.T., Liao, J., Nakatani, K., Li, J., Whitlock, J.P., Jr. & Roth, R.A. (1999) Regulation of GLUT1 gene transcription by the serine/threonine kinase Akt1. *J Biol Chem,* 274, 20281-20286.

Basta, G., Schmidt, A.M. & De Caterina, R. (2004) Advanced glycation end products and vascular inflammation: implications for accelerated atherosclerosis in diabetes. *Cardiovasc Res,* 63, 582-592.

Bath, P.M., Hassall, D.G., Gladwin, A.M., Palmer, R.M. & Martin, J.F. (1991) Nitric oxide and prostacyclin. Divergence of inhibitory effects on monocyte chemotaxis and adhesion to endothelium in vitro. *Arterioscler Thromb,* 11, 254-260.

Bauer, P.M., Fulton, D., Boo, Y.C., Sorescu, G.P., Kemp, B.E., Jo, H. & Sessa, W.C. (2003) Compensatory phosphorylation and protein-protein interactions revealed by loss of function and gain of function mutants of multiple serine phosphorylation sites in endothelial nitric-oxide synthase. *J Biol Chem,* 278, 14841-14849.

Baumgartner-Parzer, S.M., Wagner, L., Pettermann, M., Grillari, J., Gessl, A. & Waldhausl, W. (1995) High-glucose--triggered apoptosis in cultured endothelial cells. *Diabetes,* 44, 1323-1327.

Beckman, J.A., Goldfine, A.B., Gordon, M.B., Garrett, L.A. & Creager, M.A. (2002) Inhibition of protein kinase Cbeta prevents impaired endothelium-dependent vasodilation caused by hyperglycemia in humans. *Circ Res,* 90, 107-111.

Beckman, J.S. & Koppenol, W.H. (1996) Nitric oxide, superoxide, and peroxynitrite: the good, the bad, and ugly. *Am J Physiol,* 271, C1424-1437.

Beenen, O.H., Pfaffendorf, M. & van Zwieten, P.A. (1995) Contractile responses to various inotropic agents in isolated hearts obtained from hypertensive diabetic rats. *Blood Press,* 4, 372-378.

Begum, N. & Ragolia, L. (2000) High glucose and insulin inhibit VSMC MKP-1 expression by blocking iNOS via p38 MAPK activation. *Am J Physiol Cell Physiol,* 278, C81-91.

Belvisi, M.G., Stretton, C.D., Yacoub, M. & Barnes, P.J. (1992) Nitric oxide is the endogenous neurotransmitter of bronchodilator nerves in humans. *Eur J Pharmacol,* 210, 221-222.

Ben-Haroush, A., Yogev, Y. & Hod, M. (2004) Epidemiology of gestational diabetes mellitus and its association with Type 2 diabetes. *Diabet Med,* 21, 103-113.

Benter, I.F., Yousif, M.H., Griffiths, S.M., Benboubetra, M. & Akhtar, S. (2005a) Epidermal growth factor receptor tyrosine kinase-mediated signalling contributes to diabetes-induced vascular dysfunction in the mesenteric bed. *Br J Pharmacol,* 145, 829-836.

Benter, I.F., Yousif, M.H., Hollins, A.J., Griffiths, S.M. & Akhtar, S. (2005b) Diabetes-induced renal vascular dysfunction is normalized by inhibition of epidermal growth factor receptor tyrosine kinase. *J Vasc Res,* 42, 284-291.

Berg, A., Redeen, S., Ericson, A.C. & Sjostrand, S.E. (2004) Nitric oxide-an endogenous inhibitor of gastric acid secretion in isolated human gastric glands. *BMC Gastroenterol,* 4, 16.

Berk, B.C., Brock, T.A., Webb, R.C., Taubman, M.B., Atkinson, W.J., Gimbrone, M.A., Jr. & Alexander, R.W. (1985) Epidermal growth factor, a vascular smooth muscle mitogen, induces rat aortic contraction. *J Clin Invest,* 75, 1083-1086.

Bernier, S.G., Haldar, S. & Michel, T. (2000) Bradykinin-regulated interactions of the mitogen-activated protein kinase pathway with the endothelial nitric-oxide synthase. *J Biol Chem,* 275, 30707-30715.

Bierhaus, A., Hofmann, M.A., Ziegler, R. & Nawroth, P.P. (1998) AGEs and their interaction with AGE-receptors in vascular disease and diabetes mellitus. I. The AGE concept. *Cardiovasc Res,* 37, 586-600.

Bogdan, S. & Klambt, C. (2001) Epidermal growth factor receptor signaling. *Curr Biol,* 11, R292-295.

Bonventre, J.V., Gronich, J.H. & Nemenoff, R.A. (1990) Epidermal growth factor enhances glomerular mesangial cell soluble phospholipase A2 activity. *J Biol Chem,* 265, 4934-4938.

Boo, Y.C. & Jo, H. (2003) Flow-dependent regulation of endothelial nitric oxide synthase: role of protein kinases. *Am J Physiol Cell Physiol,* 285, C499-508.

Bredt, D.S. & Snyder, S.H. (1990) Isolation of nitric oxide synthetase, a calmodulin-requiring enzyme. *Proc Natl Acad Sci U S A,* 87, 682-685.

Bredt, D.S. & Snyder, S.H. (1992) Nitric oxide, a novel neuronal messenger. *Neuron,* 8, 3-11.

British Heart Foundation (2007) Statistics website [WWW] <URL: http://www.heartstats.org/datapage.asp?id=1106> [Accessed 3/8/07].

Brown, J., Reading, S.J., Jones, S., Fitchett, C.J., Howl, J., Martin, A., Longland, C.L., Michelangeli, F., Dubrova, Y.E. & Brown, C.A. (2000) Critical evaluation of ECV304 as a human endothelial cell model defined by genetic analysis and functional responses: a comparison with the human bladder cancer derived epithelial cell line T24/83. *Lab Invest,* 80, 37-45.

Brownlee, M., Vlassara, H. & Cerami, A. (1985) Nonenzymatic glycosylation products on collagen covalently trap low-density lipoprotein. *Diabetes,* 34, 938-941.

Brownlee, M. (2001) Biochemistry and molecular cell biology of diabetic complications. *Nature,* 414, 813-820.

Brunet, A., Bonni, A., Zigmond, M.J., Lin, M.Z., Juo, P., Hu, L.S., Anderson, M.J., Arden, K.C., Blenis, J. & Greenberg, M.E. (1999) Akt promotes cell survival by phosphorylating and inhibiting a Forkhead transcription factor. *Cell,* 96, 857-868.

Brzezinski, J. & Lewinski, A. (1998) Increased plasma concentration of epidermal growth factor in female patients with non-toxic nodular goitre. *Eur J Endocrinol,* 138, 388-393.

Bucala, R., Tracey, K.J. & Cerami, A. (1991) Advanced glycosylation products quench nitric oxide and mediate defective endothelium-

dependent vasodilatation in experimental diabetes. *J Clin Invest,* 87, 432-438.

Bullock, W.H., Magnuson, S.R., Choi, S., Gunn, D.E. & Rudolph, J. (2002) Prospects for kinase activity modulators in the treatment of diabetes and diabetic complications. *Curr Top Med Chem,* 2, 915-938.

Bunce, C. & Wormald, R. (2006) Leading causes of certification for blindness and partial sight in England & Wales. *BMC Public Health,* 6, 58.

Caballero, A.E. (2003) Endothelial dysfunction in obesity and insulin resistance: a road to diabetes and heart disease. *Obes Res,* 11, 1278-1289.

Cagliero, E., Maiello, M., Boeri, D., Roy, S. & Lorenzi, M. (1988) Increased expression of basement membrane components in human endothelial cells cultured in high glucose. *J Clin Invest,* 82, 735-738.

Cagliero, E., Roth, T., Roy, S. & Lorenzi, M. (1991) Characteristics and mechanisms of high-glucose-induced overexpression of basement membrane components in cultured human endothelial cells. *Diabetes,* 40, 102-110.

Cai, W., He, J.C., Zhu, L., Lu, C. & Vlassara, H. (2006) Advanced glycation end product (AGE) receptor 1 suppresses cell oxidant stress and activation signaling via EGF receptor. *Proc Natl Acad Sci U S A,* 103, 13801-13806.

Cale, J.M. & Bird, I.M. (2006) Inhibition of MEK/ERK1/2 signalling alters endothelial nitric oxide synthase activity in an agonist-dependent manner. *Biochem J,* 398, 279-288.

Cardone, M.H., Roy, N., Stennicke, H.R., Salvesen, G.S., Franke, T.F., Stanbridge, E., Frisch, S. & Reed, J.C. (1998) Regulation of cell death protease caspase-9 by phosphorylation. *Science,* 282, 1318-1321.

Carpenter, G., King, L., Jr. & Cohen, S. (1978) Epidermal growth factor stimulates phosphorylation in membrane preparations in vitro. *Nature,* 276, 409-410.

Casalini, P., Iorio, M.V., Galmozzi, E. & Menard, S. (2004) Role of HER receptors family in development and differentiation. *J Cell Physiol,* 200, 343-350.

Chattopadhyay, A., Vecchi, M., Ji, Q., Mernaugh, R. & Carpenter, G. (1999) The role of individual SH2 domains in mediating association of phospholipase C-gamma1 with the activated EGF receptor. *J Biol Chem,* 274, 26091-26097.

Chen, S., Apostolova, M.D., Cherian, M.G. & Chakrabarti, S. (2000) Interaction of endothelin-1 with vasoactive factors in mediating glucose-induced increased permeability in endothelial cells. *Lab Invest,* 80, 1311-1321.

Chen, Z.P., Mitchelhill, K.I., Michell, B.J., Stapleton, D., Rodriguez-Crespo, I., Witters, L.A., Power, D.A., Ortiz de Montellano, P.R. & Kemp, B.E. (1999) AMP-activated protein kinase phosphorylation of endothelial NO synthase. *FEBS Lett,* 443, 285-289.

Choy, J.C., Granville, D.J., Hunt, D.W. & McManus, B.M. (2001) Endothelial cell apoptosis: biochemical characteristics and potential implications for atherosclerosis. *J Mol Cell Cardiol,* 33, 1673-1690.

Chu, S. & Bohlen, H.G. (2004) High concentration of glucose inhibits glomerular endothelial eNOS through a PKC mechanism. *Am J Physiol Renal Physiol,* 287, F384-392.

Citri, A., Skaria, K.B. & Yarden, Y. (2003) The deaf and the dumb: the biology of ErbB-2 and ErbB-3. *Exp Cell Res,* 284, 54-65.

Clark, M.L. & Kumar, P.J. (2005) *Kumar & Clark clinical medicine.* Elsevier Saunders, Edinburgh; New York.

Coppey, L.J., Davidson, E.P., Rinehart, T.W., Gellett, J.S., Oltman, C.L., Lund, D.D. & Yorek, M.A. (2006) ACE inhibitor or angiotensin II receptor antagonist attenuates diabetic neuropathy in streptozotocin-induced diabetic rats. *Diabetes,* 55, 341-348.

Cosentino, F., Hishikawa, K., Katusic, Z.S. & Luscher, T.F. (1997) High glucose increases nitric oxide synthase expression and superoxide anion generation in human aortic endothelial cells. *Circulation,* 96, 25-28.

Cosentino, F., Eto, M., De Paolis, P., van der Loo, B., Bachschmid, M., Ullrich, V., Kouroedov, A., Delli Gatti, C., Joch, H., Volpe, M. & Luscher, T.F. (2003) High glucose causes upregulation of cyclooxygenase-2 and alters prostanoid profile in human endothelial cells: role of protein kinase C and reactive oxygen species. *Circulation,* 107, 1017-1023.

Coutinho, M., Gerstein, H.C., Wang, Y. & Yusuf, S. (1999) The relationship between glucose and incident cardiovascular events. A metaregression analysis of published data from 20 studies of 95,783 individuals followed for 12.4 years. *Diabetes Care,* 22, 233-240.

Cowan, K.J. & Storey, K.B. (2003) Mitogen-activated protein kinases: new signaling pathways functioning in cellular responses to environmental stress. *J Exp Biol,* 206, 1107-1115.

Craven, P.A. & DeRubertis, F.R. (1989) Protein kinase C is activated in glomeruli from streptozotocin diabetic rats. Possible mediation by glucose. *J Clin Invest,* 83, 1667-1675.

Cross, D.A., Alessi, D.R., Cohen, P., Andjelkovich, M. & Hemmings, B.A. (1995) Inhibition of glycogen synthase kinase-3 by insulin mediated by protein kinase B. *Nature,* 378, 785-789.

Cuevas, A.M. & Germain, A.M. (2004) Diet and endothelial function. *Biol Res,* 37, 225-230.

Curcio, F. & Ceriello, A. (1992) Decreased cultured endothelial cell proliferation in high glucose medium is reversed by antioxidants: new insights on the pathophysiological mechanisms of diabetic vascular complications. *In Vitro Cell Dev Biol,* 28A, 787-790.

Currie, C.J., Kraus, D., Morgan, C.L., Gill, L., Stott, N.C. & Peters, J.R. (1997) NHS acute sector expenditure for diabetes: the present, future, and excess in-patient cost of care. *Diabet Med,* 14, 686-692.

Dahlquist, G., Frisk, G., Ivarsson, S.A., Svanberg, L., Forsgren, M. & Diderholm, H. (1995) Indications that maternal coxsackie B virus infection during pregnancy is a risk factor for childhood-onset IDDM. *Diabetologia,* 38, 1371-1373.

Dahmane, A., Gil, S., Brehier, A., Davy, J. & Feger, J. (1996) Kinetic analysis of epidermal growth factor endocytosis in rat hepatocytes. Effects of diabetes. *Eur J Cell Biol,* 69, 335-342.

Daub, H., Weiss, F.U., Wallasch, C. & Ullrich, A. (1996) Role of transactivation of the EGF receptor in signalling by G-protein-coupled receptors. *Nature,* 379, 557-560.

De Caterina, R. (2000) Endothelial dysfunctions: common denominators in vascular disease. *Curr Opin Lipidol,* 11, 9-23.

Denkert, C., Warskulat, U., Hensel, F. & Haussinger, D. (1998) Osmolyte strategy in human monocytes and macrophages: involvement of p38MAPK in hyperosmotic induction of betaine and myoinositol transporters. *Arch Biochem Biophys,* 354, 172-180.

Diabetes Control and Complications Trial Research Group (1993) The effect of intensive treatment of diabetes on the development and progression of long-term complications in insulin-dependent diabetes mellitus. *N Engl J Med,* 329, 977-986.

Dimmeler, S., Fleming, I., Fisslthaler, B., Hermann, C., Busse, R. & Zeiher, A.M. (1999) Activation of nitric oxide synthase in endothelial cells by Akt-dependent phosphorylation. *Nature,* 399, 601-605.

Ding, Y., Vaziri, N.D., Coulson, R., Kamanna, V.S. & Roh, D.D. (2000) Effects of simulated hyperglycemia, insulin, and glucagon on endothelial nitric oxide synthase expression. *Am J Physiol Endocrinol Metab,* 279, E11-17.

Dittmar, T., Husemann, A., Schewe, Y., Nofer, J.R., Niggemann, B., Zanker, K.S. & Brandt, B.H. (2002) Induction of cancer cell migration by epidermal growth factor is initiated by specific phosphorylation of tyrosine 1248 of c-erbB-2 receptor via EGFR. *Faseb J,* 16, 1823-1825.

Dixon, B.S., Sharma, R.V., Dickerson, T. & Fortune, J. (1994) Bradykinin and angiotensin II: activation of protein kinase C in arterial smooth muscle. *Am J Physiol,* 266, C1406-1420.

Donath, M.Y., Storling, J., Maedler, K. & Mandrup-Poulsen, T. (2003) Inflammatory mediators and islet beta-cell failure: a link between type 1 and type 2 diabetes. *J Mol Med,* 81, 455-470.

Dora, K.A., Hinton, J.M., Walker, S.D. & Garland, C.J. (2000) An indirect influence of phenylephrine on the release of endothelium-derived vasodilators in rat small mesenteric artery. *Br J Pharmacol,* 129, 381-387.

Dorion, S., Lambert, H. & Landry, J. (2002) Activation of the p38 signaling pathway by heat shock involves the dissociation of glutathione S-transferase Mu from Ask1. *J Biol Chem,* 277, 30792-30797.

Dreux, A.C., Lamb, D.J., Modjtahedi, H. & Ferns, G.A. (2006) The epidermal growth factor receptors and their family of ligands: their putative role in atherogenesis. *Atherosclerosis,* 186, 38-53.

Du, X.L., Edelstein, D., Rossetti, L., Fantus, I.G., Goldberg, H., Ziyadeh, F., Wu, J. & Brownlee, M. (2000) Hyperglycemia-induced mitochondrial superoxide overproduction activates the hexosamine pathway and induces plasminogen activator inhibitor-1 expression by increasing Sp1 glycosylation. *Proc Natl Acad Sci U S A,* 97, 12222-12226.

Du, X.L., Edelstein, D., Dimmeler, S., Ju, Q., Sui, C. & Brownlee, M. (2001) Hyperglycemia inhibits endothelial nitric oxide synthase activity by posttranslational modification at the Akt site. *J Clin Invest,* 108, 1341-1348.

Edwards, G., Dora, K.A., Gardener, M.J., Garland, C.J. & Weston, A.H. (1998) K+ is an endothelium-derived hyperpolarizing factor in rat arteries. *Nature,* 396, 269-272.

Eguchi, S., Frank, G.D., Mifune, M. & Inagami, T. (2003) Metalloprotease-dependent ErbB ligand shedding in mediating EGFR transactivation and vascular remodelling. *Biochem Soc Trans,* 31, 1198-1202.

Engelgau, M.M., Geiss, L.S., Saaddine, J.B., Boyle, J.P., Benjamin, S.M., Gregg, E.W., Tierney, E.F., Rios-Burrows, N., Mokdad, A.H., Ford, E.S., Imperatore, G. & Narayan, K.M. (2004) The evolving diabetes burden in the United States. *Ann Intern Med,* 140, 945-950.

Evans, J.L., Goldfine, I.D., Maddux, B.A. & Grodsky, G.M. (2002) Oxidative stress and stress-activated signaling pathways: a unifying hypothesis of type 2 diabetes. *Endocr Rev,* 23, 599-622.

Fard, A., Tuck, C.H., Donis, J.A., Sciacca, R., Di Tullio, M.R., Wu, H.D., Bryant, T.A., Chen, N.T., Torres-Tamayo, M., Ramasamy, R., Berglund, L., Ginsberg, H.N., Homma, S. & Cannon, P.J. (2000) Acute elevations of plasma asymmetric dimethylarginine and impaired endothelial function in response to a high-fat meal in patients with type 2 diabetes. *Arterioscler Thromb Vasc Biol,* 20, 2039-2044.

Feldner, J.C. & Brandt, B.H. (2002) Cancer cell motility--on the road from c-erbB-2 receptor steered signaling to actin reorganization. *Exp Cell Res,* 272, 93-108.

Ferguson, K.M., Berger, M.B., Mendrola, J.M., Cho, H.S., Leahy, D.J. & Lemmon, M.A. (2003) EGF activates its receptor by removing interactions that autoinhibit ectodomain dimerization. *Mol Cell,* 11, 507-517.

Feron, O., Dessy, C., Opel, D.J., Arstall, M.A., Kelly, R.A. & Michel, T. (1998) Modulation of the endothelial nitric-oxide synthase-caveolin interaction in cardiac myocytes. Implications for the autonomic regulation of heart rate. *J Biol Chem,* 273, 30249-30254.

Fisher, G.J., Talwar, H.S., Lin, J., Lin, P., McPhillips, F., Wang, Z., Li, X., Wan, Y., Kang, S. & Voorhees, J.J. (1998) Retinoic acid inhibits induction of c-Jun protein by ultraviolet radiation that occurs

subsequent to activation of mitogen-activated protein kinase pathways in human skin in vivo. *J Clin Invest,* 101, 1432-1440.

Fitzgerald, J.S., Busch, S., Wengenmayer, T., Foerster, K., de la Motte, T., Poehlmann, T.G. & Markert, U.R. (2005) Signal transduction in trophoblast invasion. *Chem Immunol Allergy Basel Karger,* 88, 181-199.

Fleming, I., Fisslthaler, B., Dimmeler, S., Kemp, B.E. & Busse, R. (2001) Phosphorylation of Thr(495) regulates Ca(2+)/calmodulin-dependent endothelial nitric oxide synthase activity. *Circ Res,* 88, E68-75.

Florian, J.A. & Watts, S.W. (1999) Epidermal growth factor: a potent vasoconstrictor in experimental hypertension. *Am J Physiol,* 276, H976-983.

Frustaci, A., Kajstura, J., Chimenti, C., Jakoniuk, I., Leri, A., Maseri, A., Nadal-Ginard, B. & Anversa, P. (2000) Myocardial cell death in human diabetes. *Circ Res,* 87, 1123-1132.

Fujiyama, S., Matsubara, H., Nozawa, Y., Maruyama, K., Mori, Y., Tsutsumi, Y., Masaki, H., Uchiyama, Y., Koyama, Y., Nose, A., Iba, O., Tateishi, E., Ogata, N., Jyo, N., Higashiyama, S. & Iwasaka, T. (2001) Angiotensin AT(1) and AT(2) receptors differentially regulate angiopoietin-2 and vascular endothelial growth factor expression and angiogenesis by modulating heparin binding-epidermal growth factor (EGF)-mediated EGF receptor transactivation. *Circ Res,* 88, 22-29.

Fukao, M., Hattori, Y., Kanno, M., Sakuma, I. & Kitabatake, A. (1997) Alterations in endothelium-dependent hyperpolarization and relaxation in mesenteric arteries from streptozotocin-induced diabetic rats. *Br J Pharmacol,* 121, 1383-1391.

Fumo, P., Kuncio, G.S. & Ziyadeh, F.N. (1994) PKC and high glucose stimulate collagen alpha 1 (IV) transcriptional activity in a reporter mesangial cell line. *Am J Physiol,* 267, F632-638.

Furchgott, R.F. & Zawadzki, J.V. (1980) The obligatory role of endothelial cells in the relaxation of arterial smooth muscle by acetylcholine. *Nature,* 288, 373-376.

Galcheva-Gargova, Z., Konstantinov, K.N., Wu, I.H., Klier, F.G., Barrett, T. & Davis, R.J. (1996) Binding of zinc finger protein ZPR1 to the epidermal growth factor receptor. *Science,* 272, 1797-1802.

Galley, H.F. & Webster, N.R. (2004) Physiology of the endothelium. *Br J Anaesth,* 93, 105-113.

Gallis, B., Corthals, G.L., Goodlett, D.R., Ueba, H., Kim, F., Presnell, S.R., Figeys, D., Harrison, D.G., Berk, B.C., Aebersold, R. & Corson, M.A. (1999) Identification of flow-dependent endothelial nitric-oxide synthase phosphorylation sites by mass spectrometry and regulation of phosphorylation and nitric oxide production by the phosphatidylinositol 3-kinase inhibitor LY294002. *J Biol Chem,* 274, 30101-30108.

Garrett, T.P., McKern, N.M., Lou, M., Elleman, T.C., Adams, T.E., Lovrecz, G.O., Kofler, M., Jorissen, R.N., Nice, E.C., Burgess, A.W.

& Ward, C.W. (2003) The crystal structure of a truncated ErbB2 ectodomain reveals an active conformation, poised to interact with other ErbB receptors. *Mol Cell,* 11, 495-505.

Gerrity, R.G. (1981) The role of the monocyte in atherogenesis: II. Migration of foam cells from atherosclerotic lesions. *Am J Pathol,* 103, 191-200.

Giannoukakis, N. (2006) Drug evaluation: ranirestat--an aldose reductase inhibitor for the potential treatment of diabetic complications. *Curr Opin Investig Drugs,* 7, 916-923.

Goligorsky, M.S., Li, H., Brodsky, S. & Chen, J. (2002) Relationships between caveolae and eNOS: everything in proximity and the proximity of everything. *Am J Physiol Renal Physiol,* 283, F1-10.

Gomes, M.B., Cailleaux, S. & Tibirica, E. (2005) Metformin prevents the impairment of endothelium-dependent vascular relaxation induced by high glucose challenge in rabbit isolated perfused kidneys. *Naunyn Schmiedebergs Arch Pharmacol,* 372, 24-30.

Gordon, P.A. (2004) Effects of diabetes on the vascular system: current research evidence and best practice recommendations. *J Vasc Nurs,* 22, 2-11; quiz 12-13.

Graus-Porta, D., Beerli, R.R., Daly, J.M. & Hynes, N.E. (1997) ErbB-2, the preferred heterodimerization partner of all ErbB receptors, is a mediator of lateral signaling. *Embo J,* 16, 1647-1655.

Griendling, K.K. & FitzGerald, G.A. (2003) Oxidative stress and cardiovascular injury: Part I: basic mechanisms and in vivo monitoring of ROS. *Circulation,* 108, 1912-1916.

Griffith, O.W. & Stuehr, D.J. (1995) Nitric oxide synthases: properties and catalytic mechanism. *Annu Rev Physiol,* 57, 707-736.

Guerci, B., Bohme, P., Kearney-Schwartz, A., Zannad, F. & Drouin, P. (2001) Endothelial dysfunction and type 2 diabetes. Part 2: altered endothelial function and the effects of treatments in type 2 diabetes mellitus. *Diabetes Metab,* 27, 436-447.

Guzik, T.J., Korbut, R. & Adamek-Guzik, T. (2003) Nitric oxide and superoxide in inflammation and immune regulation. *J Physiol Pharmacol,* 54, 469-487.

Hackel, P.O., Zwick, E., Prenzel, N. & Ullrich, A. (1999) Epidermal growth factor receptors: critical mediators of multiple receptor pathways. *Curr Opin Cell Biol,* 11, 184-189.

Hajduch, E., Alessi, D.R., Hemmings, B.A. & Hundal, H.S. (1998) Constitutive activation of protein kinase B alpha by membrane targeting promotes glucose and system A amino acid transport, protein synthesis, and inactivation of glycogen synthase kinase 3 in L6 muscle cells. *Diabetes,* 47, 1006-1013.

Hammes, H.P. (2003) Pathophysiological mechanisms of diabetic angiopathy. *J Diabetes Complications,* 17, 16-19.

Han, J., Mandal, A.K. & Hiebert, L.M. (2005) Endothelial cell injury by high glucose and heparanase is prevented by insulin, heparin and basic fibroblast growth factor. *Cardiovasc Diabetol,* 4, 12.

Haneda, M., Kikkawa, R., Sugimoto, T., Koya, D., Araki, S., Togawa, M. & Shigeta, Y. (1995) Abnormalities in protein kinase C and MAP kinase cascade in mesangial cells cultured under high glucose conditions. *J Diabetes Complications,* 9, 246-248.

Harris, R.C., Chung, E. & Coffey, R.J. (2003) EGF receptor ligands. *Exp Cell Res,* 284, 2-13.

Hashiguchi, A., Yano, S., Morioka, M., Hamada, J., Ushio, Y., Takeuchi, Y. & Fukunaga, K. (2004) Up-regulation of endothelial nitric oxide synthase via phosphatidylinositol 3-kinase pathway contributes to ischemic tolerance in the CA1 subfield of gerbil hippocampus. *J Cereb Blood Flow Metab,* 24, 271-279.

Heijenbrok, F.J., Mathy, M.J., Pfaffendorf, M. & van Zwieten, P.A. (2000) The influence of chronic inhibition of nitric oxide synthesis on contractile and relaxant properties of rat carotid and mesenteric arteries. *Naunyn Schmiedebergs Arch Pharmacol,* 362, 504-511.

Heitzer, T., Yla-Herttuala, S., Luoma, J., Kurz, S., Munzel, T., Just, H., Olschewski, M. & Drexler, H. (1996) Cigarette smoking potentiates endothelial dysfunction of forearm resistance vessels in patients with hypercholesterolemia. Role of oxidized LDL. *Circulation,* 93, 1346-1353.

Hink, U., Tsilimingas, N., Wendt, M. & Munzel, T. (2003) Mechanisms underlying endothelial dysfunction in diabetes mellitus: therapeutic implications. *Treat Endocrinol,* 2, 293-304.

Hofmann, F., Ammendola, A. & Schlossmann, J. (2000) Rising behind NO: cGMP-dependent protein kinases. *J Cell Sci,* 113 (Pt 10), 1671-1676.

Hogan, M., Cerami, A. & Bucala, R. (1992) Advanced glycosylation endproducts block the antiproliferative effect of nitric oxide. Role in the vascular and renal complications of diabetes mellitus. *J Clin Invest,* 90, 1110-1115.

Hogikyan, R.V., Galecki, A.T., Pitt, B., Halter, J.B., Greene, D.A. & Supiano, M.A. (1998) Specific impairment of endothelium-dependent vasodilation in subjects with type 2 diabetes independent of obesity. *J Clin Endocrinol Metab,* 83, 1946-1952.

Holbro, T., Civenni, G. & Hynes, N.E. (2003) The ErbB receptors and their role in cancer progression. *Exp Cell Res,* 284, 99-110.

Hurst, R.T. & Lee, R.W. (2003) Increased incidence of coronary atherosclerosis in type 2 diabetes mellitus: mechanisms and management. *Ann Intern Med,* 139, 824-834.

Husain, S., Young, D. & Wingard, C.J. (2004) Role of PKCalpha and PKCiota in phenylephrine-induced contraction of rat corpora cavernosa. *Int J Impot Res,* 16, 325-333.

Ido, Y., Carling, D. & Ruderman, N. (2002) Hyperglycemia-induced apoptosis in human umbilical vein endothelial cells: inhibition by the AMP-activated protein kinase activation. *Diabetes,* 51, 159-167.

Igarashi, M., Wakasaki, H., Takahara, N., Ishii, H., Jiang, Z.Y., Yamauchi, T., Kuboki, K., Meier, M., Rhodes, C.J. & King, G.L.

(1999) Glucose or diabetes activates p38 mitogen-activated protein kinase via different pathways. *J Clin Invest,* 103, 185-195.

Ignarro, L.J., Buga, G.M., Wood, K.S., Byrns, R.E. & Chaudhuri, G. (1987a) Endothelium-derived relaxing factor produced and released from artery and vein is nitric oxide. *Proc Natl Acad Sci U S A,* 84, 9265-9269.

Ignarro, L.J., Byrns, R.E., Buga, G.M. & Wood, K.S. (1987b) Endothelium-derived relaxing factor from pulmonary artery and vein possesses pharmacologic and chemical properties identical to those of nitric oxide radical. *Circ Res,* 61, 866-879.

Ignarro, L.J., Buga, G.M., Byrns, R.E., Wood, K.S. & Chaudhuri, G. (1988a) Endothelium-derived relaxing factor and nitric oxide possess identical pharmacologic properties as relaxants of bovine arterial and venous smooth muscle. *J Pharmacol Exp Ther,* 246, 218-226.

Ignarro, L.J., Byrns, R.E., Buga, G.M., Wood, K.S. & Chaudhuri, G. (1988b) Pharmacological evidence that endothelium-derived relaxing factor is nitric oxide: use of pyrogallol and superoxide dismutase to study endothelium-dependent and nitric oxide-elicited vascular smooth muscle relaxation. *J Pharmacol Exp Ther,* 244, 181-189.

Ignarro, L.J., Napoli, C. & Loscalzo, J. (2002) Nitric oxide donors and cardiovascular agents modulating the bioactivity of nitric oxide: an overview. *Circ Res,* 90, 21-28.

Inoguchi, T., Battan, R., Handler, E., Sportsman, J.R., Heath, W. & King, G.L. (1992) Preferential elevation of protein kinase C isoform beta II and diacylglycerol levels in the aorta and heart of diabetic rats: differential reversibility to glycemic control by islet cell transplantation. *Proc Natl Acad Sci U S A,* 89, 11059-11063.

Jahromi, M.M. & Eisenbarth, G.S. (2006) Genetic determinants of type 1 diabetes across populations. *Ann N Y Acad Sci,* 1079, 289-299.

Jennings, P.E. (1994) From hemobiology to vascular disease: a review of the potential of gliclazide to influence the pathogenesis of diabetic vascular disease. *J Diabetes Complications,* 8, 226-230.

Jorissen, R.N., Walker, F., Pouliot, N., Garrett, T.P., Ward, C.W. & Burgess, A.W. (2003) Epidermal growth factor receptor: mechanisms of activation and signalling. *Exp Cell Res,* 284, 31-53.

Kagiyama, S., Eguchi, S., Frank, G.D., Inagami, T., Zhang, Y.C. & Phillips, M.I. (2002) Angiotensin II-induced cardiac hypertrophy and hypertension are attenuated by epidermal growth factor receptor antisense. *Circulation,* 106, 909-912.

Kamat, A. & Carpenter, G. (1997) Phospholipase C-gamma1: regulation of enzyme function and role in growth factor-dependent signal transduction. *Cytokine Growth Factor Rev,* 8, 109-117.

Kamata, H., Shibukawa, Y., Oka, S.I. & Hirata, H. (2000) Epidermal growth factor receptor is modulated by redox through multiple mechanisms. Effects of reductants and H2O2. *Eur J Biochem,* 267, 1933-1944.

Kamata, K., Miyata, N. & Kasuya, Y. (1989) Impairment of endothelium-dependent relaxation and changes in levels of cyclic GMP in aorta from streptozotocin-induced diabetic rats. *Br J Pharmacol,* 97, 614-618.

Kasayama, S., Yoshimura, M. & Oka, T. (1989) Decreased expression of hepatic epidermal growth factor receptor gene in diabetic mice. *J Mol Endocrinol,* 3, 49-56.

Kashimata, M., Hiramatsu, M. & Minami, N. (1987) Effect of streptozotocin-induced diabetes on epidermal growth factor receptors in rat liver plasma membrane. *Biochim Biophys Acta,* 923, 496-500.

Kawanabe, Y. & Nauli, S.M. (2005) Involvement of extracellular Ca2+ influx through voltage-independent Ca2+ channels in endothelin-1 function. *Cell Signal,* 17, 911-916.

Keefer, L.K., Nims, R.W., Davies, K.M. & Wink, D.A. (1996) "NONOates" (1-substituted diazen-1-ium-1,2-diolates) as nitric oxide donors: convenient nitric oxide dosage forms. *Methods Enzymol,* 268, 281-293.

Keller, D., Zeng, X., Li, X., Kapoor, M., Iordanov, M.S., Taya, Y., Lozano, G., Magun, B. & Lu, H. (1999) The p38MAPK inhibitor SB203580 alleviates ultraviolet-induced phosphorylation at serine 389 but not serine 15 and activation of p53. *Biochem Biophys Res Commun,* 261, 464-471.

Kesavadev, J.D., Short, K.R. & Nair, K.S. (2003) Diabetes in old age: an emerging epidemic. *J Assoc Physicians India,* 51, 1083-1094.

Khan, A.J., Fligiel, S.E., Liu, L., Jaszewski, R., Chandok, A. & Majumdar, A.P. (1999) Induction of EGFR tyrosine kinase in the gastric mucosa of diabetic rats. *Proc Soc Exp Biol Med,* 221, 105-110.

Kim, F., Gallis, B. & Corson, M.A. (2001) TNF-alpha inhibits flow and insulin signaling leading to NO production in aortic endothelial cells. *Am J Physiol Cell Physiol,* 280, C1057-1065.

Kim, J., Lee, C.K., Park, H.J., Kim, H.J., So, H.H., Lee, K.S., Lee, H.M., Roh, H.Y., Choi, W.S., Park, T.K. & Kim, B. (2006) Epidermal growth factor induces vasoconstriction through the phosphatidylinositol 3-kinase-mediated mitogen-activated protein kinase pathway in hypertensive rats. *J Pharmacol Sci,* 101, 135-143.

King, D.E., Mainous, A.G., 3rd, Buchanan, T.A. & Pearson, W.S. (2003) C-reactive protein and glycemic control in adults with diabetes. *Diabetes Care,* 26, 1535-1539.

Knebel, A., Rahmsdorf, H.J., Ullrich, A. & Herrlich, P. (1996) Dephosphorylation of receptor tyrosine kinases as target of regulation by radiation, oxidants or alkylating agents. *Embo J,* 15, 5314-5325.

Kolch, W. (2000) Meaningful relationships: the regulation of the Ras/Raf/MEK/ERK pathway by protein interactions. *Biochem J,* 351 Pt 2, 289-305.

Konishi, A. & Berk, B.C. (2003) Epidermal growth factor receptor transactivation is regulated by glucose in vascular smooth muscle cells. *J Biol Chem,* 278, 35049-35056.

Korc, M., Matrisian, L.M., Nakamura, R. & Magun, B.E. (1984) Epidermal growth factor binding is altered in pancreatic acini from diabetic rats. *Life Sci,* 35, 2049-2055.

Koya, D. & King, G.L. (1998) Protein kinase C activation and the development of diabetic complications. *Diabetes,* 47, 859-866.

Krentz, A.J. & Bailey, C.J. (2005) Oral antidiabetic agents: current role in type 2 diabetes mellitus. *Drugs,* 65, 385-411.

Lamping, K. & Faraci, F. (2003) Enhanced vasoconstrictor responses in eNOS deficient mice. *Nitric Oxide,* 8, 207-213.

Lane, P. & Gross, S.S. (2002) Disabling a C-terminal autoinhibitory control element in endothelial nitric-oxide synthase by phosphorylation provides a molecular explanation for activation of vascular NO synthesis by diverse physiological stimuli. *J Biol Chem,* 277, 19087-19094.

Lee, H.S., Son, S.M., Kim, Y.K., Hong, K.W. & Kim, C.D. (2003) NAD(P)H oxidase participates in the signaling events in high glucose-induced proliferation of vascular smooth muscle cells. *Life Sci,* 72, 2719-2730.

Leszczynski, D., Joenvaara, S. & Foegh, M.L. (1996) Protein kinase C-alpha regulates proliferation but not apoptosis in rat coronary vascular smooth muscle cells. *Life Sci,* 58, 599-606.

Lev-Ran, A., Hwang, D.L. & Barseghian, G. (1986) Decreased expression of liver epidermal growth factor receptors in rats with alloxan and streptozotocin diabetes. *Biochem Biophys Res Commun,* 137, 258-262.

Li, H. & Forstermann, U. (2000) Nitric oxide in the pathogenesis of vascular disease. *J Pathol,* 190, 244-254.

Liao, J., Xu, X. & Wargovich, M.J. (2000) Direct reprobing with anti-beta-actin antibody as an internal control for western blotting analysis. *Biotechniques,* 28, 216-218.

Lincoln, T.M. (2004) Cyclic GMP and phosphodiesterase 5 inhibitor therapies: what's on the horizon? *Mol Pharmacol,* 66, 11-13.

Lipsky, B.A., Berendt, A.R., Deery, H.G., Embil, J.M., Joseph, W.S., Karchmer, A.W., LeFrock, J.L., Lew, D.P., Mader, J.T., Norden, C. & Tan, J.S. (2006) Diagnosis and treatment of diabetic foot infections. *Plast Reconstr Surg,* 117, 212S-238S.

Liu, H. & Sperelakis, N. (1997) Tyrosine kinases modulate the activity of single L-type calcium channels in vascular smooth muscle cells from rat portal vein. *Can J Physiol Pharmacol,* 75, 1063-1068.

Liu, J., Garcia-Cardena, G. & Sessa, W.C. (1996) Palmitoylation of endothelial nitric oxide synthase is necessary for optimal stimulated release of nitric oxide: implications for caveolae localization. *Biochemistry,* 35, 13277-13281.

Ludvigsson, J. (2006) Why diabetes incidence increases--a unifying theory. *Ann N Y Acad Sci,* 1079, 374-382.

Lynch, J.J., Ferro, T.J., Blumenstock, F.A., Brockenauer, A.M. & Malik, A.B. (1990) Increased endothelial albumin permeability mediated by protein kinase C activation. *J Clin Invest,* 85, 1991-1998.

Makimattila, S., Liu, M.L., Vakkilainen, J., Schlenzka, A., Lahdenpera, S., Syvanne, M., Mantysaari, M., Summanen, P., Bergholm, R., Taskinen, M.R. & Yki-Jarvinen, H. (1999) Impaired endothelium-dependent vasodilation in type 2 diabetes. Relation to LDL size, oxidized LDL, and antioxidants. *Diabetes Care,* 22, 973-981.

Makino, A., Ohuchi, K. & Kamata, K. (2000) Mechanisms underlying the attenuation of endothelium-dependent vasodilatation in the mesenteric arterial bed of the streptozotocin-induced diabetic rat. *Br J Pharmacol,* 130, 549-556.

Marks, G.S., McLaughlin, B.E., Brown, L.B., Beaton, D.E., Booth, B.P., Nakatsu, K. & Brien, J.F. (1991) Interaction of glyceryl trinitrate and sodium nitroprusside with bovine pulmonary vein homogenate and 10,000 x g supernatant: biotransformation and nitric oxide formation. *Can J Physiol Pharmacol,* 69, 889-892.

Marks, G.S., McLaughlin, B.E., Nakatsu, K. & Brien, J.F. (1992) Direct evidence for nitric oxide formation from glyceryl trinitrate during incubation with intact bovine pulmonary artery. *Can J Physiol Pharmacol,* 70, 308-311.

Masters, J.R., Thomson, J.A., Daly-Burns, B., Reid, Y.A., Dirks, W.G., Packer, P., Toji, L.H., Ohno, T., Tanabe, H., Arlett, C.F., Kelland, L.R., Harrison, M., Virmani, A., Ward, T.H., Ayres, K.L. & Debenham, P.G. (2001) Short tandem repeat profiling provides an international reference standard for human cell lines. *Proc Natl Acad Sci U S A,* 98, 8012-8017.

Matsubara, M., Hayashi, N., Jing, T. & Titani, K. (2003) Regulation of endothelial nitric oxide synthase by protein kinase C. *J Biochem (Tokyo),* 133, 773-781.

Mayer, B. & Hemmens, B. (1997) Biosynthesis and action of nitric oxide in mammalian cells. *Trends Biochem Sci,* 22, 477-481.

Mayhan, W.G., Irvine, S.D. & Sharpe, G.M. (1999) Constrictor responses of resistance arterioles during diabetes mellitus. *Diabetes Res Clin Pract,* 44, 147-156.

McGinn, S., Saad, S., Poronnik, P. & Pollock, C.A. (2003) High glucose-mediated effects on endothelial cell proliferation occur via p38 MAP kinase. *Am J Physiol Endocrinol Metab,* 285, E708-717.

McVeigh, G.E., Brennan, G.M., Johnston, G.D., McDermott, B.J., McGrath, L.T., Henry, W.R., Andrews, J.W. & Hayes, J.R. (1992) Impaired endothelium-dependent and independent vasodilation in patients with type 2 (non-insulin-dependent) diabetes mellitus. *Diabetologia,* 35, 771-776.

Meininger, C.J., Marinos, R.S., Hatakeyama, K., Martinez-Zaguilan, R., Rojas, J.D., Kelly, K.A. & Wu, G. (2000) Impaired nitric oxide production in coronary endothelial cells of the spontaneously diabetic BB rat is due to tetrahydrobiopterin deficiency. *Biochem J,* 349, 353-356.

Michell, B.J., Chen, Z., Tiganis, T., Stapleton, D., Katsis, F., Power, D.A., Sim, A.T. & Kemp, B.E. (2001) Coordinated control of endothelial nitric-oxide synthase phosphorylation by protein kinase C and the cAMP-dependent protein kinase. ***J Biol Chem,*** **276, 17625-17628.**

Mineo, C., Yuhanna, I.S., Quon, M.J. & Shaul, P.W. (2003) High density lipoprotein-induced endothelial nitric-oxide synthase activation is mediated by Akt and MAP kinases. ***J Biol Chem,*** **278, 9142-9149.**

Modur, V., Zimmerman, G.A., Prescott, S.M. & McIntyre, T.M. (1996) Endothelial cell inflammatory responses to tumor necrosis factor alpha. Ceramide-dependent and -independent mitogen-activated protein kinase cascades. ***J Biol Chem,*** **271, 13094-13102.**

Moulder, S.L., Yakes, F.M., Muthuswamy, S.K., Bianco, R., Simpson, J.F. & Arteaga, C.L. (2001) Epidermal growth factor receptor (HER1) tyrosine kinase inhibitor ZD1839 (Iressa) inhibits HER2/neu (erbB2)-overexpressing breast cancer cells in vitro and in vivo. ***Cancer Res,*** **61, 8887-8895.**

Mount, P.F., Kemp, B.E. & Power, D.A. (2006) Regulation of endothelial and myocardial NO synthesis by multi-site eNOS phosphorylation. ***J Mol Cell Cardiol.***

Mullis, K.B. (1990) The unusual origin of the polymerase chain reaction. ***Sci Am,*** **262, 56-61, 64-55.**

Mungrue, I.N. & Bredt, D.S. (2004) nNOS at a glance: implications for brain and brawn. ***J Cell Sci,*** **117, 2627-2629.**

Murad, F. (1986) Cyclic guanosine monophosphate as a mediator of vasodilation. ***J Clin Invest,*** **78, 1-5.**

Muramatsu, I., Hollenberg, M.D. & Lederis, K. (1985) Vascular actions of epidermal growth factor-urogastrone: possible relationship to prostaglandin production. ***Can J Physiol Pharmacol,*** **63, 994-999.**

Myers, P.R. & Tanner, M.A. (1998) Vascular endothelial cell regulation of extracellular matrix collagen: role of nitric oxide. ***Arterioscler Thromb Vasc Biol,*** **18, 717-722.**

Nakagami, H., Morishita, R., Yamamoto, K., Yoshimura, S.I., Taniyama, Y., Aoki, M., Matsubara, H., Kim, S., Kaneda, Y. & Ogihara, T. (2001) Phosphorylation of p38 mitogen-activated protein kinase downstream of bax-caspase-3 pathway leads to cell death induced by high D-glucose in human endothelial cells. ***Diabetes,*** **50, 1472-1481.**

Nakane, M., Schmidt, H.H., Pollock, J.S., Forstermann, J.J. & Murad, F. (1993) Cloned human brain nitric oxide synthase is highly expressed in skeletal muscle. ***FEBS Lett,*** **316, 175-180.**

Nakashima, H., Suzuki, H., Ohtsu, H., Chao, J.Y., Utsunomiya, H., Frank, G.D. & Eguchi, S. (2006) Angiotensin II regulates vascular and endothelial dysfunction: recent topics of Angiotensin II type-1 receptor signaling in the vasculature. ***Curr Vasc Pharmacol,*** **4, 67-78.**

Namiki, A. & Akatsuka, N. (1990) Vascular smooth muscle relaxation induced by epidermal growth factor is endothelium-dependent. ***Eur J Pharmacol,*** **180, 247-254.**

Naruse, K., Shimizu, K., Muramatsu, M., Toki, Y., Miyazaki, Y., Okumura, K., Hashimoto, H. & Ito, T. (1994) Long-term inhibition of NO synthesis promotes atherosclerosis in the hypercholesterolemic rabbit thoracic aorta. PGH2 does not contribute to impaired endothelium-dependent relaxation. *Arterioscler Thromb,* 14, 746-752.

Newton, A.C. (2001) Protein kinase C: structural and spatial regulation by phosphorylation, cofactors, and macromolecular interactions. *Chem Rev,* 101, 2353-2364.

Nick, J.A., Avdi, N.J., Gerwins, P., Johnson, G.L. & Worthen, G.S. (1996) Activation of a p38 mitogen-activated protein kinase in human neutrophils by lipopolysaccharide. *J Immunol,* 156, 4867-4875.

Nickenig, G. & Harrison, D.G. (2002) The AT(1)-type angiotensin receptor in oxidative stress and atherogenesis: part I: oxidative stress and atherogenesis. *Circulation,* 105, 393-396.

Nishikawa, T., Edelstein, D., Du, X.L., Yamagishi, S., Matsumura, T., Kaneda, Y., Yorek, M.A., Beebe, D., Oates, P.J., Hammes, H.P., Giardino, I. & Brownlee, M. (2000) Normalizing mitochondrial superoxide production blocks three pathways of hyperglycaemic damage. *Nature,* 404, 787-790.

Niwa, K., Inanami, O., Yamamori, T., Ohta, T., Hamasu, T., Karino, T. & Kuwabara, M. (2002) Roles of protein kinase C delta in the accumulation of P53 and the induction of apoptosis in H2O2-treated bovine endothelial cells. *Free Radic Res,* 36, 1147-1153.

Nonaka, A., Kiryu, J., Tsujikawa, A., Yamashiro, K., Miyamoto, K., Nishiwaki, H., Honda, Y. & Ogura, Y. (2000) PKC-beta inhibitor (LY333531) attenuates leukocyte entrapment in retinal microcirculation of diabetic rats. *Invest Ophthalmol Vis Sci,* 41, 2702-2706.

Nose, A., Mori, Y., Uchiyama-Tanaka, Y., Kishimoto, N., Maruyama, K., Matsubara, H. & Iwasaka, T. (2003) Regulation of glucose transporter (GLUT1) gene expression by angiotensin II in mesangial cells: involvement of HB-EGF and EGF receptor transactivation. *Hypertens Res,* 26, 67-73.

Nunokawa, Y. & Tanaka, S. (1992) Interferon-gamma inhibits proliferation of rat vascular smooth muscle cells by nitric oxide generation. *Biochem Biophys Res Commun,* 188, 409-415.

Obata, T., Maegawa, H., Kashiwagi, A., Pillay, T.S. & Kikkawa, R. (1998) High glucose-induced abnormal epidermal growth factor signaling. *J Biochem (Tokyo),* 123, 813-820.

Ogiso, H., Ishitani, R., Nureki, O., Fukai, S., Yamanaka, M., Kim, J.H., Saito, K., Sakamoto, A., Inoue, M., Shirouzu, M. & Yokoyama, S. (2002) Crystal structure of the complex of human epidermal growth factor and receptor extracellular domains. *Cell,* 110, 775-787.

Oka, Y. & Orth, D.N. (1983) Human plasma epidermal growth factor/beta-urogastrone is associated with blood platelets. *J Clin Invest,* 72, 249-259.

Okamoto, M., Kahn, C.R., Maron, R. & White, M.F. (1988) Decreased autophosphorylation of EGF receptor in insulin-deficient diabetic rats. *Am J Physiol,* 254, E429-434.

Oyama, Y., Kawasaki, H., Hattori, Y. & Kanno, M. (1986) Attenuation of endothelium-dependent relaxation in aorta from diabetic rats. *Eur J Pharmacol,* 132, 75-78.

Oyekan, A.O. (2003) Contributions of nitric oxide and prostanoids and their signaling pathways to the renal medullary vasodilator effect of U46619 (9-11-dideoxy-11 alpha,9a-epoxymethano-prostaglandin F(2a)) in the rat. *J Pharmacol Exp Ther,* 304, 507-512.

Palmer, R.M., Ferrige, A.G. & Moncada, S. (1987) Nitric oxide release accounts for the biological activity of endothelium-derived relaxing factor. *Nature,* 327, 524-526.

Palmer, R.M., Ashton, D.S. & Moncada, S. (1988) Vascular endothelial cells synthesize nitric oxide from L-arginine. *Nature,* 333, 664-666.

Panza, J.A. (1997) Endothelial dysfunction in essential hypertension. *Clin Cardiol,* 20, II-26-33.

Park, C.W., Kim, J.H., Lee, J.H., Kim, Y.S., Ahn, H.J., Shin, Y.S., Kim, S.Y., Choi, E.J., Chang, Y.S. & Bang, B.K. (2000) High glucose-induced intercellular adhesion molecule-1 (ICAM-1) expression through an osmotic effect in rat mesangial cells is PKC-NF-kappa B-dependent. *Diabetologia,* 43, 1544-1553.

Paulino, E.C., de Souza, L.J., Molan, N.A., Machado, M.C. & Jancar, S. (2007) Neutrophils from acute pancreatitis patients cause a more severe in vitro endothelial damage compared with neutrophils from healthy donors and are differently regulated by endothelins. *Pancreas,* 35, 37-41.

Peppelenbosch, M.P., Tertoolen, L.G. & de Laat, S.W. (1991) Epidermal growth factor-activated calcium and potassium channels. *J Biol Chem,* 266, 19938-19944.

Pieper, G.M. & Gross, G.J. (1988) Oxygen free radicals abolish endothelium-dependent relaxation in diabetic rat aorta. *Am J Physiol,* 255, H825-833.

Pieper, G.M. (1998) Review of alterations in endothelial nitric oxide production in diabetes: protective role of arginine on endothelial dysfunction. *Hypertension,* 31, 1047-1060.

Piga, R., Naito, Y., Kokura, S., Handa, O. & Yoshikawa, T. (2006) Short-term high glucose exposure induces monocyte-endothelial cells adhesion and transmigration by increasing VCAM-1 and MCP-1 expression in human aortic endothelial cells. *Atherosclerosis.*

Podar, T. & Tuomilehto, J. (2002) The role of angiotensin converting enzyme inhibitors and angiotensin II receptor antagonists in the management of diabetic complications. *Drugs,* 62, 2007-2012.

Poitout, V. & Robertson, R.P. (2002) Minireview: Secondary beta-cell failure in type 2 diabetes--a convergence of glucotoxicity and lipotoxicity. *Endocrinology,* 143, 339-342.

Prenzel, N., Fischer, O.M., Streit, S., Hart, S. & Ullrich, A. (2001) The epidermal growth factor receptor family as a central element for

cellular signal transduction and diversification. *Endocr Relat Cancer,* 8, 11-31.

Quehenberger, P., Bierhaus, A., Fasching, P., Muellner, C., Klevesath, M., Hong, M., Stier, G., Sattler, M., Schleicher, E., Speiser, W. & Nawroth, P.P. (2000) Endothelin 1 transcription is controlled by nuclear factor-kappaB in AGE-stimulated cultured endothelial cells. *Diabetes,* 49, 1561-1570.

Radha, V., Vimaleswaran, K.S., Deepa, R. & Mohan, V. (2003) The genetics of diabetes mellitus. *Indian J Med Res,* 117, 225-238.

Radomski, M.W., Palmer, R.M. & Moncada, S. (1990) An L-arginine/nitric oxide pathway present in human platelets regulates aggregation. *Proc Natl Acad Sci U S A,* 87, 5193-5197.

Raingeaud, J., Gupta, S., Rogers, J.S., Dickens, M., Han, J., Ulevitch, R.J. & Davis, R.J. (1995) Pro-inflammatory cytokines and environmental stress cause p38 mitogen-activated protein kinase activation by dual phosphorylation on tyrosine and threonine. *J Biol Chem,* 270, 7420-7426.

Randriamboavonjy, V. & Fleming, I. (2005) Endothelial nitric oxide synthase (eNOS) in platelets: how is it regulated and what is it doing there? *Pharmacol Rep,* 57 Suppl, 59-65.

Rang, H.P., Dale, M.M. & Ritter, J.M. (1999) *Pharmacology.* Churchill Livingstone, New York.

Rao, G.N. (1996) Hydrogen peroxide induces complex formation of SHC-Grb2-SOS with receptor tyrosine kinase and activates Ras and extracellular signal-regulated protein kinases group of mitogen-activated protein kinases. *Oncogene,* 13, 713-719.

Rask-Madsen, C. & King, G.L. (2005) Proatherosclerotic mechanisms involving protein kinase C in diabetes and insulin resistance. *Arterioscler Thromb Vasc Biol,* 25, 487-496.

Reddy, G.K. (2004) AGE-related cross-linking of collagen is associated with aortic wall matrix stiffness in the pathogenesis of drug-induced diabetes in rats. *Microvasc Res,* 68, 132-142.

Reddy, K.G., Nair, R.N., Sheehan, H.M. & Hodgson, J.M. (1994) Evidence that selective endothelial dysfunction may occur in the absence of angiographic or ultrasound atherosclerosis in patients with risk factors for atherosclerosis. *J Am Coll Cardiol,* 23, 833-843.

Riad, A., Unger, D., Du, J., Westermann, D., Mohr, Z., Sobirey, M., Dorenkamp, M., Schultheiss, H.P. & Tschope, C. (2007) Chronic inhibition of p38MAPK improves cardiac and endothelial function in experimental diabetes mellitus. *Eur J Pharmacol,* 554, 40-45.

Ribeiro, M.L., Farina, M., Billi, S., Perez Martinez, S., Branes, M.C., Villalon, M. & Franchi, A. (2005) Effect of in vivo administration of epidermal growth factor on prostaglandin production and NOS activity in term rat placentae. Possible participation of placental EGF receptors. *Placenta,* 26, 758-765.

Rijken, P.J., van Hal, G.J., van der Heyden, M.A., Verkleij, A.J. & Boonstra, J. (1998) Actin polymerization is required for negative

feedback regulation of epidermal growth factor-induced signal transduction. *Exp Cell Res,* 243, 254-262.

Rosen, L.B. & Greenberg, M.E. (1996) Stimulation of growth factor receptor signal transduction by activation of voltage-sensitive calcium channels. *Proc Natl Acad Sci U S A,* 93, 1113-1118.

Rosette, C. & Karin, M. (1996) Ultraviolet light and osmotic stress: activation of the JNK cascade through multiple growth factor and cytokine receptors. *Science,* 274, 1194-1197.

Roskoski, R., Jr. (2004) The ErbB/HER receptor protein-tyrosine kinases and cancer. *Biochem Biophys Res Commun,* 319, 1-11.

Russo, G., Leopold, J.A. & Loscalzo, J. (2002) Vasoactive substances: nitric oxide and endothelial dysfunction in atherosclerosis. *Vascul Pharmacol,* 38, 259-269.

Saad, S., Stevens, V.A., Wassef, L., Poronnik, P., Kelly, D.J., Gilbert, R.E. & Pollock, C.A. (2005) High glucose transactivates the EGF receptor and up-regulates serum glucocorticoid kinase in the proximal tubule. *Kidney Int,* 68, 985-997.

Sacco, R.L. (2002) Reducing the risk of stroke in diabetes: what have we learned that is new? *Diabetes Obes Metab,* 4 Suppl 1, S27-34.

Sako, Y., Minoghchi, S. & Yanagida, T. (2000) Single-molecule imaging of EGFR signalling on the surface of living cells. *Nat Cell Biol,* 2, 168-172.

Salt, I.P., Morrow, V.A., Brandie, F.M., Connell, J.M. & Petrie, J.R. (2003) High glucose inhibits insulin-stimulated nitric oxide production without reducing endothelial nitric-oxide synthase Ser1177 phosphorylation in human aortic endothelial cells. *J Biol Chem,* 278, 18791-18797.

Sayed-Ahmed, N., Besbas, N., Mundy, J., Muchaneta-Kubara, E., Cope, G., Pearson, C. & el Nahas, M. (1996) Upregulation of epidermal growth factor and its receptor in the kidneys of rats with streptozotocin-induced diabetes. *Exp Nephrol,* 4, 330-339.

Schalkwijk, C.G. & Stehouwer, C.D. (2005) Vascular complications in diabetes mellitus: the role of endothelial dysfunction. *Clin Sci (Lond),* 109, 143-159.

Schaudies, R.P. & Savage, C.R., Jr. (1986) Isolation of rat epidermal growth factor (r-EGF): chemical, biological and immunological comparisons with mouse and human EGF. *Comp Biochem Physiol B,* 84, 497-505.

Scherrer, U., Randin, D., Vollenweider, P., Vollenweider, L. & Nicod, P. (1994) Nitric oxide release accounts for insulin's vascular effects in humans. *J Clin Invest,* 94, 2511-2515.

Schiekofer, S., Andrassy, M., Chen, J., Rudofsky, G., Schneider, J., Wendt, T., Stefan, N., Humpert, P., Fritsche, A., Stumvoll, M., Schleicher, E., Haring, H.U., Nawroth, P.P. & Bierhaus, A. (2003) Acute hyperglycemia causes intracellular formation of CML and activation of ras, p42/44 MAPK, and nuclear factor kappaB in PBMCs. *Diabetes,* 52, 621-633.

Schlessinger, J. (2000) Cell signaling by receptor tyrosine kinases. *Cell,* 103, 211-225.

Schmidt, K., Gibraeil, H.D. & Mayer, B. (2002) Lack of involvement of extracellular signal-regulated kinase (ERK) in the agonist-induced endothelial nitric oxide synthesis. *Biochem Pharmacol,* 63, 1137-1142.

Sen, P., Chakraborty, P.K. & Raha, S. (2007) Activation of p38MAPK by repetitive low-grade oxidative stress leads to pro-survival effects. *Biochim Biophys Acta,* 1773, 367-374.

Seshiah, P.N., Weber, D.S., Rocic, P., Valppu, L., Taniyama, Y. & Griendling, K.K. (2002) Angiotensin II stimulation of NAD(P)H oxidase activity: upstream mediators. *Circ Res,* 91, 406-413.

Sheetz, M.J. & King, G.L. (2002) Molecular understanding of hyperglycemia's adverse effects for diabetic complications. *Jama,* 288, 2579-2588.

Shi, L.B., Huang, J.H. & Han, B.S. (2007) Hypoxia inducible factor-1alpha meidates protective effects of ischemic preconditioning on ECV-304 endothelial cells. *World J Gastroenterol,* 13, 2369-2373.

Shiba, T., Inoguchi, T., Sportsman, J.R., Heath, W.F., Bursell, S. & King, G.L. (1993) Correlation of diacylglycerol level and protein kinase C activity in rat retina to retinal circulation. *Am J Physiol,* 265, E783-793.

Shinozaki, K., Kashiwagi, A., Nishio, Y., Okamura, T., Yoshida, Y., Masada, M., Toda, N. & Kikkawa, R. (1999) Abnormal biopterin metabolism is a major cause of impaired endothelium-dependent relaxation through nitric oxide/O2- imbalance in insulin-resistant rat aorta. *Diabetes,* 48, 2437-2445.

Sillau, A.H., McCullough, R.E., Dyckes, R., White, M.M. & Moore, L.G. (2002) Chronic hypoxia increases MCA contractile response to U-46619 by reducing NO production and/or activity. *J Appl Physiol,* 92, 1859-1864.

Singh, A.B. & Harris, R.C. (2005) Autocrine, paracrine and juxtacrine signaling by EGFR ligands. *Cell Signal,* 17, 1183-1193.

Singh, R., Singh, A.K., Alavi, N. & Leehey, D.J. (2003) Mechanism of increased angiotensin II levels in glomerular mesangial cells cultured in high glucose. *J Am Soc Nephrol,* 14, 873-880.

Sissom, J.F., Stenzel, W.K. & Warshaw, J.B. (1987) Decreased binding of epidermal growth factor in placentas from streptozotocin-diabetic rats. *J Clin Invest,* 80, 242-247.

Sorensen, V.R., Mathiesen, E.R., Clausen, P., Flyvbjerg, A. & Feldt-Rasmussen, B. (2005) Impaired vascular function during short-term poor glycaemic control in Type 1 diabetic patients. *Diabet Med,* 22, 871-876.

Srivastava, A.K. (2002) High glucose-induced activation of protein kinase signaling pathways in vascular smooth muscle cells: a potential role in the pathogenesis of vascular dysfunction in diabetes (review). *Int J Mol Med,* 9, 85-89.

Steinberg, H.O., Bayazeed, B., Hook, G., Johnson, A., Cronin, J. & Baron, A.D. (1997) Endothelial dysfunction is associated with cholesterol levels in the high normal range in humans. *Circulation,* 96, 3287-3293.

Storey, K.B. (2004) *Functional metabolism: regulation and adaptation.* John Wiley & Sons, Hoboken, N.J.; [Great Britain].

Sudic, D., Razmara, M., Forslund, M., Ji, Q., Hjemdahl, P. & Li, N. (2006) High glucose levels enhance platelet activation: involvement of multiple mechanisms. *Br J Haematol,* 133, 315-322.

Sudol, M. (1998) From Src Homology domains to other signaling modules: proposal of the 'protein recognition code'. *Oncogene,* 17, 1469-1474.

Takahashi, K., Ghatei, M.A., Lam, H.C., O'Halloran, D.J. & Bloom, S.R. (1990a) Elevated plasma endothelin in patients with diabetes mellitus. *Diabetologia,* 33, 306-310.

Takahashi, K., Sawasaki, Y., Hata, J., Mukai, K. & Goto, T. (1990b) Spontaneous transformation and immortalization of human endothelial cells. *In Vitro Cell Dev Biol,* 26, 265-274.

Takeishi, Y., Ping, P., Bolli, R., Kirkpatrick, D.L., Hoit, B.D. & Walsh, R.A. (2000) Transgenic overexpression of constitutively active protein kinase C epsilon causes concentric cardiac hypertrophy. *Circ Res,* 86, 1218-1223.

Taylor, A.A. (2001) Pathophysiology of hypertension and endothelial dysfunction in patients with diabetes mellitus. *Endocrinol Metab Clin North Am,* 30, 983-997.

Taylor, P.D., Graves, J.E. & Poston, L. (1995) Selective impairment of acetylcholine-mediated endothelium-dependent relaxation in isolated resistance arteries of the streptozotocin-induced diabetic rat. *Clin Sci (Lond),* 88, 519-524.

Tesfamariam, B., Brown, M.L., Deykin, D. & Cohen, R.A. (1990) Elevated glucose promotes generation of endothelium-derived vasoconstrictor prostanoids in rabbit aorta. *J Clin Invest,* 85, 929-932.

Tesfamariam, B., Brown, M.L. & Cohen, R.A. (1991) Elevated glucose impairs endothelium-dependent relaxation by activating protein kinase C. *J Clin Invest,* 87, 1643-1648.

Tesfamariam, B., Palacino, J.J., Weisbrod, R.M. & Cohen, R.A. (1993) Aldose reductase inhibition restores endothelial cell function in diabetic rabbit aorta. *J Cardiovasc Pharmacol,* 21, 205-211.

Thomas, S.R., Chen, K. & Keaney, J.F., Jr. (2002) Hydrogen peroxide activates endothelial nitric-oxide synthase through coordinated phosphorylation and dephosphorylation via a phosphoinositide 3-kinase-dependent signaling pathway. *J Biol Chem,* 277, 6017-6024.

Tice, D.A., Biscardi, J.S., Nickles, A.L. & Parsons, S.J. (1999) Mechanism of biological synergy between cellular Src and epidermal growth factor receptor. *Proc Natl Acad Sci U S A,* 96, 1415-1420.

Tocris bioscience (2007a) AG825: Material Safety Data Sheet [WWW] <URL:http://www.tocris.com/literature/D__Literature_tempfiles_60371msds.pdf> [Accessed 5/8/07].

Tocris bioscience (2007b) AG1478 hydrochloride: Material Safety Data Sheet [WWW]
<URL:http://www.tocris.com/literature/D_Literature_tempfiles_11256msds.pdf> [Accessed 5/8/07].
Tognini, G., Ferrozzi, F., Bova, D., Bini, P. & Zompatori, M. (2003) Diabetes mellitus: CT findings of unusual complications related to the disease: a pictorial essay. *Clin Imaging,* 27, 325-329.
Tommasi, S., Fedele, V., Lacalamita, R., Crapolicchio, A., Perlino, E., Bellizzi, A. & Paradiso, A. (2004) Molecular and functional characteristics of erbB2 in normal and cancer breast cells. *Cancer Lett,* 209, 215-222.
Towbin, H., Staehelin, T. & Gordon, J. (1979) Electrophoretic transfer of proteins from polyacrylamide gels to nitrocellulose sheets: procedure and some applications. *Proc Natl Acad Sci U S A,* 76, 4350-4354.
Tzahar, E., Waterman, H., Chen, X., Levkowitz, G., Karunagaran, D., Lavi, S., Ratzkin, B.J. & Yarden, Y. (1996) A hierarchical network of interreceptor interactions determines signal transduction by Neu differentiation factor/neuregulin and epidermal growth factor. *Mol Cell Biol,* 16, 5276-5287.
UK Prospective Diabetes Study (UKPDS) Group (1998) Intensive blood-glucose control with sulphonylureas or insulin compared with conventional treatment and risk of complications in patients with type 2 diabetes. *Lancet,* 352, 837-853.
Vaidyula, V.R., Boden, G. & Rao, A.K. (2006) Platelet and monocyte activation by hyperglycemia and hyperinsulinemia in healthy subjects. *Platelets,* 17, 577-585.
Vanhoutte, P.M. (2001) Endothelial adrenoceptors. *J Cardiovasc Pharmacol,* 38, 796-808.
Varma, S., Lal, B.K., Zheng, R., Breslin, J.W., Saito, S., Pappas, P.J., Hobson, R.W., 2nd & Duran, W.N. (2005) Hyperglycemia alters PI3k and Akt signaling and leads to endothelial cell proliferative dysfunction. *Am J Physiol Heart Circ Physiol,* 289, H1744-1751.
Vasquez-Vivar, J., Kalyanaraman, B., Martasek, P., Hogg, N., Masters, B.S., Karoui, H., Tordo, P. & Pritchard, K.A., Jr. (1998) Superoxide generation by endothelial nitric oxide synthase: the influence of cofactors. *Proc Natl Acad Sci U S A,* 95, 9220-9225.
Vedernikov, Y.P., Belfort, M.A., Saade, G.R. & Garfield, R.E. (2001) Inhibition of cyclooxygenase but not nitric oxide synthase influences effects on the human omental artery of the thromboxane A2 mimetic U46619 and 17beta-estradiol. *Am J Obstet Gynecol,* 185, 182-189.
Vijan, S. & Hayward, R.A. (2003) Treatment of hypertension in type 2 diabetes mellitus: blood pressure goals, choice of agents, and setting priorities in diabetes care. *Ann Intern Med,* 138, 593-602.
Wagenknecht, L.E., Zaccaro, D., Espeland, M.A., Karter, A.J., O'Leary, D.H. & Haffner, S.M. (2003) Diabetes and progression of carotid

atherosclerosis: the insulin resistance atherosclerosis study. *Arterioscler Thromb Vasc Biol,* 23, 1035-1041.

Wan, Y.S., Wang, Z.Q., Voorhees, J. & Fisher, G. (2001) EGF receptor crosstalks with cytokine receptors leading to the activation of c-Jun kinase in response to UV irradiation in human keratinocytes. *Cell Signal,* 13, 139-144.

Wang, A., Nomura, M., Patan, S. & Ware, J.A. (2002) Inhibition of protein kinase Calpha prevents endothelial cell migration and vascular tube formation in vitro and myocardial neovascularization in vivo. *Circ Res,* 90, 609-616.

Ward, A., O'Brien, J.A. & Salas, M. (2005) Cost-effectiveness of oral hypoglycaemic agents for the treatment of type 2 diabetes mellitus. *Expert Opin Pharmacother,* 6, 601-608.

Warmuth, I., Harth, Y., Matsui, M.S., Wang, N. & DeLeo, V.A. (1994) Ultraviolet radiation induces phosphorylation of the epidermal growth factor receptor. *Cancer Res,* 54, 374-376.

Watts, G.F., O'Brien, S.F., Silvester, W. & Millar, J.A. (1996) Impaired endothelium-dependent and independent dilatation of forearm resistance arteries in men with diet-treated non-insulin-dependent diabetes: role of dyslipidaemia. *Clin Sci (Lond),* 91, 567-573.

Way, K.J., Katai, N. & King, G.L. (2001) Protein kinase C and the development of diabetic vascular complications. *Diabet Med,* 18, 945-959.

Webb, R.C. (2003) Smooth muscle contraction and relaxation. *Adv Physiol Educ,* 27, 201-206.

White, C.R., Brock, T.A., Chang, L.Y., Crapo, J., Briscoe, P., Ku, D., Bradley, W.A., Gianturco, S.H., Gore, J., Freeman, B.A. & et al. (1994) Superoxide and peroxynitrite in atherosclerosis. *Proc Natl Acad Sci U S A,* 91, 1044-1048.

Wild, S., Roglic, G., Green, A., Sicree, R. & King, H. (2004) Global prevalence of diabetes: estimates for the year 2000 and projections for 2030. *Diabetes Care,* 27, 1047-1053.

Williams, S.B., Cusco, J.A., Roddy, M.A., Johnstone, M.T. & Creager, M.A. (1996) Impaired nitric oxide-mediated vasodilation in patients with non-insulin-dependent diabetes mellitus. *J Am Coll Cardiol,* 27, 567-574.

Williamson, J.R., Chang, K., Frangos, M., Hasan, K.S., Ido, Y., Kawamura, T., Nyengaard, J.R., van den Enden, M., Kilo, C. & Tilton, R.G. (1993) Hyperglycemic pseudohypoxia and diabetic complications. *Diabetes,* 42, 801-813.

Wilson, P.S., Thompson, W.J., Moore, T.M., Khimenko, P.L. & Taylor, A.E. (1997) Vasoconstriction increases pulmonary nitric oxide synthesis and circulating cyclic GMP. *J Surg Res,* 70, 75-83.

World Health Organization (1999) Definition, diagnosis and classification of diabetes mellitus and its complications. Report of a WHO consultation. Geneva. *Arterioscler Thromb Vasc Biol.*

World Health Organization (2006) Diabetes. Fact Sheet No 312 [WWW]

<URL: http://www.who.int/mediacentre/factsheets/fs312/en/ > [Accessed 3/8/07].

Worthylake, R., Opresko, L.K. & Wiley, H.S. (1999) ErbB-2 amplification inhibits down-regulation and induces constitutive activation of both ErbB-2 and epidermal growth factor receptors. *J Biol Chem,* 274, 8865-8874.

Xia, P., Inoguchi, T., Kern, T.S., Engerman, R.L., Oates, P.J. & King, G.L. (1994) Characterization of the mechanism for the chronic activation of diacylglycerol-protein kinase C pathway in diabetes and hypergalactosemia. *Diabetes,* 43, 1122-1129.

Yamauchi, T., Ueki, K., Tobe, K., Tamemoto, H., Sekine, N., Wada, M., Honjo, M., Takahashi, M., Takahashi, T., Hirai, H., Tushima, T., Akanuma, Y., Fujita, T., Komuro, I., Yazaki, Y. & Kadowaki, T. (1997) Tyrosine phosphorylation of the EGF receptor by the kinase Jak2 is induced by growth hormone. *Nature,* 390, 91-96.

Yang, M.L., Guh, J.Y., Lai, Y.H., Yang, Y.L., Chang, C.C., Tsai, J.H. & Chuang, L.Y. (1997) Effects of high glucose culture on EGF effects and EGF receptors in the LLC-PK1 cells. *Am J Nephrol,* 17, 193-198.

Yao, R. & Cooper, G.M. (1995) Requirement for phosphatidylinositol-3 kinase in the prevention of apoptosis by nerve growth factor. *Science,* 267, 2003-2006.

Yarden, Y. (2001) The EGFR family and its ligands in human cancer. signalling mechanisms and therapeutic opportunities. *Eur J Cancer,* 37 Suppl 4, S3-8.

Yoon, J.W. & Jun, H.S. (2006) Viruses cause type 1 diabetes in animals. *Ann N Y Acad Sci,* 1079, 138-146.

Yousif, M.H., Benter, I.F. & Akhtar, S. (2005) The role of tyrosine kinase-mediated pathways in diabetes-induced alterations in responsiveness of rat carotid artery. *Auton Autacoid Pharmacol,* 25, 69-78.

Yousif, M.H., Benter, I.F., Hares, N., Canatan, H. & Akhtar, S. (2006) Phosphoinositide 3-kinase mediated signalling contributes to development of diabetes-induced abnormal vascular reactivity of rat carotid artery. *Cell Biochem Funct,* 24, 13-22.

Yu, X., Sharma, K.D., Takahashi, T., Iwamoto, R. & Mekada, E. (2002) Ligand-independent dimer formation of epidermal growth factor receptor (EGFR) is a step separable from ligand-induced EGFR signaling. *Mol Biol Cell,* 13, 2547-2557.

Zackrisson, U., Mikuni, M., Wallin, A., Delbro, D., Hedin, L. & Brannstrom, M. (1996) Cell-specific localization of nitric oxide synthases (NOS) in the rat ovary during follicular development, ovulation and luteal formation. *Hum Reprod,* 11, 2667-2673.

Zeng, G., Nystrom, F.H., Ravichandran, L.V., Cong, L.N., Kirby, M., Mostowski, H. & Quon, M.J. (2000) Roles for insulin receptor, PI3-kinase, and Akt in insulin-signaling pathways related to production of nitric oxide in human vascular endothelial cells. *Circulation,* 101, 1539-1545.

Zhang, H.T., O'Rourke, D.M., Zhao, H., Murali, R., Mikami, Y., Davis, J.G., Greene, M.I. & Qian, X. (1998) Absence of autophosphorylation site Y882 in the p185neu oncogene product correlates with a reduction of transforming potential. ***Oncogene,*** **16, 2835-2842.**

Zhang, L., Zalewski, A., Liu, Y., Mazurek, T., Cowan, S., Martin, J.L., Hofmann, S.M., Vlassara, H. & Shi, Y. (2003) Diabetes-induced oxidative stress and low-grade inflammation in porcine coronary arteries. ***Circulation,*** **108, 472-478.**

Zheng, J., Bird, I.M., Melsaether, A.N. & Magness, R.R. (1999) Activation of the mitogen-activated protein kinase cascade is necessary but not sufficient for basic fibroblast growth factor- and epidermal growth factor-stimulated expression of endothelial nitric oxide synthase in ovine fetoplacental artery endothelial cells. ***Endocrinology,*** **140, 1399-1407.**

Zierath, J.R. & Kawano, Y. (2003) The effect of hyperglycaemia on glucose disposal and insulin signal transduction in skeletal muscle. ***Best Pract Res Clin Endocrinol Metab,*** **17, 385-398.**

Zimmet, P., Alberti, K.G. & Shaw, J. (2001) Global and societal implications of the diabetes epidemic. ***Nature,*** **414, 782-787.**

Zuurbier, C.J., Demirci, C., Koeman, A., Vink, H. & Ince, C. (2005) Short-term hyperglycemia increases endothelial glycocalyx permeability and acutely decreases lineal density of capillaries with flowing red blood cells. ***J Appl Physiol,*** **99, 1471-1476.**

Appendix

PUBLICATIONS AND PRESENTATIONS

Research Articles

Benter, I.F., Yousif, M.H., Hollins, A.J., **Griffiths, S.M.** & Akhtar, S. (2005) Diabetes-induced renal vascular dysfunction is normalized by inhibition of epidermal growth factor receptor tyrosine kinase. *J Vasc Res,* 42, 284-291.

Benter, I.F., Yousif, M.H., **Griffiths, S.M.**, Benboubetra, M. & Akhtar, S. (2005) Epidermal growth factor receptor tyrosine kinase-mediated signalling contributes to diabetes-induced vascular dysfunction in the mesenteric bed. *Br J Pharmacol,* 145, 829-836.

Poster Presentations

Griffiths, S.M., Yousif, M.H., Benter, I.F., Hollins, A.J., Akhtar, S. (2005) The Effect of Hyperglycaemia on EGFR Signalling and its Potential Role in Diabetes-induced Vascular Dysfunction. Keystone Symposia. Diabetes Mellitus: Molecular Mechanisms, Genetics and New Therapies. Keystone Resort, Keystone, Colorado.

Griffiths S.M. (2005) The Effect of Hyperglycaemia on EGFR Signalling and its Potential Role in Diabetes-induced Vascular Dysfunction. Annual Presentations by Britain's Top Younger Scientists, Engineers and Technologists at the House of Commons.

Griffiths S.M., Yousif M.H., Benter I.F., Hollins A.J., Akhtar S. (2005) "The effect of hyperglycaemia on EGFR signalling and its potential role in diabetes-induced vascular dysfunction" British Pharmaceutical Conference. Journal of Pharmacy and Pharmacology 57, s-37.

Griffiths, S.M., Benboubetra, M., Yousif, M.H., Benter,I.H., Akhtar, S. (2004) The role of EGFR signalling in diabetes-induced vascular dysfunction. Postgraduate research day poster.

Griffiths, S.M., Yousif, M.H., Benter, I.F., and Akhtar, S. (2004) The Role of EGFR in Hyperglycaemia-induced Endothelial Cell Dysfunction. Biochemical Society Focused Meeting. Kinases in Diabetes. Hulme Hall, University of Manchester, UK.*

Hollins A.J., Omidi Y., Fox S.P., **Griffiths S.**, Akhtar S. (2004) "Polyethylenimine-mediated delivery of small interfering RNA targeting the epidermal growth factor receptor: a comparison of linear and branched polymer architecture" British Pharmaceutical Conference. Journal of Pharmacy and Pharmacology 56, s-20, no.53.

Benboubetra M., Omidi Y., Yousif M., **Griffiths S.,** Benbter I. and Akhtar S., (2004) Microarray-based gene expression profiling in streptozotocin-induced diabetes: role of receptor tyrosine kinases in vascular dysfunction, *31st Annual Meeting & Exposition of the Controlled Release Society, June 12-16, 2004,* Honolulu, Hawaii, USA.

Oral Presentations

Griffiths S.M. (2005) The role of EGFR signalling cascade in diabetes-induced vascular dysfunction. Cardiovascular IRG Away-day. Miskin Manor Country Hotel.

Griffiths, S.M., Yousif, M.H., Benter, I.F., Hollins, A.J., Akhtar, S. (2005) The Effect of Hyperglycaemia on EGFR Signalling and its Potential Role in Diabetes Induced Vascular Dysfunction. Welsh school of pharmacy postgraduate research day.

* First prize poster